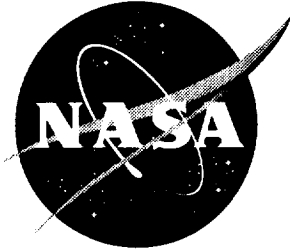


NASA/TM-1999-209701



# Subsonic Investigation of Leading-Edge Flaps Designed for Vortex- and Attached-Flow on a High-Speed Civil Transport Configuration

*Bryan A. Campbell, Guy T. Kemmerly, and Kevin J. Kjerstad  
Langley Research Center, Hampton, Virginia*

*Victor R. Lessard  
ViGYAN, Inc., Hampton, Virginia*

---

December 1999

## The NASA STI Program Office . . . in Profile

Since its founding, NASA has been dedicated to the advancement of aeronautics and space science. The NASA Scientific and Technical Information (STI) Program Office plays a key part in helping NASA maintain this important role.

The NASA STI Program Office is operated by Langley Research Center, the lead center for NASA's scientific and technical information. The NASA STI Program Office provides access to the NASA STI Database, the largest collection of aeronautical and space science STI in the world. The Program Office is also NASA's institutional mechanism for disseminating the results of its research and development activities. These results are published by NASA in the NASA STI Report Series, which includes the following report types:

- **TECHNICAL PUBLICATION.** Reports of completed research or a major significant phase of research that present the results of NASA programs and include extensive data or theoretical analysis. Includes compilations of significant scientific and technical data and information deemed to be of continuing reference value. NASA counterpart of peer-reviewed formal professional papers, but having less stringent limitations on manuscript length and extent of graphic presentations.
- **TECHNICAL MEMORANDUM.** Scientific and technical findings that are preliminary or of specialized interest, e.g., quick release reports, working papers, and bibliographies that contain minimal annotation. Does not contain extensive analysis.
- **CONTRACTOR REPORT.** Scientific and technical findings by NASA-sponsored contractors and grantees.

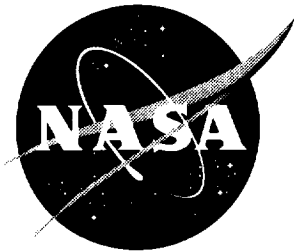
- **CONFERENCE PUBLICATION.** Collected papers from scientific and technical conferences, symposia, seminars, or other meetings sponsored or co-sponsored by NASA.
- **SPECIAL PUBLICATION.** Scientific, technical, or historical information from NASA programs, projects, and missions, often concerned with subjects having substantial public interest.
- **TECHNICAL TRANSLATION.** English-language translations of foreign scientific and technical material pertinent to NASA's mission.

Specialized services that complement the STI Program Office's diverse offerings include creating custom thesauri, building customized databases, organizing and publishing research results . . . even providing videos.

For more information about the NASA STI Program Office, see the following:

- Access the NASA STI Program Home Page at <http://www.sti.nasa.gov>
- Email your question via the Internet to [help@sti.nasa.gov](mailto:help@sti.nasa.gov)
- Fax your question to the NASA STI Help Desk at (301) 621-0134
- Telephone the NASA STI Help Desk at (301) 621-0390
- Write to:  
NASA STI Help Desk  
NASA Center for AeroSpace Information  
7121 Standard Drive  
Hanover, MD 21076-1320

NASA/TM-1999-209701



# Subsonic Investigation of Leading-Edge Flaps Designed for Vortex- and Attached-Flow on a High-Speed Civil Transport Configuration

*Bryan A. Campbell, Guy T. Kemmerly, and Kevin J. Kjerstad  
Langley Research Center, Hampton, Virginia*

*Victor R. Lessard  
ViGYAN, Inc., Hampton, Virginia*

National Aeronautics and  
Space Administration

Langley Research Center  
Hampton, Virginia 23681-2199

---

December 1999

---

Available from:

NASA Center for AeroSpace Information (CASI)  
7121 Standard Drive  
Hanover, MD 21076-1320  
(301) 621-0390

National Technical Information Service (NTIS)  
5285 Port Royal Road  
Springfield, VA 22161-2171  
(703) 605-6000

## Summary

A wind tunnel investigation of two separate leading-edge flaps, designed for vortex- and attached-flow respectively, were conducted on a High Speed Civil Transport (HSCT) configuration in the Langley 14- by 22-Foot Subsonic Tunnel. Data were obtained over a Mach number range of 0.12 to 0.27, with corresponding chord Reynolds numbers of  $2.50 \times 10^6$  to  $5.50 \times 10^6$ . Variations of the leading-edge flap deflection angle were tested with outboard leading-edge flaps deflected  $0^\circ$  and  $26.4^\circ$ . Trailing-edge flaps were deflected  $0^\circ$ ,  $10^\circ$ ,  $12.9^\circ$  and  $20^\circ$ . The longitudinal and lateral aerodynamic data are presented without analysis. A complete tabulated data listing is also presented herein. The data associated with each deflected leading-edge flap indicate L/D improvements over the undeflected configuration. These improvements may be instrumental in providing the necessary lift augmentation required by an actual HSCT during the climb-out and landing phases of the flight envelope. However, further tests will have to be done to assess their full potential.

## Introduction

Proposed High-Speed Civil Transport (HSCT) configurations have supersonic cruise speeds above Mach 2, and hence incorporate a high degree of leading-edge sweep for supersonic cruise efficiency. However, high leading-edge sweep is not conducive to efficient performance at subsonic speeds such as encountered during take-off, climbout, approach and landing. Therefore, investigations are continuing at the NASA Langley Research Center to study ways of improving the subsonic capabilities of conceptual HSCT configurations.

One area of investigation involves the tendency for highly swept wings to develop leading-edge vortical flow at moderate to high angles of attack. It has been observed in previous wind tunnel investigations (references 1 & 2) that during the subsonic climbout phase of the flight envelope, these wings tend to produce large upper surface vortex structures. Although these vortices may provide significant lift augmentation, they often result in increased drag and a poorer L/D. Increased drag requires a corresponding increase in engine thrust, thereby adversely affecting the community noise characteristics.

Over the years, several methods have been tried to manipulate the vortex flow field on the wings of configurations similar to HSCT concepts in order to improve their low speed performance (references 3 thru 8). This test investigates the use of two leading-edge flap systems to enhance low-speed, high-lift. The first system, a vortex flap on the  $71^\circ$  inboard section of this

model, was designed to use leading-edge flow separation advantageously by rotating the vortex-induced suction force forward, thus providing a measure of leading-edge thrust. The second system, referred to as a mission adaptive flap (MA), was designed to significantly reduce flow separation by keeping the leading-edge of the flap aligned with the local upwash field. This results in a flap with a considerable amount of twist and camber. Both flap systems were tested with a variety of trailing-edge flap deflections.

The results presented herein were acquired at the NASA Langley 14- by 22-Foot Subsonic Tunnel. Data were obtained for the cruise and high-lift configurations (without vertical tails) for an angle-of-attack range from  $-2^\circ$  to  $20^\circ$  over a Mach number range of 0.12 to 0.27. The corresponding Reynolds number, based on the mean aerodynamic chord, ranged from  $2.5 \times 10^6$  to  $5.5 \times 10^6$ , respectively.

### Symbols & Abbreviations

$a$	speed of sound, $\frac{ft}{sec}$
$b$	wing span, $ft$
$C_A$	axial-force coefficient, $\frac{\text{Axial force}}{qS}$
$C_D$	drag coefficient, $\frac{\text{Drag}}{qS}$
$C_L$	lift coefficient, $\frac{\text{Lift}}{qS}$
$C_l$	rolling moment coefficient, $\frac{\text{Rolling moment}}{qSb}$
$C_m$	pitching moment coefficient, $\frac{\text{Pitching moment}}{qS\bar{c}}$
$C_N$	normal force coefficient, $\frac{\text{Normal force}}{qS}$
$C_n$	yawing moment coefficient, $\frac{\text{Yawing moment}}{qSb}$
$C_Y$	side force coefficient, $\frac{\text{Side-force}}{qS}$
$\bar{c}$	mean aerodynamic chord, $ft$
$D$	drag, $lb$

<i>L</i>	lift, <i>lb</i>
<i>L/D</i>	lift-to-drag ratio
<i>M</i>	Mach number, $\frac{V}{a}$
<i>q</i>	dynamic pressure, $\frac{lb}{ft^2}$
<i>R</i>	Reynolds number, $\frac{\rho V c}{\mu}$
<i>S</i>	wing reference area, $ft^2$
<i>V</i>	velocity, $\frac{ft}{sec}$
$\alpha$	angle of attack, <i>deg</i>
$\beta$	angle of sideslip, <i>deg</i>
$\delta$	flap deflection angle, normal to hinge line (positive down), <i>deg</i>
$\mu$	viscosity, $\frac{lb \cdot sec}{ft^2}$
$\rho$	density, $\frac{slugs}{ft^3}$

**Subscripts:**

<i>L</i>	leading edge (Indicates all leading-edge flaps unless followed by the subscript 1, 2, or 3.)
<i>T</i>	trailing edge (Indicates all trailing-edge flaps unless followed by the subscript 1, 2, or 3.)
$\infty$	free stream conditions
1, 2, 3	flap location as defined in Figure 2.

**Abbreviations:**

HSCT	high-speed civil transport
i	inboard wing
o	outboard wing

## **Model Description**

### **Wind Tunnel Model**

A geometric description of the model tested in this investigation is presented in figure 1. The wing has an inboard sweep of  $71^\circ$  and an outboard sweep of  $50^\circ$  with no twist or camber. The flap systems, shown in figure 2, consist of leading-edge flap segments and partial span trailing-edge flap segments spaced to accommodate engine nacelle placement. Tests were conducted for each of the leading-edge flaps along with the undeflected leading-edge configuration. Trailing-edge flaps were deflected  $0^\circ$ ,  $10^\circ$ ,  $12.9^\circ$  and  $20^\circ$  for each of the leading-edge flaps. Transition grit (number 60 size) was applied to both the forebody and the wing upper surface leading-edge to fix boundary-layer transition from laminar to turbulent flow. During this investigation the model had no canards, tail surfaces, or engine nacelles. The geometric characteristics are presented in Table 1.

### **Vortex Flap**

The vortex flap, shown on the model in figure 3, was designed for the inboard  $71^\circ$  swept section using Frink's vortex flap design code (reference 9). The design conditions included a lift coefficient of  $C_L = 0.8$ , a vortex flap deflection of  $40^\circ$ , with an outboard leading-edge deflection of  $26.4^\circ$ , and all trailing-edge flaps at  $20^\circ$ . The resulting configuration is shown in figure 4. During the investigation, the vortex flap was also tested at  $30^\circ$  and  $50^\circ$  deflections.

### **Attached Flow Flap**

An attached flow flap, shown on the model in figure 5, was also designed for the entire wing leading-edge. The flap was designed using Carlson's wing design code (reference 10) and is referred to as a mission adaptive flap because the local flap deflection angle increases as a function of wing span to account for the increasing upwash field. By keeping the flap aligned with the local upwash, leading-edge flow separation can be significantly reduced. The amount of local deflection shown in figure 5 represents what is required for a design lift coefficient of  $C_L = 0.45$ . Additionally, the flap possesses a high degree of camber to maintain a smooth hinge line radius and thus reduce the possibility of hinge line separation. To ensure a smooth transition between the inboard and the outboard sections, the inboard and outboard flap segments were manufactured such that no gap existed at the crank. Gaps at the crank would normally exist due to deflecting



leading-edge flaps on hinge lines with different sweeps.

The difference in the design  $C_L$  between the two flap systems resulted from a change in program focus occurring after the design of the vortex flap was completed and fabrication was started. However, each flap system was tested over a large range of lift coefficients thereby providing overlapping data for both design conditions.

### Test Conditions & Instrumentation

Tests were conducted in the Langley 14- by 22-Foot Subsonic Tunnel (reference 11). Test Mach numbers, dynamic pressures, and Reynolds numbers based on the wing mean aerodynamic chord were as follows:

Mach number, $M$	Dynamic pressure, $q$ , $psf$	Reynolds number, $R$ , $\times 10^6$
0.12	20	2.50
0.18	50	3.90
0.22	70	4.50
0.27	110	5.50

Tests were conducted over an angle-of-attack range from  $-2^\circ$  to  $20^\circ$ ; with most configurations also tested through  $\pm 5^\circ$  of sideslip. All configurations had zero roll angle.

A six-component strain-gauge balance mounted inside the fuselage measured the forces and moments. The accuracy of this strain-gauge balance is presented in Appendix A.

Angle of attack was measured by an accelerometer installed in the model; whereas, the angle of sideslip was measured via a digital encoder mounted to the turntable drive mechanism of the model support system.

The data were corrected for jet-boundary and blockage effects according to the methods of references 12 and 13. No corrections were made for flow angularity or local support system flow interference.

## Presentation of Data

An index to the aerodynamic data acquired during this investigation is presented in Table 2, with a complete tabular listing of the data being presented in Table 3. Plots depicting the longitudinal and lateral aerodynamic data are presented herein, without analysis, in the following groupings:

Topic	Figure
<b>Vortex Flap Aerodynamics</b>	
Tunnel dynamic pressure effects . . . . .	6
Sideslip effects, undeflected flaps, $q=110$ psf . . . . .	7
Trailing-edge flap effects, $\delta_L=0^\circ$ , $q=70$ psf . . . . .	8
Trailing-edge flap effects, $\delta_L=0^\circ$ , $q=110$ psf . . . . .	9
Sideslip effects, $\delta_L=0^\circ$ , $\delta_T=20^\circ$ , $q=110$ psf . . . . .	10
Effects of $\delta_{L1/2}=40^\circ/0^\circ$ , $\delta_T=20^\circ$ , $q=70$ psf . . . . .	11
Sideslip effects, $\delta_{L1/2}=40^\circ/0^\circ$ , $\delta_T=20^\circ$ , $q=110$ psf . . . . .	12
Effects of $\delta_L$ combinations with $\delta_T=20^\circ$ , $q=70$ psf . . . . .	13
Sideslip effects, $\delta_{L1/2}=30^\circ/26.4^\circ$ , $\delta_T=20^\circ$ , $q=110$ psf . . . . .	14
Sideslip effects, $\delta_{L1/2}=40^\circ/26.4^\circ$ , $\delta_T=20^\circ$ , $q=110$ psf . . . . .	15
Sideslip effects, $\delta_{L1/2}=50^\circ/26.4^\circ$ , $\delta_T=20^\circ$ , $q=110$ psf . . . . .	16
Effects of deflecting outboard trailing-edge flap with $\delta_{L1/2}=40^\circ/26.4^\circ$ , $q=70$ psf . . . . .	17
Effects of deflecting outboard trailing-edge flap with $\delta_{L1/2}=40^\circ/26.4^\circ$ , $q=110$ psf . . . . .	18
<b>Attached Flow Flap Aerodynamics</b>	
Tunnel dynamic pressure effects . . . . .	19
Sideslip effects, undeflected flaps, $q=110$ psf . . . . .	20
Trailing-edge flap effects, $\delta_L=0^\circ$ , $q=70$ psf . . . . .	21
Trailing-edge flap effects, $\delta_L=0^\circ$ , $q=110$ psf . . . . .	22
Sideslip effects, $\delta_L=0^\circ$ , $\delta_{T1/2/3}=10^\circ/10^\circ/20^\circ$ , $q=110$ psf . . . . .	23
Tunnel dynamic pressure effects, $\delta_L=MA$ , $\delta_T=0^\circ$ . . . . .	24
Sideslip effects, $\delta_L=MA$ , $\delta_T=0^\circ$ , $q=110$ psf . . . . .	25
Comparison of $\delta_L=MA$ with $\delta_L=0^\circ$ ; $\delta_T=0^\circ$ , $q=70$ psf . . . . .	26
Comparison of $\delta_L=MA$ with $\delta_L=0^\circ$ ; $\delta_T=0^\circ$ , $q=110$ psf . . . . .	27
Effects of trailing-edge flap deflections, $\delta_L=MA$ , $q=70$ psf . . . . .	28
Effects of trailing-edge flap deflections, $\delta_L=MA$ , $q=110$ psf . . . . .	29
Sideslip effects, $\delta_L=MA$ , $\delta_{T1/2/3}=10^\circ/10^\circ/0^\circ$ , $q=110$ psf . . . . .	30
Sideslip effects, $\delta_L=MA$ , $\delta_{T1/2/3}=10^\circ/10^\circ/12.9^\circ$ , $q=110$ psf . . . . .	31
Sideslip effects, $\delta_L=MA$ , $\delta_{T1/2/3}=10^\circ/10^\circ/20^\circ$ , $q=110$ psf . . . . .	32

**Table 1.**  
**Geometric Characteristics Of Basic Model**

The wing reference area is defined by extending the inboard leading edge and the outboard trailing edge of the cruise configuration planform projection to the centerline (see Figure 1.).

Aspect ratio	2.116
Reference area, ft <sup>2</sup>	10.664
Gross area, ft <sup>2</sup>	11.005
Span, ft	4.750
Root chord, ft	5.288
Tip chord, ft	0.529
Reference mean aerodynamic chord, ft	3.071
Leading-edge sweep, degrees:	
At body station 1.943 ft	71.0
At body station 6.299 ft	50.0

**Table 2.**  
**Index to Data in Table 3.**

Note: Alpha sweep is defined as  $\alpha = -2^\circ$  through  $20^\circ$ ,  $\Delta = 2^\circ$ . Runs with the vortex flap were limited to a maximum of  $16^\circ$  at  $q=110$  psf due to the internal balance pitching moment limitations.

Run	q (psf)	$\alpha$ (deg)	$\beta$ (deg)	L.E. Flap Type	$\delta_{L1}$ (deg)	$\delta_{L2}$ (deg)	$\delta_{T1,2,3}$ (deg)
10	20	sweep	0	MA	-	-	0/0/0
11	50	↓	↓	↓	↓	↓	↓
12	70	↓	↓	↓	↓	↓	↓
13	110	↓	↓	↓	↓	↓	↓
14	70	sweep	0	MA	-	-	0/0/0
15	110	↓	-5	↓	↓	↓	↓
16	110	↓	+5	↓	↓	↓	↓
17	70	sweep	0	MA	-	-	10/10/0
18	110	↓	0	↓	↓	↓	↓
19	↓	↓	+5	↓	↓	↓	↓
20	↓	↓	-5	↓	↓	↓	↓
21	70	sweep	0	MA	-	-	10/10/12.9
22	110	↓	0	↓	↓	↓	↓
23	↓	↓	+5	↓	↓	↓	↓
24	↓	↓	-5	↓	↓	↓	↓
25	70	sweep	0	MA	-	-	10/10/20
26	110	↓	0	↓	↓	↓	↓
27	↓	↓	-5	↓	↓	↓	↓
28	↓	↓	+5	↓	↓	↓	↓
29	20	sweep	0	NONE	0	0	0/0/0
30	50	↓	↓	↓	↓	↓	↓
31	70	↓	↓	↓	↓	↓	↓

Run	q (psf)	$\alpha$ (deg)	$\beta$ (deg)	L.E. Flap Type	$\delta_{L1}$ (deg)	$\delta_{L2}$ (deg)	$\delta_{T1,2,3}$ (deg)
32	110	sweep	0	NONE	0	0	0/0/0
33	110	↓	+5	↓	↓	↓	↓
34	110	↓	-5	↓	↓	↓	↓
36	20	sweep	0	NONE	0	0	0/0/0
37	50	↓	↓	↓	↓	↓	↓
38	70	↓	↓	↓	↓	↓	↓
39	110	↓	↓	↓	↓	↓	↓
40	↓	sweep	+5	NONE	0	0	0/0/0
41	↓	sweep	-5	NONE	0	0	0/0/0
42	70	sweep	0	NONE	0	0	10/10/20
43	110	↓	0	↓	↓	↓	↓
44	↓	↓	+5	↓	↓	↓	↓
45	↓	↓	-5	↓	↓	↓	↓
46	20	sweep	0	VOR	0	0	0/0/0
47	50	↓	↓	↓	↓	↓	↓
48	70	↓	↓	↓	↓	↓	↓
49	110	↓	↓	↓	↓	↓	↓
50	↓	↓	+5	↓	↓	↓	↓
51	↓	↓	-5	↓	↓	↓	↓
52	70	sweep	0	VOR	0	0	20/20/20
53	110	↓	↓	↓	↓	↓	↓
54	↓	↓	+5	↓	↓	↓	↓
55	↓	↓	-5	↓	↓	↓	↓
56	70	sweep	0	VOR	40	0	20/20/20
57	110	↓	↓	↓	↓	↓	↓
58	↓	↓	+5	↓	↓	↓	↓
59	↓	↓	-5	↓	↓	↓	↓

Run	q (psf)	$\alpha$ (deg)	$\beta$ (deg)	L.E. Flap Type	$\delta_{L1}$ (deg)	$\delta_{L2}$ (deg)	$\delta_{T1,2,3}$ (deg)
60	70	sweep	0	VOR	40	26.4	20 / 20 / 20
61	110						
62			+5				
63	↓	↓	-5	↓	↓	↓	↓
64	70	sweep	0	VOR	30	26.4	20 / 20 / 20
65	110						
66			+5				
67	↓	↓	-5	↓	↓	↓	↓
68	70	sweep	0	VOR	50	26.4	20 / 20 / 20
69							
70			+5				
71	↓	↓	-5	↓	↓	↓	↓
72	70	sweep	0	VOR	40	26.4	10 / 10 / 12.9
73	110	sweep	0	VOR	40	26.4	10 / 10 / 12.9

**Table 3**  
**Tabulated Force and Moment Data**

NASA Langley Research Center 14- by 22-Foot Subsonic Tunnel Test 395

Run	Point	R/10 <sup>6</sup>	M	q	$\alpha$	$\beta$	C <sub>N</sub>	C <sub>A</sub>	C <sub>L</sub>	C <sub>D</sub>	C <sub>m</sub>	C <sub>i</sub>	C <sub>n</sub>	C <sub>y</sub>	L/D
10.	1.	2.36	0.12	19.97	-2.05	0.00	-0.1506	0.0247	-0.1496	0.0301	-0.0150	0.0000	0.0001	0.0008	-4.97
10.	2.	2.36	0.12	19.98	0.07	0.00	-0.0435	0.0190	-0.0435	0.0189	-0.0036	0.0000	-0.0001	-0.0002	-2.30
10.	3.	2.36	0.12	19.98	2.00	0.00	0.0458	0.0131	0.0453	0.0147	0.0051	-0.0001	-0.0004	-0.0019	3.09
10.	4.	2.36	0.12	19.99	4.05	0.00	0.1301	0.0057	0.1293	0.0149	0.0130	-0.0003	-0.0005	-0.0025	8.69
10.	5.	2.36	0.12	20.05	6.05	0.00	0.2104	-0.0036	0.2096	0.0188	0.0228	-0.0003	-0.0006	-0.0035	11.17
10.	6.	2.36	0.12	20.02	8.02	0.00	0.2858	-0.0129	0.2848	0.0274	0.0361	-0.0003	-0.0009	-0.0044	10.38
10.	7.	2.36	0.12	20.01	10.03	0.00	0.3587	-0.0232	0.3572	0.0401	0.0523	-0.0003	-0.0012	-0.0049	8.91
10.	8.	2.36	0.12	19.95	12.00	0.00	0.4446	-0.0313	0.4414	0.0625	0.0716	-0.0009	-0.0020	-0.0038	7.07
10.	9.	2.35	0.12	19.92	14.02	0.00	0.5435	-0.0336	0.5355	0.1002	0.0991	-0.0003	-0.0021	-0.0067	5.35
10.	10.	2.35	0.12	19.93	16.01	0.00	0.6721	-0.0363	0.6560	0.1521	0.1271	-0.0001	-0.0019	-0.0092	4.31
10.	11.	2.35	0.12	19.95	18.06	0.00	0.7824	-0.0391	0.7560	0.2075	0.1633	-0.0002	-0.0021	-0.0099	3.64
10.	12.	2.35	0.12	19.86	20.09	0.00	0.8902	-0.0417	0.8504	0.2692	0.2022	-0.0014	0.0021	-0.0028	3.16
11.	1.	3.70	0.18	50.06	-1.99	0.00	-0.1439	0.0241	-0.1429	0.0291	-0.0146	-0.0002	0.0001	0.0010	-4.91
11.	2.	3.69	0.19	50.11	-0.04	0.00	-0.0467	0.0189	-0.0467	0.0189	-0.0038	-0.0001	0.0000	0.0003	-2.47
11.	3.	3.68	0.18	49.91	2.00	0.00	0.0468	0.0126	0.0464	0.0142	0.0055	0.0000	-0.0002	-0.0009	3.26
11.	4.	3.68	0.18	50.00	4.07	0.00	0.1328	0.0048	0.1321	0.0143	0.0135	-0.0003	-0.0003	-0.0011	9.25
11.	5.	3.68	0.18	49.94	6.07	0.00	0.2115	-0.0044	0.2108	0.0181	0.0228	-0.0003	-0.0004	-0.0016	11.63
11.	6.	3.68	0.19	50.11	8.05	0.00	0.2878	-0.0137	0.2869	0.0270	0.0361	-0.0003	-0.0006	-0.0027	10.62
11.	7.	3.67	0.18	49.88	10.04	0.00	0.3603	-0.0241	0.3589	0.0395	0.0515	-0.0003	-0.0009	-0.0036	9.09
11.	8.	3.67	0.18	49.82	12.01	0.00	0.4425	-0.0337	0.4398	0.0599	0.0700	-0.0006	-0.0011	-0.0034	7.34
11.	9.	3.66	0.18	49.67	14.00	0.00	0.5386	-0.0347	0.5310	0.0976	0.0991	-0.0006	-0.0010	-0.0063	5.44
11.	10.	3.67	0.18	50.05	16.03	0.00	0.6669	-0.0373	0.6513	0.1499	0.1261	-0.0011	-0.0016	-0.0072	4.35
11.	11.	3.66	0.18	49.77	18.01	0.00	0.7790	-0.0405	0.7533	0.2044	0.1617	-0.0004	-0.0014	-0.0072	3.68
11.	12.	3.66	0.18	49.83	20.01	0.00	0.8794	-0.0432	0.8411	0.2629	0.1980	-0.0014	0.0030	0.0003	3.20
12.	1.	4.29	0.22	69.89	-1.99	0.00	-0.1448	0.0244	-0.1438	0.0294	-0.0146	-0.0001	0.0002	0.0013	-4.88
12.	2.	4.29	0.22	69.99	0.09	0.00	-0.0414	0.0187	-0.0414	0.0187	-0.0032	-0.0002	0.0000	0.0006	-2.22
12.	3.	4.28	0.22	69.84	2.02	0.00	0.0482	0.0128	0.0477	0.0144	0.0058	-0.0002	-0.0002	-0.0005	3.30
12.	4.	4.28	0.22	70.05	4.02	0.00	0.1307	0.0052	0.1301	0.0144	0.0136	-0.0004	-0.0003	-0.0009	9.05
12.	5.	4.27	0.22	69.80	6.05	0.00	0.2088	-0.0040	0.2081	0.0181	0.0227	-0.0004	-0.0003	-0.0011	11.47
12.	6.	4.28	0.22	70.05	8.01	0.00	0.2850	-0.0134	0.2841	0.0267	0.0357	-0.0004	-0.0005	-0.0021	10.63
12.	7.	4.27	0.22	69.76	10.06	0.00	0.3597	-0.0242	0.3584	0.0394	0.0514	-0.0003	-0.0008	-0.0031	9.09
12.	8.	4.27	0.22	69.87	12.01	0.00	0.4397	-0.0342	0.4372	0.0588	0.0693	-0.0005	-0.0009	-0.0026	7.44
12.	9.	4.26	0.22	69.75	14.07	0.00	0.5376	-0.0348	0.5299	0.0980	0.0996	-0.0010	-0.0008	-0.0057	5.41
12.	10.	4.27	0.22	70.13	16.07	0.00	0.6643	-0.0376	0.6488	0.1492	0.1265	-0.0014	-0.0014	-0.0060	4.35
12.	11.	4.26	0.22	70.08	18.03	0.00	0.7729	-0.0409	0.7476	0.2023	0.1608	-0.0006	-0.0010	-0.0055	3.70
12.	12.	4.25	0.22	69.73	19.94	0.00	0.8742	-0.0439	0.8367	0.2595	0.1968	-0.0019	0.0039	0.0028	3.22
13.	1.	5.26	0.28	110.30	-2.01	0.00	-0.1458	0.0242	-0.1448	0.0294	-0.0144	0.0000	0.0002	0.0018	-4.93
13.	2.	5.24	0.28	110.04	0.02	0.00	-0.0460	0.0189	-0.0460	0.0189	-0.0039	-0.0003	0.0001	0.0011	-2.44
13.	3.	5.23	0.28	109.87	2.08	0.00	0.0484	0.0125	0.0479	0.0143	0.0059	-0.0003	-0.0001	0.0000	3.35
13.	4.	5.22	0.28	110.09	4.00	0.00	0.1264	0.0053	0.1257	0.0142	0.0131	-0.0006	-0.0002	-0.0002	8.85
13.	5.	5.22	0.28	110.15	6.04	0.00	0.2059	-0.0040	0.2052	0.0178	0.0224	-0.0005	-0.0003	-0.0007	11.50
13.	6.	5.21	0.28	110.03	8.10	0.00	0.2864	-0.0139	0.2855	0.0269	0.0361	-0.0003	-0.0005	-0.0013	10.62
13.	7.	5.20	0.28	110.17	10.07	0.00	0.3577	-0.0245	0.3564	0.0389	0.0509	-0.0002	-0.0006	-0.0023	9.16
13.	8.	5.20	0.28	110.19	12.00	0.00	0.4352	-0.0349	0.4329	0.0571	0.0680	-0.0006	-0.0009	-0.0015	7.59
13.	9.	5.18	0.28	109.88	13.98	0.00	0.5217	-0.0380	0.5155	0.0901	0.0964	-0.0025	-0.0017	-0.0008	5.72
13.	10.	5.18	0.28	110.31	16.11	0.00	0.6430	-0.0391	0.6286	0.1423	0.1266	0.0010	-0.0011	-0.0026	4.42
13.	11.	5.16	0.28	110.04	18.06	0.00	0.7646	-0.0415	0.7398	0.1995	0.1593	-0.0007	0.0005	-0.0025	3.71
13.	12.	5.16	0.28	110.21	20.08	0.00	0.8840	-0.0444	0.8455	0.2643	0.1987	-0.0006	0.0011	-0.0023	3.20
14.	4.	4.32	0.22	70.33	-2.03	0.00	-0.1396	0.0234	-0.1387	0.0284	-0.0148	0.0003	0.0001	-0.0009	-4.88



NASA Langley Research Center 14- by 22-Foot Subsonic Tunnel Test 395

Run	Point	R/10 <sup>6</sup>	M	q	$\alpha$	$\beta$	C <sub>N</sub>	C <sub>A</sub>	C <sub>L</sub>	C <sub>D</sub>	C <sub>m</sub>	C <sub>l</sub>	C <sub>n</sub>	C <sub>y</sub>	L/D
14.	5.	4.32	0.22	70.24	-0.08	0.00	-0.0428	0.0182	-0.0427	0.0182	-0.0042	0.0002	0.0000	-0.0018	-2.34
14.	6.	4.32	0.22	70.15	2.03	0.00	0.0557	0.0115	0.0553	0.0135	0.0058	0.0002	-0.0003	-0.0031	4.11
14.	7.	4.33	0.22	70.14	4.01	0.00	0.1366	0.0040	0.1360	0.0136	0.0132	0.0001	-0.0004	-0.0036	10.02
14.	8.	4.33	0.22	70.10	6.07	0.00	0.2165	-0.0053	0.2159	0.0178	0.0229	0.0001	-0.0003	-0.0042	12.15
14.	9.	4.34	0.22	70.37	8.00	0.00	0.2919	-0.0147	0.2911	0.0264	0.0359	0.0001	-0.0005	-0.0052	11.02
14.	10.	4.33	0.22	70.14	10.01	0.00	0.3659	-0.0252	0.3647	0.0393	0.0515	0.0001	-0.0008	-0.0063	9.28
14.	11.	4.33	0.22	70.19	12.02	0.00	0.4460	-0.0354	0.4436	0.0590	0.0697	-0.0003	-0.0012	-0.0048	7.52
14.	12.	4.33	0.22	69.97	14.09	0.00	0.5443	-0.0388	0.5373	0.0960	0.0979	-0.0020	-0.0025	-0.0035	5.60
14.	13.	4.33	0.22	70.04	16.04	0.00	0.6516	-0.0412	0.6376	0.1419	0.1263	0.0021	-0.0023	-0.0039	4.49
14.	14.	4.33	0.22	69.79	18.04	0.00	0.7679	-0.0425	0.7433	0.1993	0.1607	0.0022	-0.0004	-0.0057	3.73
14.	15.	4.33	0.22	69.97	20.06	0.00	0.8860	-0.0449	0.8477	0.2643	0.1982	-0.0025	0.0050	0.0016	3.21
15.	1.	5.55	0.28	109.90	-2.00	-5.01	-0.1324	0.0234	-0.1315	0.0281	-0.0176	-0.0009	0.0027	0.0072	-4.68
15.	2.	5.57	0.28	110.85	-0.04	-5.01	-0.0397	0.0186	-0.0397	0.0186	-0.0065	-0.0001	0.0025	0.0058	-2.13
15.	3.	5.54	0.28	110.32	2.04	-5.01	0.0545	0.0119	0.0540	0.0139	0.0030	0.0016	0.0022	0.0047	3.90
15.	4.	5.52	0.28	109.64	4.04	-5.01	0.1385	0.0040	0.1379	0.0138	0.0125	0.0031	0.0018	0.0033	9.98
15.	5.	5.52	0.28	109.68	6.02	-5.01	0.2149	-0.0056	0.2143	0.0172	0.0215	0.0055	0.0010	0.0001	12.47
15.	6.	5.53	0.28	110.26	8.00	-5.01	0.2895	-0.0166	0.2889	0.0241	0.0323	0.0100	0.0018	-0.0039	11.97
15.	7.	5.51	0.28	109.56	10.02	-5.01	0.3639	-0.0272	0.3630	0.0370	0.0475	0.0100	0.0017	-0.0036	9.80
15.	8.	5.52	0.28	110.22	12.02	-5.01	0.4425	-0.0367	0.4405	0.0570	0.0655	0.0114	0.0014	-0.0107	7.73
15.	9.	5.52	0.28	110.16	14.01	-5.01	0.5398	-0.0426	0.5341	0.0904	0.0893	0.0127	0.0029	-0.0226	5.91
15.	10.	5.51	0.28	109.87	16.14	-5.01	0.6443	-0.0443	0.6312	0.1381	0.1215	0.0157	0.0002	-0.0266	4.57
15.	11.	5.53	0.28	110.80	18.12	-5.01	0.7484	-0.0432	0.7247	0.1937	0.1581	0.0160	-0.0047	-0.0285	3.74
15.	12.	5.52	0.28	110.22	20.15	-5.01	0.8544	-0.0433	0.8171	0.2560	0.1970	0.0186	-0.0087	-0.0306	3.19
16.	1.	5.52	0.28	110.45	-2.03	5.02	-0.1491	0.0234	-0.1482	0.0287	-0.0194	0.0035	-0.0024	-0.0100	-5.16
16.	2.	5.51	0.28	110.14	-0.01	5.02	-0.0505	0.0188	-0.0505	0.0188	-0.0085	0.0019	-0.0025	-0.0096	-2.69
16.	3.	5.50	0.28	109.94	2.02	5.02	0.0444	0.0129	0.0439	0.0145	0.0007	0.0001	-0.0026	-0.0098	3.03
16.	4.	5.50	0.28	109.61	4.01	5.02	0.1309	0.0052	0.1303	0.0144	0.0101	-0.0013	-0.0026	-0.0106	9.06
16.	5.	5.50	0.28	110.01	6.09	5.02	0.2147	-0.0044	0.2139	0.0186	0.0216	-0.0037	-0.0018	-0.0093	11.51
16.	6.	5.51	0.28	110.25	8.06	5.02	0.2930	-0.0147	0.2921	0.0268	0.0335	-0.0078	-0.0020	-0.0061	10.89
16.	7.	5.50	0.28	109.88	10.02	5.02	0.3666	-0.0249	0.3654	0.0398	0.0480	-0.0087	-0.0024	-0.0069	9.19
16.	8.	5.51	0.28	110.16	12.06	5.02	0.4498	-0.0327	0.4467	0.0627	0.0680	-0.0105	-0.0031	0.0016	7.13
16.	9.	5.51	0.28	110.20	14.02	5.02	0.5436	-0.0390	0.5368	0.0949	0.0914	-0.0109	-0.0038	0.0106	5.66
16.	10.	5.51	0.28	110.10	16.08	5.02	0.6470	-0.0413	0.6331	0.1410	0.1220	-0.0138	-0.0029	0.0109	4.49
16.	11.	5.50	0.28	109.85	17.99	5.02	0.7331	-0.0407	0.7098	0.1896	0.1552	-0.0137	0.0010	0.0123	3.74
16.	12.	5.51	0.28	110.17	20.06	5.02	0.8553	-0.0392	0.8169	0.2590	0.1977	-0.0180	0.0067	0.0149	3.15
17.	2.	4.80	0.22	69.93	-2.00	0.00	-0.0699	0.0235	-0.0690	0.0259	-0.0229	-0.0002	0.0002	0.0007	-2.66
17.	3.	4.79	0.22	69.91	-0.08	0.00	0.0202	0.0185	0.0202	0.0185	-0.0115	0.0000	0.0001	0.0002	1.09
17.	4.	4.79	0.22	69.87	2.03	0.00	0.1149	0.0121	0.1144	0.0162	-0.0021	0.0000	-0.0002	-0.0007	7.07
17.	5.	4.79	0.22	70.09	4.07	0.00	0.1960	0.0040	0.1952	0.0180	0.0060	-0.0001	-0.0002	-0.0011	10.85
17.	6.	4.78	0.22	70.04	6.01	0.00	0.2713	-0.0050	0.2703	0.0237	0.0157	0.0001	-0.0001	-0.0014	11.40
17.	7.	4.77	0.22	69.85	8.04	0.00	0.3517	-0.0151	0.3503	0.0346	0.0294	0.0000	-0.0002	-0.0019	10.11
17.	8.	4.78	0.22	69.97	10.02	0.00	0.4273	-0.0261	0.4253	0.0492	0.0439	0.0000	-0.0004	-0.0025	8.64
17.	9.	4.78	0.22	70.13	12.06	0.00	0.5084	-0.0360	0.5047	0.0720	0.0640	-0.0001	-0.0006	-0.0012	7.01
17.	10.	4.77	0.22	69.76	14.02	0.00	0.6087	-0.0385	0.5999	0.1114	0.0891	-0.0009	-0.0016	0.0002	5.39
17.	11.	4.77	0.22	69.91	16.01	0.00	0.7188	-0.0400	0.7020	0.1616	0.1195	0.0027	-0.0020	0.0015	4.34
17.	12.	4.77	0.22	70.00	18.04	0.00	0.8338	-0.0412	0.8056	0.2214	0.1549	0.0041	-0.0015	-0.0007	3.64
17.	13.	4.77	0.22	69.88	19.99	0.00	0.9640	-0.0430	0.9206	0.2921	0.1893	-0.0010	0.0018	0.0020	3.15
18.	1.	5.92	0.27	110.36	-2.08	0.00	-0.0744	0.0230	-0.0735	0.0257	-0.0233	-0.0001	0.0002	0.0003	-2.86
18.	2.	5.90	0.27	109.96	0.06	0.00	0.0256	0.0175	0.0256	0.0176	-0.0110	0.0000	0.0001	-0.0001	1.46



Run	Point	R/10 <sup>6</sup>	M	q	$\alpha$	$\beta$	C <sub>N</sub>	C <sub>A</sub>	C <sub>L</sub>	C <sub>D</sub>	C <sub>m</sub>	C <sub>i</sub>	C <sub>n</sub>	C <sub>y</sub>	L/D
22.	4.	5.86	0.27	110.26	4.05	0.00	0.2607	0.0030	0.2598	0.0216	-0.0143	-0.0005	-0.0003	-0.0009	12.00
22.	5.	5.85	0.27	110.22	6.02	0.00	0.3347	-0.0064	0.3336	0.0292	-0.0042	-0.0007	-0.0002	-0.0011	11.44
22.	6.	5.84	0.27	109.82	8.02	0.00	0.4052	-0.0164	0.4035	0.0408	0.0123	-0.0004	-0.0003	-0.0012	9.88
22.	7.	5.84	0.27	109.79	10.04	0.00	0.4810	-0.0282	0.4785	0.0569	0.0277	-0.0005	-0.0005	-0.0017	8.41
22.	8.	5.83	0.27	109.73	12.00	0.01	0.5572	-0.0380	0.5530	0.0798	0.0472	-0.0005	-0.0002	-0.0009	6.93
22.	9.	5.84	0.27	110.09	14.02	0.00	0.6574	-0.0401	0.6476	0.1219	0.0738	-0.0009	-0.0004	-0.0013	5.31
22.	10.	5.83	0.27	109.77	16.01	0.00	0.7610	-0.0390	0.7422	0.1744	0.1062	-0.0003	0.0000	-0.0018	4.25
22.	11.	5.83	0.27	109.86	18.01	0.00	0.8904	-0.0395	0.8590	0.2404	0.1398	-0.0009	0.0012	0.0004	3.57
22.	12.	5.83	0.27	110.09	20.03	0.00	1.0029	-0.0407	0.9562	0.3085	0.1795	-0.0023	0.0034	0.0048	3.10
23.	1.	5.82	0.27	109.77	-2.00	5.01	-0.0172	0.0218	-0.0164	0.0224	-0.0457	0.0013	-0.0027	-0.0094	-0.73
23.	2.	5.81	0.27	109.70	0.02	5.01	0.0785	0.0176	0.0785	0.0177	-0.0347	-0.0007	-0.0025	-0.0091	4.44
23.	3.	5.81	0.27	109.89	2.01	5.01	0.1719	0.0115	0.1713	0.0176	-0.0266	-0.0029	-0.0026	-0.0090	9.71
23.	4.	5.81	0.27	109.96	4.03	5.01	0.2564	0.0032	0.2556	0.0214	-0.0168	-0.0048	-0.0025	-0.0099	11.93
23.	5.	5.81	0.27	109.77	6.02	5.01	0.3343	-0.0070	0.3331	0.0286	-0.0045	-0.0083	-0.0017	-0.0089	11.66
23.	6.	5.82	0.27	110.37	7.99	5.01	0.4069	-0.0181	0.4055	0.0393	0.0084	-0.0113	-0.0018	-0.0050	10.32
23.	7.	5.81	0.27	109.95	10.01	5.01	0.4792	-0.0292	0.4769	0.0554	0.0248	-0.0103	-0.0020	-0.0056	8.61
23.	8.	5.81	0.27	110.04	12.05	5.01	0.5626	-0.0374	0.5580	0.0820	0.0450	-0.0119	-0.0032	0.0055	6.81
23.	9.	5.81	0.27	109.73	14.01	5.01	0.6566	-0.0413	0.6471	0.1204	0.0714	-0.0150	-0.0030	0.0144	5.37
23.	10.	5.81	0.27	109.76	16.00	5.01	0.7499	-0.0421	0.7325	0.1683	0.1041	-0.0165	-0.0019	0.0149	4.35
23.	11.	5.81	0.27	109.92	18.01	5.01	0.8460	-0.0395	0.8168	0.2264	0.1408	-0.0168	0.0029	0.0162	3.61
23.	12.	5.81	0.27	109.87	20.04	5.01	0.9651	-0.0388	0.9199	0.2974	0.1805	-0.0214	0.0078	0.0194	3.09
24.	1.	5.80	0.27	110.04	-2.00	-5.01	-0.0045	0.0213	-0.0037	0.0214	-0.0441	0.0004	0.0029	0.0077	-0.17
24.	2.	5.80	0.27	110.07	0.07	-5.01	0.0910	0.0170	0.0910	0.0171	-0.0329	0.0021	0.0026	0.0068	5.32
24.	3.	5.80	0.27	109.93	2.03	-5.01	0.1783	0.0110	0.1778	0.0174	-0.0244	0.0039	0.0025	0.0058	10.21
24.	4.	5.81	0.27	110.25	4.05	-5.01	0.2616	0.0026	0.2608	0.0214	-0.0145	0.0061	0.0020	0.0050	12.20
24.	5.	5.80	0.27	109.76	6.00	-5.01	0.3324	-0.0069	0.3313	0.0282	-0.0050	0.0094	0.0013	0.0022	11.73
24.	6.	5.80	0.27	110.04	8.03	-5.01	0.4031	-0.0176	0.4016	0.0394	0.0085	0.0122	0.0018	-0.0013	10.19
24.	7.	5.80	0.27	109.96	10.02	-5.01	0.4756	-0.0287	0.4733	0.0553	0.0246	0.0116	0.0021	-0.0010	8.55
24.	8.	5.80	0.27	109.98	12.02	-5.01	0.5575	-0.0378	0.5532	0.0803	0.0426	0.0123	0.0026	-0.0100	6.89
24.	9.	5.80	0.27	109.91	14.00	-5.01	0.6514	-0.0412	0.6420	0.1191	0.0692	0.0162	0.0033	-0.0197	5.39
24.	10.	5.80	0.27	109.77	16.00	-5.01	0.7471	-0.0421	0.7298	0.1674	0.1024	0.0178	0.0007	-0.0235	4.36
24.	11.	5.80	0.27	110.09	18.03	-5.01	0.8452	-0.0402	0.8162	0.2258	0.1387	0.0167	-0.0033	-0.0237	3.61
24.	12.	5.80	0.27	110.10	20.06	-5.01	0.9643	-0.0392	0.9192	0.2969	0.1782	0.0214	-0.0077	-0.0252	3.10
25.	2.	4.87	0.22	70.21	-2.06	0.00	0.0267	0.0237	0.0275	0.0228	-0.0500	0.0000	0.0001	0.0010	1.21
25.	3.	4.85	0.22	69.83	0.03	0.00	0.1268	0.0194	0.1268	0.0196	-0.0386	0.0004	0.0001	0.0004	6.48
25.	4.	4.85	0.22	69.95	2.04	0.00	0.2157	0.0140	0.2150	0.0219	-0.0298	0.0005	0.0000	-0.0001	9.83
25.	5.	4.85	0.22	70.37	4.06	0.00	0.2939	0.0059	0.2927	0.0270	-0.0211	0.0003	0.0000	-0.0006	10.85
25.	6.	4.85	0.22	70.33	6.03	0.00	0.3653	-0.0029	0.3636	0.0359	-0.0104	0.0003	0.0001	-0.0009	10.13
25.	7.	4.84	0.22	70.36	8.06	0.00	0.4344	-0.0131	0.4319	0.0486	0.0068	0.0003	-0.0002	-0.0008	8.88
25.	8.	4.83	0.22	70.07	10.10	0.00	0.5118	-0.0254	0.5084	0.0657	0.0221	0.0004	-0.0004	-0.0015	7.74
25.	9.	4.84	0.22	70.23	12.06	0.00	0.5928	-0.0349	0.5870	0.0909	0.0416	0.0002	-0.0004	0.0004	6.46
25.	10.	4.83	0.22	70.17	14.01	0.00	0.6908	-0.0366	0.6791	0.1334	0.0670	-0.0017	-0.0014	0.0029	5.09
25.	11.	4.82	0.22	69.91	16.03	0.00	0.7926	-0.0365	0.7718	0.1860	0.0997	0.0006	-0.0008	0.0073	4.15
25.	12.	4.81	0.22	69.56	18.03	0.00	0.9061	-0.0345	0.8722	0.2504	0.1353	0.0011	0.0026	0.0074	3.48
25.	13.	4.81	0.22	69.59	20.04	0.00	1.0314	-0.0353	0.9810	0.3238	0.1741	-0.0036	0.0084	0.0136	3.03
26.	1.	5.99	0.27	110.21	-2.09	0.00	0.0201	0.0238	0.0210	0.0231	-0.0498	0.0003	0.0001	0.0002	0.91
26.	2.	5.97	0.27	109.74	0.05	0.00	0.1204	0.0193	0.1204	0.0195	-0.0379	0.0006	0.0002	-0.0002	6.18
26.	3.	5.98	0.28	110.44	2.03	0.00	0.2110	0.0139	0.2103	0.0215	-0.0293	0.0009	0.0001	-0.0009	9.78
26.	4.	5.97	0.27	110.16	4.05	0.00	0.2890	0.0057	0.2879	0.0264	-0.0210	0.0007	0.0001	-0.0011	10.92





NASA Langley Research Center 14- by 22-Foot Subsonic Tunnel Test 395

Run	Point	R/10 <sup>6</sup>	M	q	$\alpha$	$\beta$	C <sub>N</sub>	C <sub>A</sub>	C <sub>L</sub>	C <sub>D</sub>	C <sub>m</sub>	C <sub>i</sub>	C <sub>n</sub>	C <sub>y</sub>	L/D
34.	7.	5.80	0.28	110.00	10.03	-5.01	0.4491	0.0018	0.4419	0.0807	0.0702	0.0114	0.0007	-0.0009	5.48
34.	8.	5.80	0.28	110.25	12.06	-5.01	0.5442	0.0013	0.5320	0.1160	0.0959	0.0117	0.0005	-0.0017	4.59
34.	9.	5.80	0.28	110.21	14.07	-5.01	0.6489	0.0004	0.6293	0.1595	0.1218	0.0137	0.0002	-0.0025	3.95
34.	10.	5.80	0.28	110.26	16.05	-5.01	0.7564	-0.0005	0.7271	0.2105	0.1499	0.0167	-0.0013	-0.0048	3.45
34.	11.	5.80	0.28	110.14	18.01	-5.01	0.8612	-0.0014	0.8195	0.2673	0.1794	0.0196	-0.0026	-0.0071	3.07
34.	12.	5.79	0.27	109.81	20.03	-5.01	0.9718	-0.0022	0.9137	0.3339	0.2125	0.0232	-0.0059	-0.0111	2.74
36.	2.	2.49	0.12	19.96	-2.04	0.00	-0.0549	0.0092	-0.0546	0.0111	-0.0057	0.0000	0.0000	0.0005	-4.91
36.	3.	2.49	0.12	19.95	0.04	0.00	0.0221	0.0099	0.0221	0.0099	0.0038	0.0004	0.0000	0.0006	2.22
36.	4.	2.49	0.12	19.96	2.03	0.00	0.0940	0.0096	0.0936	0.0129	0.0134	0.0006	-0.0002	-0.0002	7.24
36.	5.	2.49	0.12	19.93	4.02	0.00	0.1711	0.0090	0.1701	0.0211	0.0235	0.0002	-0.0003	-0.0009	8.07
36.	6.	2.49	0.12	19.91	6.01	0.00	0.2611	0.0086	0.2587	0.0361	0.0382	0.0004	-0.0003	-0.0012	7.17
36.	7.	2.51	0.12	20.26	8.08	0.00	0.3788	0.0075	0.3740	0.0612	0.0569	0.0006	-0.0005	-0.0014	6.11
36.	8.	2.51	0.12	20.30	10.05	0.00	0.4665	0.0069	0.4582	0.0890	0.0763	0.0004	-0.0006	-0.0024	5.15
36.	9.	2.51	0.12	20.29	12.05	0.00	0.5611	0.0066	0.5473	0.1246	0.1023	-0.0005	-0.0006	-0.0023	4.39
36.	10.	2.51	0.12	20.25	14.00	0.00	0.6664	0.0062	0.6451	0.1687	0.1289	-0.0009	-0.0003	-0.0025	3.82
36.	11.	2.51	0.12	20.19	16.00	0.00	0.7742	0.0057	0.7427	0.2210	0.1579	-0.0015	0.0004	-0.0021	3.36
36.	12.	2.51	0.12	20.21	18.02	0.00	0.8886	0.0053	0.8433	0.2826	0.1897	-0.0025	0.0021	-0.0003	2.98
36.	13.	2.51	0.12	20.18	20.02	0.00	1.0014	0.0048	0.9393	0.3505	0.2233	-0.0058	0.0062	0.0057	2.68
37.	1.	3.93	0.18	50.08	-2.07	0.00	-0.0563	0.0080	-0.0560	0.0100	-0.0058	0.0002	0.0000	-0.0001	-5.58
37.	2.	3.93	0.18	50.04	0.06	0.00	0.0219	0.0087	0.0219	0.0087	0.0037	0.0005	0.0000	0.0001	2.50
37.	3.	3.93	0.18	50.06	2.02	0.00	0.0942	0.0082	0.0939	0.0116	0.0134	0.0006	-0.0002	-0.0002	8.10
37.	4.	3.92	0.18	50.02	4.06	0.00	0.1724	0.0074	0.1714	0.0197	0.0231	0.0002	-0.0002	-0.0004	8.71
37.	5.	3.92	0.18	50.06	6.02	0.00	0.2592	0.0067	0.2571	0.0341	0.0374	0.0001	-0.0002	-0.0002	7.54
37.	6.	3.92	0.18	50.06	8.02	0.00	0.3616	0.0057	0.3573	0.0566	0.0537	0.0004	-0.0003	-0.0007	6.32
37.	7.	3.92	0.18	50.06	10.05	0.00	0.4620	0.0051	0.4540	0.0864	0.0747	0.0002	-0.0003	-0.0009	5.25
37.	8.	3.92	0.18	50.08	12.02	0.00	0.5556	0.0049	0.5424	0.1215	0.1008	-0.0004	-0.0003	-0.0007	4.46
37.	9.	3.92	0.18	50.09	14.01	0.00	0.6599	0.0045	0.6392	0.1656	0.1276	-0.0008	-0.0002	-0.0012	3.86
37.	10.	3.91	0.18	49.88	16.09	0.00	0.7728	0.0040	0.7415	0.2200	0.1584	-0.0014	0.0005	-0.0005	3.37
37.	11.	3.91	0.18	49.87	18.06	0.00	0.8849	0.0032	0.8404	0.2799	0.1883	-0.0020	0.0016	0.0009	3.00
37.	12.	3.91	0.18	49.74	20.09	0.00	0.9987	0.0024	0.9371	0.3485	0.2215	-0.0041	0.0049	0.0057	2.69
38.	1.	4.62	0.22	70.07	-2.03	0.00	-0.0555	0.0078	-0.0552	0.0097	-0.0058	0.0001	-0.0001	-0.0004	-5.67
38.	2.	4.61	0.22	69.98	0.08	0.00	0.0220	0.0084	0.0220	0.0084	0.0037	0.0004	-0.0001	-0.0005	2.61
38.	3.	4.61	0.22	70.10	2.08	0.00	0.0955	0.0078	0.0951	0.0113	0.0136	0.0006	-0.0002	-0.0007	8.39
38.	4.	4.60	0.22	69.88	4.02	0.00	0.1692	0.0069	0.1683	0.0188	0.0226	0.0002	-0.0002	-0.0005	8.94
38.	5.	4.60	0.22	69.94	6.04	0.00	0.2581	0.0061	0.2560	0.0335	0.0371	0.0001	-0.0002	-0.0005	7.65
38.	6.	4.61	0.22	70.03	8.09	0.00	0.3632	0.0051	0.3589	0.0566	0.0539	0.0004	-0.0002	-0.0008	6.34
38.	7.	4.61	0.22	70.01	10.06	0.00	0.4598	0.0045	0.4519	0.0855	0.0745	0.0001	-0.0003	-0.0009	5.29
38.	8.	4.61	0.22	70.20	12.00	0.00	0.5505	0.0042	0.5376	0.1196	0.0999	-0.0002	-0.0003	-0.0010	4.50
38.	9.	4.60	0.22	69.94	14.00	0.00	0.6543	0.0035	0.6341	0.1632	0.1263	-0.0007	-0.0002	-0.0008	3.89
38.	10.	4.60	0.22	69.90	16.09	0.00	0.7676	0.0028	0.7368	0.2174	0.1572	-0.0013	0.0005	-0.0001	3.39
38.	11.	4.60	0.22	69.85	18.05	0.00	0.8752	0.0020	0.8315	0.2756	0.1867	-0.0017	0.0015	0.0013	3.02
38.	12.	4.59	0.22	69.58	20.07	0.00	0.9861	0.0013	0.9257	0.3428	0.2200	-0.0037	0.0055	0.0072	2.70
39.	1.	5.73	0.28	110.29	-2.09	0.00	-0.0586	0.0075	-0.0583	0.0096	-0.0061	0.0000	-0.0001	-0.0005	-6.06
39.	2.	5.71	0.28	110.01	0.03	0.00	0.0195	0.0081	0.0195	0.0081	0.0034	0.0005	0.0000	-0.0004	2.40
39.	3.	5.70	0.28	110.05	2.04	0.00	0.0932	0.0075	0.0929	0.0109	0.0132	0.0006	-0.0002	-0.0006	8.53
39.	4.	5.70	0.28	110.21	4.08	0.00	0.1695	0.0065	0.1686	0.0186	0.0227	0.0002	-0.0001	-0.0005	9.06
39.	5.	5.69	0.28	110.00	6.04	0.00	0.2542	0.0055	0.2522	0.0324	0.0361	0.0001	-0.0001	-0.0004	7.78
39.	6.	5.69	0.28	110.10	8.05	0.00	0.3562	0.0044	0.3520	0.0547	0.0531	0.0003	-0.0002	-0.0005	6.43
39.	7.	5.69	0.28	110.16	10.09	0.00	0.4537	0.0037	0.4460	0.0839	0.0740	0.0006	-0.0003	-0.0006	5.32

NASA Langley Research Center 14- by 22-Foot Subsonic Tunnel Test 395

Run	Point	R/10 <sup>6</sup>	M	q	$\alpha$	$\beta$	C <sub>N</sub>	C <sub>A</sub>	C <sub>L</sub>	C <sub>D</sub>	C <sub>m</sub>	C <sub>l</sub>	C <sub>n</sub>	C <sub>y</sub>	L/D
39.	8.	5.69	0.28	110.11	12.08	0.00	0.5470	0.0033	0.5342	0.1187	0.0996	-0.0001	-0.0003	-0.0008	4.50
39.	9.	5.68	0.28	110.00	14.03	0.00	0.6484	0.0026	0.6284	0.1612	0.1260	-0.0008	-0.0001	-0.0006	3.90
39.	10.	5.69	0.28	110.35	16.02	0.00	0.7547	0.0017	0.7250	0.2118	0.1546	-0.0014	0.0005	0.0002	3.42
39.	11.	5.68	0.28	110.09	18.09	0.00	0.8691	0.0011	0.8258	0.2735	0.1856	-0.0016	0.0018	0.0021	3.02
39.	12.	5.68	0.28	110.01	20.07	0.00	0.9786	0.0005	0.9190	0.3394	0.2175	-0.0030	0.0047	0.0064	2.71
40.	1.	5.67	0.28	110.04	-2.01	4.99	-0.0664	0.0075	-0.0661	0.0099	-0.0097	0.0021	-0.0014	-0.0026	-6.70
40.	2.	5.67	0.28	110.04	-0.01	4.99	0.0078	0.0083	0.0078	0.0082	-0.0008	-0.0002	-0.0016	-0.0034	0.95
40.	3.	5.67	0.28	110.17	2.06	4.99	0.0849	0.0077	0.0846	0.0108	0.0082	-0.0021	-0.0019	-0.0038	7.84
40.	4.	5.67	0.28	110.36	4.06	4.99	0.1653	0.0068	0.1644	0.0186	0.0193	-0.0032	-0.0020	-0.0042	8.86
40.	5.	5.67	0.28	110.31	6.08	4.99	0.2570	0.0055	0.2550	0.0329	0.0324	-0.0040	-0.0015	-0.0035	7.75
40.	6.	5.66	0.28	110.14	8.00	4.99	0.3504	0.0043	0.3464	0.0534	0.0485	-0.0067	-0.0014	-0.0031	6.48
40.	7.	5.67	0.28	110.38	10.00	4.99	0.4440	0.0034	0.4367	0.0812	0.0693	-0.0099	-0.0013	-0.0030	5.38
40.	8.	5.67	0.28	110.44	12.05	4.99	0.5396	0.0027	0.5271	0.1164	0.0956	-0.0105	-0.0011	-0.0026	4.53
40.	9.	5.67	0.28	110.51	14.05	4.99	0.6308	0.0023	0.6113	0.1567	0.1230	-0.0110	-0.0006	-0.0020	3.90
40.	10.	5.66	0.28	110.11	16.07	4.99	0.7207	0.0019	0.6920	0.2031	0.1520	-0.0115	0.0007	-0.0005	3.41
40.	11.	5.66	0.28	110.07	18.05	4.99	0.8156	0.0015	0.7750	0.2563	0.1813	-0.0135	0.0031	0.0023	3.02
40.	12.	5.66	0.28	110.08	20.07	4.99	0.9168	0.0013	0.8607	0.3185	0.2125	-0.0156	0.0067	0.0071	2.70
41.	1.	5.64	0.28	109.83	-2.04	-5.00	-0.0592	0.0076	-0.0589	0.0097	-0.0090	0.0007	0.0017	0.0034	-6.09
41.	2.	5.65	0.28	110.14	0.02	-5.00	0.0157	0.0082	0.0157	0.0082	0.0005	0.0025	0.0017	0.0028	1.90
41.	3.	5.66	0.28	110.30	2.06	-5.00	0.0905	0.0077	0.0902	0.0110	0.0101	0.0044	0.0017	0.0026	8.23
41.	4.	5.65	0.28	110.31	4.09	-5.00	0.1712	0.0067	0.1703	0.0190	0.0212	0.0054	0.0017	0.0024	8.95
41.	5.	5.66	0.28	110.47	6.03	-5.00	0.2569	0.0056	0.2549	0.0328	0.0329	0.0058	0.0011	0.0017	7.77
41.	6.	5.66	0.28	110.47	8.02	-5.00	0.3511	0.0047	0.3470	0.0541	0.0502	0.0088	0.0010	0.0009	6.42
41.	7.	5.66	0.28	110.38	10.03	-5.01	0.4479	0.0040	0.4403	0.0826	0.0713	0.0115	0.0009	0.0011	5.33
41.	8.	5.64	0.28	109.80	12.09	-5.01	0.5433	0.0034	0.5305	0.1181	0.0972	0.0119	0.0009	0.0009	4.49
41.	9.	5.65	0.28	109.99	13.99	-5.00	0.6405	0.0027	0.6209	0.1589	0.1226	0.0135	0.0004	0.0002	3.91
41.	10.	5.65	0.28	110.05	16.06	-5.01	0.7550	0.0021	0.7250	0.2128	0.1518	0.0171	-0.0008	-0.0012	3.41
41.	11.	5.64	0.27	109.66	18.07	-5.01	0.8630	0.0013	0.8200	0.2715	0.1822	0.0204	-0.0028	-0.0038	3.02
41.	12.	5.65	0.28	110.13	20.03	-5.01	0.9682	0.0007	0.9094	0.3353	0.2138	0.0240	-0.0059	-0.0073	2.71
42.	3.	4.62	0.22	70.19	-2.03	0.04	0.1087	0.0171	0.1092	0.0133	-0.0432	-0.0006	0.0000	0.0002	8.23
42.	4.	4.61	0.22	70.04	0.05	0.04	0.1842	0.0171	0.1842	0.0174	-0.0342	-0.0003	0.0000	0.0005	10.57
42.	5.	4.61	0.22	69.94	2.07	0.04	0.2577	0.0164	0.2570	0.0259	-0.0234	-0.0005	-0.0001	0.0001	9.93
42.	6.	4.61	0.22	69.86	4.07	0.04	0.3306	0.0150	0.3287	0.0388	-0.0111	-0.0010	0.0000	0.0002	8.47
42.	7.	4.62	0.22	70.08	6.08	0.04	0.4152	0.0143	0.4114	0.0588	0.0050	-0.0008	-0.0001	0.0000	7.00
42.	8.	4.61	0.22	69.99	8.02	0.04	0.5033	0.0136	0.4964	0.0845	0.0248	-0.0002	-0.0002	-0.0001	5.87
42.	9.	4.62	0.22	70.04	10.02	0.04	0.5909	0.0135	0.5796	0.1174	0.0494	-0.0004	-0.0003	-0.0003	4.94
42.	10.	4.62	0.22	70.11	12.05	0.04	0.6835	0.0147	0.6654	0.1586	0.0777	-0.0007	-0.0003	-0.0005	4.19
42.	11.	4.61	0.22	69.70	14.09	0.04	0.7911	0.0156	0.7635	0.2098	0.1052	-0.0014	-0.0001	-0.0009	3.64
42.	12.	4.60	0.22	69.61	16.01	0.04	0.8942	0.0162	0.8551	0.2649	0.1335	-0.0017	0.0005	-0.0003	3.23
42.	13.	4.60	0.22	69.38	18.08	0.04	1.0112	0.0167	0.9561	0.3329	0.1648	-0.0026	0.0018	0.0011	2.87
42.	14.	4.60	0.22	69.48	20.04	0.04	1.1199	0.0168	1.0463	0.4034	0.1973	-0.0046	0.0056	0.0061	2.59
43.	1.	5.74	0.28	109.77	-2.08	0.04	0.1020	0.0162	0.1025	0.0126	-0.0430	-0.0003	0.0000	-0.0003	8.16
43.	2.	5.74	0.28	110.46	0.03	0.04	0.1792	0.0163	0.1792	0.0165	-0.0337	0.0001	0.0000	-0.0001	10.85
43.	3.	5.71	0.28	109.78	2.08	0.04	0.2529	0.0153	0.2522	0.0247	-0.0229	0.0001	-0.0002	-0.0006	10.21
43.	4.	5.71	0.28	109.80	4.07	0.04	0.3254	0.0139	0.3236	0.0373	-0.0110	-0.0005	-0.0001	-0.0004	8.67
43.	5.	5.72	0.28	110.12	6.02	0.04	0.4038	0.0129	0.4002	0.0558	0.0041	-0.0009	0.0000	-0.0005	7.18
43.	6.	5.71	0.28	110.14	8.04	0.04	0.4978	0.0120	0.4912	0.0823	0.0245	0.0002	-0.0002	-0.0004	5.96
43.	7.	5.71	0.28	110.08	10.06	0.04	0.5863	0.0118	0.5752	0.1152	0.0493	0.0003	-0.0003	-0.0006	4.99
43.	8.	5.71	0.28	110.08	12.04	0.04	0.6745	0.0127	0.6571	0.1547	0.0764	-0.0004	-0.0004	-0.0005	4.25

NASA Langley Research Center 14- by 22-Foot Subsonic Tunnel Test 395

Run	Point	R/10 <sup>6</sup>	M	q	$\alpha$	$\beta$	C <sub>N</sub>	C <sub>A</sub>	C <sub>L</sub>	C <sub>D</sub>	C <sub>m</sub>	C <sub>l</sub>	C <sub>n</sub>	C <sub>y</sub>	L/D
43.	9.	5.71	0.28	110.35	14.07	0.04	0.7801	0.0133	0.7534	0.2046	0.1037	-0.0012	-0.0001	-0.0004	3.68
43.	10.	5.71	0.28	110.28	16.07	0.04	0.8870	0.0139	0.8485	0.2614	0.1329	-0.0014	0.0004	-0.0001	3.25
43.	11.	5.70	0.28	109.85	18.03	0.04	0.9946	0.0140	0.9415	0.3243	0.1625	-0.0024	0.0023	0.0022	2.90
43.	12.	5.70	0.27	109.91	20.03	0.04	1.1035	0.0143	1.0318	0.3953	0.1937	-0.0035	0.0042	0.0048	2.61
44.	1.	5.70	0.28	109.99	-2.02	5.00	0.0925	0.0162	0.0930	0.0130	-0.0456	-0.0023	-0.0008	-0.0047	7.15
44.	2.	5.79	0.28	114.06	-0.05	5.00	0.1602	0.0160	0.1602	0.0159	-0.0366	-0.0045	-0.0011	-0.0052	10.05
44.	3.	5.70	0.28	110.39	2.09	5.00	0.2440	0.0152	0.2432	0.0243	-0.0274	-0.0067	-0.0015	-0.0060	10.02
44.	4.	5.69	0.28	109.67	4.02	5.00	0.3192	0.0138	0.3174	0.0366	-0.0144	-0.0077	-0.0016	-0.0065	8.68
44.	5.	5.69	0.28	109.86	6.02	5.00	0.4039	0.0125	0.4003	0.0554	0.0004	-0.0069	-0.0012	-0.0054	7.23
44.	6.	5.70	0.28	110.22	8.02	5.00	0.4919	0.0120	0.4855	0.0813	0.0211	-0.0098	-0.0012	-0.0044	5.97
44.	7.	5.72	0.28	110.82	10.03	5.00	0.5780	0.0119	0.5670	0.1135	0.0452	-0.0124	-0.0014	-0.0040	5.00
44.	8.	5.70	0.28	110.15	12.06	5.00	0.6668	0.0123	0.6495	0.1528	0.0730	-0.0138	-0.0012	-0.0037	4.25
44.	9.	5.69	0.28	109.80	14.08	5.00	0.7612	0.0128	0.7352	0.1996	0.1019	-0.0142	-0.0004	-0.0030	3.68
44.	10.	5.71	0.28	110.23	16.01	5.00	0.8444	0.0131	0.8080	0.2478	0.1296	-0.0145	0.0008	-0.0019	3.26
44.	11.	5.70	0.28	110.02	18.04	5.00	0.9376	0.0131	0.8875	0.3056	0.1601	-0.0161	0.0032	0.0005	2.90
44.	12.	5.71	0.28	110.04	20.07	5.00	1.0411	0.0139	0.9731	0.3737	0.1925	-0.0174	0.0069	0.0047	2.60
45.	1.	5.70	0.28	110.15	-2.03	-5.02	0.0981	0.0162	0.0986	0.0128	-0.0454	0.0048	0.0015	0.0034	7.71
45.	2.	5.70	0.28	110.26	0.03	-5.02	0.1718	0.0163	0.1718	0.0165	-0.0362	0.0068	0.0014	0.0032	10.40
45.	3.	5.70	0.28	110.27	2.05	-5.02	0.2478	0.0154	0.2471	0.0244	-0.0258	0.0085	0.0013	0.0032	10.11
45.	4.	5.70	0.28	110.13	4.09	-5.02	0.3255	0.0140	0.3236	0.0376	-0.0125	0.0093	0.0012	0.0030	8.62
45.	5.	5.70	0.28	110.28	5.99	-5.02	0.4040	0.0129	0.4005	0.0556	0.0018	0.0082	0.0008	0.0019	7.20
45.	6.	5.70	0.28	110.27	8.09	-5.02	0.4958	0.0125	0.4891	0.0830	0.0232	0.0113	0.0006	0.0011	5.90
45.	7.	5.70	0.28	110.19	10.05	-5.02	0.5806	0.0128	0.5694	0.1151	0.0474	0.0131	0.0007	0.0007	4.95
45.	8.	5.71	0.28	110.52	12.03	-5.02	0.6690	0.0132	0.6515	0.1539	0.0744	0.0140	0.0005	0.0006	4.23
45.	9.	5.71	0.28	110.22	14.02	-5.02	0.7640	0.0134	0.7380	0.2001	0.1020	0.0150	0.0000	0.0005	3.69
45.	10.	5.70	0.28	109.99	16.08	-5.02	0.8562	0.0136	0.8190	0.2527	0.1324	0.0150	-0.0014	-0.0014	3.24
45.	11.	5.70	0.27	109.84	18.06	-5.02	0.9492	0.0140	0.8981	0.3105	0.1618	0.0158	-0.0030	-0.0034	2.89
45.	12.	5.71	0.28	110.48	20.08	-5.02	1.0477	0.0144	0.9791	0.3766	0.1937	0.0175	-0.0065	-0.0078	2.60
46.	2.	2.48	0.12	19.98	-2.04	0.03	-0.0589	0.0099	-0.0585	0.0120	-0.0121	0.0001	0.0001	0.0001	-4.89
46.	3.	2.48	0.12	20.05	0.02	0.03	0.0194	0.0111	0.0194	0.0111	0.0053	0.0006	0.0000	-0.0003	1.74
46.	4.	2.48	0.12	20.06	2.00	0.03	0.0964	0.0114	0.0959	0.0147	0.0240	0.0008	-0.0003	-0.0012	6.50
46.	5.	2.48	0.12	20.03	4.02	0.03	0.1787	0.0114	0.1774	0.0240	0.0437	0.0003	-0.0003	-0.0016	7.38
46.	6.	2.48	0.12	20.14	6.09	0.03	0.2790	0.0113	0.2763	0.0411	0.0716	0.0003	-0.0005	-0.0014	6.72
46.	7.	2.48	0.12	20.00	8.04	0.03	0.3825	0.0105	0.3772	0.0644	0.1018	0.0010	-0.0007	-0.0029	5.86
46.	8.	2.48	0.12	20.07	10.07	0.03	0.4890	0.0105	0.4797	0.0967	0.1361	0.0008	-0.0009	-0.0036	4.96
46.	9.	2.48	0.12	20.08	12.03	0.03	0.5968	0.0100	0.5816	0.1354	0.1734	0.0003	-0.0009	-0.0041	4.30
46.	10.	2.48	0.12	20.10	14.02	0.03	0.7108	0.0099	0.6872	0.1835	0.2153	0.0002	-0.0007	-0.0042	3.74
46.	11.	2.48	0.12	20.03	16.00	0.03	0.8321	0.0098	0.7972	0.2411	0.2605	-0.0009	0.0001	-0.0030	3.31
46.	12.	2.48	0.12	20.03	18.06	0.03	0.9604	0.0091	0.9103	0.3095	0.3075	-0.0012	0.0015	-0.0015	2.94
46.	13.	2.47	0.12	19.99	20.03	0.03	1.0794	0.0082	1.0113	0.3811	0.3558	-0.0020	0.0050	0.0029	2.65
47.	1.	3.89	0.18	49.99	-2.02	0.03	-0.0579	0.0085	-0.0576	0.0105	-0.0121	0.0002	0.0000	0.0002	-5.46
47.	2.	3.88	0.18	50.02	0.00	0.03	0.0197	0.0094	0.0197	0.0094	0.0052	0.0006	0.0000	0.0001	2.10
47.	3.	3.88	0.18	50.01	2.03	0.03	0.0975	0.0095	0.0971	0.0130	0.0242	0.0008	-0.0002	-0.0002	7.48
47.	4.	3.88	0.18	50.02	4.06	0.03	0.1789	0.0093	0.1778	0.0221	0.0439	0.0003	-0.0002	-0.0004	8.05
47.	5.	3.88	0.18	50.02	6.08	0.03	0.2750	0.0091	0.2724	0.0385	0.0704	0.0002	-0.0003	-0.0008	7.08
47.	6.	3.88	0.18	50.06	8.01	0.03	0.3770	0.0089	0.3721	0.0618	0.1007	0.0008	-0.0005	-0.0014	6.02
47.	7.	3.88	0.18	50.11	10.07	0.03	0.4846	0.0085	0.4757	0.0939	0.1356	0.0007	-0.0005	-0.0018	5.06
47.	8.	3.88	0.18	50.24	12.07	0.03	0.5934	0.0082	0.5785	0.1333	0.1733	0.0002	-0.0005	-0.0016	4.34
47.	9.	3.87	0.18	49.94	14.01	0.03	0.7044	0.0081	0.6815	0.1800	0.2142	-0.0001	-0.0003	-0.0010	3.79



NASA Langley Research Center 14- by 22-Foot Subsonic Tunnel Test 395

Run	Point	R/10 <sup>6</sup>	M	q	$\alpha$	$\beta$	C <sub>N</sub>	C <sub>A</sub>	C <sub>L</sub>	C <sub>D</sub>	C <sub>m</sub>	C <sub>l</sub>	C <sub>n</sub>	C <sub>y</sub>	L/D
47.	10.	3.88	0.18	50.26	16.02	0.03	0.8216	0.0078	0.7875	0.2366	0.2577	-0.0006	0.0003	-0.0001	3.33
47.	11.	3.87	0.18	50.06	18.20	0.03	0.9622	0.0069	0.9119	0.3101	0.3087	-0.0009	0.0018	0.0015	2.94
47.	12.	3.87	0.18	50.06	20.10	0.03	1.0856	0.0067	1.0172	0.3832	0.3553	-0.0026	0.0053	0.0058	2.65
48.	1.	4.55	0.22	70.09	-2.04	0.03	-0.0589	0.0086	-0.0585	0.0107	-0.0123	0.0002	0.0000	0.0001	-5.46
48.	2.	4.54	0.22	69.96	0.08	0.03	0.0227	0.0094	0.0227	0.0095	0.0060	0.0005	0.0000	0.0000	2.39
48.	3.	4.55	0.22	70.44	2.03	0.03	0.0970	0.0094	0.0967	0.0128	0.0245	0.0007	-0.0001	-0.0004	7.54
48.	4.	4.55	0.22	70.34	4.03	0.03	0.1789	0.0092	0.1779	0.0218	0.0446	0.0004	-0.0001	-0.0004	8.15
48.	5.	4.55	0.22	70.46	6.08	0.03	0.2738	0.0088	0.2713	0.0380	0.0702	0.0001	-0.0003	-0.0008	7.13
48.	6.	4.56	0.22	70.55	8.02	0.03	0.3738	0.0084	0.3690	0.0610	0.1008	0.0007	-0.0004	-0.0012	6.05
48.	7.	4.53	0.22	69.77	10.06	0.03	0.4820	0.0080	0.4732	0.0929	0.1356	0.0006	-0.0004	-0.0012	5.09
48.	8.	4.53	0.22	69.68	12.07	0.03	0.5921	0.0077	0.5774	0.1326	0.1733	0.0003	-0.0004	-0.0008	4.35
48.	9.	4.52	0.22	69.50	14.03	0.03	0.7024	0.0077	0.6795	0.1794	0.2140	0.0000	-0.0002	-0.0005	3.79
48.	10.	4.52	0.22	69.38	16.04	0.03	0.8221	0.0073	0.7881	0.2364	0.2581	-0.0005	0.0004	-0.0001	3.33
48.	11.	4.51	0.22	69.22	18.05	0.03	0.9491	0.0066	0.9003	0.3033	0.3038	-0.0005	0.0015	0.0011	2.97
48.	12.	4.50	0.22	68.97	20.08	0.03	1.0785	0.0061	1.0109	0.3796	0.3526	-0.0023	0.0051	0.0056	2.66
49.	1.	5.62	0.28	109.93	-2.03	0.03	-0.0591	0.0084	-0.0588	0.0105	-0.0122	0.0001	0.0000	0.0002	-5.58
49.	2.	5.60	0.28	109.55	-0.03	0.03	0.0171	0.0091	0.0171	0.0091	0.0048	0.0005	0.0001	0.0002	1.88
49.	3.	5.60	0.28	109.56	2.07	0.03	0.0984	0.0090	0.0980	0.0126	0.0251	0.0007	-0.0001	-0.0003	7.78
49.	4.	5.58	0.28	109.19	4.08	0.03	0.1789	0.0086	0.1779	0.0214	0.0450	0.0004	-0.0001	-0.0003	8.32
49.	5.	5.58	0.28	109.19	6.04	0.03	0.2678	0.0082	0.2654	0.0366	0.0685	0.0000	-0.0002	-0.0009	7.26
49.	6.	5.58	0.28	109.26	8.01	0.03	0.3698	0.0079	0.3651	0.0598	0.1002	0.0006	-0.0003	-0.0008	6.11
49.	7.	5.60	0.28	110.53	10.06	0.03	0.4757	0.0075	0.4671	0.0913	0.1346	0.0007	-0.0004	-0.0006	5.12
49.	8.	5.59	0.28	109.83	12.04	0.03	0.5844	0.0069	0.5701	0.1298	0.1717	0.0005	-0.0003	-0.0007	4.39
49.	9.	5.59	0.28	110.16	14.10	0.03	0.6986	0.0068	0.6759	0.1784	0.2135	0.0003	-0.0001	-0.0005	3.79
49.	10.	5.58	0.28	109.90	16.07	0.03	0.8173	0.0061	0.7837	0.2343	0.2572	-0.0003	0.0004	-0.0004	3.34
50.	1.	5.60	0.28	110.90	-2.04	5.03	-0.0715	0.0088	-0.0712	0.0113	-0.0185	0.0028	-0.0014	-0.0024	-6.29
50.	2.	5.59	0.28	111.01	-0.07	5.02	0.0042	0.0093	0.0043	0.0093	-0.0011	0.0001	-0.0016	-0.0032	0.46
50.	3.	5.58	0.28	110.47	2.06	5.02	0.0885	0.0094	0.0881	0.0126	0.0180	-0.0024	-0.0019	-0.0037	7.01
50.	4.	5.56	0.28	109.85	4.03	5.02	0.1734	0.0089	0.1723	0.0211	0.0400	-0.0043	-0.0022	-0.0045	8.15
50.	5.	5.56	0.28	109.66	6.02	5.02	0.2692	0.0084	0.2669	0.0368	0.0657	-0.0055	-0.0020	-0.0048	7.25
50.	6.	5.57	0.28	110.03	8.08	5.02	0.3724	0.0079	0.3676	0.0606	0.0965	-0.0093	-0.0018	-0.0041	6.07
50.	7.	5.57	0.28	110.23	10.08	5.02	0.4741	0.0074	0.4655	0.0910	0.1301	-0.0121	-0.0019	-0.0039	5.11
50.	8.	5.58	0.28	110.55	12.07	5.02	0.5829	0.0068	0.5686	0.1298	0.1672	-0.0148	-0.0018	-0.0038	4.38
50.	9.	5.57	0.28	110.28	14.02	5.02	0.6930	0.0061	0.6709	0.1754	0.2059	-0.0172	-0.0012	-0.0030	3.83
50.	10.	5.57	0.28	110.35	15.07	5.02	0.7535	0.0060	0.7260	0.2036	0.2283	-0.0182	-0.0006	-0.0023	3.57
51.	1.	5.57	0.28	110.53	-2.04	-5.02	-0.0592	0.0088	-0.0588	0.0109	-0.0156	0.0005	0.0018	0.0036	-5.37
51.	2.	5.56	0.28	110.35	0.06	-5.02	0.0195	0.0095	0.0195	0.0095	0.0025	0.0028	0.0017	0.0034	2.05
51.	3.	5.56	0.28	110.29	2.09	-5.02	0.0985	0.0095	0.0981	0.0131	0.0216	0.0053	0.0017	0.0031	7.50
51.	4.	5.56	0.28	110.44	4.03	-5.02	0.1796	0.0090	0.1785	0.0217	0.0427	0.0067	0.0017	0.0031	8.21
51.	5.	5.56	0.28	110.46	6.01	-5.02	0.2696	0.0086	0.2672	0.0371	0.0664	0.0079	0.0014	0.0029	7.21
51.	6.	5.54	0.28	109.86	8.07	-5.02	0.3712	0.0083	0.3664	0.0608	0.0972	0.0117	0.0014	0.0032	6.03
51.	7.	5.56	0.28	110.35	10.06	-5.02	0.4751	0.0078	0.4664	0.0915	0.1303	0.0145	0.0016	0.0037	5.10
51.	8.	5.56	0.28	110.31	12.05	-5.02	0.5838	0.0075	0.5694	0.1304	0.1675	0.0166	0.0015	0.0034	4.37
51.	9.	5.55	0.28	110.31	14.11	-5.02	0.7015	0.0070	0.6786	0.1796	0.2086	0.0188	0.0012	0.0028	3.78
51.	10.	5.55	0.28	110.07	15.04	-5.02	0.7572	0.0065	0.7295	0.2047	0.2287	0.0197	0.0008	0.0022	3.56
52.	2.	4.57	0.22	69.95	-1.96	-0.06	0.1623	0.0232	0.1630	0.0177	-0.0527	-0.0002	0.0002	-0.0004	9.20
52.	3.	4.56	0.22	69.88	0.08	-0.06	0.2412	0.0235	0.2412	0.0240	-0.0361	0.0001	0.0000	-0.0003	10.05

NASA Langley Research Center 14- by 22-Foot Subsonic Tunnel Test 395

Run	Point	R/10 <sup>6</sup>	M	q	$\alpha$	$\beta$	C <sub>N</sub>	C <sub>A</sub>	C <sub>L</sub>	C <sub>D</sub>	C <sub>m</sub>	C <sub>l</sub>	C <sub>n</sub>	C <sub>y</sub>	L/D
52.	4.	4.55	0.22	69.81	2.04	-0.07	0.3175	0.0232	0.3165	0.0349	-0.0151	-0.0001	-0.0001	-0.0008	9.07
52.	5.	4.55	0.22	69.90	4.01	-0.07	0.3952	0.0231	0.3927	0.0512	0.0066	-0.0007	-0.0001	-0.0008	7.67
52.	6.	4.55	0.22	69.99	5.96	-0.07	0.4822	0.0231	0.4772	0.0739	0.0335	-0.0002	-0.0002	-0.0014	6.46
52.	7.	4.55	0.22	70.09	8.08	-0.07	0.5870	0.0234	0.5779	0.1068	0.0719	0.0001	-0.0004	-0.0016	5.41
52.	8.	4.55	0.22	70.17	10.01	-0.07	0.6875	0.0240	0.6728	0.1447	0.1069	0.0001	-0.0004	-0.0018	4.65
52.	9.	4.54	0.22	70.04	12.06	-0.07	0.7982	0.0254	0.7753	0.1938	0.1474	0.0000	-0.0003	-0.0016	4.00
52.	10.	4.54	0.22	69.87	14.05	-0.07	0.9124	0.0269	0.8785	0.2504	0.1894	-0.0004	0.0000	-0.0014	3.51
52.	11.	4.53	0.22	69.89	16.00	-0.07	1.0265	0.0278	0.9790	0.3132	0.2333	-0.0011	0.0009	-0.0004	3.13
52.	12.	4.53	0.22	69.97	17.98	-0.07	1.1467	0.0292	1.0817	0.3860	0.2794	-0.0016	0.0025	0.0021	2.80
52.	13.	4.53	0.22	69.78	19.98	-0.07	1.2762	0.0299	1.1892	0.4693	0.3292	-0.0032	0.0063	0.0069	2.53
53.	1.	5.60	0.28	109.82	-2.01	-0.06	0.1557	0.0224	0.1563	0.0170	-0.0528	-0.0003	0.0001	-0.0005	9.21
53.	2.	5.59	0.28	109.40	-0.01	-0.07	0.2330	0.0225	0.2330	0.0227	-0.0365	-0.0001	0.0001	-0.0004	10.28
53.	3.	5.57	0.28	109.07	1.98	-0.07	0.3089	0.0220	0.3080	0.0330	-0.0156	-0.0002	-0.0001	-0.0007	9.33
53.	4.	5.58	0.28	109.70	4.05	-0.07	0.3910	0.0215	0.3885	0.0496	0.0077	-0.0008	0.0000	-0.0008	7.83
53.	5.	5.58	0.28	109.67	6.02	-0.07	0.4768	0.0212	0.4719	0.0719	0.0339	-0.0003	-0.0002	-0.0013	6.56
53.	6.	5.59	0.28	110.55	8.04	-0.07	0.5743	0.0214	0.5656	0.1027	0.0698	0.0001	-0.0002	-0.0015	5.51
53.	7.	5.58	0.28	110.00	10.07	-0.07	0.6817	0.0217	0.6674	0.1423	0.1073	0.0004	-0.0002	-0.0018	4.69
53.	8.	5.57	0.28	110.07	11.98	-0.07	0.7839	0.0227	0.7621	0.1870	0.1443	0.0003	0.0000	-0.0021	4.08
53.	9.	5.56	0.28	109.84	14.03	-0.07	0.8999	0.0242	0.8672	0.2443	0.1872	-0.0001	0.0004	-0.0018	3.55
53.	10.	5.56	0.28	110.02	16.02	-0.07	1.0132	0.0255	0.9668	0.3074	0.2310	-0.0011	0.0012	-0.0006	3.14
54.	1.	5.55	0.28	110.00	-2.03	5.00	0.1414	0.0219	0.1421	0.0170	-0.0584	-0.0030	-0.0009	-0.0047	8.36
54.	2.	5.54	0.28	109.80	-0.03	5.00	0.2183	0.0222	0.2183	0.0223	-0.0420	-0.0060	-0.0012	-0.0055	9.79
54.	3.	5.55	0.28	110.22	2.05	5.00	0.3016	0.0220	0.3006	0.0331	-0.0213	-0.0085	-0.0013	-0.0061	9.09
54.	4.	5.54	0.28	109.78	3.97	5.00	0.3831	0.0215	0.3807	0.0485	0.0022	-0.0090	-0.0017	-0.0067	7.85
54.	5.	5.55	0.28	110.36	6.06	5.00	0.4751	0.0210	0.4702	0.0719	0.0328	-0.0100	-0.0014	-0.0071	6.54
54.	6.	5.55	0.28	110.36	8.05	5.00	0.5710	0.0214	0.5623	0.1024	0.0661	-0.0126	-0.0013	-0.0061	5.49
54.	7.	5.53	0.28	109.94	10.00	5.00	0.6671	0.0219	0.6532	0.1390	0.1018	-0.0144	-0.0015	-0.0062	4.70
54.	8.	5.53	0.28	110.09	12.05	5.00	0.7698	0.0222	0.7482	0.1844	0.1410	-0.0168	-0.0015	-0.0074	4.06
54.	9.	5.53	0.28	109.96	14.06	5.00	0.8700	0.0237	0.8382	0.2369	0.1818	-0.0180	-0.0007	-0.0068	3.54
54.	10.	5.53	0.28	109.99	15.97	5.00	0.9686	0.0244	0.9245	0.2929	0.2218	-0.0189	0.0002	-0.0061	3.16
54.	11.	5.52	0.28	109.89	17.02	5.00	1.0269	0.0246	0.9747	0.3276	0.2453	-0.0195	0.0014	-0.0051	2.98
55.	1.	5.50	0.28	109.70	-1.97	-5.00	0.1523	0.0221	0.1529	0.0170	-0.0553	0.0049	0.0012	0.0038	9.02
55.	2.	5.51	0.28	110.29	0.08	-5.00	0.2294	0.0224	0.2294	0.0229	-0.0381	0.0073	0.0012	0.0036	10.03
55.	3.	5.51	0.28	110.26	1.94	-5.00	0.3033	0.0222	0.3024	0.0328	-0.0187	0.0089	0.0012	0.0034	9.23
55.	4.	5.50	0.28	109.83	3.99	-5.00	0.3871	0.0217	0.3846	0.0491	0.0069	0.0096	0.0013	0.0032	7.83
55.	5.	5.51	0.28	110.07	6.04	-5.00	0.4769	0.0214	0.4720	0.0723	0.0346	0.0108	0.0009	0.0031	6.53
55.	6.	5.50	0.28	109.69	8.06	-5.00	0.5718	0.0217	0.5631	0.1028	0.0665	0.0139	0.0010	0.0029	5.48
55.	7.	5.51	0.28	110.36	10.02	-5.00	0.6664	0.0221	0.6524	0.1393	0.1024	0.0151	0.0013	0.0035	4.68
55.	8.	5.50	0.28	110.08	12.04	-5.00	0.7675	0.0227	0.7459	0.1842	0.1414	0.0168	0.0015	0.0040	4.05
55.	9.	5.50	0.28	110.02	14.07	-5.00	0.8726	0.0237	0.8406	0.2377	0.1822	0.0178	0.0011	0.0039	3.54
55.	10.	5.50	0.28	109.91	16.03	-5.00	0.9759	0.0250	0.9311	0.2966	0.2230	0.0185	0.0005	0.0037	3.14
56.	2.	4.38	0.22	69.95	-2.02	0.00	0.1137	0.0341	0.1148	0.0301	-0.0838	0.0002	0.0005	0.0008	3.82
56.	3.	4.37	0.22	69.96	0.05	0.00	0.2064	0.0293	0.2063	0.0296	-0.0623	0.0007	0.0004	0.0001	6.97
56.	4.	4.37	0.22	69.89	2.07	0.00	0.2952	0.0243	0.2941	0.0353	-0.0439	0.0003	0.0001	-0.0013	8.34
56.	5.	4.37	0.22	70.21	4.01	0.00	0.3736	0.0197	0.3713	0.0463	-0.0312	-0.0003	0.0003	-0.0012	8.03
56.	6.	4.37	0.22	70.09	6.03	0.00	0.4444	0.0152	0.4404	0.0626	-0.0138	-0.0001	0.0001	-0.0012	7.04
56.	7.	4.36	0.22	69.88	8.03	0.00	0.5109	0.0093	0.5046	0.0815	0.0098	0.0001	-0.0002	-0.0010	6.19
56.	8.	4.36	0.22	70.18	10.04	0.00	0.5828	0.0027	0.5734	0.1055	0.0317	0.0001	-0.0002	-0.0009	5.44
56.	9.	4.36	0.22	70.11	12.06	0.00	0.6426	-0.0031	0.6291	0.1327	0.0566	0.0001	0.0002	-0.0015	4.74

NASA Langley Research Center 14- by 22-Foot Subsonic Tunnel Test 395

Run	Point	R/10 <sup>6</sup>	M	q	$\alpha$	$\beta$	C <sub>N</sub>	C <sub>A</sub>	C <sub>L</sub>	C <sub>D</sub>	C <sub>m</sub>	C <sub>i</sub>	C <sub>n</sub>	C <sub>y</sub>	L/D
56.	10.	4.36	0.22	70.20	14.05	0.00	0.7101	-0.0102	0.6913	0.1643	0.0816	0.0003	0.0010	-0.0010	4.21
56.	11.	4.35	0.22	69.93	16.00	0.00	0.7956	-0.0192	0.7701	0.2030	0.1086	0.0012	0.0031	0.0006	3.79
56.	12.	4.35	0.22	70.04	18.07	0.00	0.8775	-0.0289	0.8432	0.2474	0.1459	0.0027	0.0063	0.0073	3.41
56.	13.	4.34	0.22	69.87	20.00	0.00	0.9605	-0.0360	0.9149	0.2977	0.1817	0.0020	0.0117	0.0161	3.07
57.	1.	5.37	0.28	109.81	-2.00	0.00	0.1105	0.0345	0.1116	0.0307	-0.0835	0.0000	0.0003	0.0003	3.63
57.	2.	5.37	0.28	109.97	0.03	0.00	0.2008	0.0295	0.2008	0.0298	-0.0624	0.0007	0.0003	-0.0002	6.74
57.	3.	5.36	0.28	109.64	1.99	0.00	0.2859	0.0244	0.2848	0.0346	-0.0443	0.0005	0.0002	-0.0011	8.24
57.	4.	5.36	0.28	109.74	4.07	0.00	0.3701	0.0190	0.3678	0.0457	-0.0304	-0.0003	0.0003	-0.0010	8.05
57.	5.	5.36	0.28	110.18	6.10	0.00	0.4407	0.0144	0.4367	0.0618	-0.0135	0.0001	0.0002	-0.0009	7.07
57.	6.	5.36	0.28	110.03	8.06	0.00	0.5064	0.0084	0.5003	0.0801	0.0098	0.0002	-0.0001	-0.0004	6.24
57.	7.	5.36	0.28	110.32	10.08	0.00	0.5772	0.0015	0.5681	0.1036	0.0322	0.0003	-0.0001	-0.0007	5.48
57.	8.	5.36	0.28	110.30	12.05	0.00	0.6345	-0.0043	0.6214	0.1297	0.0568	0.0002	0.0002	-0.0012	4.79
57.	9.	5.35	0.28	110.00	14.02	0.00	0.7020	-0.0114	0.6839	0.1607	0.0817	0.0002	0.0011	-0.0006	4.26
57.	10.	5.34	0.28	109.95	16.08	0.00	0.7919	-0.0212	0.7668	0.2011	0.1105	0.0010	0.0031	0.0015	3.81
57.	11.	5.33	0.28	109.73	17.98	0.00	0.8697	-0.0300	0.8364	0.2425	0.1452	0.0026	0.0064	0.0082	3.45
57.	12.	5.33	0.28	109.67	20.01	0.00	0.9621	-0.0374	0.9168	0.2971	0.1837	0.0018	0.0108	0.0156	3.09
58.	1.	5.32	0.28	109.93	-2.09	5.00	0.0932	0.0355	0.0944	0.0321	-0.0912	-0.0004	-0.0048	-0.0178	2.94
58.	2.	5.33	0.28	110.09	0.07	5.00	0.1883	0.0308	0.1883	0.0311	-0.0692	-0.0028	-0.0044	-0.0162	6.05
58.	3.	5.32	0.28	109.93	2.01	5.00	0.2717	0.0258	0.2706	0.0356	-0.0517	-0.0045	-0.0041	-0.0149	7.60
58.	4.	5.31	0.28	109.99	4.07	5.00	0.3582	0.0204	0.3558	0.0462	-0.0352	-0.0048	-0.0034	-0.0128	7.70
58.	5.	5.31	0.28	109.99	6.01	5.00	0.4320	0.0148	0.4281	0.0606	-0.0149	-0.0056	-0.0023	-0.0103	7.07
58.	6.	5.31	0.28	109.94	8.01	5.00	0.5019	0.0093	0.4957	0.0801	0.0066	-0.0069	-0.0018	-0.0082	6.19
58.	7.	5.31	0.28	110.00	9.99	5.00	0.5655	0.0033	0.5563	0.1025	0.0304	-0.0092	-0.0019	-0.0076	5.43
58.	8.	5.31	0.28	109.91	12.00	5.00	0.6331	-0.0031	0.6200	0.1299	0.0542	-0.0078	-0.0011	-0.0061	4.77
58.	9.	5.31	0.28	110.27	14.00	5.00	0.6932	-0.0097	0.6750	0.1599	0.0803	-0.0054	0.0009	-0.0026	4.22
58.	10.	5.31	0.28	110.11	16.01	5.00	0.7724	-0.0176	0.7473	0.1981	0.1087	-0.0062	0.0037	0.0011	3.77
58.	11.	5.31	0.28	109.97	17.98	5.00	0.8692	-0.0254	0.8345	0.2467	0.1416	-0.0057	0.0079	0.0099	3.38
58.	12.	5.31	0.28	110.15	20.02	5.00	0.9435	-0.0322	0.8975	0.2956	0.1833	-0.0051	0.0128	0.0212	3.04
59.	1.	5.29	0.28	109.97	-2.00	-5.02	0.1078	0.0351	0.1089	0.0313	-0.0869	0.0022	0.0046	0.0147	3.47
59.	2.	5.30	0.28	110.36	-0.09	-5.02	0.1900	0.0307	0.1901	0.0305	-0.0672	0.0041	0.0042	0.0134	6.23
59.	3.	5.29	0.28	109.97	2.00	-5.02	0.2787	0.0256	0.2776	0.0356	-0.0485	0.0056	0.0036	0.0116	7.81
59.	4.	5.29	0.28	110.12	4.02	-5.02	0.3615	0.0206	0.3592	0.0463	-0.0323	0.0069	0.0027	0.0076	7.75
59.	5.	5.29	0.28	110.07	6.02	-5.02	0.4331	0.0152	0.4291	0.0612	-0.0136	0.0074	0.0016	0.0053	7.01
59.	6.	5.29	0.28	110.30	8.03	-5.02	0.4987	0.0100	0.4924	0.0805	0.0079	0.0080	0.0015	0.0041	6.12
59.	7.	5.29	0.28	110.03	10.06	-5.02	0.5667	0.0035	0.5574	0.1036	0.0319	0.0100	0.0019	0.0042	5.38
59.	8.	5.29	0.28	110.20	12.02	-5.02	0.6319	-0.0026	0.6186	0.1304	0.0552	0.0083	0.0017	0.0042	4.74
59.	9.	5.29	0.28	110.07	14.03	-5.02	0.6933	-0.0095	0.6750	0.1605	0.0808	0.0049	0.0015	0.0040	4.21
59.	10.	5.29	0.28	110.20	15.99	-5.02	0.7663	-0.0168	0.7413	0.1969	0.1080	0.0052	0.0002	0.0022	3.77
59.	11.	5.29	0.28	110.17	18.10	-5.02	0.8553	-0.0261	0.8211	0.2433	0.1415	0.0066	-0.0001	0.0033	3.38
59.	12.	5.29	0.28	110.20	20.03	-5.02	0.9398	-0.0331	0.8943	0.2937	0.1798	0.0040	-0.0056	-0.0122	3.05
60.	2.	4.43	0.22	70.04	-2.02	0.03	0.0796	0.0349	0.0808	0.0320	-0.0784	-0.0004	0.0002	0.0010	2.52
60.	3.	4.43	0.22	70.14	0.05	0.03	0.1797	0.0274	0.1797	0.0276	-0.0589	0.0001	0.0000	-0.0002	6.50
60.	4.	4.42	0.22	70.03	2.04	0.03	0.2683	0.0192	0.2674	0.0290	-0.0419	0.0003	-0.0003	-0.0012	9.22
60.	5.	4.41	0.22	69.93	4.01	0.03	0.3417	0.0113	0.3401	0.0356	-0.0282	-0.0001	-0.0002	-0.0011	9.57
60.	6.	4.42	0.22	70.11	6.03	0.03	0.4106	0.0028	0.4080	0.0465	-0.0126	-0.0007	-0.0001	-0.0010	8.78
60.	7.	4.42	0.22	70.16	8.08	0.03	0.4927	-0.0093	0.4891	0.0609	0.0078	-0.0005	0.0000	-0.0010	8.02
60.	8.	4.41	0.22	70.21	10.01	0.03	0.5692	-0.0219	0.5644	0.0785	0.0272	-0.0006	0.0001	-0.0015	7.19
60.	9.	4.42	0.22	70.34	12.04	0.03	0.6492	-0.0354	0.6423	0.1023	0.0504	-0.0006	0.0003	-0.0016	6.28
60.	10.	4.41	0.22	70.01	14.10	0.03	0.7264	-0.0468	0.7159	0.1335	0.0777	0.0002	0.0008	0.0002	5.36

NASA Langley Research Center 14- by 22-Foot Subsonic Tunnel Test 395

Run	Point	R/10 <sup>6</sup>	M	q	$\alpha$	$\beta$	C <sub>N</sub>	C <sub>A</sub>	C <sub>L</sub>	C <sub>D</sub>	C <sub>m</sub>	C <sub>i</sub>	C <sub>n</sub>	C <sub>y</sub>	L/D
60.	11.	4.41	0.22	70.20	16.08	0.03	0.7969	-0.0550	0.7810	0.1701	0.1096	-0.0010	0.0037	0.0035	4.59
60.	12.	4.41	0.22	70.04	18.08	0.03	0.8795	-0.0600	0.8547	0.2186	0.1469	-0.0022	0.0079	0.0111	3.91
60.	13.	4.40	0.22	70.07	20.03	0.03	0.9675	-0.0661	0.9317	0.2724	0.1830	-0.0042	0.0135	0.0192	3.42
61.	1.	5.47	0.28	110.24	-2.06	0.03	0.0732	0.0353	0.0744	0.0326	-0.0787	-0.0003	-0.0001	0.0004	2.28
61.	2.	5.45	0.28	109.89	0.10	0.03	0.1761	0.0274	0.1761	0.0278	-0.0586	0.0001	-0.0002	-0.0003	6.34
61.	3.	5.45	0.28	109.98	2.04	0.03	0.2623	0.0190	0.2614	0.0286	-0.0421	0.0002	-0.0003	-0.0013	9.14
61.	4.	5.45	0.28	110.14	4.06	0.03	0.3383	0.0107	0.3367	0.0350	-0.0283	0.0000	-0.0002	-0.0010	9.61
61.	5.	5.45	0.28	110.13	6.04	0.03	0.4066	0.0022	0.4041	0.0455	-0.0133	-0.0006	-0.0001	-0.0008	8.88
61.	6.	5.44	0.28	110.08	8.07	0.03	0.4876	-0.0098	0.4841	0.0596	0.0072	-0.0005	-0.0001	-0.0008	8.12
61.	7.	5.44	0.28	109.97	10.02	0.03	0.5640	-0.0227	0.5594	0.0769	0.0273	-0.0005	0.0001	-0.0014	7.28
61.	8.	5.44	0.28	110.24	12.07	0.03	0.6437	-0.0364	0.6371	0.1005	0.0508	-0.0006	0.0004	-0.0015	6.34
61.	9.	5.43	0.28	110.15	14.02	0.03	0.7164	-0.0473	0.7065	0.1295	0.0770	-0.0003	0.0007	0.0003	5.46
61.	10.	5.42	0.28	109.80	15.99	0.03	0.7902	-0.0559	0.7750	0.1661	0.1080	-0.0006	0.0036	0.0032	4.67
61.	11.	5.43	0.28	110.21	18.01	0.03	0.8700	-0.0605	0.8461	0.2140	0.1462	-0.0019	0.0075	0.0099	3.95
61.	12.	5.43	0.28	110.16	20.03	0.03	0.9611	-0.0663	0.9257	0.2700	0.1840	-0.0036	0.0132	0.0182	3.43
62.	1.	5.42	0.28	110.11	-2.04	5.02	0.0605	0.0354	0.0617	0.0332	-0.0843	0.0017	-0.0051	-0.0168	1.86
62.	2.	5.41	0.28	110.06	0.00	5.02	0.1579	0.0285	0.1579	0.0286	-0.0658	-0.0010	-0.0048	-0.0154	5.52
62.	3.	5.41	0.28	110.11	2.06	5.02	0.2503	0.0204	0.2494	0.0296	-0.0488	-0.0036	-0.0042	-0.0141	8.42
62.	4.	5.40	0.28	109.82	4.03	5.02	0.3294	0.0119	0.3278	0.0354	-0.0326	-0.0056	-0.0036	-0.0119	9.25
62.	5.	5.41	0.28	109.88	6.08	5.02	0.4078	0.0014	0.4053	0.0451	-0.0132	-0.0078	-0.0022	-0.0093	8.98
62.	6.	5.42	0.28	110.55	8.01	5.02	0.4827	-0.0096	0.4793	0.0586	0.0043	-0.0102	-0.0021	-0.0052	8.18
62.	7.	5.42	0.28	110.45	10.07	5.02	0.5628	-0.0224	0.5580	0.0775	0.0261	-0.0120	-0.0026	-0.0039	7.20
62.	8.	5.41	0.28	110.10	12.04	5.02	0.6442	-0.0342	0.6372	0.1024	0.0480	-0.0136	-0.0028	0.0000	6.22
62.	9.	5.40	0.28	109.78	14.02	5.02	0.7207	-0.0457	0.7102	0.1321	0.0746	-0.0159	-0.0016	0.0054	5.38
62.	10.	5.41	0.28	110.05	16.07	5.02	0.7934	-0.0540	0.7774	0.1699	0.1090	-0.0162	0.0019	0.0116	4.58
62.	11.	5.41	0.28	110.17	18.09	5.02	0.8641	-0.0570	0.8391	0.2166	0.1509	-0.0145	0.0092	0.0187	3.87
62.	12.	5.40	0.28	109.96	20.04	5.02	0.9445	-0.0615	0.9083	0.2688	0.1887	-0.0167	0.0151	0.0254	3.38
63.	1.	5.39	0.28	110.01	-2.09	-5.02	0.0683	0.0348	0.0695	0.0323	-0.0820	-0.0005	0.0052	0.0137	2.15
63.	2.	5.39	0.28	110.24	0.01	-5.02	0.1652	0.0279	0.1652	0.0281	-0.0625	0.0020	0.0048	0.0120	5.88
63.	3.	5.39	0.28	110.17	2.08	-5.02	0.2593	0.0197	0.2584	0.0294	-0.0454	0.0052	0.0041	0.0098	8.79
63.	4.	5.38	0.28	110.08	4.02	-5.02	0.3359	0.0114	0.3343	0.0354	-0.0296	0.0078	0.0031	0.0058	9.45
63.	5.	5.38	0.28	109.94	6.07	-5.02	0.4108	0.0014	0.4084	0.0454	-0.0118	0.0092	0.0021	0.0029	9.00
63.	6.	5.38	0.28	110.04	8.08	-5.02	0.4857	-0.0096	0.4823	0.0596	0.0063	0.0113	0.0026	-0.0001	8.10
63.	7.	5.38	0.28	110.00	10.01	-5.02	0.5619	-0.0218	0.5571	0.0773	0.0267	0.0129	0.0033	-0.0013	7.21
63.	8.	5.39	0.28	110.23	12.03	-5.02	0.6419	-0.0346	0.6350	0.1014	0.0502	0.0153	0.0039	-0.0037	6.27
63.	9.	5.38	0.28	109.88	14.03	-5.02	0.7185	-0.0443	0.7078	0.1330	0.0770	0.0149	0.0037	-0.0053	5.32
63.	10.	5.38	0.28	110.06	16.01	-5.02	0.7879	-0.0521	0.7717	0.1694	0.1094	0.0135	0.0011	-0.0094	4.56
63.	11.	5.38	0.28	109.90	18.07	-5.02	0.8667	-0.0579	0.8419	0.2163	0.1465	0.0122	-0.0018	-0.0122	3.89
63.	12.	5.38	0.28	110.16	20.01	-5.02	0.9455	-0.0628	0.9100	0.2675	0.1849	0.0156	-0.0085	-0.0232	3.40
64.	3.	4.71	0.22	69.91	-1.97	-0.01	0.0903	0.0308	0.0913	0.0277	-0.0721	-0.0009	0.0004	0.0007	3.29
64.	4.	4.70	0.22	69.82	-0.02	-0.01	0.1865	0.0250	0.1865	0.0251	-0.0530	-0.0003	0.0002	-0.0001	7.44
64.	5.	4.71	0.22	70.23	2.05	-0.01	0.2761	0.0177	0.2753	0.0279	-0.0353	0.0002	-0.0001	-0.0007	9.88
64.	6.	4.70	0.22	70.04	4.01	-0.01	0.3469	0.0113	0.3453	0.0360	-0.0233	0.0002	0.0000	-0.0008	9.59
64.	7.	4.70	0.22	70.11	6.05	-0.01	0.4175	0.0034	0.4148	0.0479	-0.0055	-0.0004	0.0000	-0.0013	8.65
64.	8.	4.69	0.22	70.11	7.99	-0.01	0.4957	-0.0066	0.4918	0.0632	0.0177	0.0002	0.0001	-0.0016	7.78
64.	9.	4.69	0.22	69.96	9.96	-0.01	0.5758	-0.0178	0.5702	0.0832	0.0420	0.0001	0.0002	-0.0018	6.85
64.	10.	4.68	0.22	69.95	12.04	-0.01	0.6620	-0.0284	0.6534	0.1118	0.0715	0.0003	0.0004	-0.0012	5.84
64.	11.	4.68	0.22	69.97	13.96	-0.01	0.7439	-0.0356	0.7304	0.1469	0.1033	0.0015	0.0012	0.0006	4.97
64.	12.	4.67	0.22	69.87	15.99	-0.01	0.8310	-0.0416	0.8103	0.1913	0.1399	-0.0005	0.0037	0.0024	4.24

NASA Langley Research Center 14- by 22-Foot Subsonic Tunnel Test 395

Run	Point	R/10 <sup>6</sup>	M	q	$\alpha$	$\beta$	C <sub>N</sub>	C <sub>A</sub>	C <sub>L</sub>	C <sub>D</sub>	C <sub>m</sub>	C <sub>l</sub>	C <sub>n</sub>	C <sub>y</sub>	L/D
64.	13.	4.68	0.22	70.33	17.99	-0.01	0.9228	-0.0455	0.8917	0.2446	0.1793	-0.0024	0.0076	0.0097	3.65
64.	14.	4.67	0.22	70.01	20.03	-0.01	1.0336	-0.0479	0.9874	0.3127	0.2250	-0.0046	0.0126	0.0208	3.16
65.	1.	5.79	0.28	109.99	-2.00	-0.01	0.0828	0.0317	0.0838	0.0288	-0.0721	-0.0011	0.0006	-0.0004	2.91
65.	2.	5.77	0.28	109.51	-0.02	-0.01	0.1797	0.0257	0.1798	0.0258	-0.0536	-0.0004	0.0004	-0.0007	6.98
65.	3.	5.78	0.28	110.22	1.97	-0.01	0.2675	0.0187	0.2667	0.0282	-0.0369	-0.0001	0.0003	-0.0015	9.47
65.	4.	5.77	0.28	109.96	4.06	-0.01	0.3416	0.0119	0.3399	0.0364	-0.0245	-0.0005	0.0004	-0.0017	9.33
65.	5.	5.76	0.28	109.79	5.99	-0.01	0.4085	0.0041	0.4058	0.0473	-0.0063	0.0000	0.0006	-0.0017	8.57
65.	6.	5.77	0.28	110.25	8.02	-0.01	0.4890	-0.0067	0.4851	0.0624	0.0182	0.0011	0.0006	-0.0019	7.77
65.	7.	5.77	0.28	110.22	9.96	-0.01	0.5660	-0.0177	0.5605	0.0817	0.0428	0.0009	0.0007	-0.0026	6.86
65.	8.	5.76	0.28	110.13	12.00	-0.01	0.6498	-0.0285	0.6415	0.1088	0.0721	0.0010	0.0009	-0.0018	5.90
65.	9.	5.75	0.28	109.83	13.98	-0.01	0.7336	-0.0362	0.7207	0.1440	0.1045	0.0018	0.0011	0.0000	5.01
65.	10.	5.75	0.28	109.90	16.01	-0.01	0.8235	-0.0420	0.8031	0.1890	0.1420	0.0007	0.0037	0.0020	4.25
65.	11.	5.74	0.28	109.90	18.04	-0.01	0.9212	-0.0464	0.8902	0.2440	0.1822	-0.0016	0.0074	0.0089	3.65
65.	12.	5.74	0.28	109.94	20.02	-0.01	1.0246	-0.0477	0.9790	0.3094	0.2247	-0.0035	0.0124	0.0181	3.16
66.	1.	5.72	0.28	109.87	-2.00	5.00	0.0650	0.0331	0.0661	0.0309	-0.0771	0.0021	-0.0030	-0.0141	2.14
66.	2.	5.71	0.28	109.72	0.08	5.00	0.1647	0.0279	0.1646	0.0282	-0.0582	-0.0007	-0.0026	-0.0129	5.83
66.	3.	5.71	0.28	109.81	1.99	5.00	0.2505	0.0213	0.2496	0.0303	-0.0426	-0.0032	-0.0017	-0.0111	8.25
66.	4.	5.71	0.28	109.82	4.02	5.00	0.3286	0.0136	0.3268	0.0369	-0.0241	-0.0046	-0.0015	-0.0094	8.85
66.	5.	5.71	0.28	110.04	6.06	5.00	0.4057	0.0047	0.4030	0.0481	-0.0038	-0.0059	-0.0010	-0.0088	8.37
66.	6.	5.71	0.28	110.08	7.98	5.00	0.4830	-0.0053	0.4790	0.0627	0.0170	-0.0089	-0.0010	-0.0044	7.64
66.	7.	5.70	0.28	109.74	9.98	5.00	0.5655	-0.0166	0.5598	0.0828	0.0416	-0.0113	-0.0015	-0.0010	6.76
66.	8.	5.69	0.28	109.64	12.05	5.00	0.6531	-0.0272	0.6444	0.1112	0.0686	-0.0134	-0.0014	0.0041	5.80
66.	9.	5.69	0.28	109.43	14.00	5.00	0.7331	-0.0359	0.7200	0.1444	0.1014	-0.0151	0.0003	0.0074	4.99
66.	10.	5.70	0.28	109.91	16.02	5.00	0.8128	-0.0405	0.7924	0.1877	0.1408	-0.0169	0.0041	0.0122	4.22
66.	11.	5.70	0.28	110.02	18.03	5.00	0.9099	-0.0431	0.8786	0.2435	0.1827	-0.0198	0.0097	0.0198	3.61
66.	12.	5.70	0.28	109.96	20.02	5.00	1.0160	-0.0456	0.9702	0.3084	0.2260	-0.0225	0.0138	0.0273	3.15
67.	1.	5.69	0.28	110.02	-2.03	-5.00	0.0729	0.0331	0.0740	0.0306	-0.0741	0.0001	0.0046	0.0094	2.42
67.	2.	5.69	0.28	110.16	-0.09	-5.00	0.1654	0.0280	0.1655	0.0278	-0.0565	0.0028	0.0043	0.0074	5.95
67.	3.	5.68	0.28	109.83	1.99	-5.00	0.2597	0.0205	0.2588	0.0298	-0.0399	0.0063	0.0034	0.0041	8.69
67.	4.	5.68	0.28	110.00	3.98	-5.00	0.3352	0.0129	0.3335	0.0365	-0.0225	0.0089	0.0029	0.0023	9.13
67.	5.	5.68	0.28	110.09	6.02	-5.00	0.4084	0.0043	0.4057	0.0477	-0.0040	0.0103	0.0024	0.0006	8.51
67.	6.	5.68	0.28	109.83	7.97	-5.00	0.4837	-0.0055	0.4798	0.0624	0.0168	0.0130	0.0029	-0.0032	7.68
67.	7.	5.68	0.28	109.87	9.95	-5.00	0.5659	-0.0163	0.5602	0.0828	0.0412	0.0152	0.0035	-0.0059	6.76
67.	8.	5.68	0.28	110.03	12.03	-5.00	0.6517	-0.0273	0.6431	0.1106	0.0709	0.0168	0.0034	-0.0079	5.81
67.	9.	5.69	0.28	110.29	14.00	-5.00	0.7334	-0.0347	0.7200	0.1456	0.1022	0.0168	0.0025	-0.0089	4.95
67.	10.	5.68	0.28	109.85	16.02	-5.00	0.8239	-0.0407	0.8031	0.1907	0.1375	0.0188	0.0005	-0.0100	4.21
67.	11.	5.68	0.28	110.14	17.99	-5.00	0.9102	-0.0450	0.8796	0.2411	0.1761	0.0195	-0.0010	-0.0123	3.65
67.	12.	5.68	0.28	110.18	20.08	-5.00	1.0157	-0.0474	0.9702	0.3075	0.2219	0.0210	-0.0050	-0.0231	3.16
68.	2.	4.59	0.22	69.79	-2.02	0.00	0.0688	0.0384	0.0701	0.0360	-0.0837	-0.0005	0.0002	0.0007	1.95
68.	3.	4.57	0.22	69.69	0.02	0.00	0.1650	0.0310	0.1649	0.0311	-0.0654	0.0000	0.0002	-0.0002	5.30
68.	4.	4.57	0.22	69.92	2.03	0.00	0.2553	0.0223	0.2543	0.0316	-0.0487	0.0001	0.0001	-0.0014	8.04
68.	5.	4.57	0.22	69.90	4.03	0.00	0.3311	0.0137	0.3294	0.0373	-0.0347	-0.0002	0.0001	-0.0009	8.83
68.	6.	4.57	0.22	70.01	6.01	0.00	0.4057	0.0049	0.4029	0.0480	-0.0186	-0.0001	0.0005	-0.0002	8.40
68.	7.	4.57	0.22	69.95	8.02	0.00	0.4892	-0.0051	0.4851	0.0640	-0.0010	0.0011	0.0008	0.0000	7.58
68.	8.	4.56	0.22	69.92	10.02	0.00	0.5589	-0.0163	0.5532	0.0823	0.0205	0.0022	0.0015	-0.0011	6.72
68.	9.	4.56	0.22	70.00	12.03	0.00	0.6364	-0.0308	0.6288	0.1039	0.0388	0.0006	0.0013	0.0003	6.05
68.	10.	4.56	0.22	70.03	14.01	0.00	0.7093	-0.0450	0.6991	0.1299	0.0587	0.0001	0.0012	0.0033	5.38
68.	11.	4.56	0.22	70.19	15.99	0.00	0.7700	-0.0545	0.7553	0.1618	0.0842	-0.0017	0.0044	0.0064	4.67
68.	12.	4.56	0.22	70.18	18.00	0.00	0.8451	-0.0630	0.8232	0.2038	0.1111	-0.0023	0.0081	0.0162	4.04

NASA Langley Research Center 14- by 22-Foot Subsonic Tunnel Test 395

Run	Point	R/10 <sup>6</sup>	M	q	$\alpha$	$\beta$	C <sub>N</sub>	C <sub>A</sub>	C <sub>L</sub>	C <sub>D</sub>	C <sub>m</sub>	C <sub>i</sub>	C <sub>n</sub>	C <sub>y</sub>	L/D
68.	13.	4.56	0.22	70.16	20.00	0.00	0.9220	-0.0717	0.8909	0.2508	0.1430	0.0012	0.0132	0.0238	3.55
69.	1.	5.65	0.28	109.94	-2.03	0.00	0.0618	0.0397	0.0632	0.0374	-0.0826	0.0002	0.0006	-0.0009	1.69
69.	2.	5.62	0.28	109.91	0.01	0.00	0.1571	0.0324	0.1571	0.0325	-0.0649	0.0006	0.0007	-0.0016	4.83
69.	3.	5.61	0.28	110.00	2.01	0.00	0.2455	0.0238	0.2445	0.0326	-0.0481	0.0013	0.0007	-0.0027	7.50
69.	4.	5.61	0.28	110.16	4.02	0.00	0.3235	0.0147	0.3217	0.0377	-0.0343	0.0007	0.0006	-0.0020	8.53
69.	5.	5.60	0.28	110.00	6.03	0.00	0.3982	0.0054	0.3954	0.0477	-0.0185	0.0005	0.0008	-0.0007	8.29
69.	6.	5.60	0.28	110.15	8.00	0.00	0.4835	-0.0060	0.4797	0.0622	-0.0026	0.0002	0.0007	0.0011	7.71
69.	7.	5.60	0.28	110.13	10.01	0.00	0.5574	-0.0196	0.5523	0.0787	0.0188	0.0008	0.0005	0.0015	7.02
69.	8.	5.59	0.28	109.76	12.00	0.00	0.6307	-0.0330	0.6238	0.1002	0.0377	-0.0002	0.0007	0.0014	6.22
69.	9.	5.59	0.28	110.05	14.02	0.00	0.7040	-0.0469	0.6944	0.1267	0.0582	-0.0008	0.0008	0.0036	5.48
69.	10.	5.59	0.28	110.13	16.03	0.00	0.7661	-0.0562	0.7518	0.1595	0.0849	-0.0010	0.0044	0.0059	4.71
69.	11.	5.59	0.28	110.22	17.98	0.00	0.8387	-0.0647	0.8177	0.1999	0.1116	-0.0021	0.0079	0.0150	4.09
69.	12.	5.59	0.28	110.40	20.03	0.00	0.9112	-0.0716	0.8806	0.2475	0.1465	0.0022	0.0141	0.0233	3.56
70.	1.	5.56	0.28	109.49	-2.02	5.00	0.0536	0.0399	0.0549	0.0380	-0.0886	0.0010	-0.0055	-0.0190	1.44
70.	2.	5.56	0.28	109.88	0.02	5.00	0.1489	0.0328	0.1489	0.0329	-0.0712	-0.0008	-0.0054	-0.0182	4.52
70.	3.	5.56	0.28	109.69	2.04	5.00	0.2402	0.0242	0.2392	0.0329	-0.0544	-0.0030	-0.0049	-0.0178	7.26
70.	4.	5.56	0.28	110.01	4.04	5.00	0.3192	0.0153	0.3173	0.0381	-0.0375	-0.0038	-0.0046	-0.0171	8.32
70.	5.	5.56	0.28	110.07	6.03	5.00	0.3986	0.0048	0.3959	0.0472	-0.0196	-0.0059	-0.0027	-0.0126	8.38
70.	6.	5.56	0.28	109.96	8.03	5.00	0.4798	-0.0073	0.4761	0.0606	-0.0025	-0.0097	-0.0020	-0.0078	7.86
70.	7.	5.56	0.28	110.14	10.03	5.00	0.5581	-0.0198	0.5530	0.0788	0.0156	-0.0111	-0.0026	-0.0089	7.01
70.	8.	5.56	0.28	110.17	12.02	5.00	0.6294	-0.0321	0.6223	0.1010	0.0356	-0.0109	-0.0028	-0.0087	6.16
70.	9.	5.55	0.28	109.88	13.99	5.00	0.7062	-0.0456	0.6963	0.1281	0.0552	-0.0122	-0.0020	-0.0046	5.43
70.	10.	5.55	0.28	109.93	16.03	5.00	0.7677	-0.0528	0.7525	0.1632	0.0848	-0.0130	0.0023	0.0000	4.61
70.	11.	5.55	0.28	110.03	17.99	5.00	0.8312	-0.0611	0.8095	0.2010	0.1127	-0.0117	0.0069	0.0102	4.03
70.	12.	5.56	0.28	110.30	20.00	5.00	0.9084	-0.0715	0.8781	0.2463	0.1438	-0.0110	0.0116	0.0206	3.57
71.	1.	5.55	0.28	110.40	-2.03	-5.00	0.0603	0.0396	0.0617	0.0375	-0.0864	-0.0005	0.0064	0.0181	1.65
71.	2.	5.54	0.28	110.25	0.04	-5.00	0.1562	0.0321	0.1562	0.0323	-0.0681	0.0016	0.0059	0.0158	4.84
71.	3.	5.53	0.28	109.77	2.03	-5.00	0.2452	0.0237	0.2442	0.0326	-0.0520	0.0038	0.0056	0.0143	7.50
71.	4.	5.53	0.28	110.23	4.02	-5.00	0.3249	0.0147	0.3231	0.0378	-0.0358	0.0054	0.0047	0.0121	8.56
71.	5.	5.53	0.28	110.29	6.04	-5.00	0.4005	0.0045	0.3978	0.0472	-0.0195	0.0074	0.0026	0.0069	8.44
71.	6.	5.54	0.28	110.45	8.04	-5.00	0.4780	-0.0069	0.4743	0.0609	-0.0029	0.0114	0.0026	0.0041	7.79
71.	7.	5.53	0.28	110.13	10.03	-5.00	0.5562	-0.0193	0.5510	0.0790	0.0152	0.0125	0.0034	0.0058	6.98
71.	8.	5.53	0.28	110.19	12.04	-5.00	0.6310	-0.0323	0.6238	0.1014	0.0356	0.0119	0.0040	0.0084	6.15
71.	9.	5.53	0.28	110.25	14.06	-5.00	0.7068	-0.0440	0.6963	0.1307	0.0574	0.0122	0.0042	0.0071	5.33
71.	10.	5.53	0.28	109.99	16.03	-5.00	0.7684	-0.0531	0.7532	0.1632	0.0832	0.0129	0.0023	0.0028	4.61
71.	11.	5.53	0.28	110.02	18.04	-5.00	0.8363	-0.0614	0.8142	0.2031	0.1100	0.0097	0.0004	-0.0006	4.01
71.	12.	5.52	0.28	109.76	20.00	-5.00	0.9035	-0.0708	0.8732	0.2452	0.1422	0.0107	-0.0065	-0.0145	3.56
72.	2.	4.56	0.22	70.06	-2.02	-0.01	-0.0111	0.0289	-0.0101	0.0292	-0.0637	-0.0012	0.0002	0.0015	-0.34
72.	3.	4.55	0.22	69.98	0.09	-0.01	0.0923	0.0211	0.0922	0.0213	-0.0439	-0.0009	0.0000	0.0005	4.34
72.	4.	4.54	0.22	69.85	2.08	-0.01	0.1828	0.0128	0.1822	0.0195	-0.0273	-0.0010	-0.0002	-0.0004	9.32
72.	5.	4.53	0.22	69.66	4.06	-0.01	0.2606	0.0042	0.2596	0.0228	-0.0135	-0.0011	-0.0002	0.0000	11.37
72.	6.	4.53	0.22	69.81	6.07	-0.01	0.3312	-0.0040	0.3298	0.0315	0.0010	-0.0012	-0.0001	0.0003	10.49
72.	7.	4.55	0.22	70.47	8.06	-0.01	0.4057	-0.0145	0.4037	0.0431	0.0205	-0.0011	-0.0001	0.0006	9.36
72.	8.	4.55	0.22	70.24	10.03	-0.01	0.4833	-0.0270	0.4806	0.0585	0.0409	-0.0009	-0.0001	0.0000	8.22
72.	9.	4.55	0.22	70.29	12.03	-0.01	0.5629	-0.0404	0.5590	0.0789	0.0631	-0.0009	0.0002	-0.0004	7.08
72.	10.	4.54	0.22	70.10	15.07	-0.01	0.6828	-0.0570	0.6741	0.1240	0.1022	0.0000	0.0017	0.0035	5.44
72.	11.	4.54	0.22	70.06	14.09	-0.01	0.6429	-0.0529	0.6365	0.1067	0.0885	-0.0010	0.0006	0.0016	5.97
72.	12.	4.54	0.22	70.14	16.06	-0.01	0.7255	-0.0615	0.7142	0.1434	0.1170	-0.0008	0.0035	0.0064	4.98
72.	13.	4.53	0.22	69.99	18.01	-0.01	0.7987	-0.0673	0.7804	0.1852	0.1532	-0.0027	0.0075	0.0122	4.21

NASA Langley Research Center 14- by 22-Foot Subsonic Tunnel Test 395

Run	Point	R/10 <sup>6</sup>	M	q	$\alpha$	$\beta$	C <sub>N</sub>	C <sub>A</sub>	C <sub>L</sub>	C <sub>D</sub>	C <sub>m</sub>	C <sub>l</sub>	C <sub>n</sub>	C <sub>Y</sub>	LD
72.	14.	4.53	0.22	70.11	20.09	-0.01	0.8946	-0.0744	0.8657	0.2402	0.1909	-0.0046	0.0134	0.0214	3.60
73.	1.	5.61	0.28	110.07	-2.07	-0.01	-0.0186	0.0289	-0.0175	0.0295	-0.0638	-0.0009	0.0000	0.0011	-0.59
73.	2.	5.61	0.28	109.88	-0.03	-0.01	0.0812	0.0215	0.0812	0.0215	-0.0444	-0.0007	-0.0001	0.0006	3.79
73.	3.	5.61	0.28	110.19	2.07	-0.01	0.1773	0.0125	0.1767	0.0190	-0.0266	-0.0007	-0.0003	-0.0007	9.29
73.	4.	5.60	0.28	110.04	4.06	-0.01	0.2551	0.0038	0.2541	0.0221	-0.0132	-0.0008	-0.0002	-0.0002	11.51
73.	5.	5.59	0.28	109.93	6.09	-0.01	0.3266	-0.0047	0.3252	0.0304	0.0010	-0.0009	-0.0001	0.0001	10.69
73.	6.	5.59	0.28	110.20	8.06	-0.01	0.4017	-0.0154	0.3999	0.0417	0.0209	-0.0006	-0.0002	0.0004	9.59
73.	7.	5.59	0.28	110.36	10.02	-0.01	0.4774	-0.0277	0.4749	0.0566	0.0411	-0.0004	-0.0001	-0.0001	8.39
73.	8.	5.58	0.28	109.99	12.07	-0.01	0.5572	-0.0415	0.5536	0.0770	0.0636	-0.0007	0.0003	-0.0003	7.19
73.	9.	5.58	0.28	110.00	13.97	-0.01	0.6305	-0.0527	0.6246	0.1024	0.0871	-0.0007	0.0006	0.0011	6.10
73.	10.	5.57	0.28	109.95	16.01	-0.01	0.7139	-0.0623	0.7034	0.1388	0.1171	0.0001	0.0032	0.0052	5.07
73.	11.	5.57	0.28	110.00	18.08	-0.01	0.7986	-0.0682	0.7803	0.1853	0.1559	-0.0025	0.0079	0.0128	4.21
73.	12.	5.58	0.28	110.42	20.09	-0.01	0.8887	-0.0746	0.8603	0.2380	0.1922	-0.0041	0.0131	0.0197	3.61

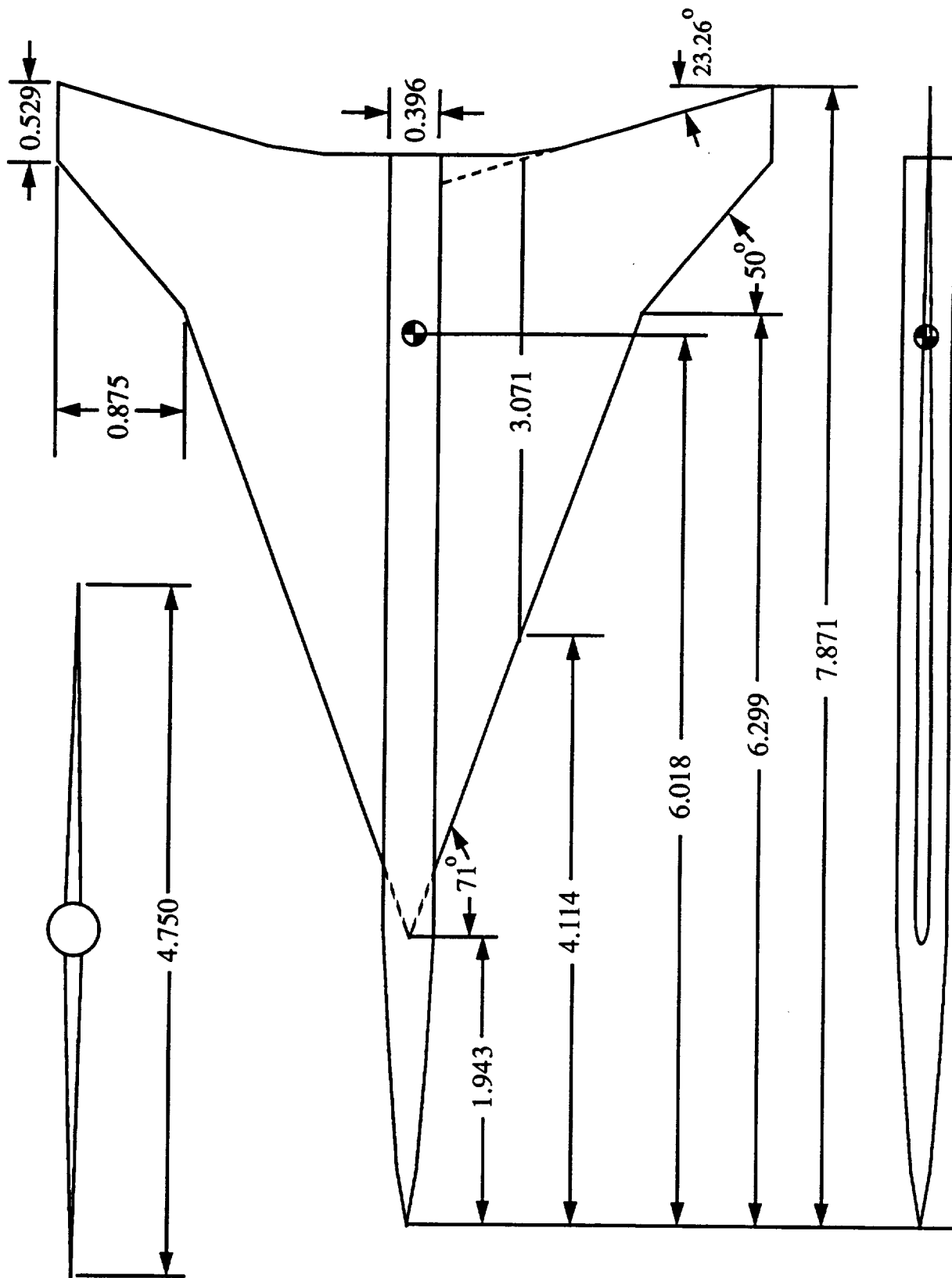


Figure 1. Geometric characteristics of the model. All linear dimensions are in feet.



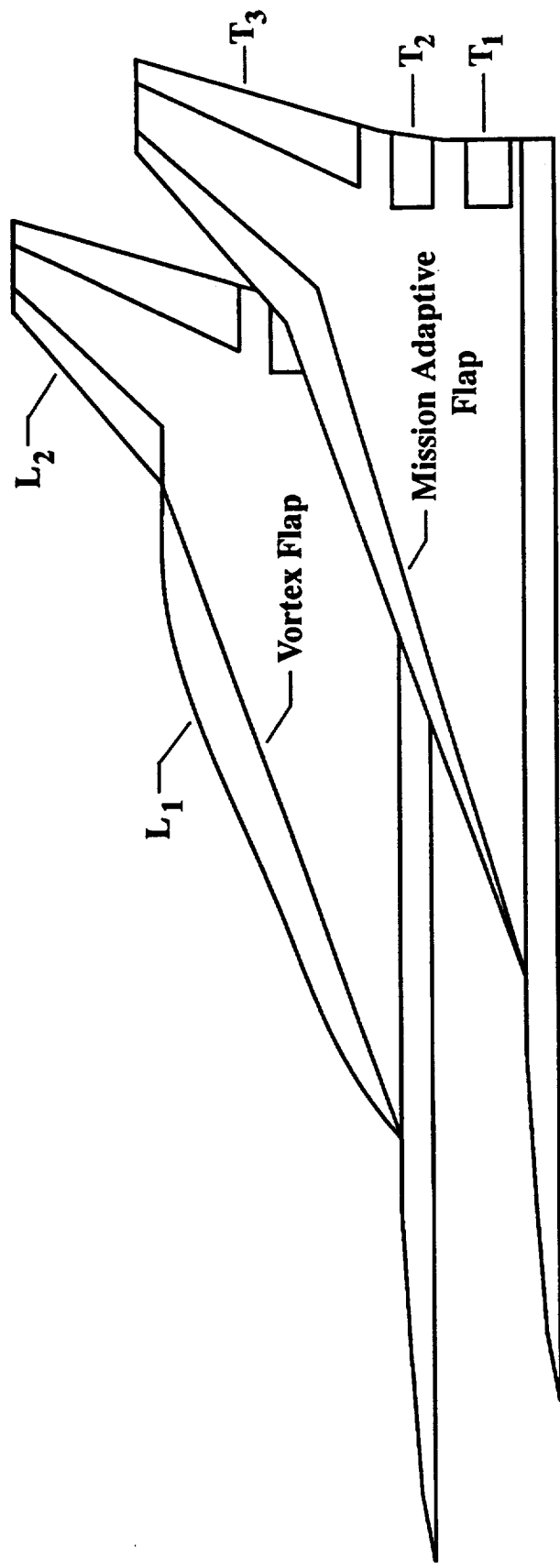


Figure 2. Flap designations for both leading- and trailing-edge flap segments.

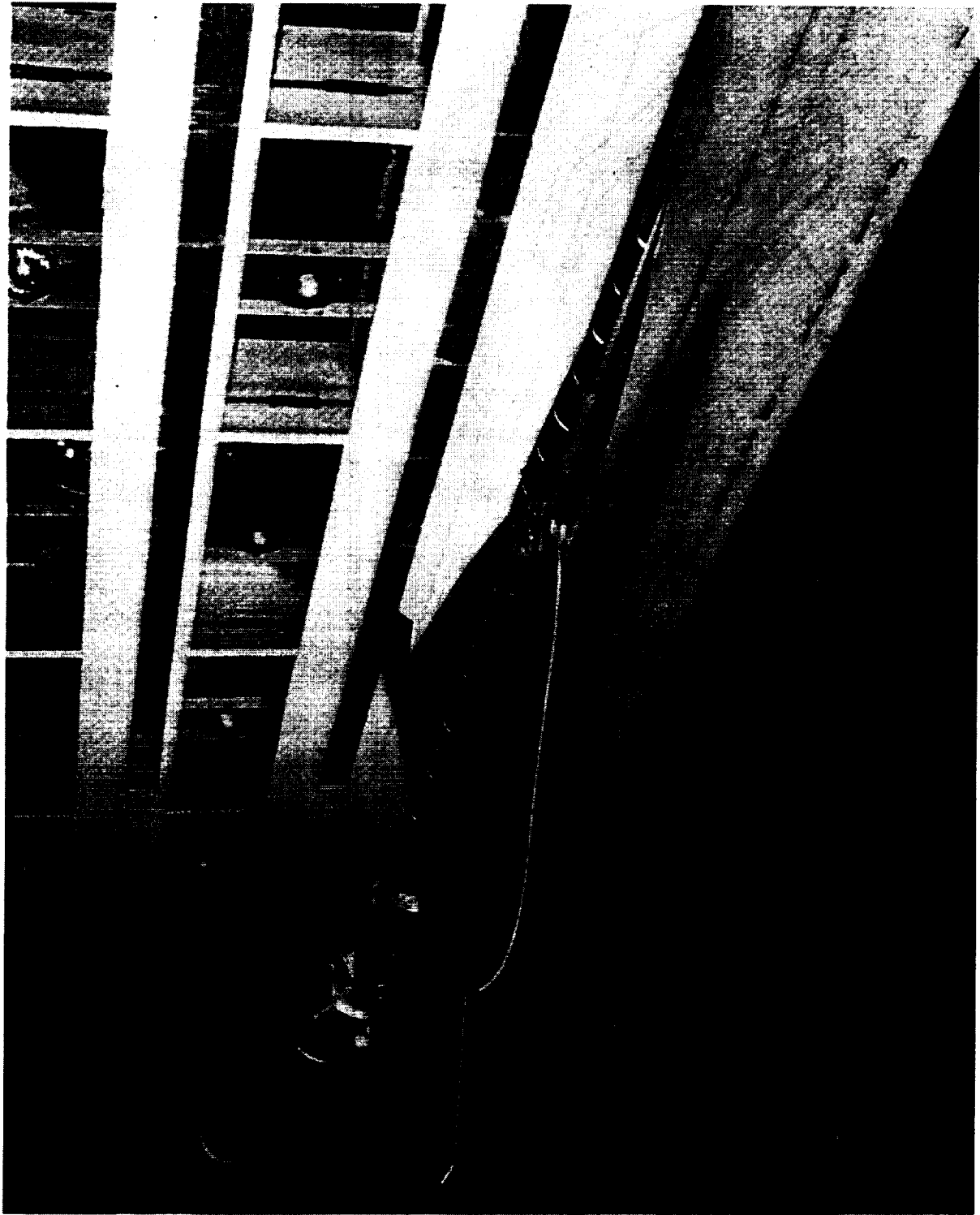


Figure 3. Vortex flap configuration of model mounted in the 14- by 22-Foot Subsonic Tunnel.

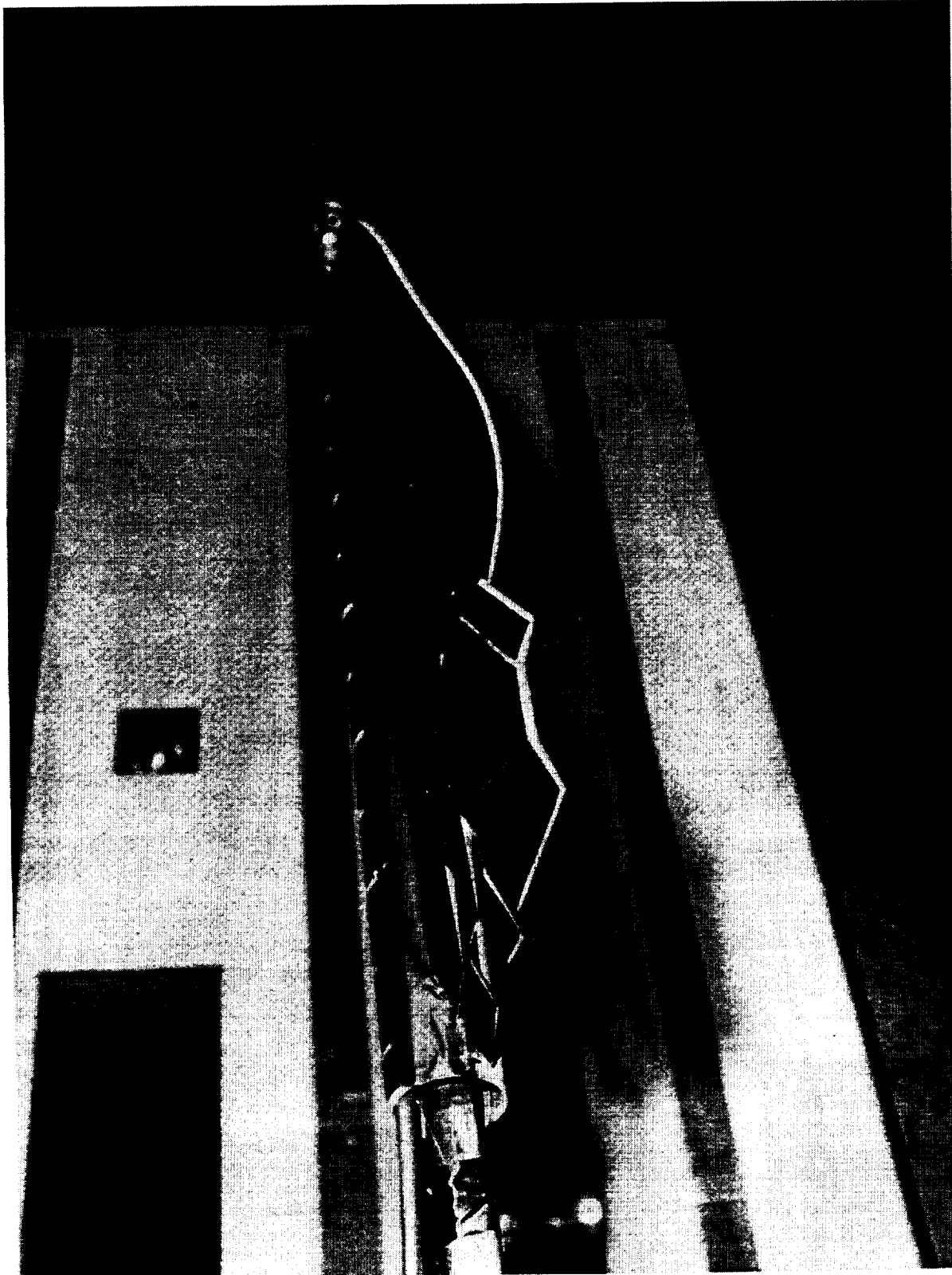


Figure 4. Side view of vortex flap configuration with leading-edges at  $\delta_{L1/2} = 40^\circ/26.4^\circ$ ,  
and  $\delta_{T1/2\beta} = 20^\circ/20^\circ/20^\circ$ .

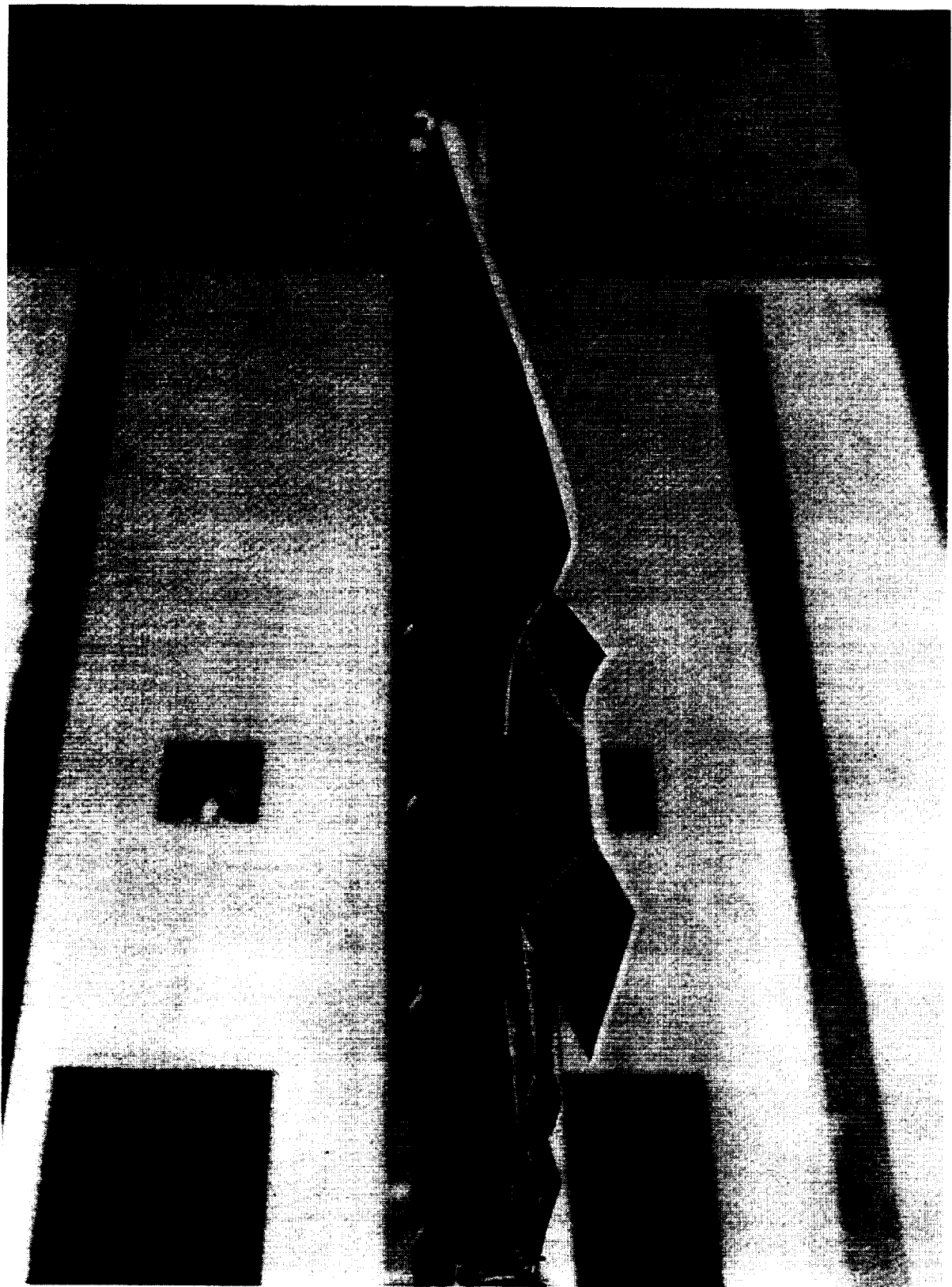
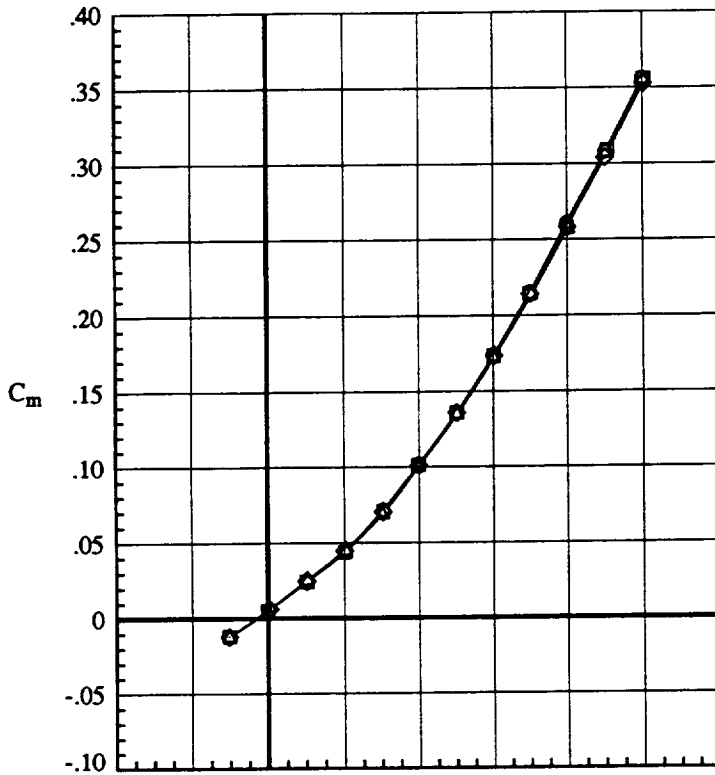
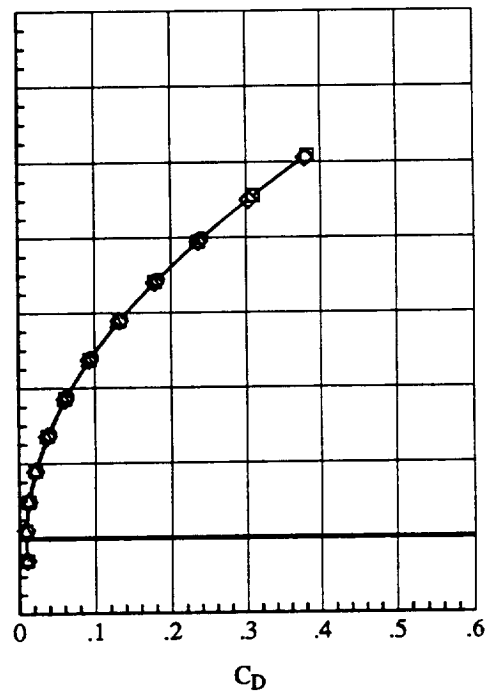
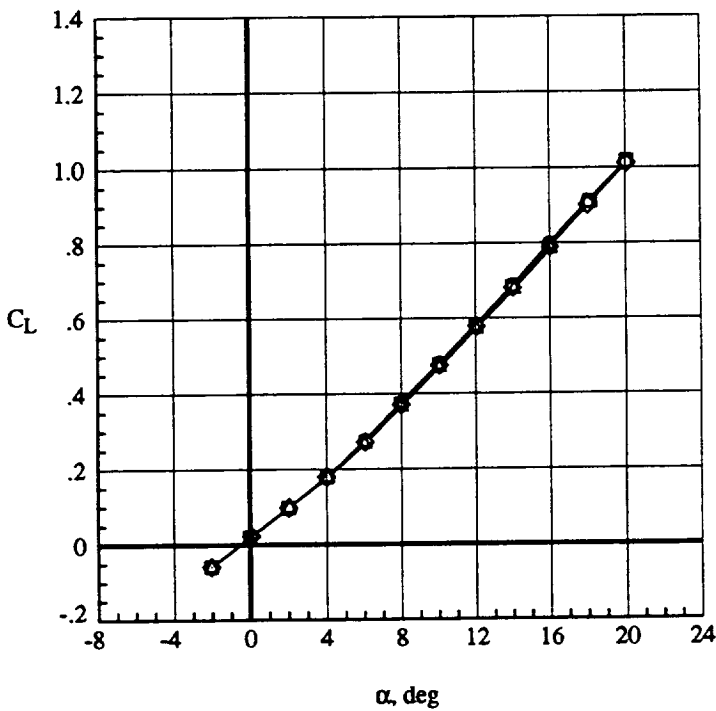


Figure 5. Side view of mission adaptive leading-edge flap configuration with trailing edges at  $\delta_{T1}/\rho\beta = 10^\circ/10^\circ/12.9^\circ$ .

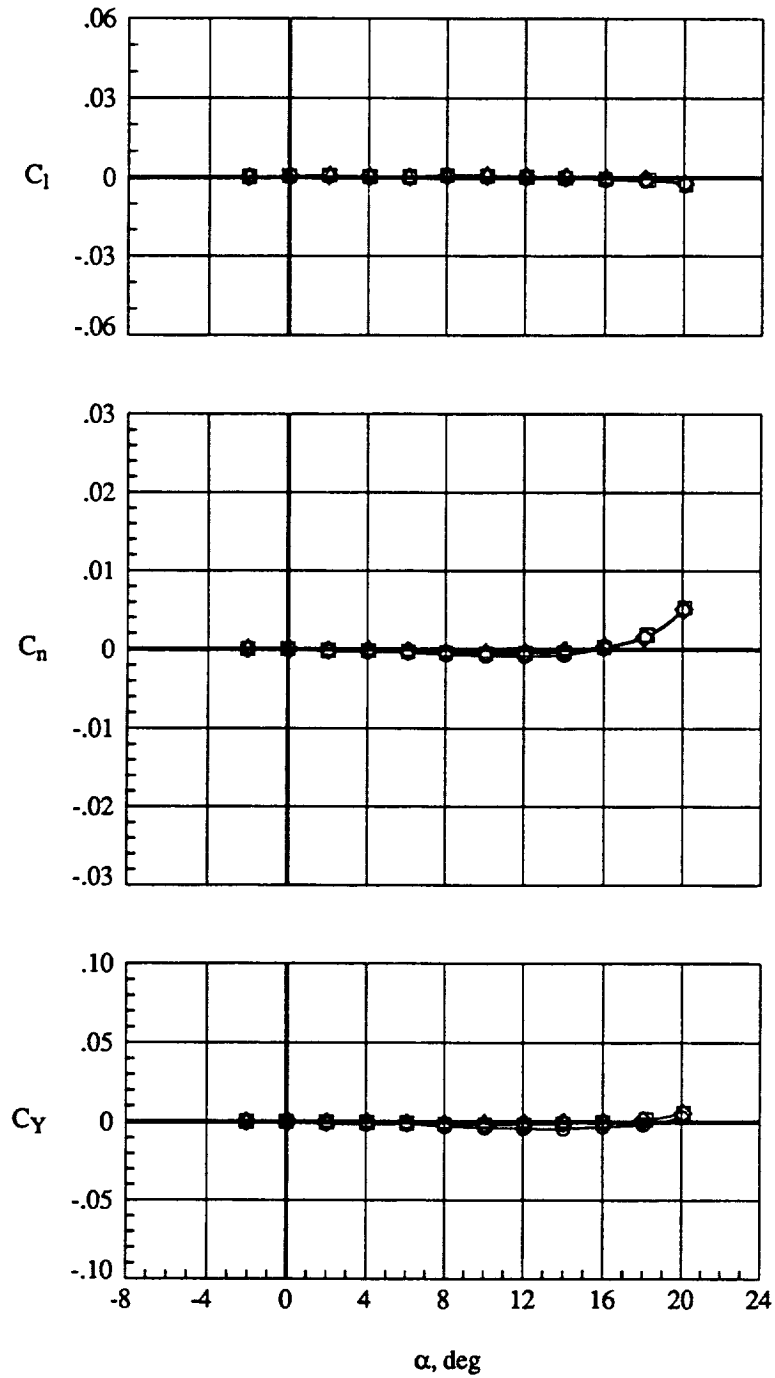


Run	$\beta$ , deg	q	
○	46.	0.	20.
□	47.	0.	50.
◇	48.	0.	70.
△	49.	0.	110.

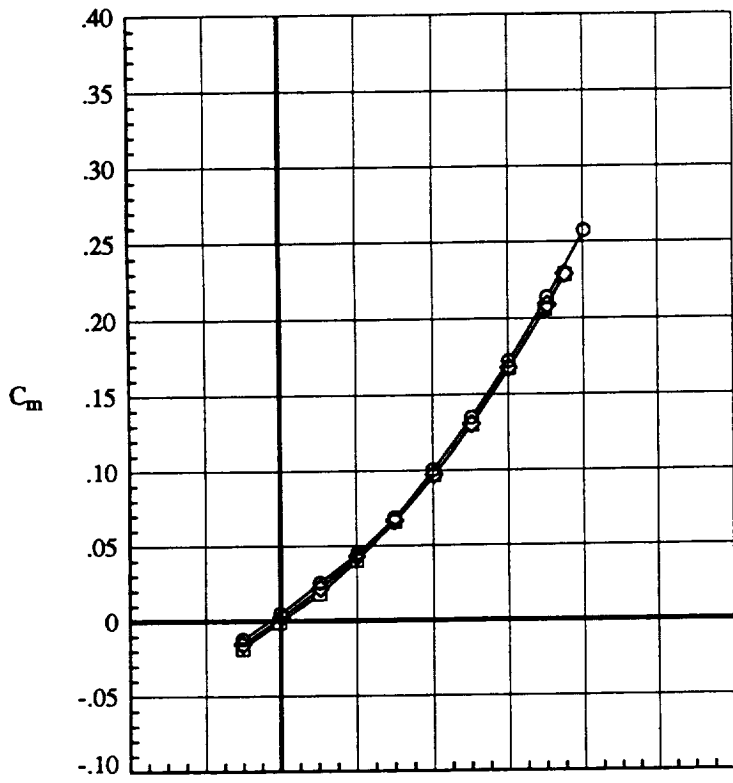


(a) Longitudinal aerodynamics  
 Figure 6. Effect of tunnel dynamic pressure with vortex flap at  $\delta_L = 0^\circ$ ;  $\delta_T = 0^\circ$ .

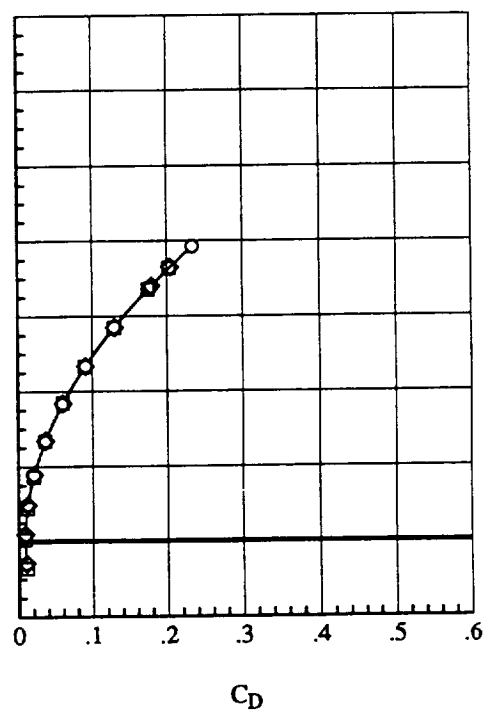
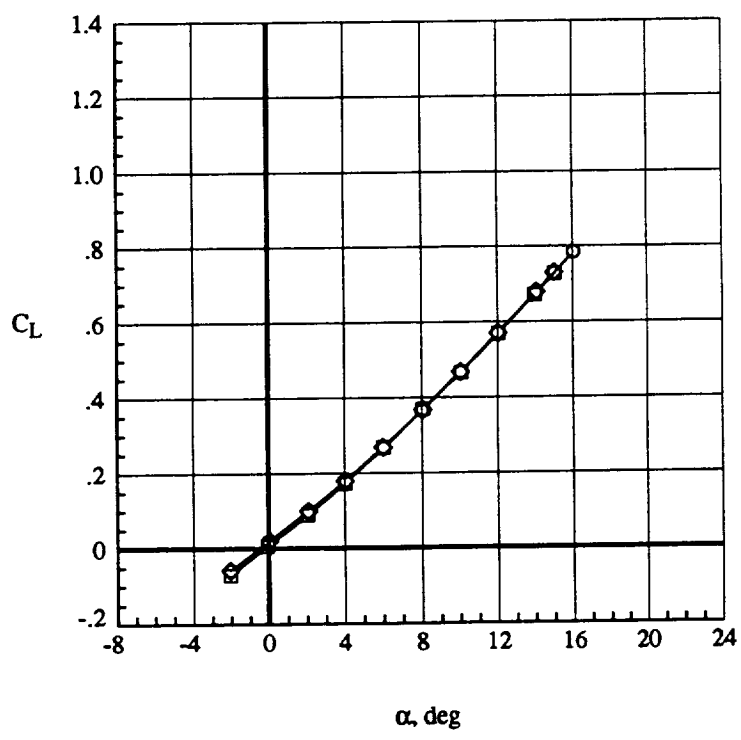
	Run	$\beta$ , deg	q
○	46.	0.	20.
□	47.	0.	50.
◇	48.	0.	70.
△	49.	0.	110.



(b) Lateral aerodynamics  
Figure 6. Concluded.

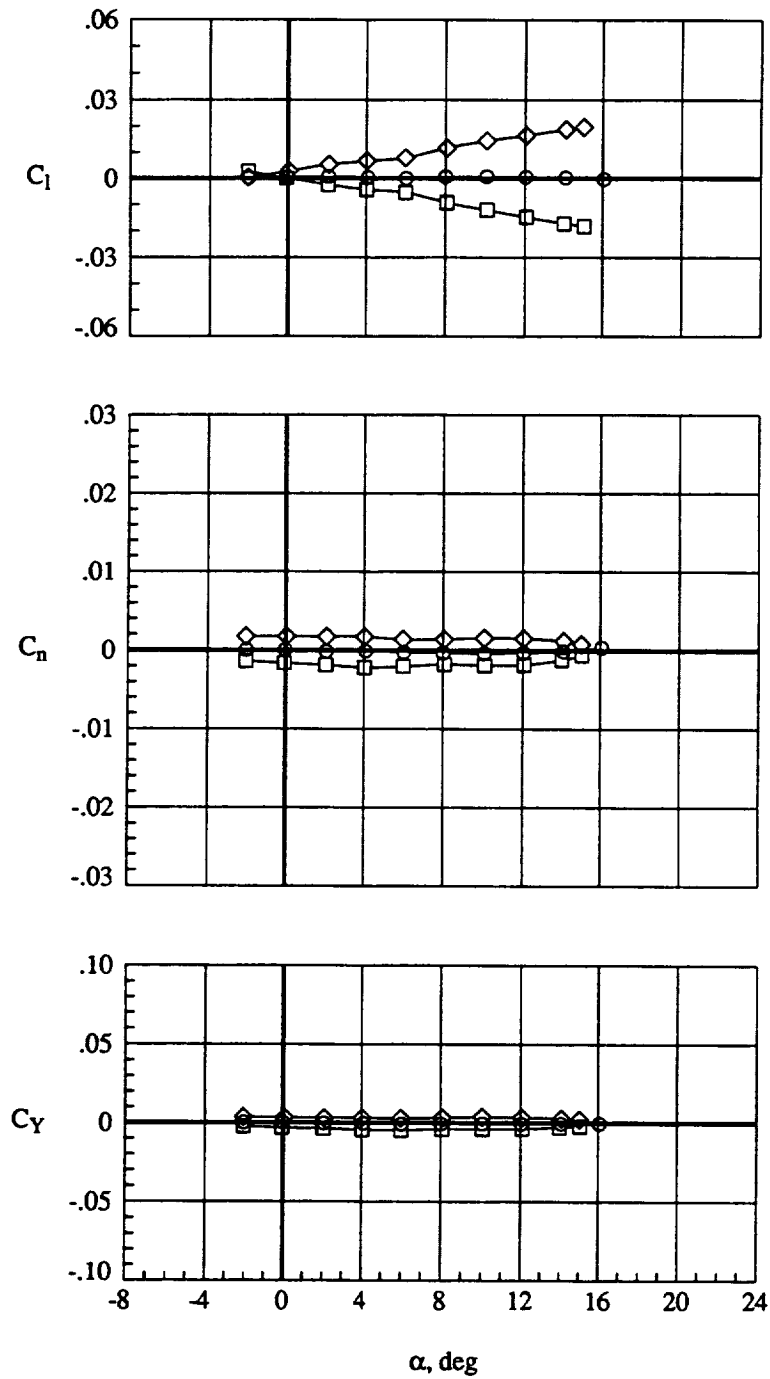


Run	$\beta$ , deg	Configuration
○	49.	$\delta_L = 0^\circ, \delta_T = 0^\circ$
□	50.	$\delta_L = 0^\circ, \delta_T = 0^\circ$
◇	51.	$\delta_L = 0^\circ, \delta_T = 0^\circ$



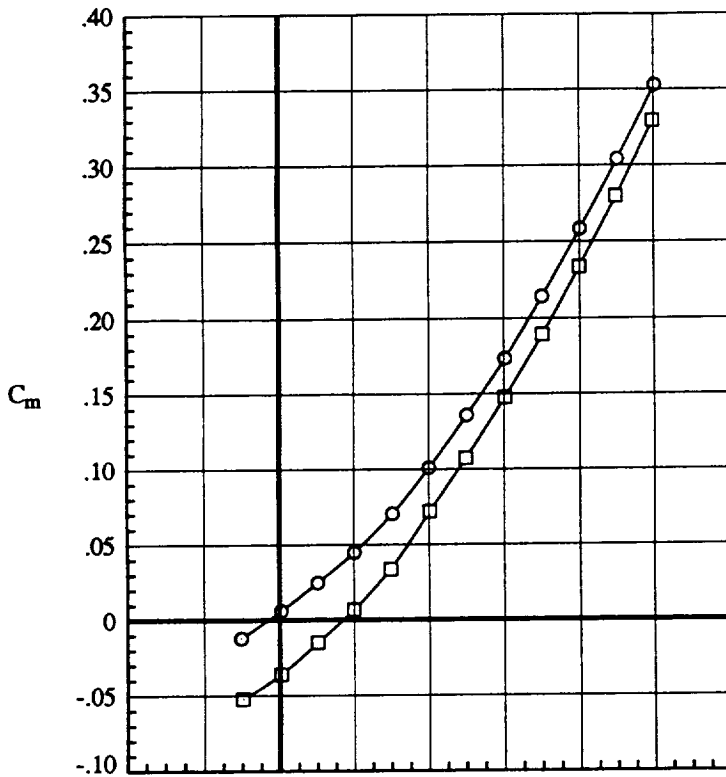
(a) Longitudinal aerodynamics  
 Figure 7. Effect of sideslip with vortex flap at  $\delta_L = 0^\circ, \delta_T = 0^\circ, q=110$  psf.

	Run	$\beta$ , deg	Configuration
○	49.	0.	$\delta_L = 0^\circ, \delta_T = 0^\circ$
□	50.	5.	$\delta_L = 0^\circ, \delta_T = 0^\circ$
◇	51.	-5.	$\delta_L = 0^\circ, \delta_T = 0^\circ$

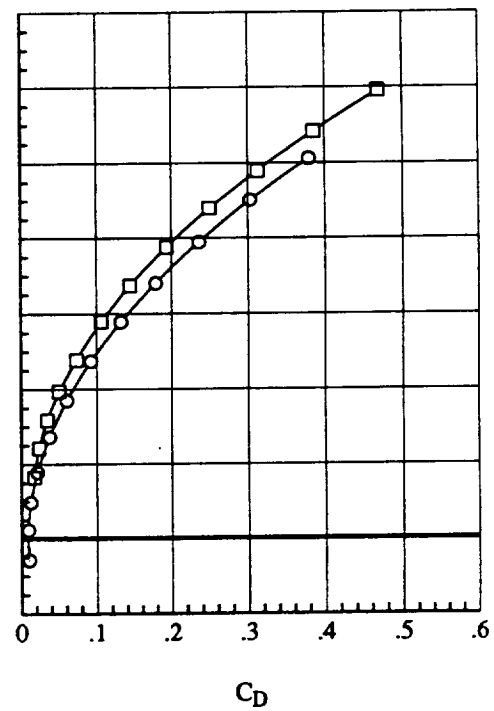
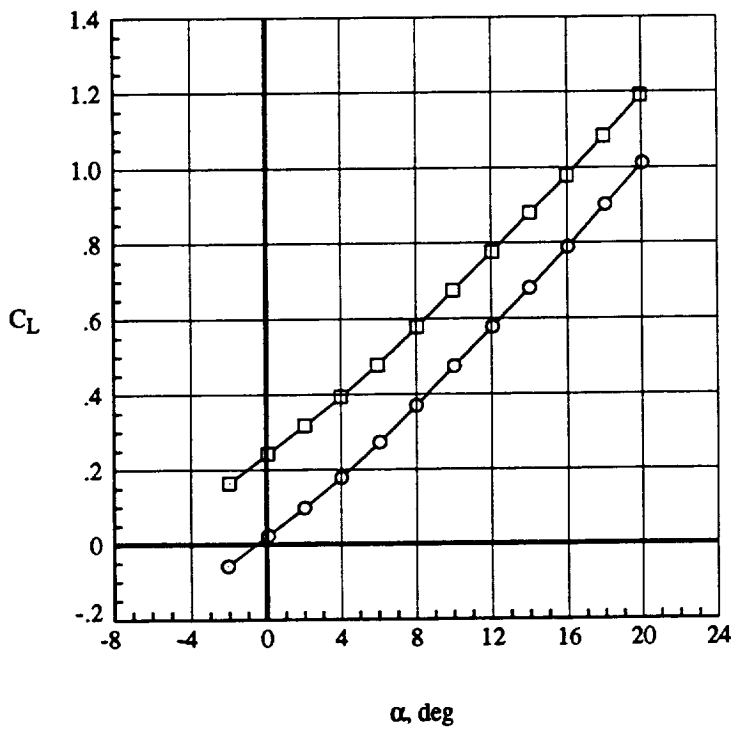


(b) Lateral aerodynamics  
Figure 7. Concluded.



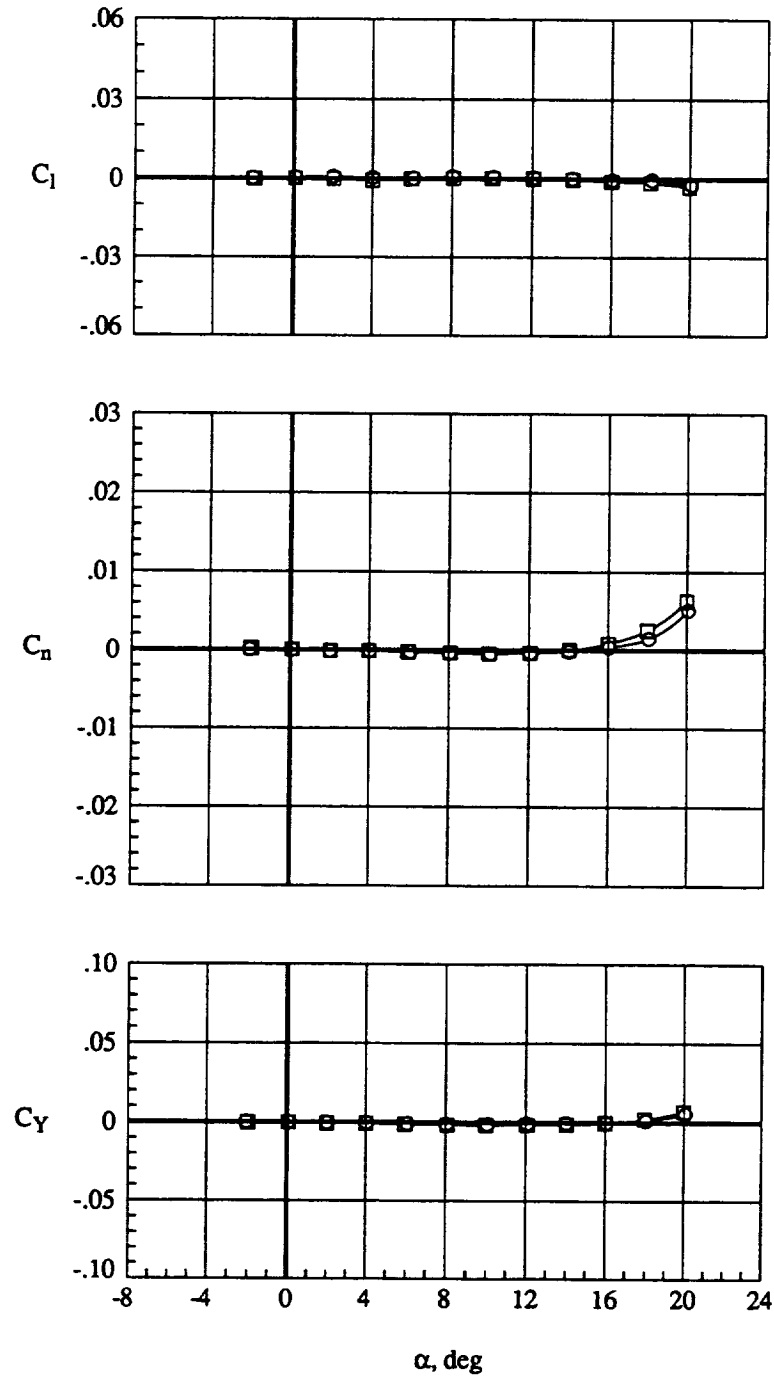


Run	$\beta$ , deg	Configuration
○	48.	$\delta_L = 0^\circ, \delta_T = 0^\circ$
□	52.	$\delta_L = 0^\circ, \delta_T = 20^\circ$



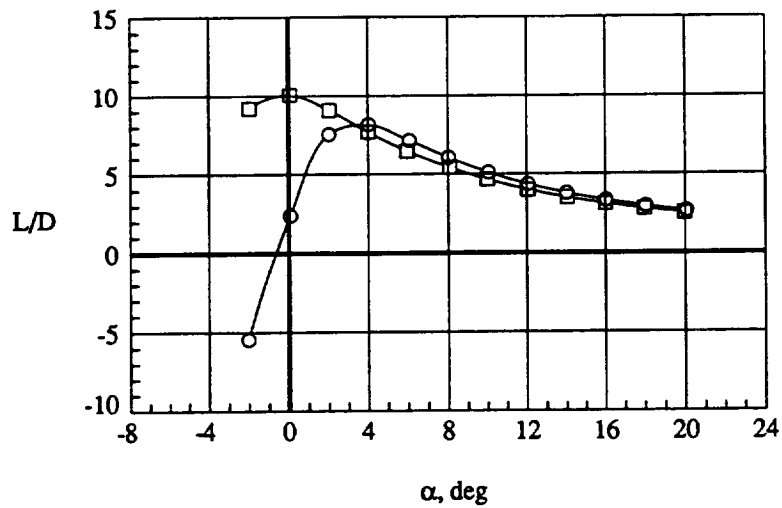
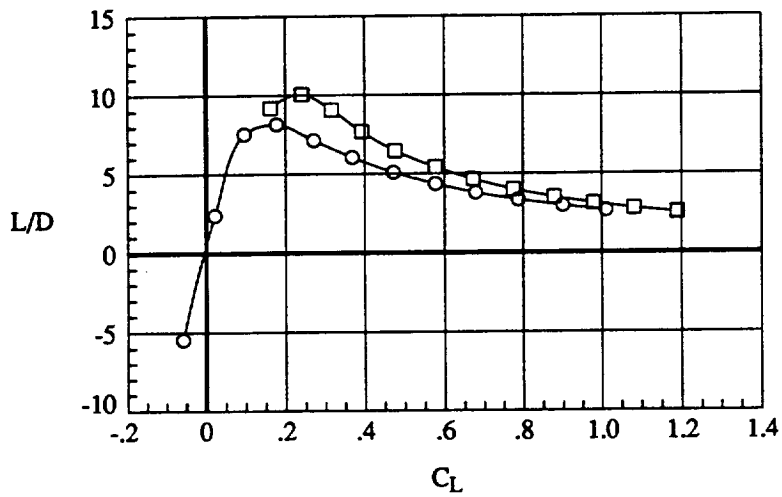
(a) Longitudinal aerodynamics  
 Figure 8. Effect of trailing-edge flaps with vortex flap at  $\delta_L = 0^\circ, q=70$  psf.

	Run	$\beta$ , deg	Configuration
○	48.	0.	$\delta_L = 0^\circ, \delta_T = 0^\circ$
□	52.	0.	$\delta_L = 0^\circ, \delta_T = 20^\circ$

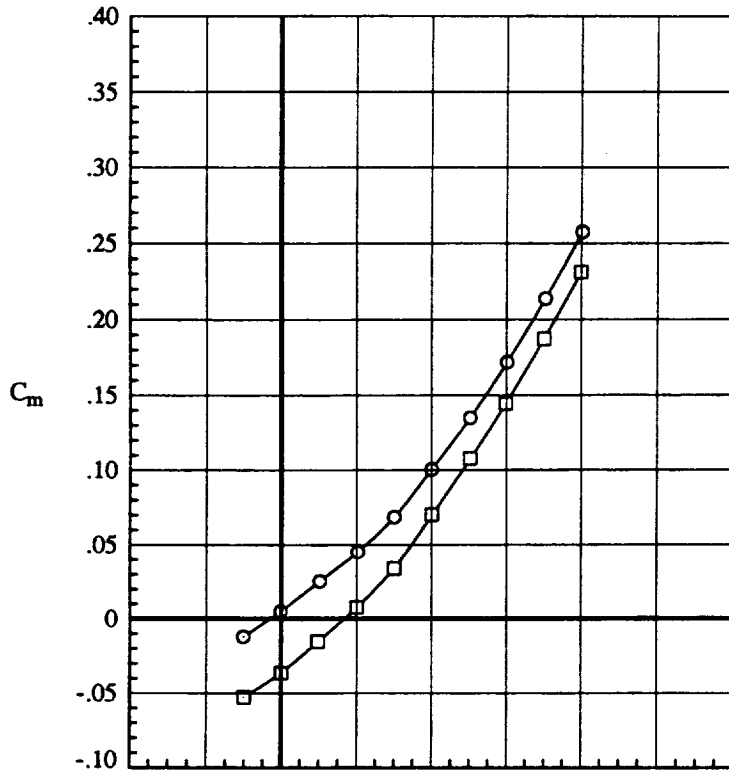


(b) Lateral aerodynamics  
Figure 8. Continued.

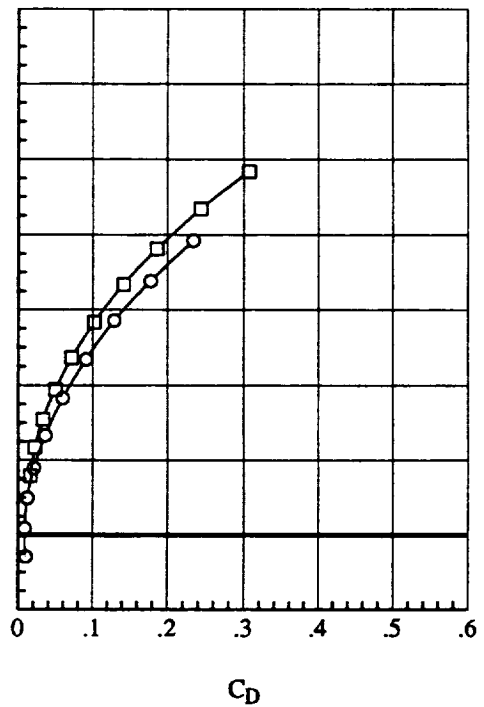
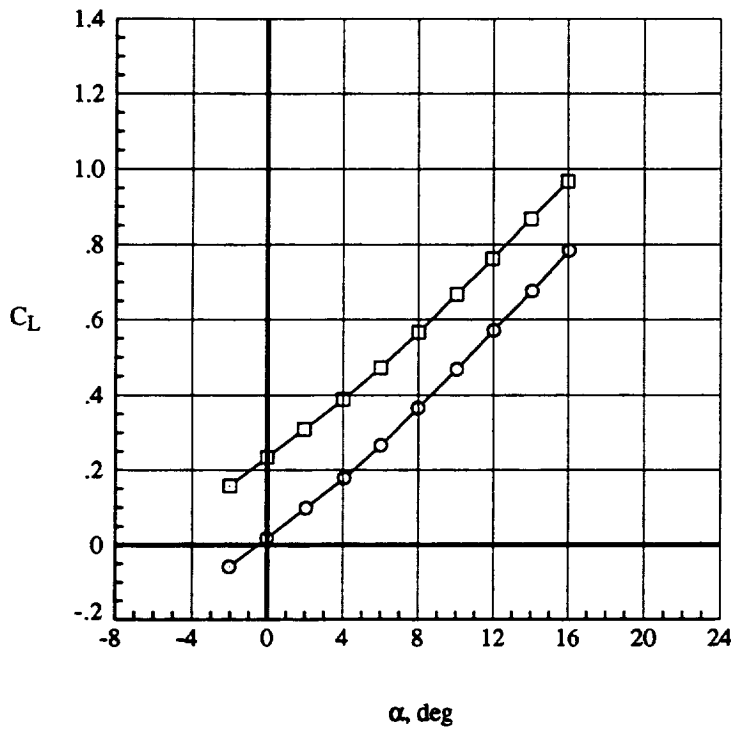
	Run	$\beta$ , deg	Configuration
○	48.	0.	$\delta_L = 0^\circ, \delta_T = 0^\circ$
□	52.	0.	$\delta_L = 0^\circ, \delta_T = 20^\circ$



(c) Lift / Drag performance  
Figure 8. Concluded.



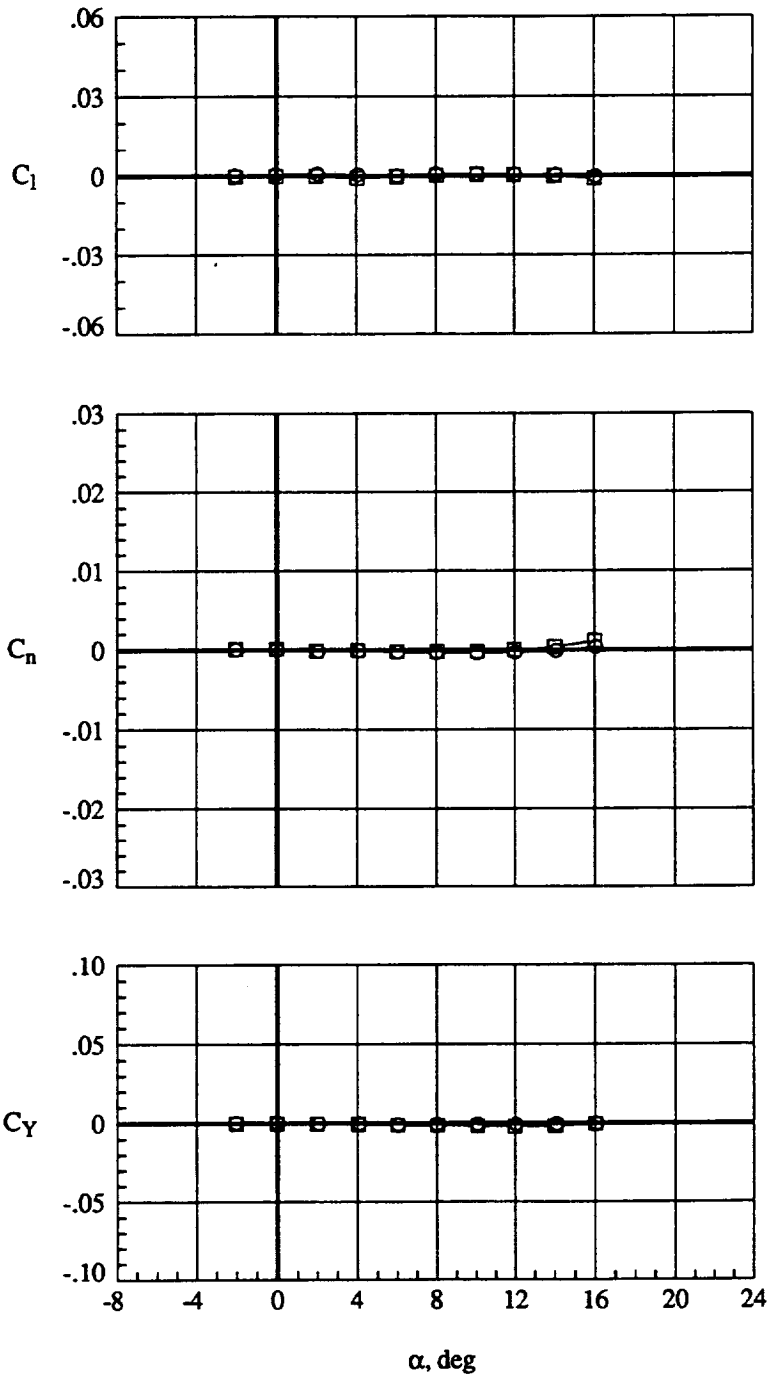
Run	$\beta$ , deg	Configuration	
○	49.	0.	$\delta_L = 0^\circ, \delta_T = 0^\circ$
□	53.	0.	$\delta_L = 0^\circ, \delta_T = 20^\circ$



(a) Longitudinal aerodynamics

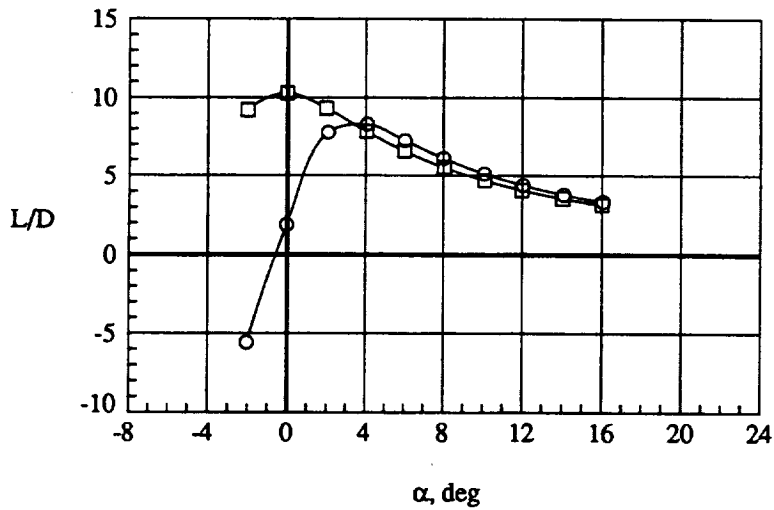
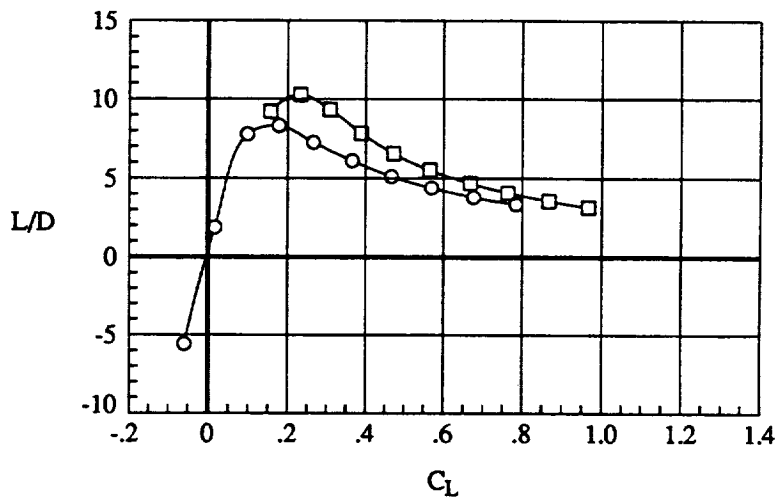
Figure 9. Effect of trailing-edge flaps with vortex flap at  $\delta_L = 0^\circ, q=110$  psf.

	Run	$\beta$ , deg	Configuration
○	49.	0.	$\delta_L = 0^\circ, \delta_T = 0^\circ$
□	53.	0.	$\delta_L = 0^\circ, \delta_T = 20^\circ$

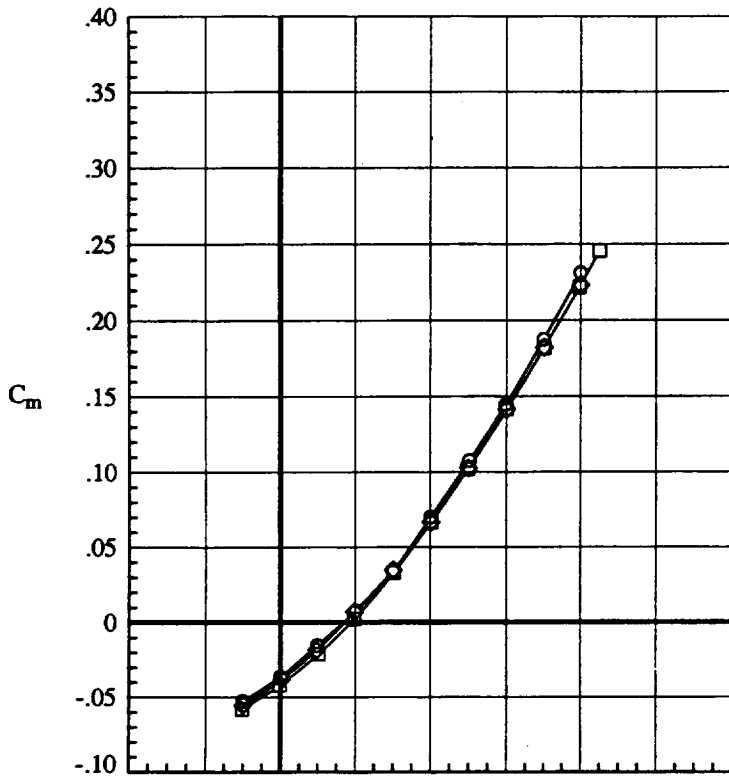


(b) Lateral aerodynamics  
Figure 9. Continued.

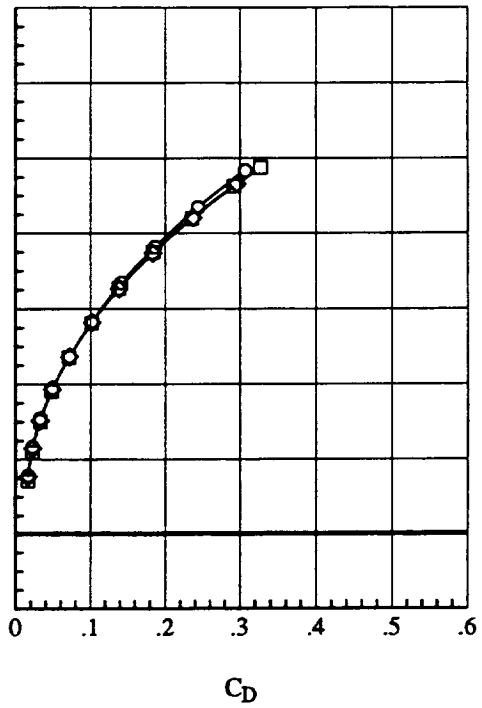
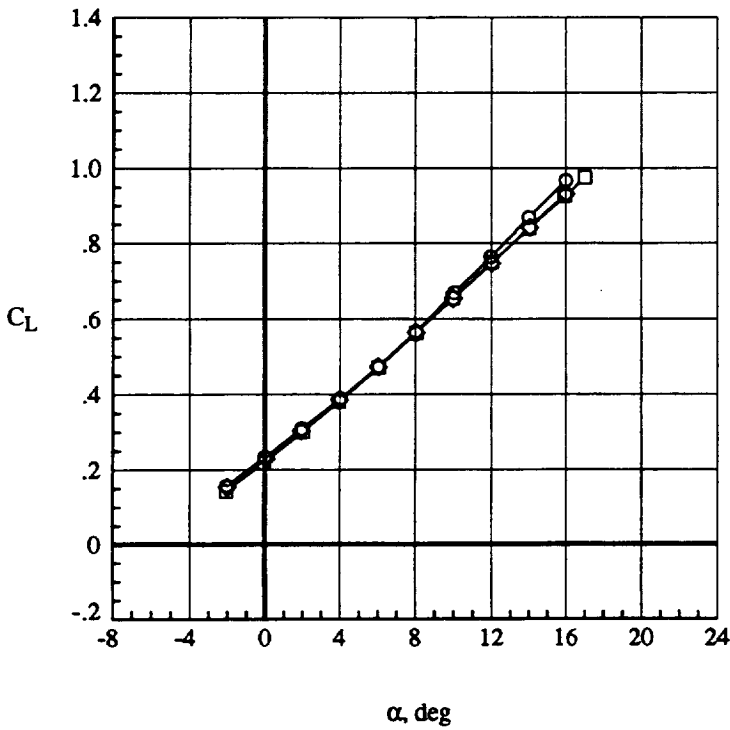
	Run	$\beta$ , deg	Configuration
○	49.	0.	$\delta_L = 0^\circ, \delta_T = 0^\circ$
□	53.	0.	$\delta_L = 0^\circ, \delta_T = 20^\circ$



(c) Lift / Drag performance  
Figure 9. Concluded.

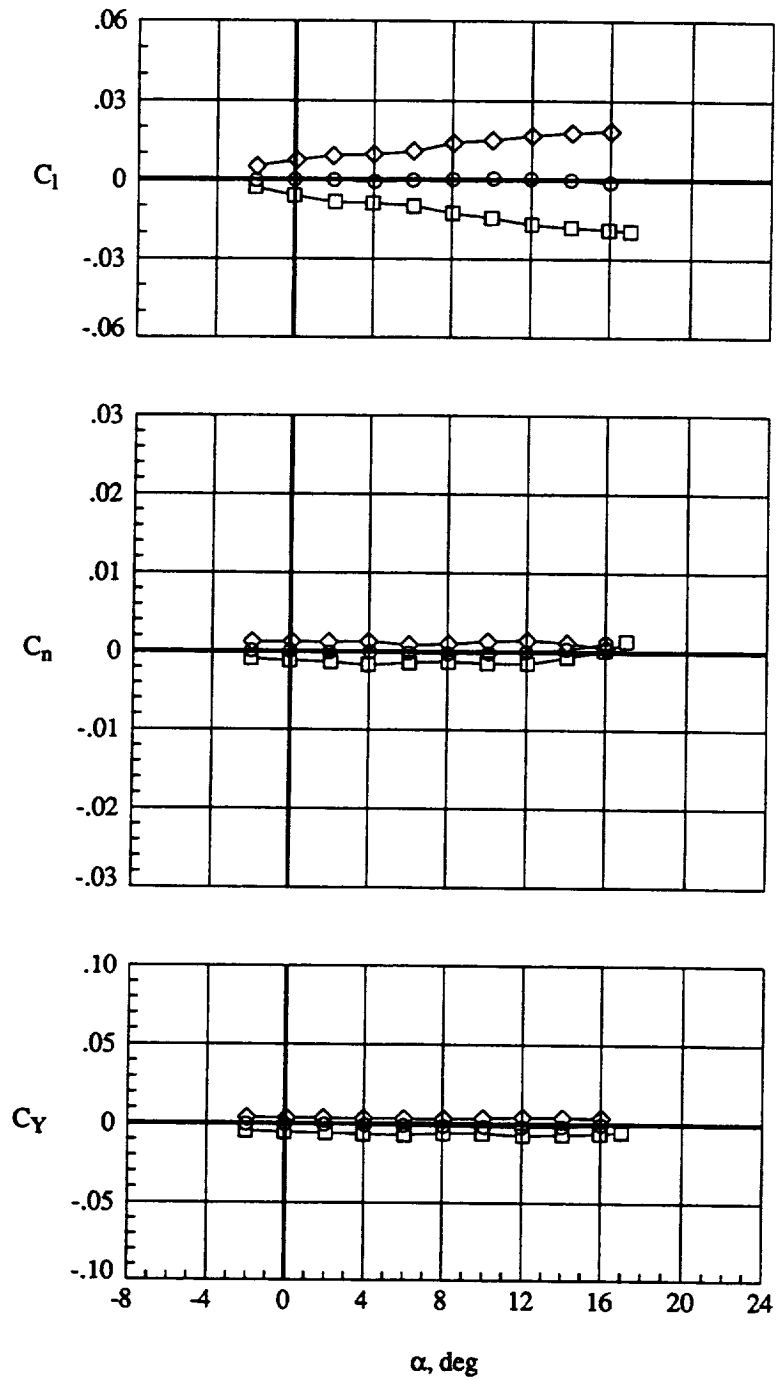


Run	$\beta$ , deg	Configuration
○	53. 0.	$\delta_L = 0^\circ, \delta_T = 20^\circ$
□	54. 5.	$\delta_L = 0^\circ, \delta_T = 20^\circ$
◇	55. -5.	$\delta_L = 0^\circ, \delta_T = 20^\circ$



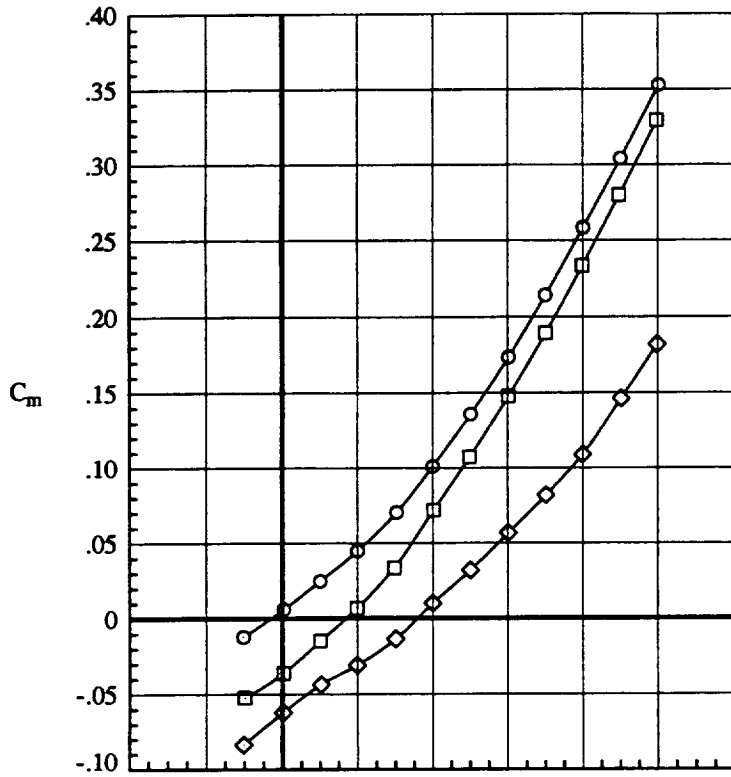
(a) Longitudinal aerodynamics  
 Figure 10. Effect of sideslip with vortex flap at  $\delta_L = 0^\circ; \delta_T = 20^\circ, q = 110$  psf.

	Run	$\beta$ , deg	Configuration
○	53.	0.	$\delta_L = 0^\circ, \delta_T = 20^\circ$
□	54.	5.	$\delta_L = 0^\circ, \delta_T = 20^\circ$
◇	55.	-5.	$\delta_L = 0^\circ, \delta_T = 20^\circ$

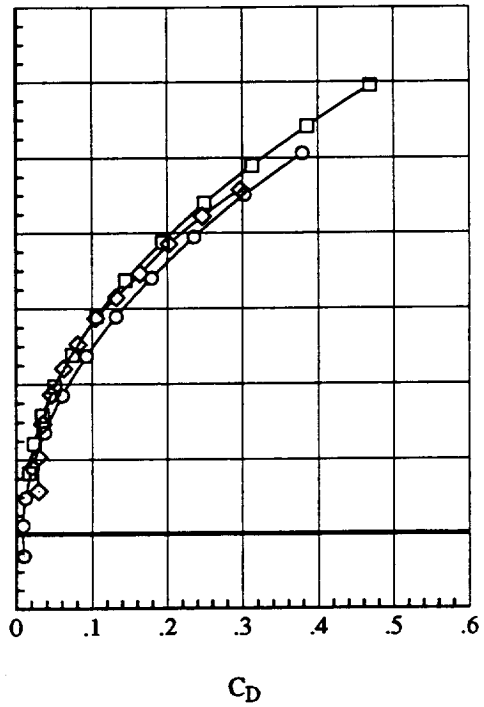
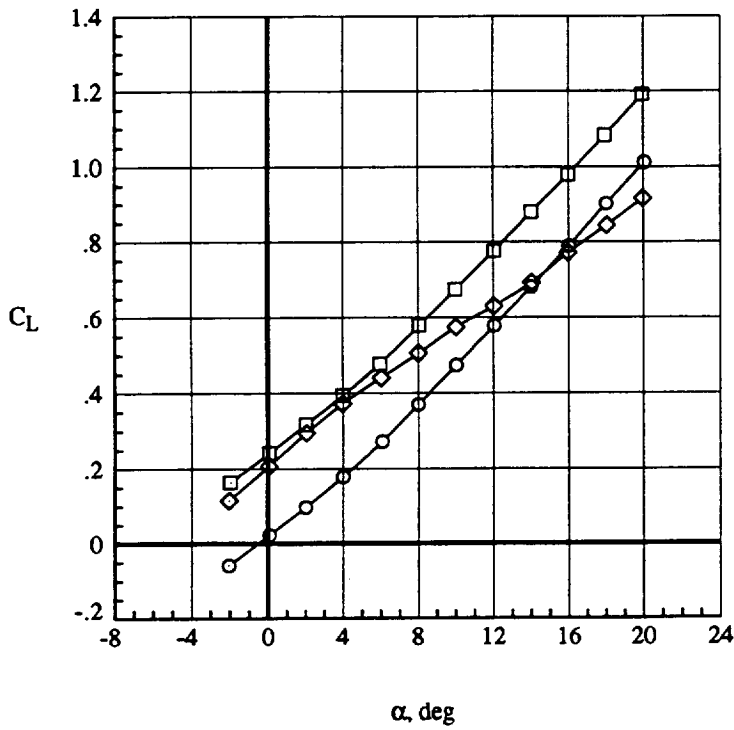


(b) Lateral aerodynamics  
Figure 10. Concluded.



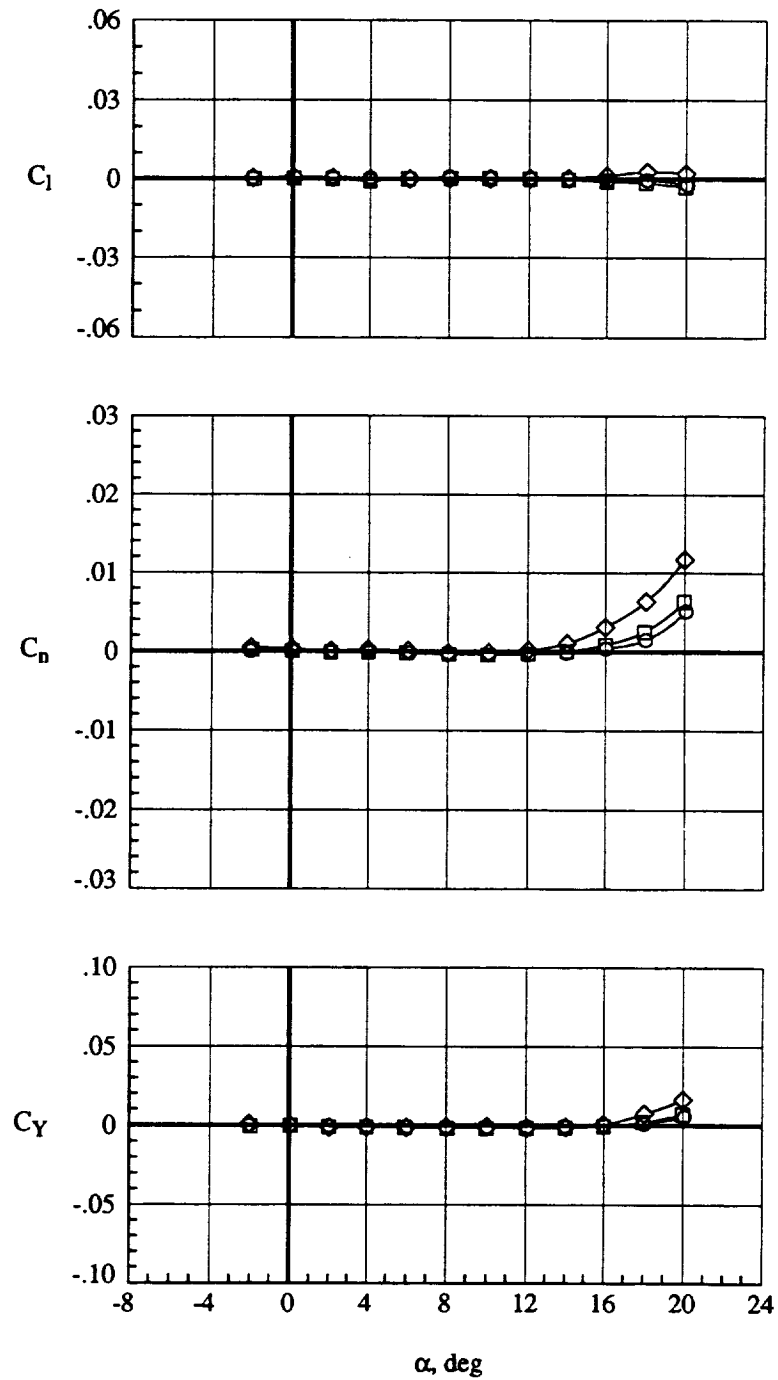


Run	$\beta$ , deg	Configuration	
○	48.	0.	$\delta_L = 0^\circ, \delta_T = 0^\circ$
□	52.	0.	$\delta_L = 0^\circ, \delta_T = 20^\circ$
◇	56.	0.	$\delta_{L-1/2} = 40^\circ / 0^\circ, \delta_T = 20^\circ$



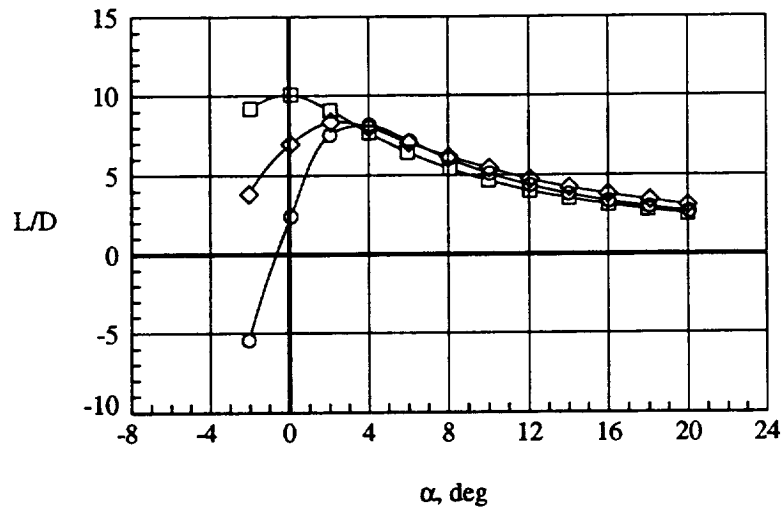
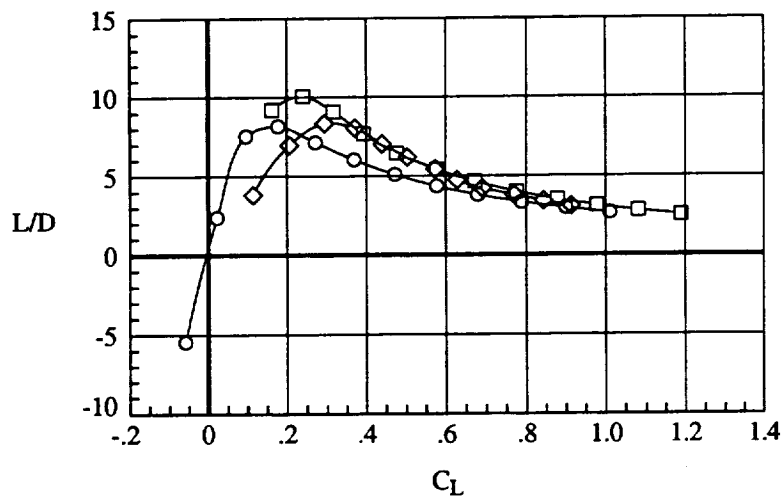
(a) Longitudinal aerodynamics  
 Figure 11. Effect of deflected vortex flap with  $\delta_T = 20^\circ$ ,  $q=70$  psf.

	Run	$\beta$ , deg	Configuration
○	48.	0.	$\delta_L = 0^\circ, \delta_T = 0^\circ$
□	52.	0.	$\delta_L = 0^\circ, \delta_T = 20^\circ$
◇	56.	0.	$\delta_{L1/2} = 40^\circ / 0^\circ, \delta_T = 20^\circ$

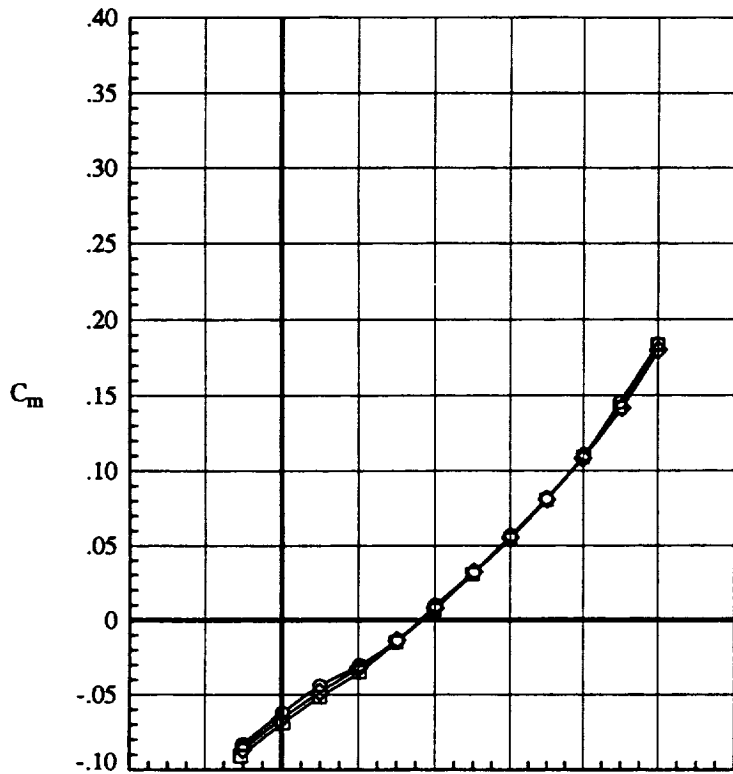


(b) Lateral aerodynamics  
Figure 11. Continued.

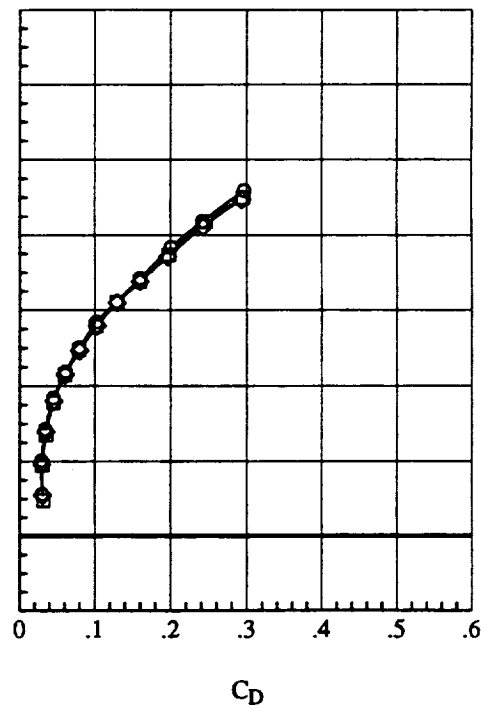
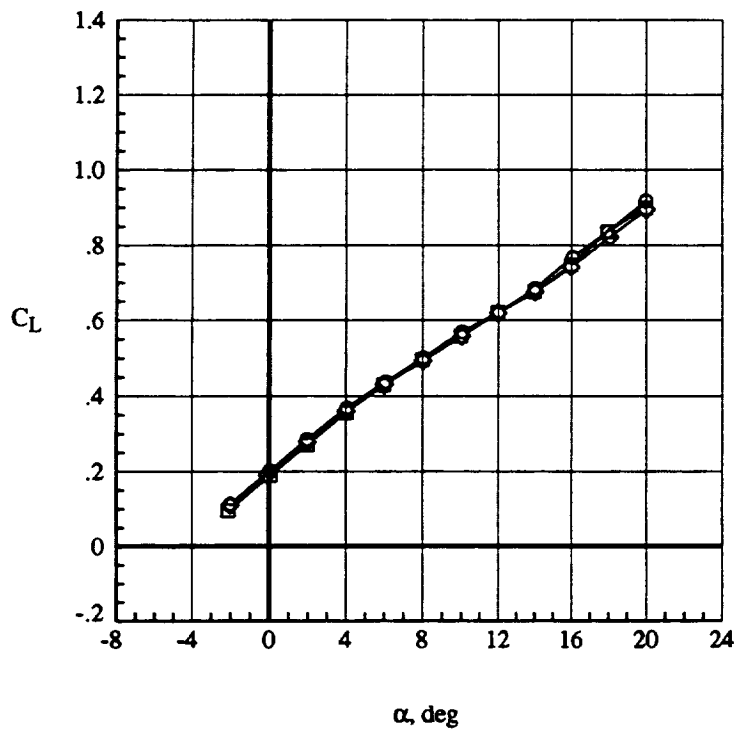
	Run	$\beta$ , deg	Configuration
○	48.	0.	$\delta_L = 0^\circ, \delta_T = 0^\circ$
□	52.	0.	$\delta_L = 0^\circ, \delta_T = 20^\circ$
◇	56.	0.	$\delta_{L1/2} = 40^\circ / 0^\circ, \delta_T = 20^\circ$



(c) Lift / Drag performance  
Figure 11. Concluded.



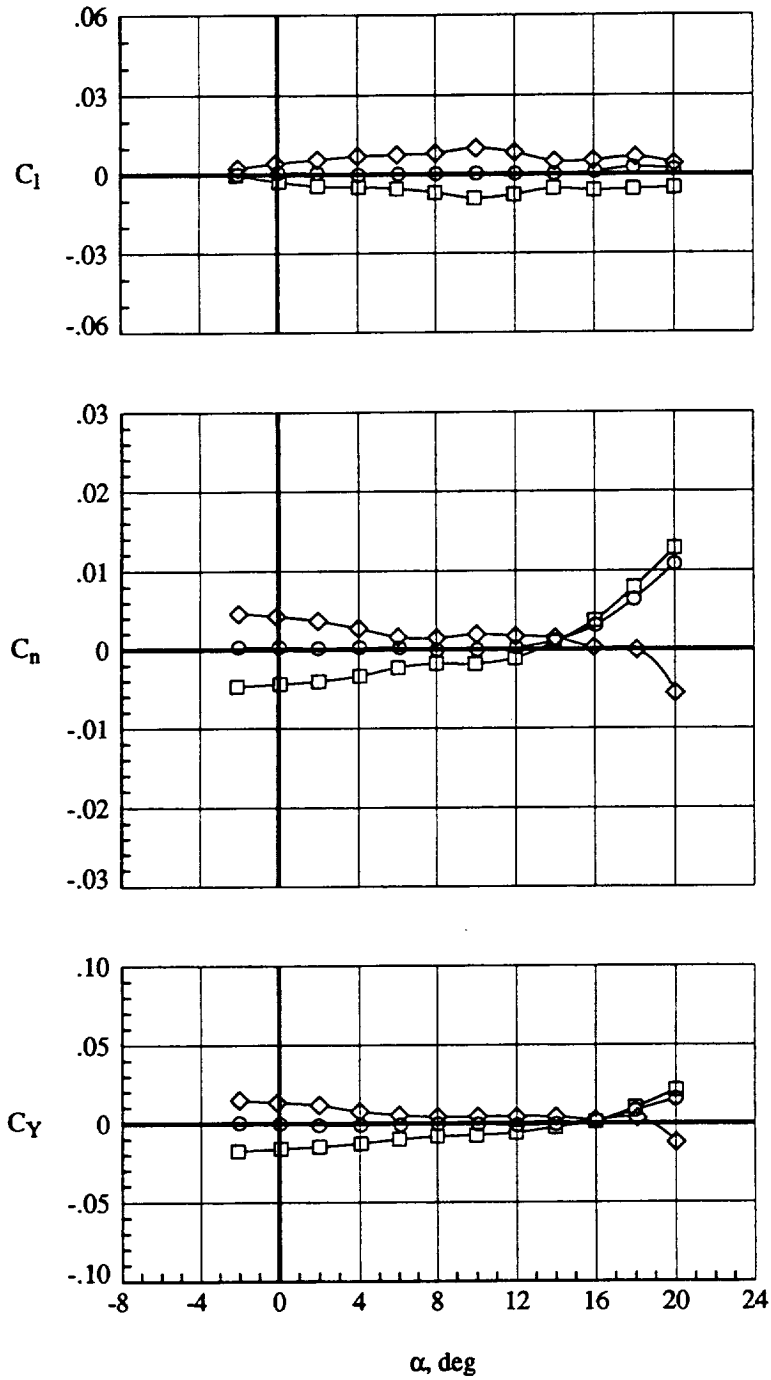
Run	$\beta$ , deg	Configuration
○	57.	0. $\delta_{L1/2} = 40^\circ / 0^\circ, \delta_T = 20^\circ$
□	58.	5. $\delta_{L1/2} = 40^\circ / 0^\circ, \delta_T = 20^\circ$
◇	59.	-5. $\delta_{L1/2} = 40^\circ / 0^\circ, \delta_T = 20^\circ$



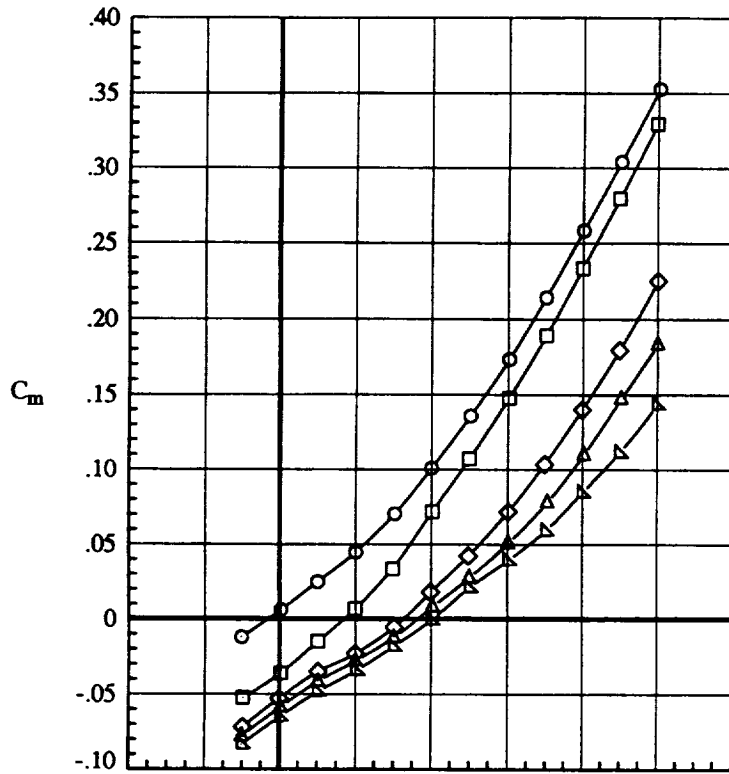
(a) Longitudinal aerodynamics

Figure 12. Effect of sideslip with deflected vortex flap and  $\delta_T = 20^\circ$ ;  $q = 110$  psf.

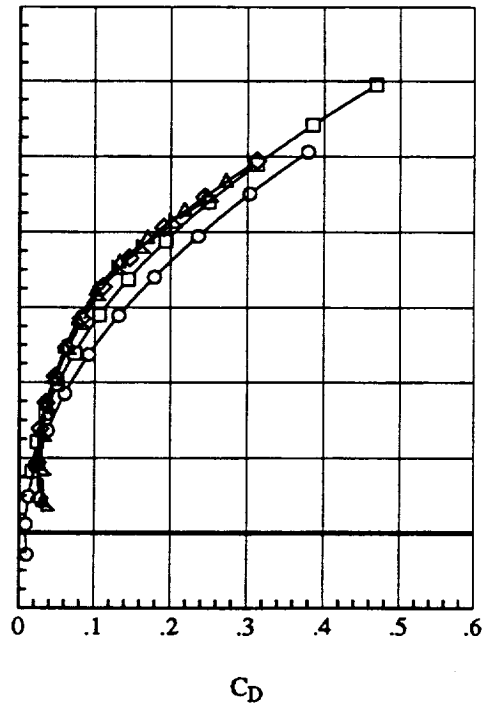
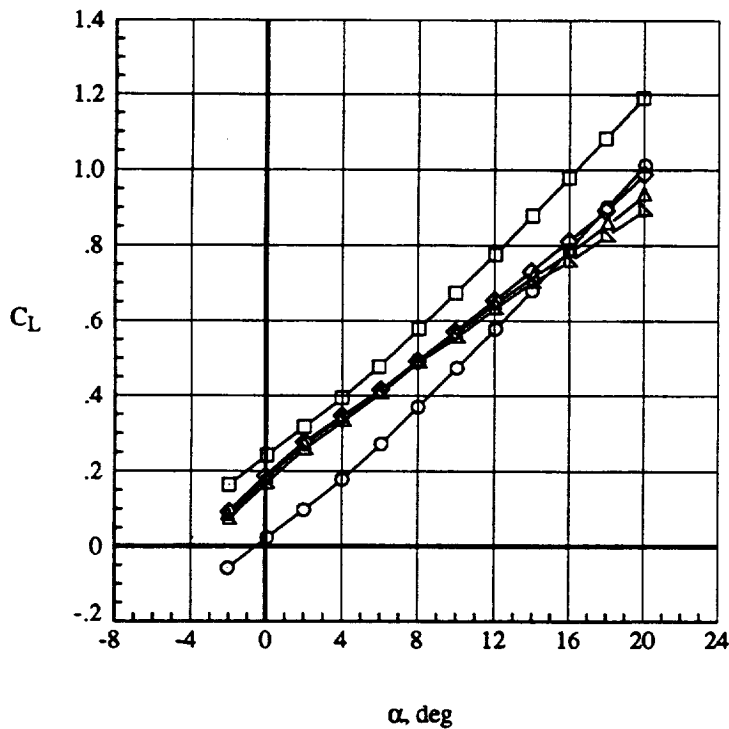
	Run	$\beta$ , deg	Configuration
○	57.	0.	$\delta_{L1/2} = 40^\circ / 0^\circ, \delta_T = 20^\circ$
□	58.	5.	$\delta_{L1/2} = 40^\circ / 0^\circ, \delta_T = 20^\circ$
◇	59.	-5.	$\delta_{L1/2} = 40^\circ / 0^\circ, \delta_T = 20^\circ$



(b) Lateral aerodynamics  
Figure 12. Concluded.



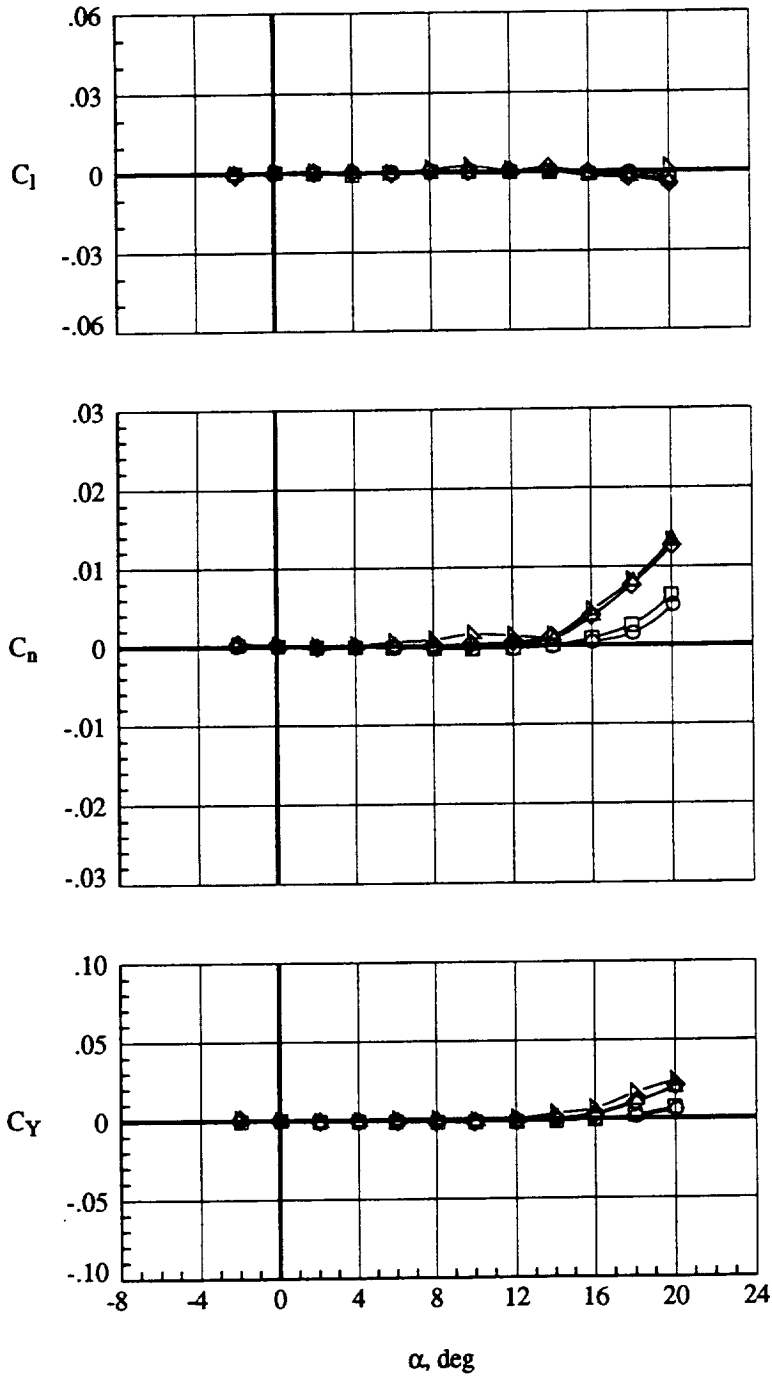
Run	$\beta$ , deg	Configuration	
○	48.	0.	$\delta_L = 0^\circ, \delta_T = 0^\circ$
□	52.	0.	$\delta_L = 0^\circ, \delta_T = 20^\circ$
◇	64.	0.	$\delta_{L_{1/2}} = 30^\circ / 26.4^\circ, \delta_T = 20^\circ$
△	60.	0.	$\delta_{L_{1/2}} = 40^\circ / 26.4^\circ, \delta_T = 20^\circ$
▽	68.	0.	$\delta_{L_{1/2}} = 50^\circ / 26.4^\circ, \delta_T = 20^\circ$



(a) Longitudinal aerodynamics

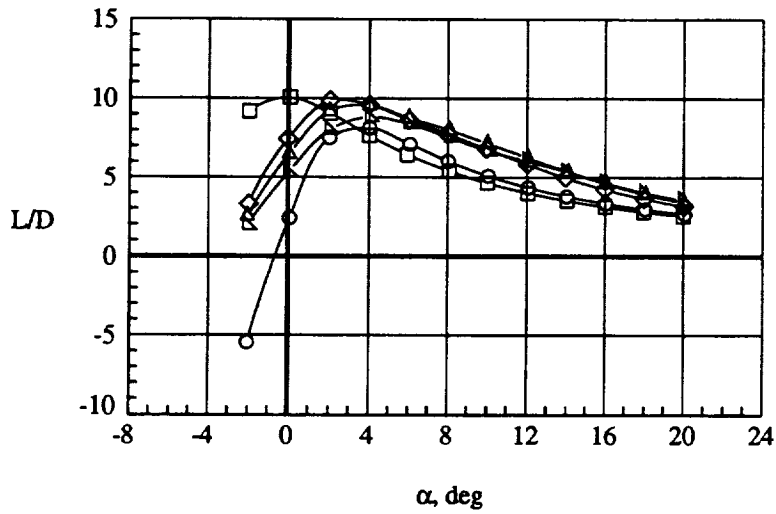
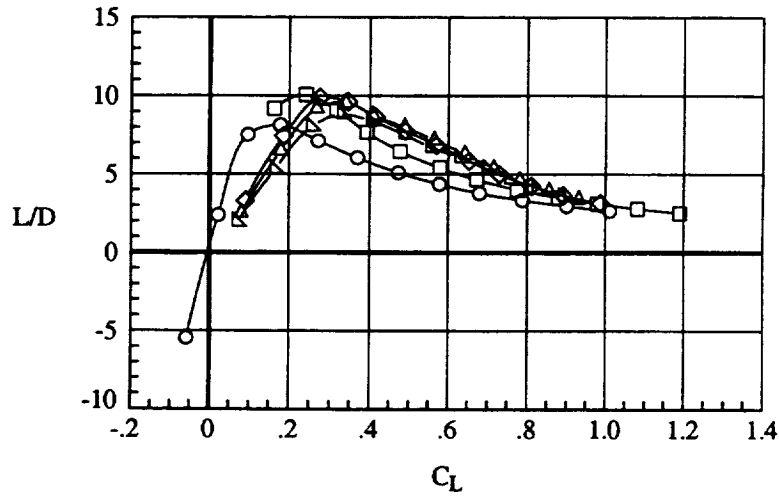
Figure 13. Effect of deflecting the vortex flap with the outboard leading-edge flap.  $\delta_T = 20^\circ, q=70$  psf.

	Run	$\beta$ , deg	Configuration
○	48.	0.	$\delta_L = 0^\circ, \delta_T = 0^\circ$
□	52.	0.	$\delta_L = 0^\circ, \delta_T = 20^\circ$
◇	64.	0.	$\delta_{L1/2} = 30^\circ / 26.4^\circ, \delta_T = 20^\circ$
△	60.	0.	$\delta_{L1/2} = 40^\circ / 26.4^\circ, \delta_T = 20^\circ$
▴	68.	0.	$\delta_{L1/2} = 50^\circ / 26.4^\circ, \delta_T = 20^\circ$



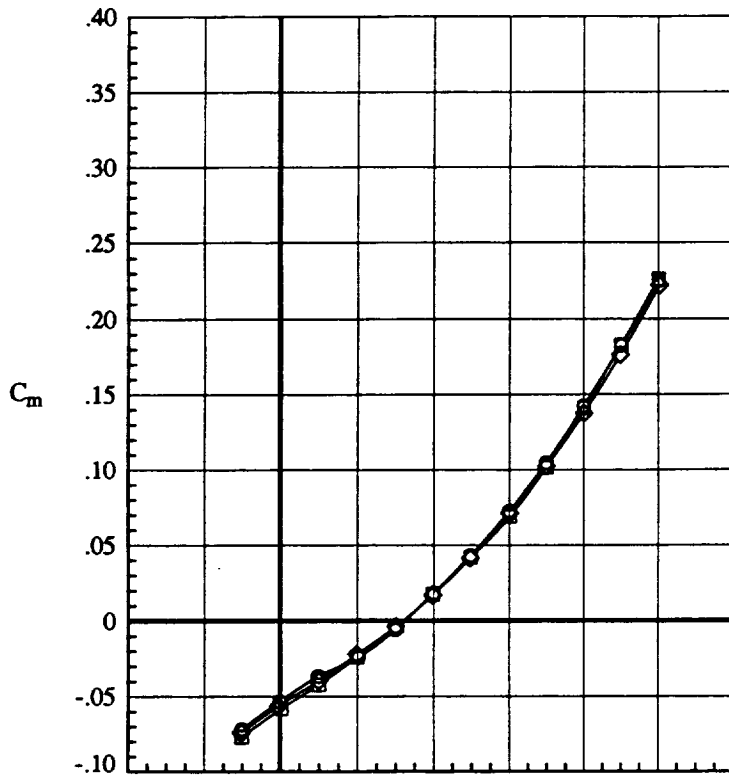
(b) Lateral aerodynamics  
Figure 13. Continued.

	Run	$\beta$ , deg	Configuration
○	48.	0.	$\delta_L = 0^\circ, \delta_T = 0^\circ$
□	52.	0.	$\delta_L = 0^\circ, \delta_T = 20^\circ$
◇	64.	0.	$\delta_{L1/2} = 30^\circ / 26.4^\circ, \delta_T = 20^\circ$
△	60.	0.	$\delta_{L1/2} = 40^\circ / 26.4^\circ, \delta_T = 20^\circ$
▴	68.	0.	$\delta_{L1/2} = 50^\circ / 26.4^\circ, \delta_T = 20^\circ$

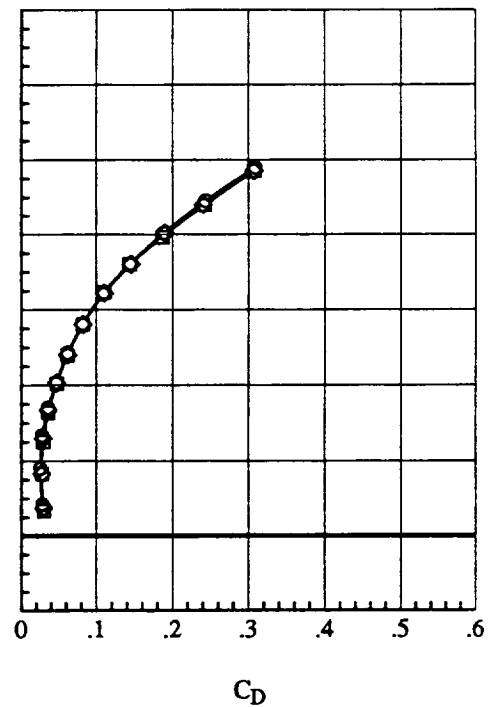
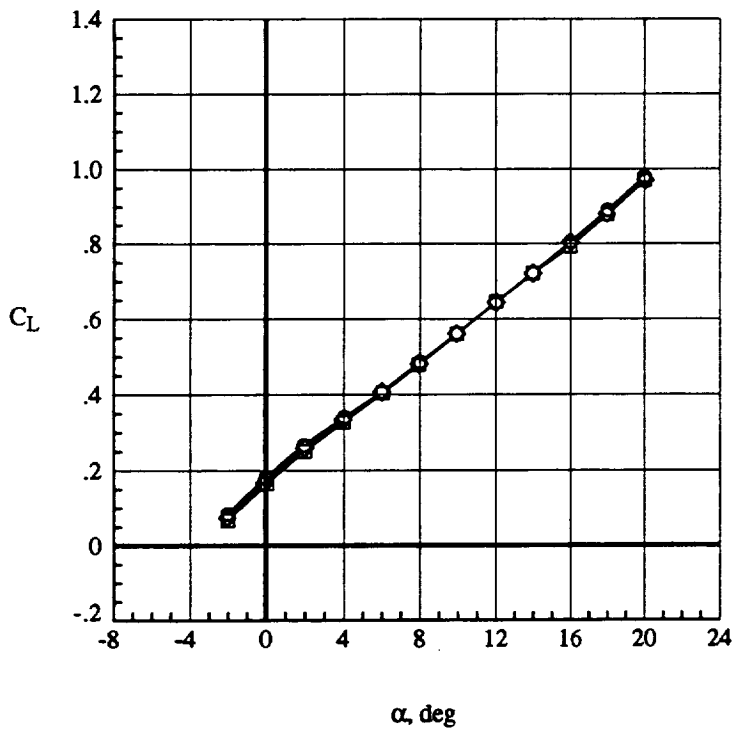


(c) Lift / Drag performance  
Figure 13. Concluded.





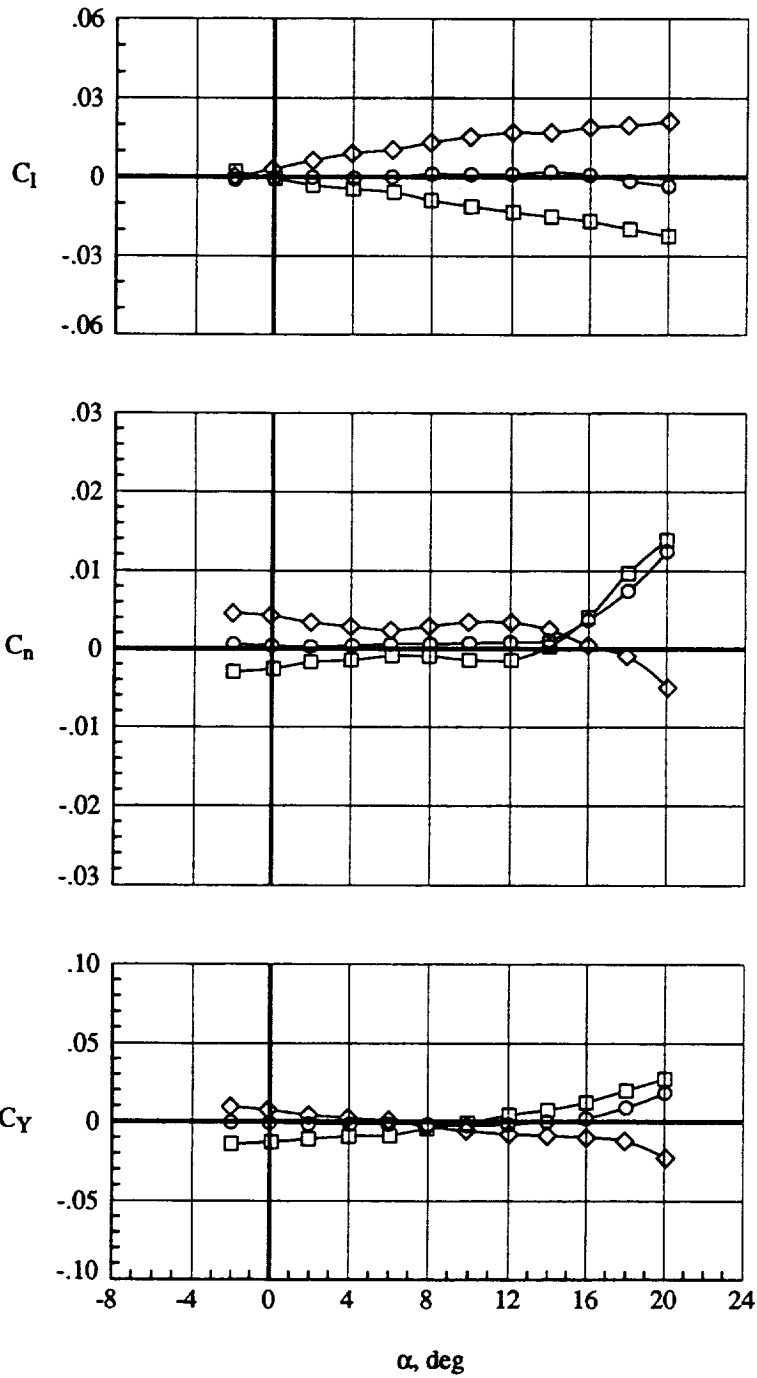
Run	$\beta$ , deg	Configuration
○	65.	0. $\delta_{L_{1/2}} = 30^\circ / 26.4^\circ, \delta_T = 20^\circ$
□	66.	5. $\delta_{L_{1/2}} = 30^\circ / 26.4^\circ, \delta_T = 20^\circ$
◇	67.	-5. $\delta_{L_{1/2}} = 30^\circ / 26.4^\circ, \delta_T = 20^\circ$



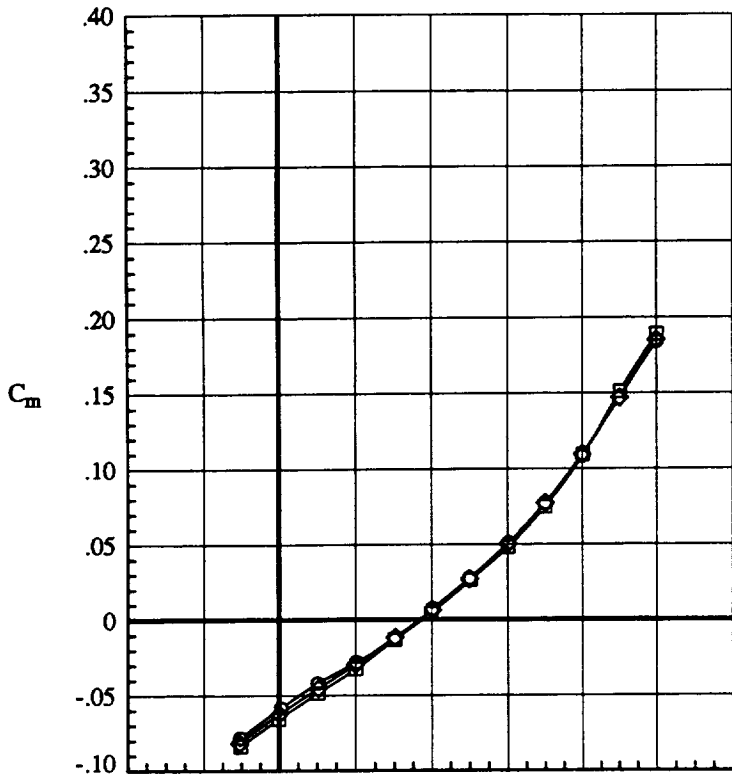
(a) Longitudinal aerodynamics

Figure 14. Effect of sideslip with vortex flap at  $\delta_{L_1} = 30^\circ$  and outboard leading-edge flap at  $\delta_{L_2} = 26.4^\circ, \delta_T = 20^\circ, q = 110$  psf.

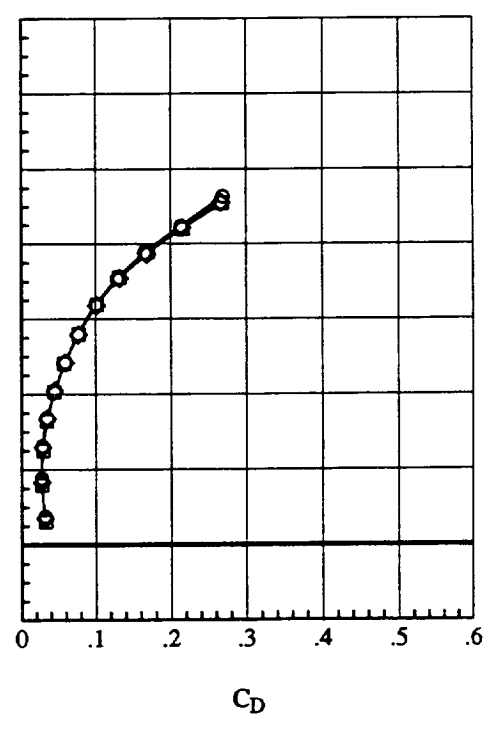
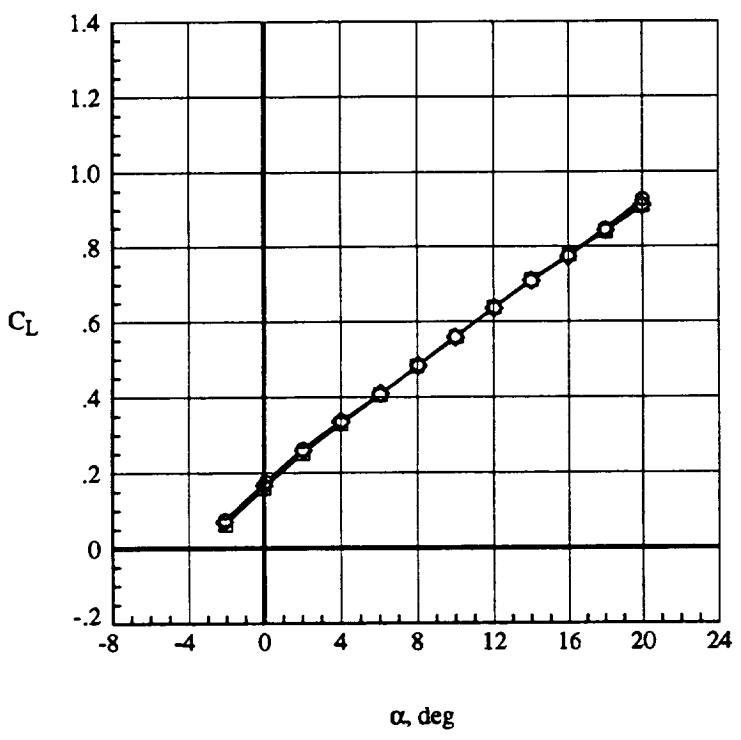
	Run	$\beta$ , deg	Configuration
○	65.	0.	$\delta_{L_{1/2}} = 30^\circ / 26.4^\circ, \delta_T = 20^\circ$
□	66.	5.	$\delta_{L_{1/2}} = 30^\circ / 26.4^\circ, \delta_T = 20^\circ$
◇	67.	-5.	$\delta_{L_{1/2}} = 30^\circ / 26.4^\circ, \delta_T = 20^\circ$



(b) Lateral aerodynamics  
Figure 14. Concluded.

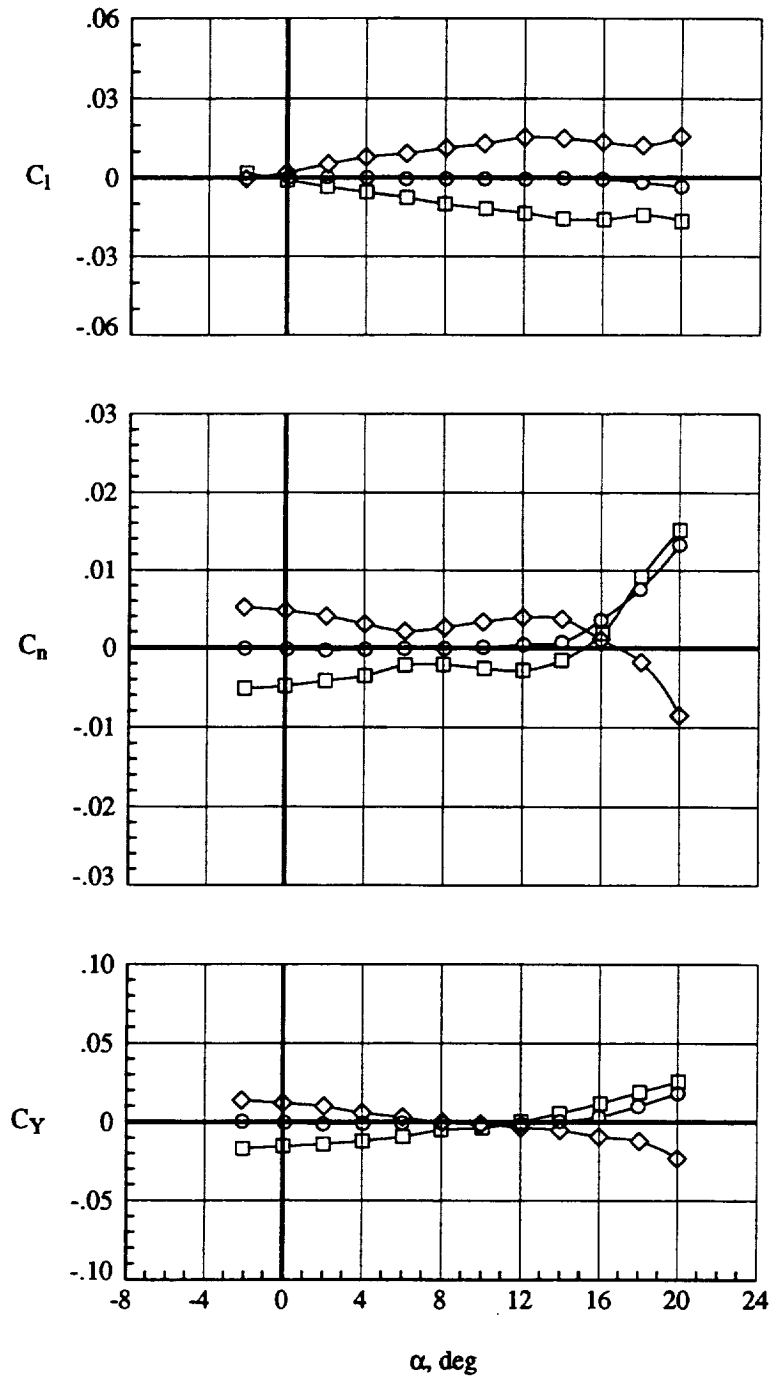


Run	$\beta$ , deg	Configuration
○	61. 0.	$\delta_{L_{1/2}} = 40^\circ / 26.4^\circ, \delta_T = 20^\circ$
□	62. 5.	$\delta_{L_{1/2}} = 40^\circ / 26.4^\circ, \delta_T = 20^\circ$
◇	63. -5.	$\delta_{L_{1/2}} = 40^\circ / 26.4^\circ, \delta_T = 20^\circ$

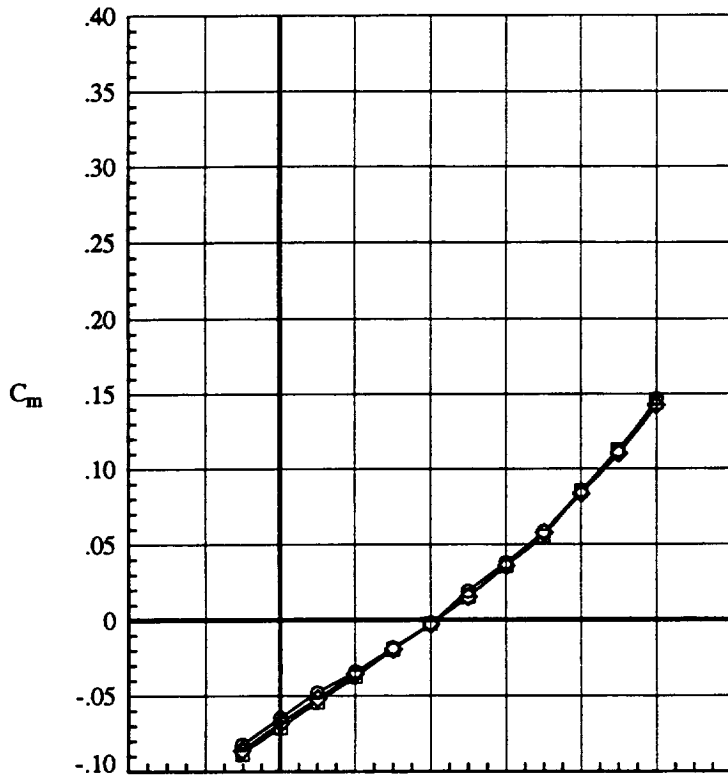


(a) Longitudinal aerodynamics  
 Figure 15. Effect of sideslip with vortex flap at  $\delta_{L_1} = 40^\circ$  and outboard leading-edge flap at  $\delta_{L_2} = 26.4^\circ, \delta_T = 20^\circ, q=110$  psf.

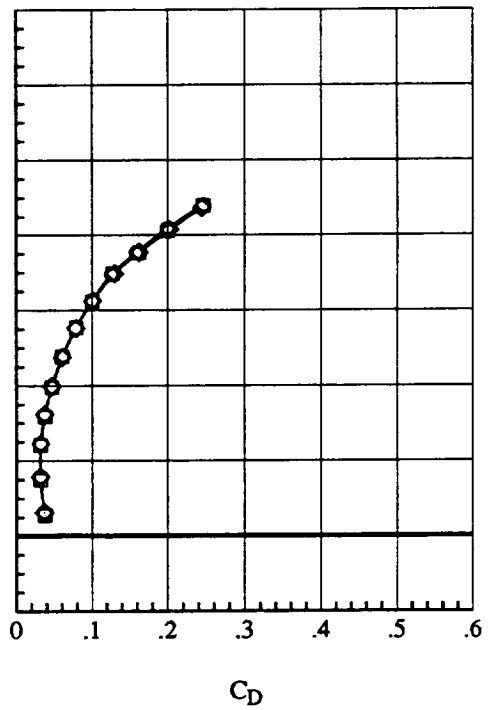
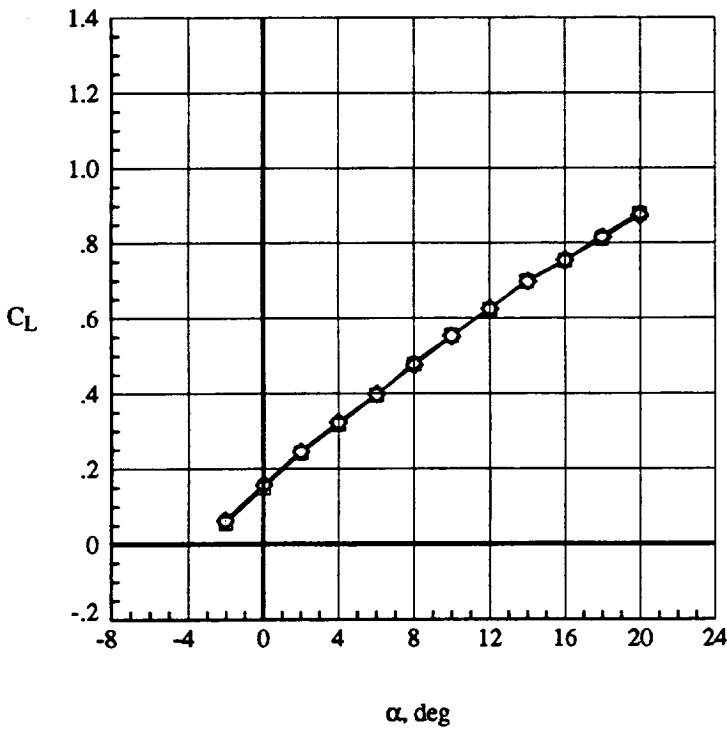
	Run	$\beta$ , deg	Configuration
○	61.	0.	$\delta_{L_{1/2}} = 40^\circ / 26.4^\circ, \delta_T = 20^\circ$
□	62.	5.	$\delta_{L_{1/2}} = 40^\circ / 26.4^\circ, \delta_T = 20^\circ$
◇	63.	-5.	$\delta_{L_{1/2}} = 40^\circ / 26.4^\circ, \delta_T = 20^\circ$



(b) Lateral aerodynamics  
Figure 15. Concluded.



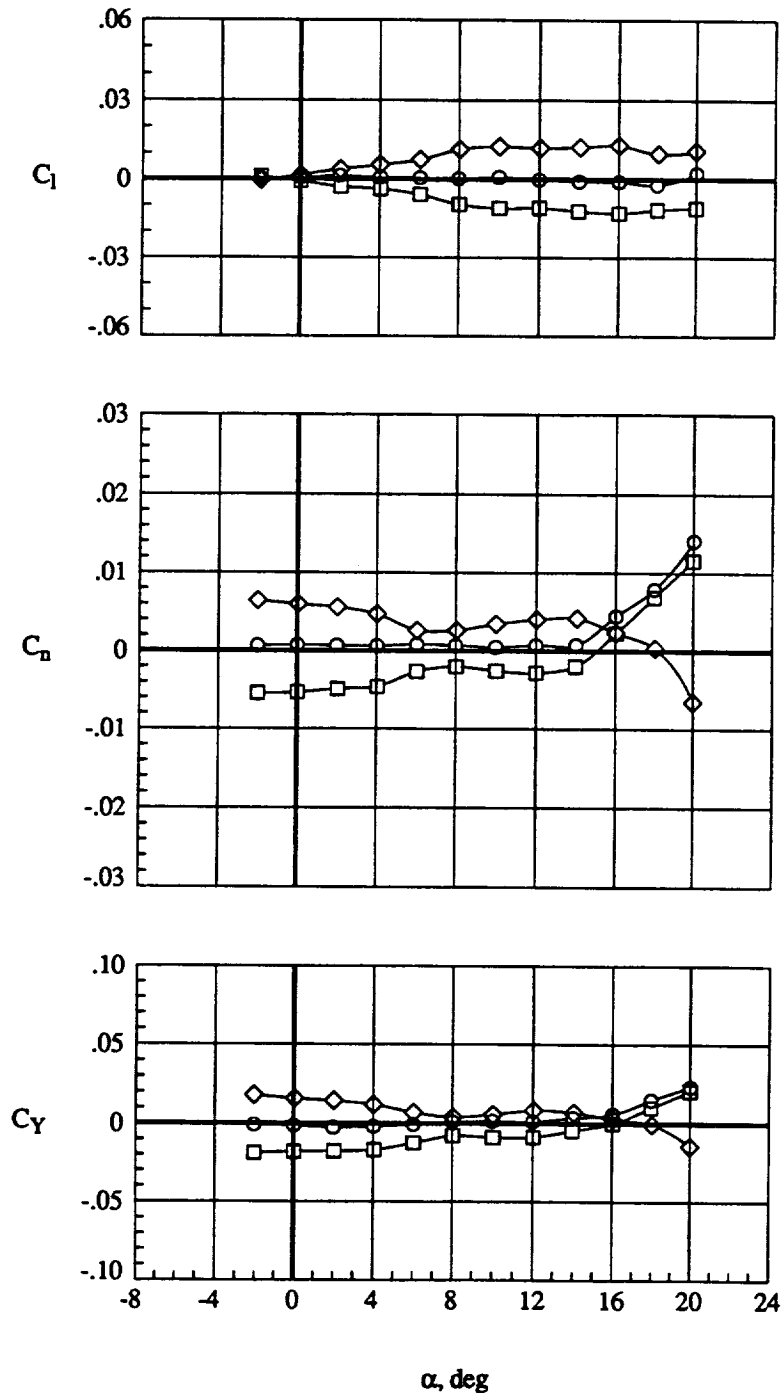
Run	$\beta$ , deg	Configuration
○	69.	0. $\delta_{L_{1/2}} = 50^\circ / 26.4^\circ, \delta_T = 20^\circ$
□	70.	5. $\delta_{L_{1/2}} = 50^\circ / 26.4^\circ, \delta_T = 20^\circ$
◇	71.	-5. $\delta_{L_{1/2}} = 50^\circ / 26.4^\circ, \delta_T = 20^\circ$



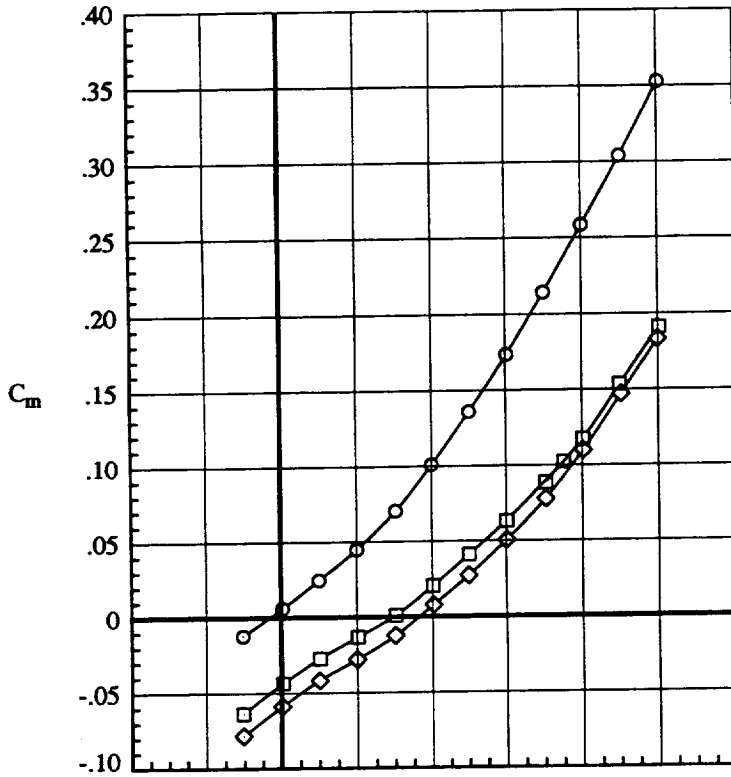
(a) Longitudinal aerodynamics

Figure 16. Effect of sideslip with vortex flap at  $\delta_{L_1} = 50^\circ$  and outboard leading-edge flap at  $\delta_{L_2} = 26.4^\circ, \delta_T = 20^\circ, q=110$  psf.

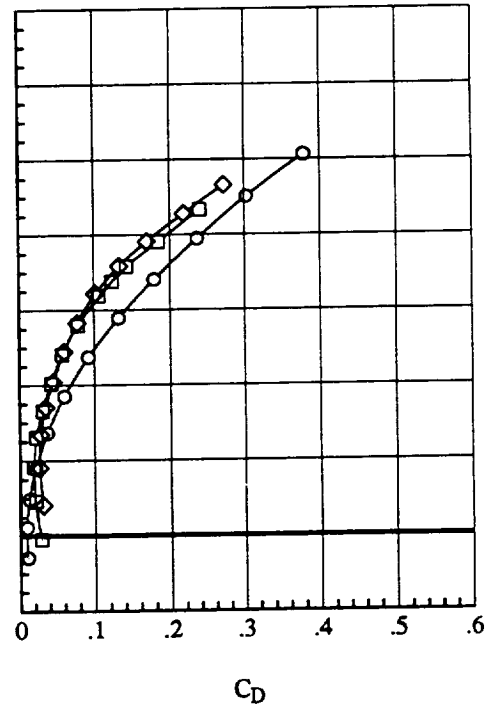
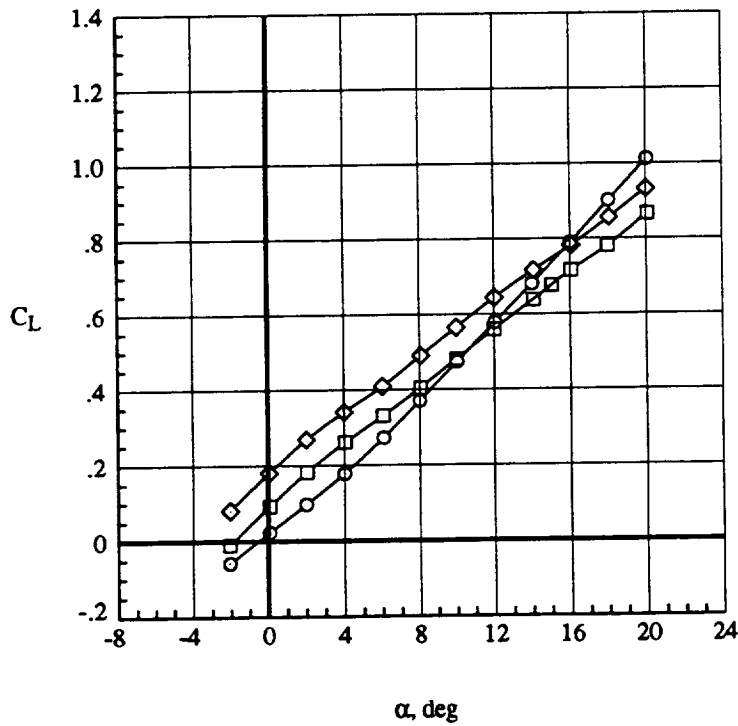
Run	$\beta$ , deg	Configuration
○	69.	0. $\delta_{L_{1/2}} = 50^\circ / 26.4^\circ, \delta_T = 20^\circ$
□	70.	5. $\delta_{L_{1/2}} = 50^\circ / 26.4^\circ, \delta_T = 20^\circ$
◇	71.	-5. $\delta_{L_{1/2}} = 50^\circ / 26.4^\circ, \delta_T = 20^\circ$



(b) Lateral aerodynamics  
Figure 16. Concluded.



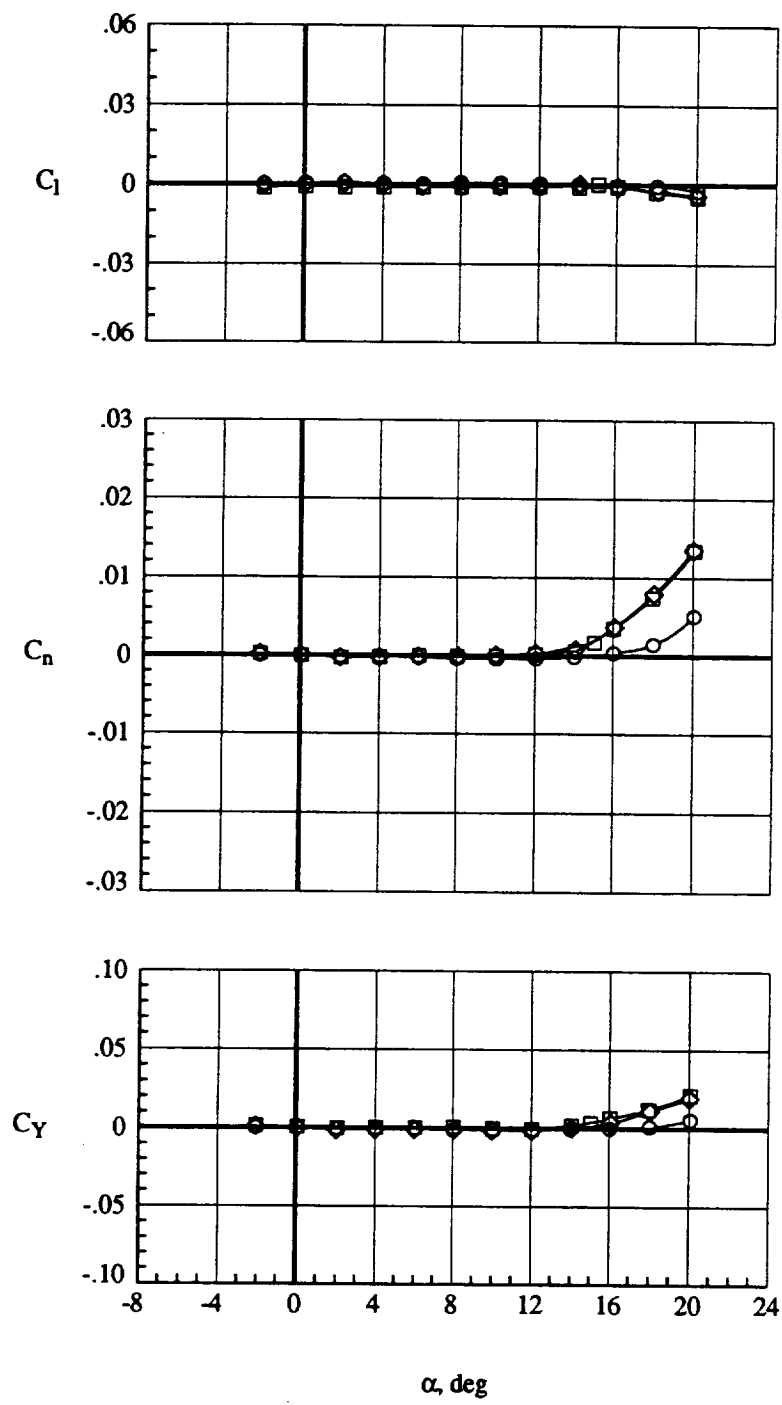
Run	$\beta$ , deg	Configuration
○	48.	$\delta_L = 0^\circ, \delta_T = 0^\circ$
□	72.	$\delta_{T_{1/2/3}} = 10^\circ / 10^\circ / 12.9^\circ$
◇	60.	$\delta_T = 20^\circ$



(a) Longitudinal aerodynamics

Figure 17. Effect of deflecting outboard trailing-edge flap with  $\delta_{L_{1/2}} = 40^\circ / 26.4^\circ$ ,  $q = 70$  psf.

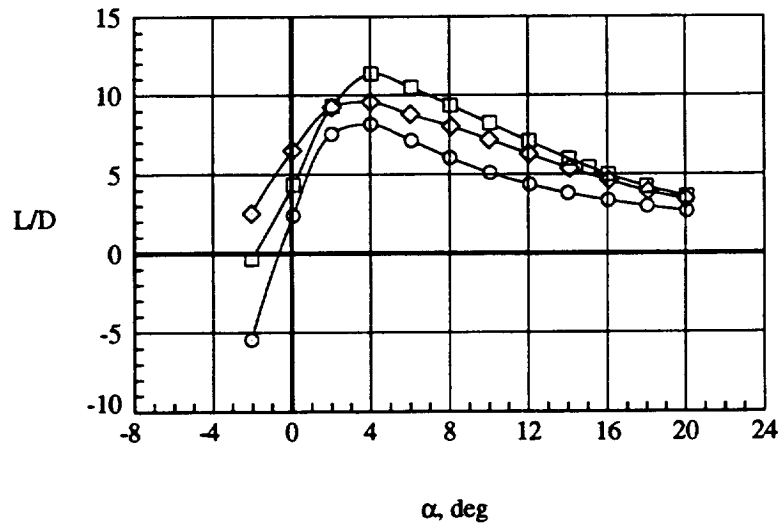
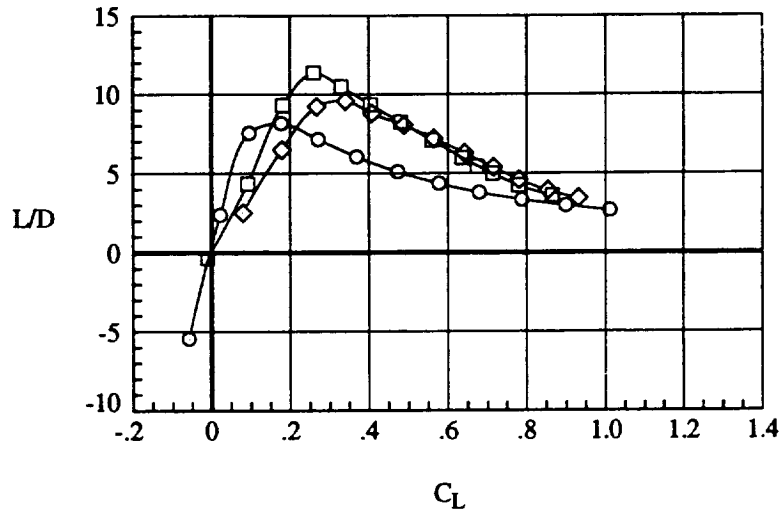
Run	$\beta$ , deg	Configuration
○	48.	$\delta_L = 0^\circ, \delta_T = 0^\circ$
□	72.	$\delta_{T_{1/2/3}} = 10^\circ / 10^\circ / 12.9^\circ$
◇	60.	$\delta_T = 20^\circ$



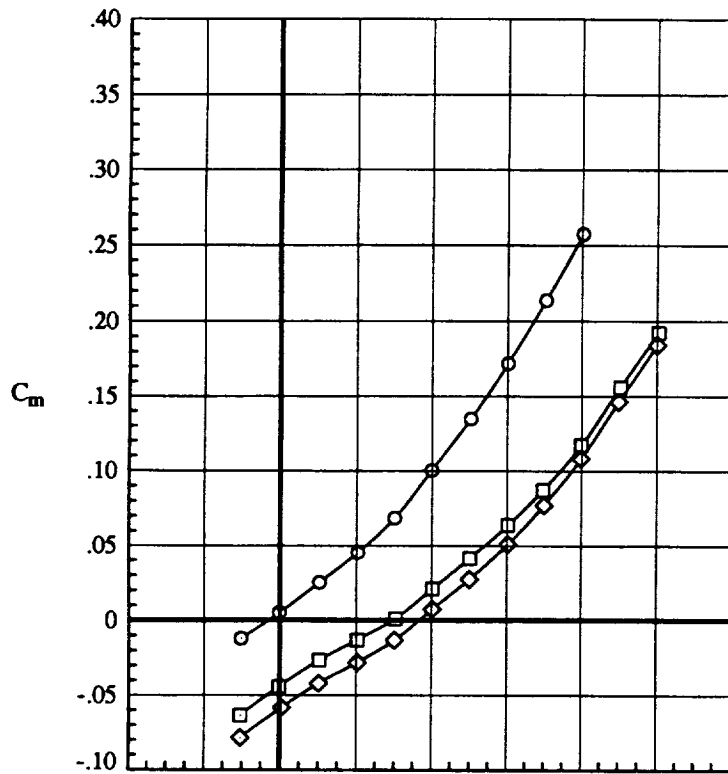
(b) Lateral aerodynamics  
 Figure 17. Continued.  
 60



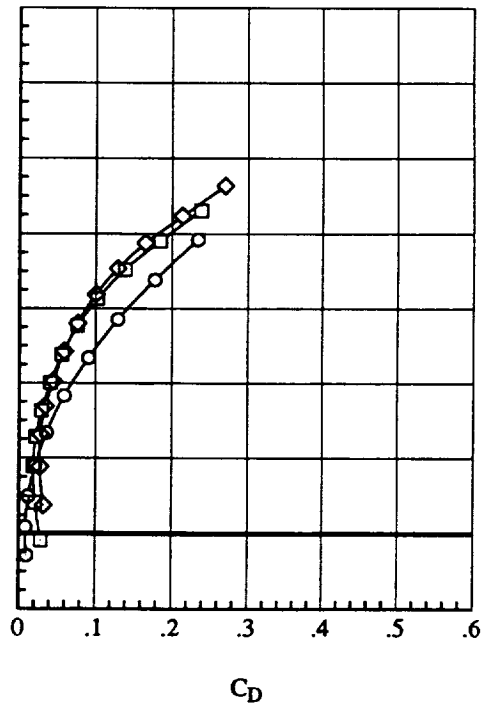
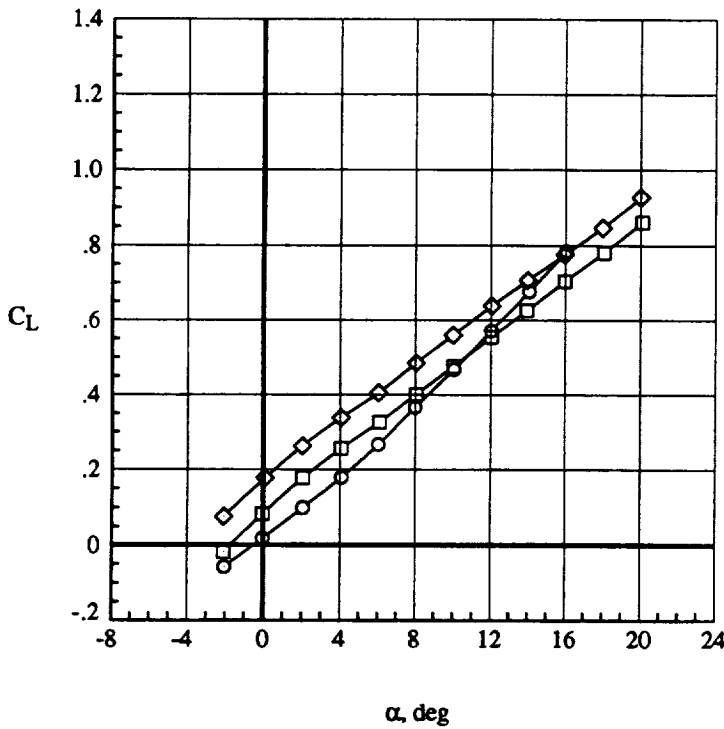
	Run	$\beta$ , deg	Configuration
○	48.	0.	$\delta_L = 0^\circ, \delta_T = 0^\circ$
□	72.	0.	$\delta_{T_{1/2/3}} = 10^\circ / 10^\circ / 12.9^\circ$
◇	60.	0.	$\delta_T = 20^\circ$



(c) Lift / Drag performance  
Figure 17. Concluded.



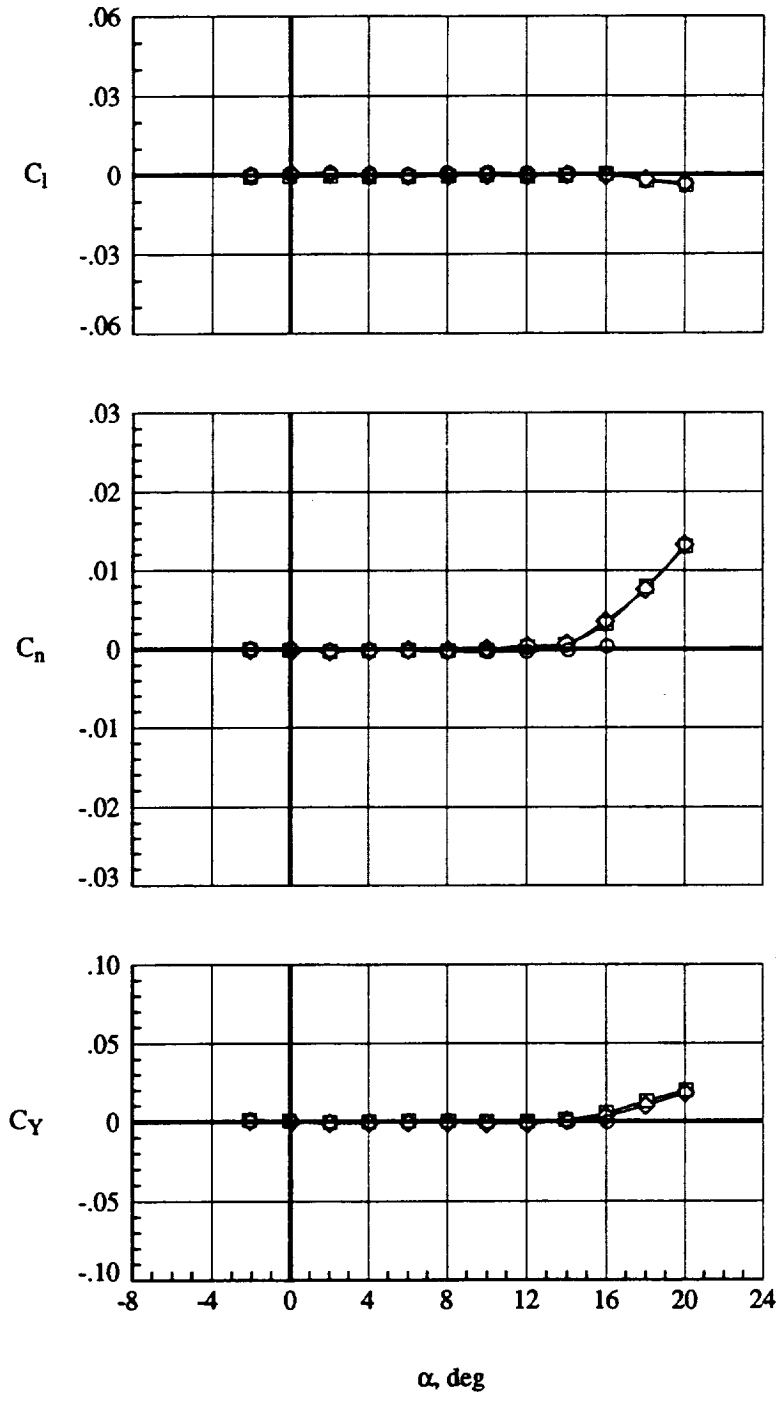
Run	$\beta$ , deg	Configuration
○	49.	$\delta_L = 0^\circ, \delta_T = 0^\circ$
□	73.	$\delta_{T_{1/23}} = 10^\circ / 10^\circ / 12.9^\circ$
◇	61.	$\delta_T = 20^\circ$



(a) Longitudinal aerodynamics

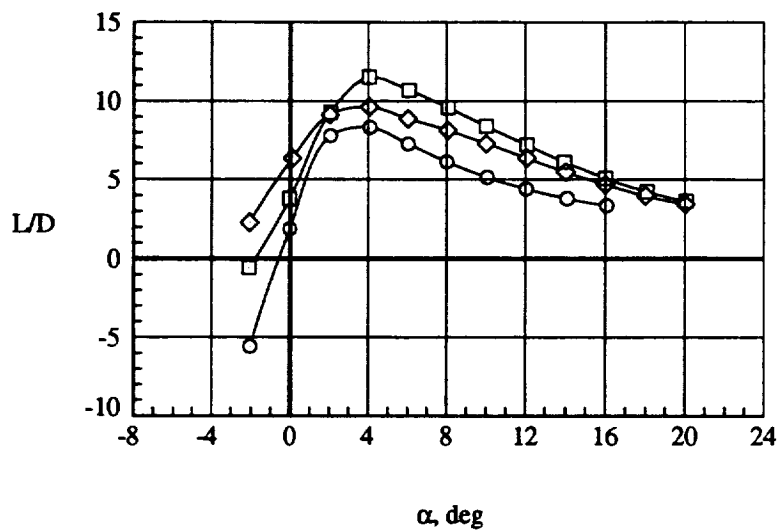
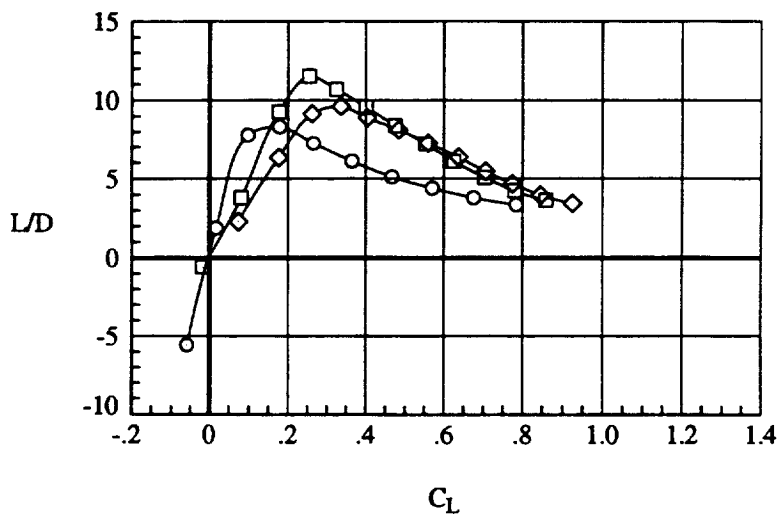
Figure 18. Effect of deflecting outboard trailing-edge flap with  $\delta_{L_{1/2}} = 40^\circ / 26.4^\circ$ ,  $q=110$  psf.

	Run	$\beta$ , deg	Configuration
○	49.	0.	$\delta_L = 0^\circ, \delta_T = 0^\circ$
□	73.	0.	$\delta_{T_{1/2/3}} = 10^\circ / 10^\circ / 12.9^\circ$
◇	61.	0.	$\delta_T = 20^\circ$

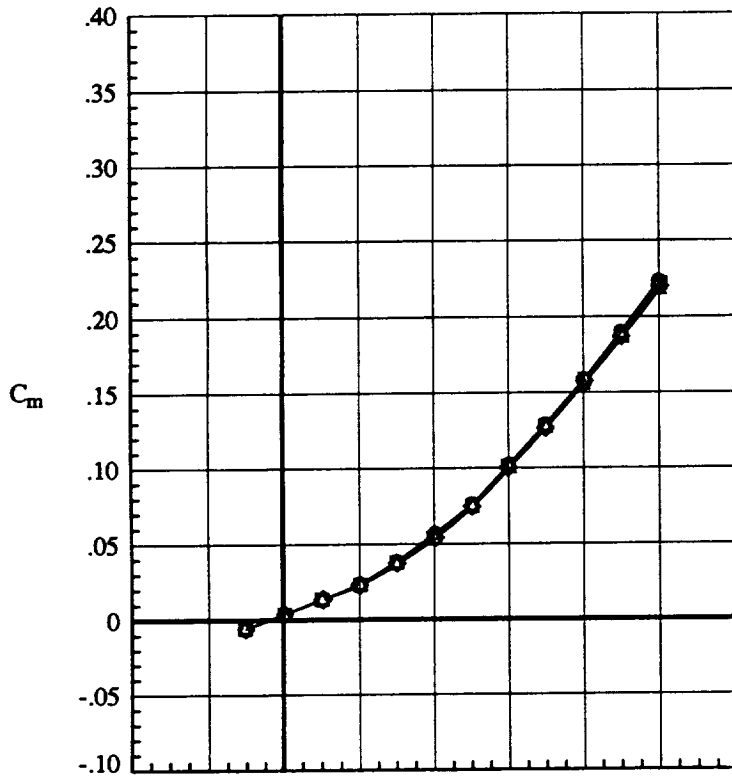


(b) Lateral aerodynamics  
Figure 18. Continued.

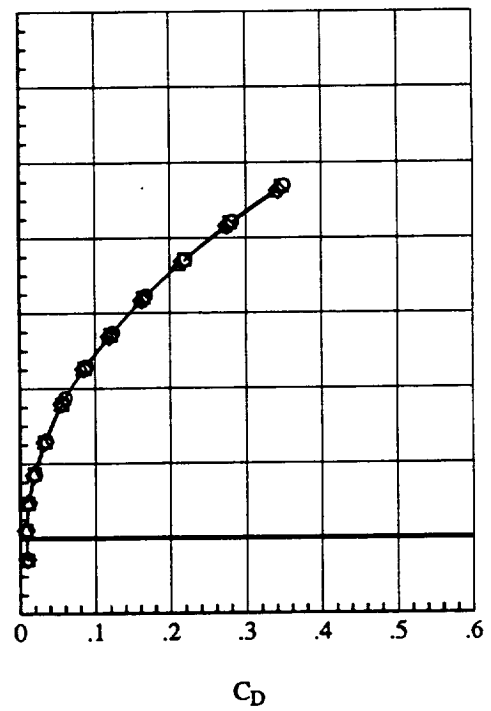
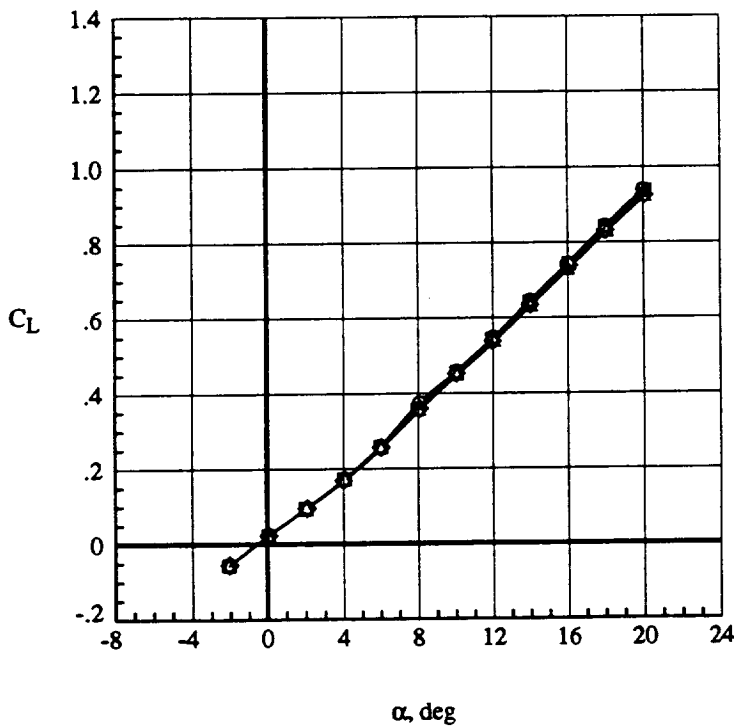
Run	$\beta$ , deg	Configuration
○	49.	$\delta_L = 0^\circ, \delta_T = 0^\circ$
□	73.	$\delta_{T_{1/2/3}} = 10^\circ / 10^\circ / 12.9^\circ$
◇	61.	$\delta_T = 20^\circ$



(c) Lift / Drag performance  
Figure 18. Concluded.



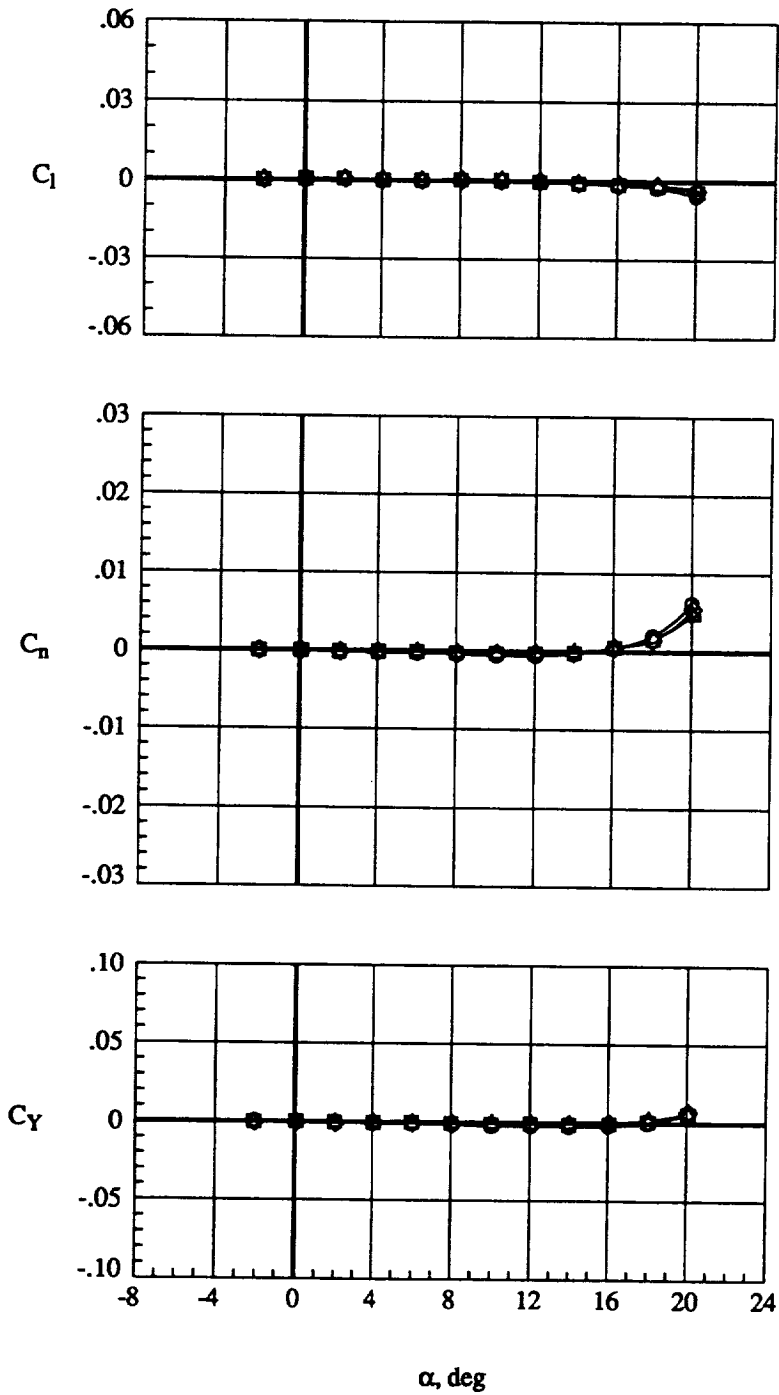
	Run	$\beta$ , deg	q
○	36.	0.	20.
□	37.	0.	50.
◇	38.	0.	70.
△	39.	110.	



(a) Longitudinal aerodynamics

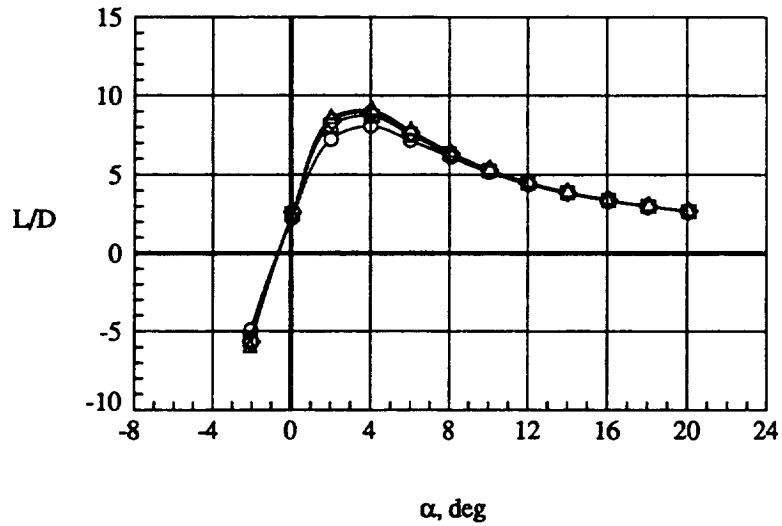
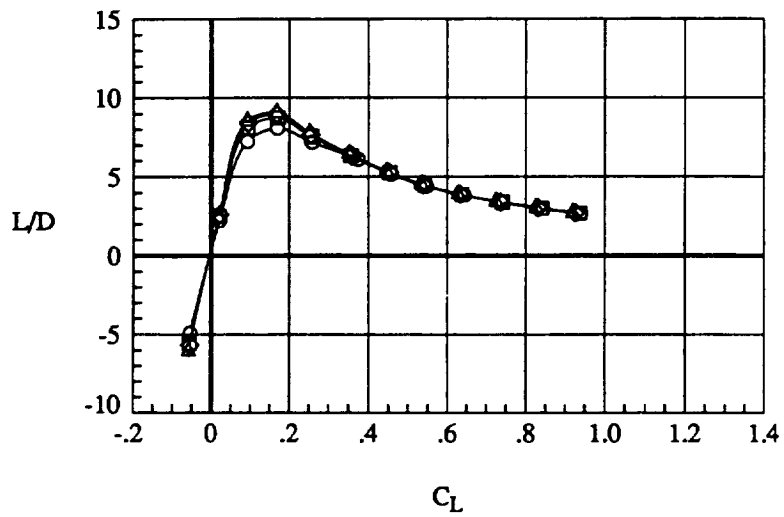
Figure 19. Effect of tunnel dynamic pressure on the baseline configuration,  $\delta_L = 0^\circ$ , and  $\delta_T = 0^\circ$ .

	Run	$\beta$ , deg	q
○	36.	0.	20.
□	37.	0.	50.
◇	38.	0.	70.
△	39.	0.	110.

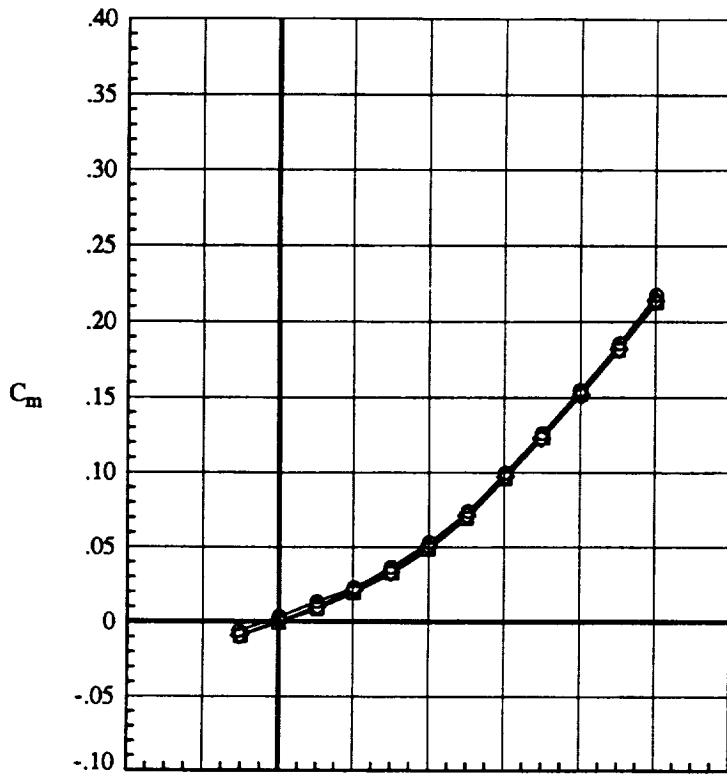


(b) Lateral aerodynamics  
Figure 19. Continued.

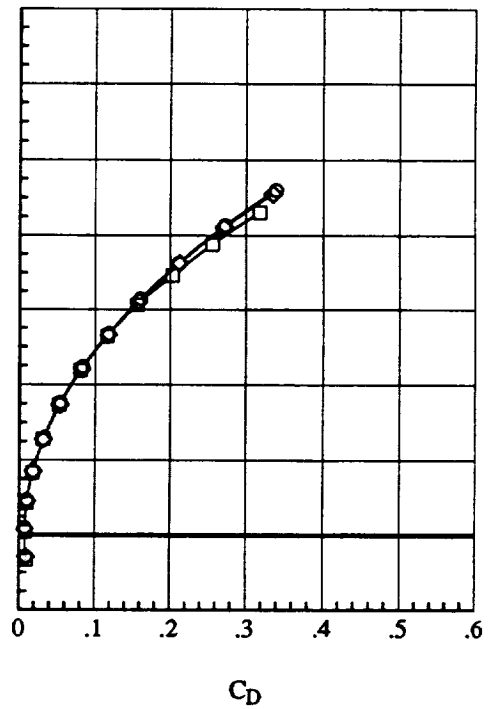
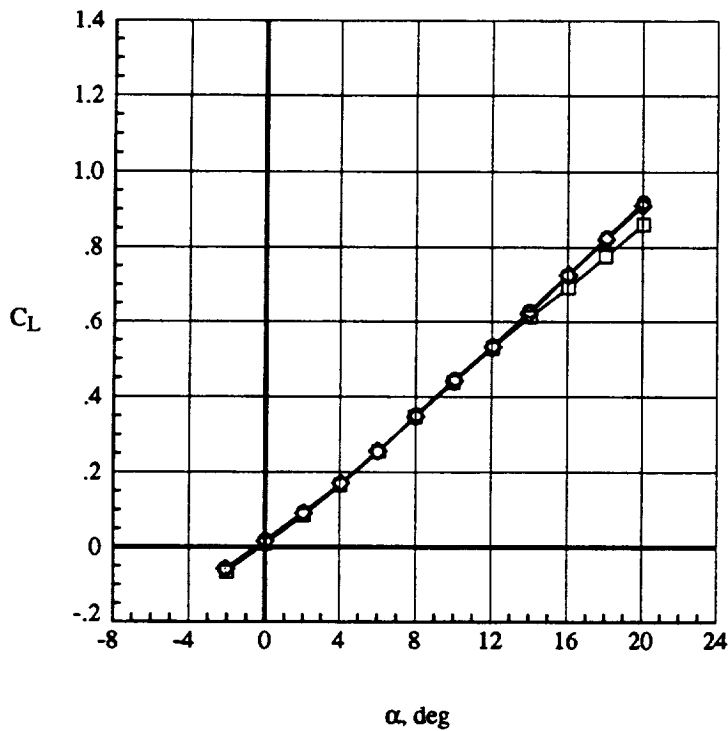
	Run	$\beta$ , deg	q
○	36.	0.	20.
□	37.	0.	50.
◇	38.	0.	70.
△	39.	0.	110.



(c) Lift / Drag performance  
Figure 19. Concluded.



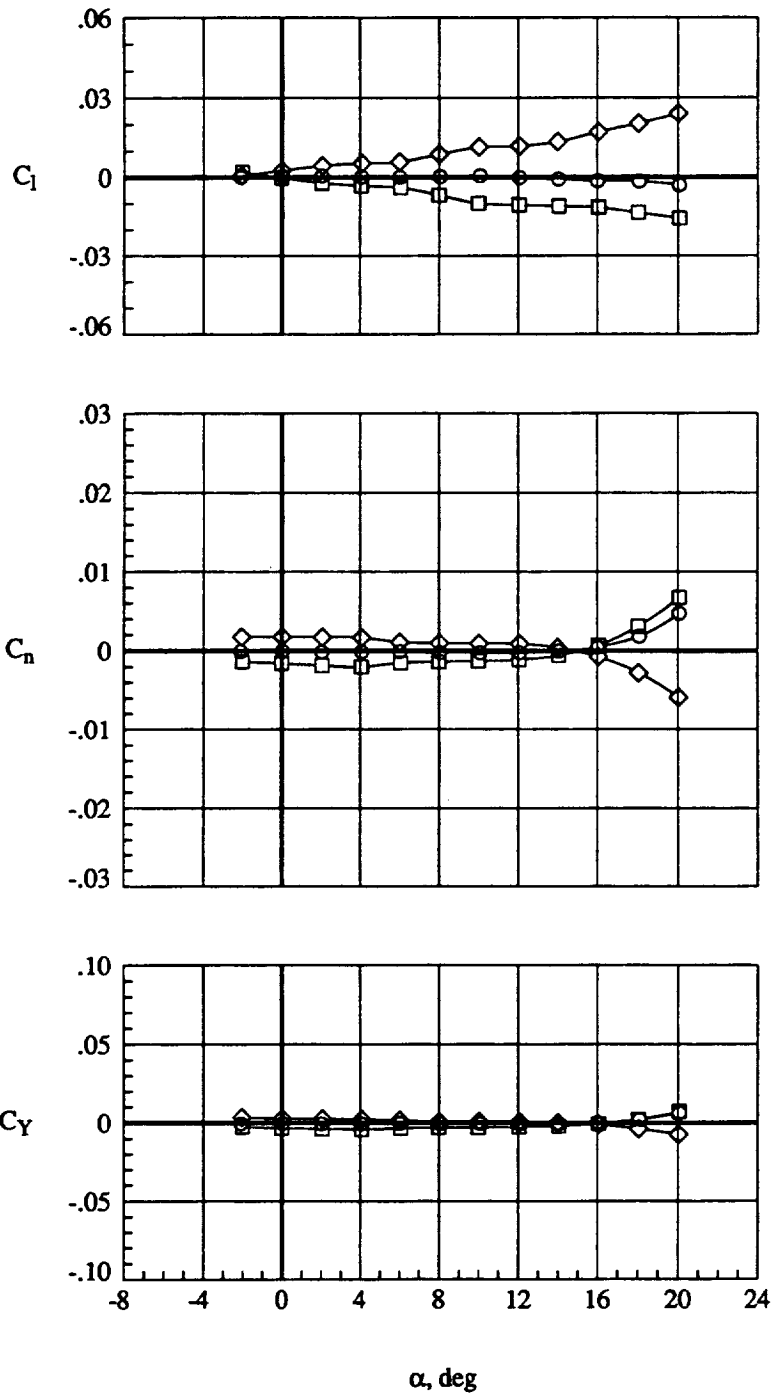
Run	$\beta$ , deg	Configuration
○	39.	$\delta_L = 0^\circ, \delta_T = 0^\circ$
□	40.	$\delta_L = 0^\circ, \delta_T = 0^\circ$
◇	41.	$\delta_L = 0^\circ, \delta_T = 0^\circ$



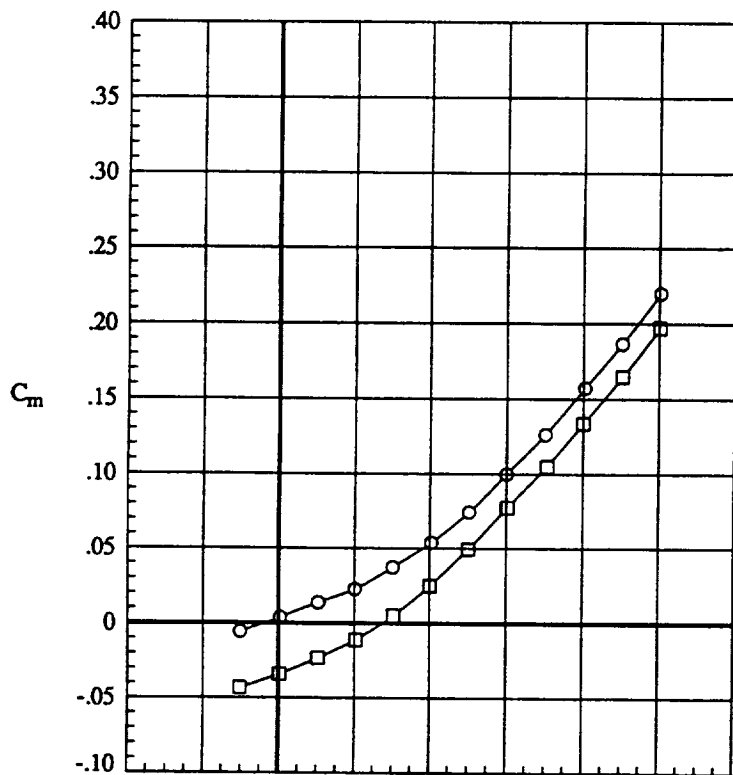
(a) Longitudinal aerodynamics  
 Figure 20. Effect of sideslip on baseline configuration,  $q=110$  psf.



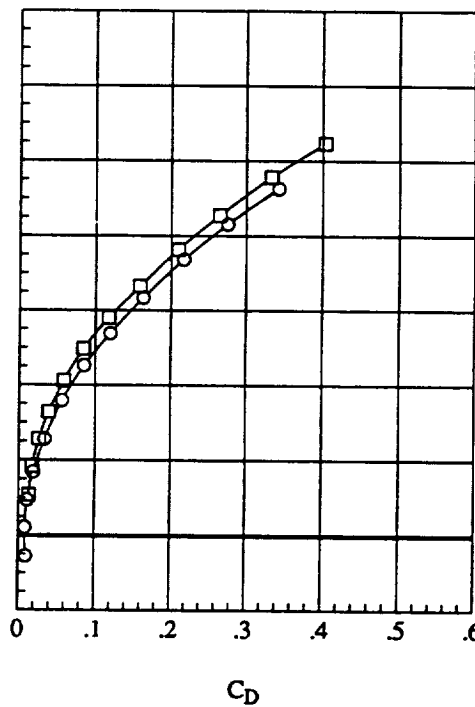
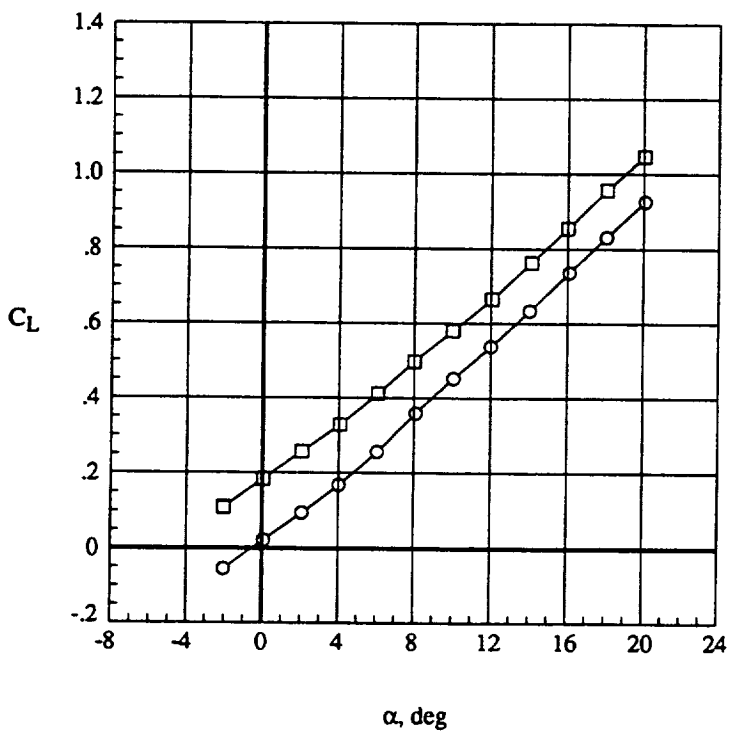
Run	$\beta$ , deg	Configuration
○	39.	$\delta_L = 0^\circ, \delta_T = 0^\circ$
□	40.	$\delta_L = 0^\circ, \delta_T = 0^\circ$
◇	41.	$\delta_L = 0^\circ, \delta_T = 0^\circ$



(b) Lateral aerodynamics  
Figure 20. Concluded.



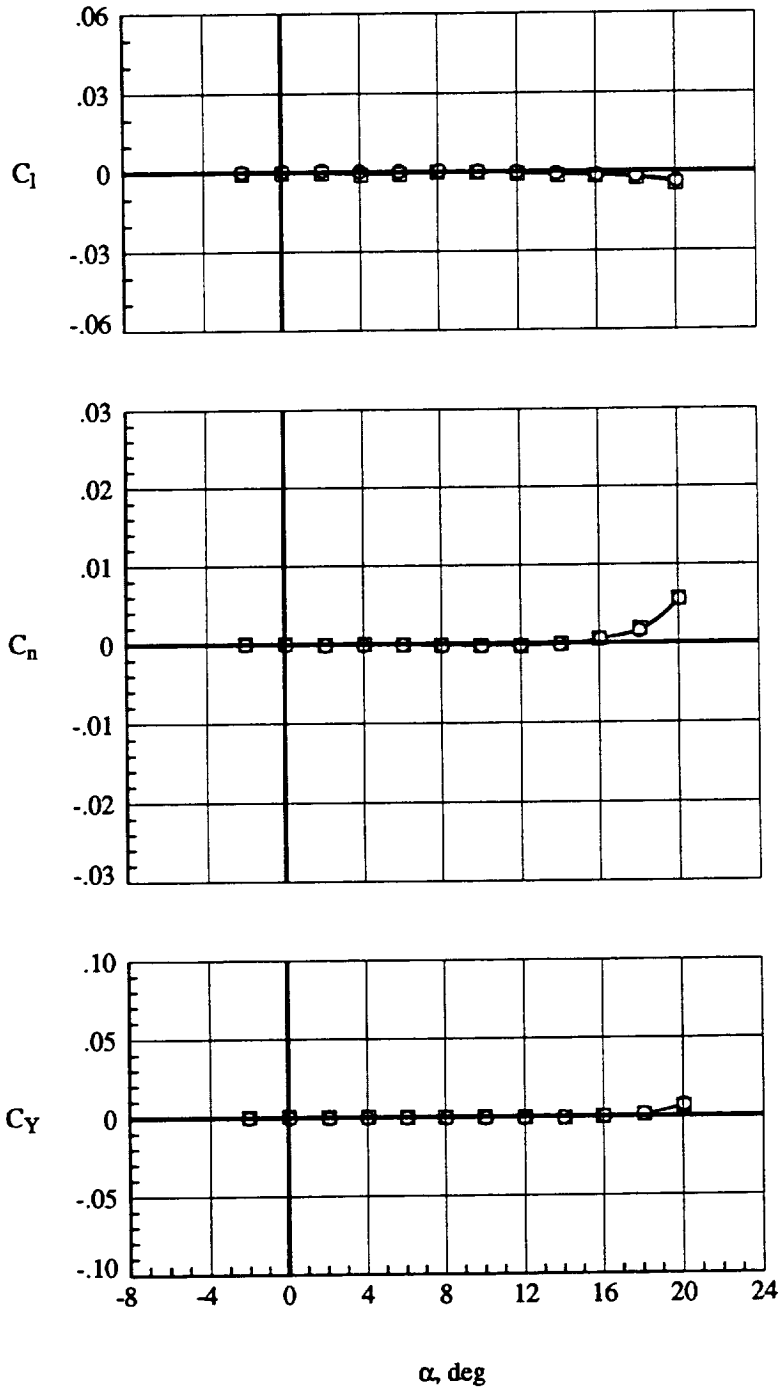
Run	$\beta$ , deg	Configuration
○	38.	0. $\delta_L = 0^\circ, \delta_T = 0^\circ$
□	42.	0. $\delta_L = 0^\circ, \delta_{T_{1/2\beta}} = 10^\circ/10^\circ/20^\circ$



(a) Longitudinal aerodynamics

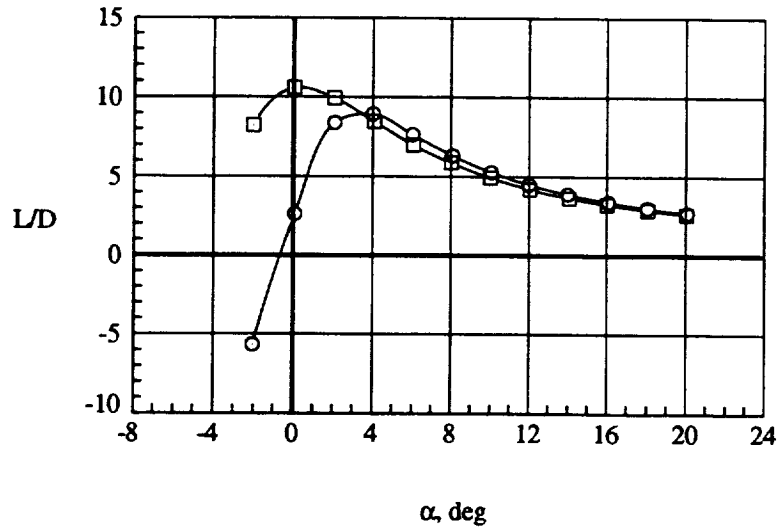
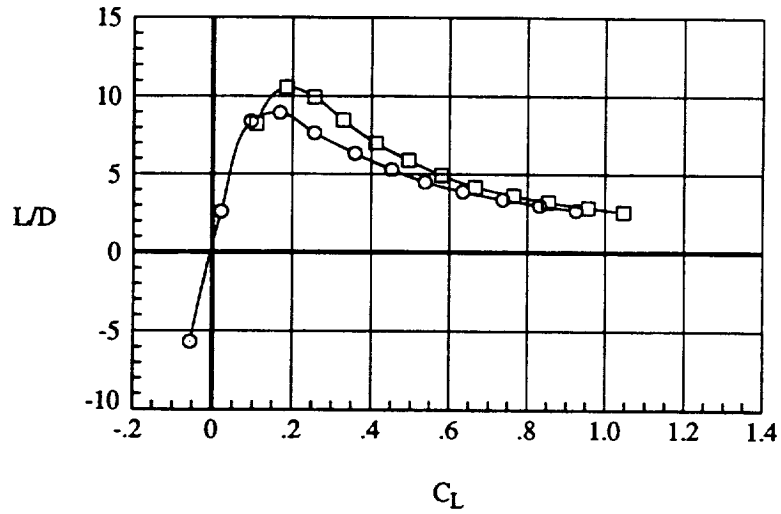
Figure 21. Effect of trailing-edge flaps on baseline configuration.  $\delta_L = 0^\circ, q=70$  psf.

	Run	$\beta$ , deg	Configuration
○	38.	0.	$\delta_L = 0^\circ, \delta_T = 0^\circ$
□	42.	0.	$\delta_L = 0^\circ, \delta_{T_{1/2/3}} = 10^\circ/10^\circ/20^\circ$

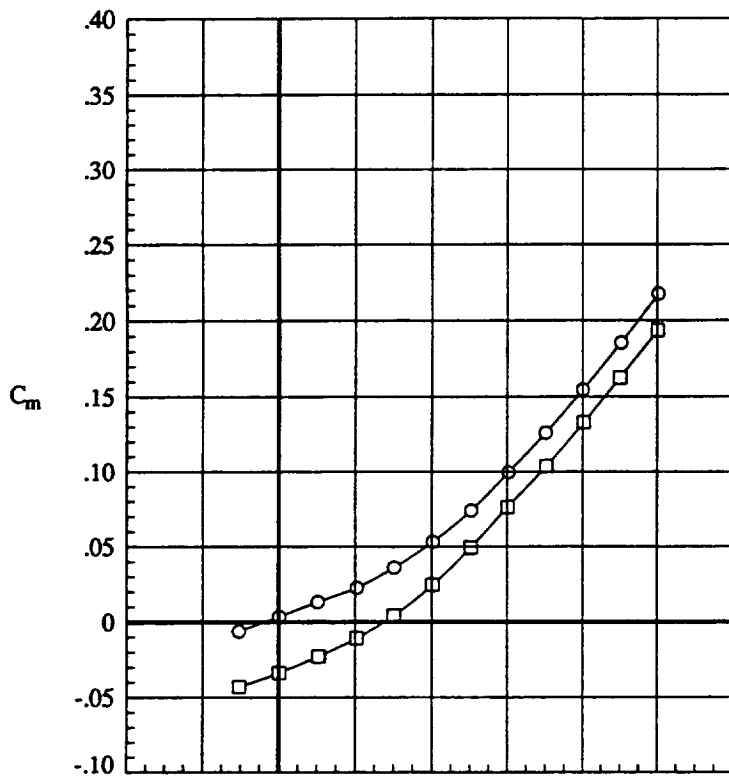


(b) Lateral aerodynamics  
Figure 21. Continued.

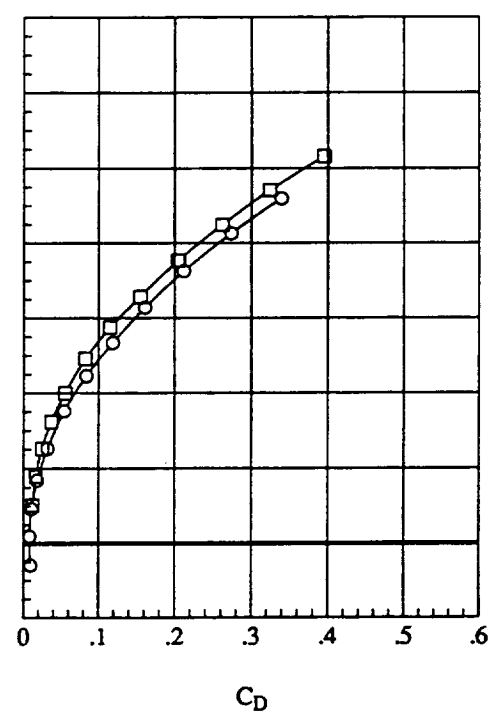
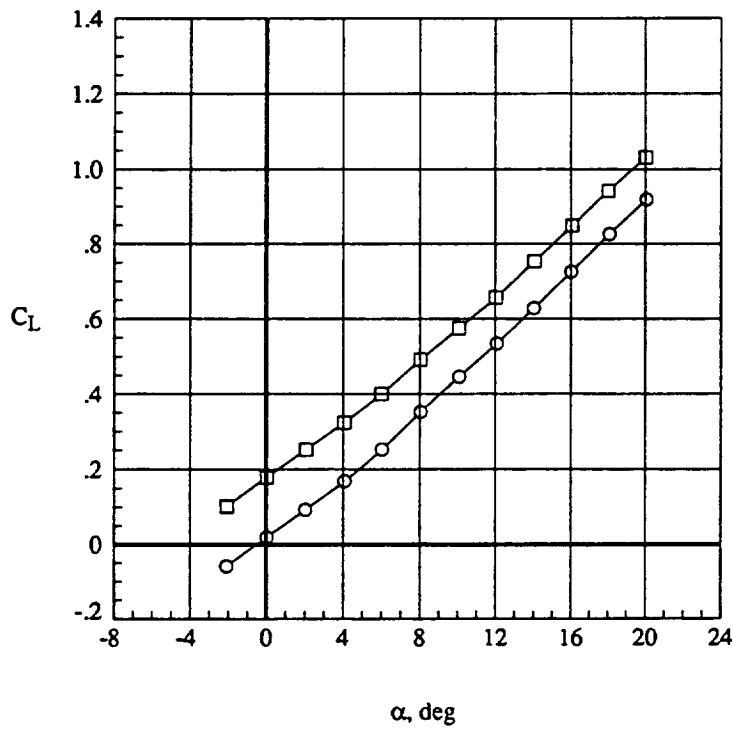
Run	$\beta$ , deg	Configuration
○	38.	$\delta_L = 0^\circ, \delta_T = 0^\circ$
□	42.	$\delta_L = 0^\circ, \delta_{T_{1/2/3}} = 10^\circ/10^\circ/20^\circ$



(c) Lift / Drag performance  
Figure 21. Concluded.

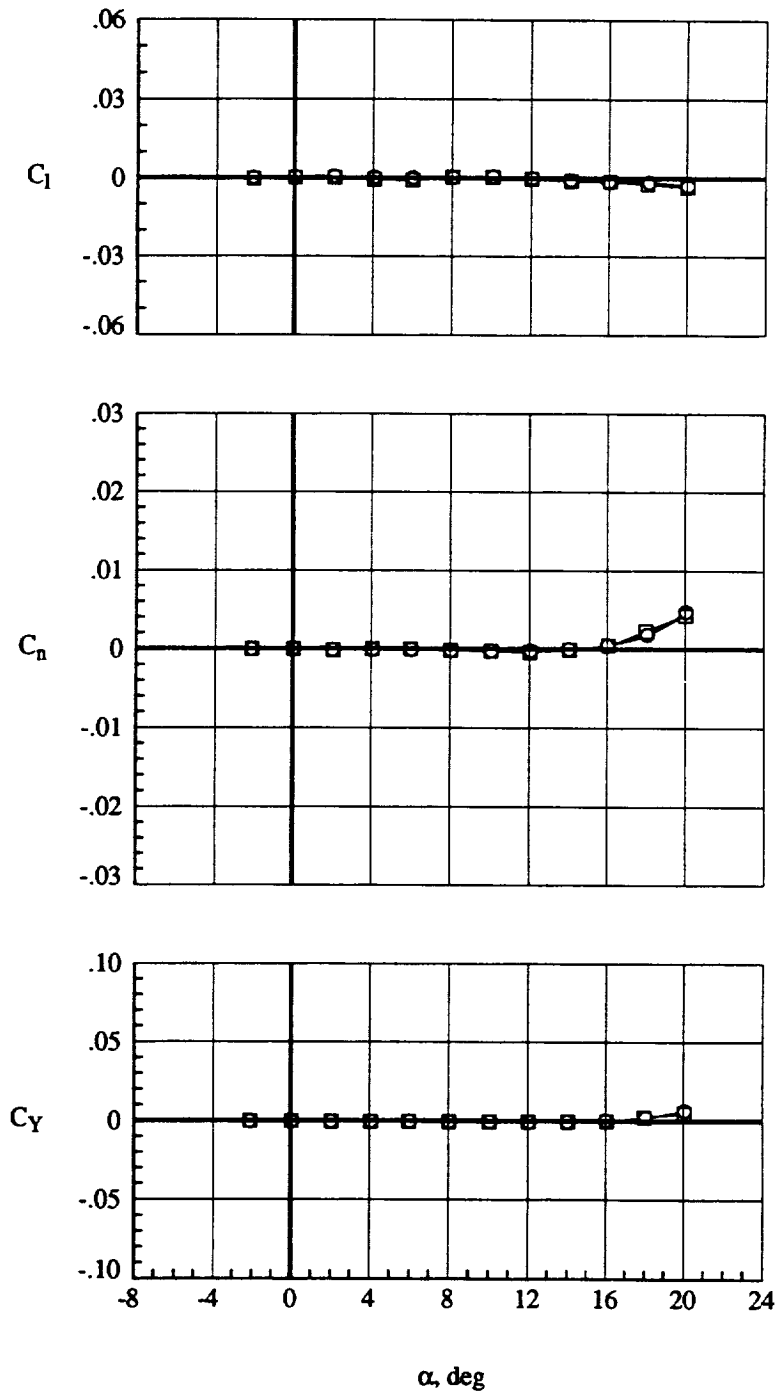


Run	$\beta$ , deg	Configuration
○	39.	$\delta_L = 0^\circ, \delta_T = 0^\circ$
□	43.	$\delta_L = 0^\circ, \delta_{T_{1/2\beta}} = 10^\circ/10^\circ/20^\circ$



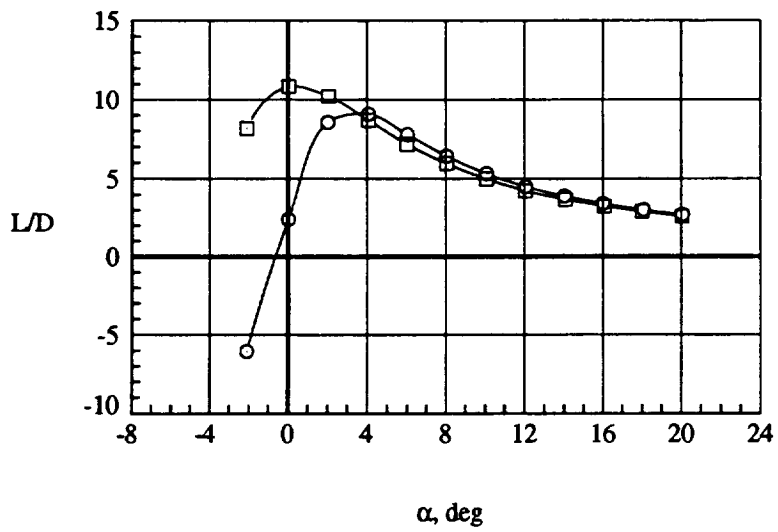
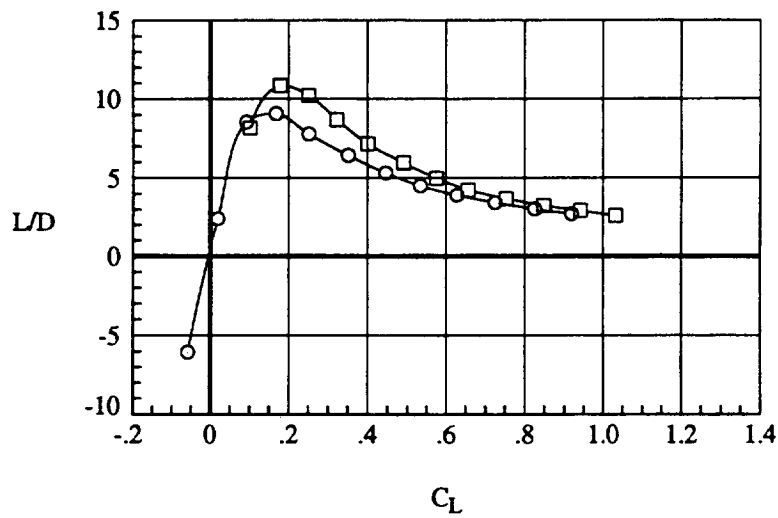
(a) Longitudinal aerodynamics  
 Figure 22. Effect of trailing-edge flaps on baseline configuration,  $q=110$  psf.

	Run	$\beta$ , deg	Configuration
○	39.	0.	$\delta_L = 0^\circ, \delta_T = 0^\circ$
□	43.	0.	$\delta_L = 0^\circ, \delta_{T_{1/2/3}} = 10^\circ/10^\circ/20^\circ$

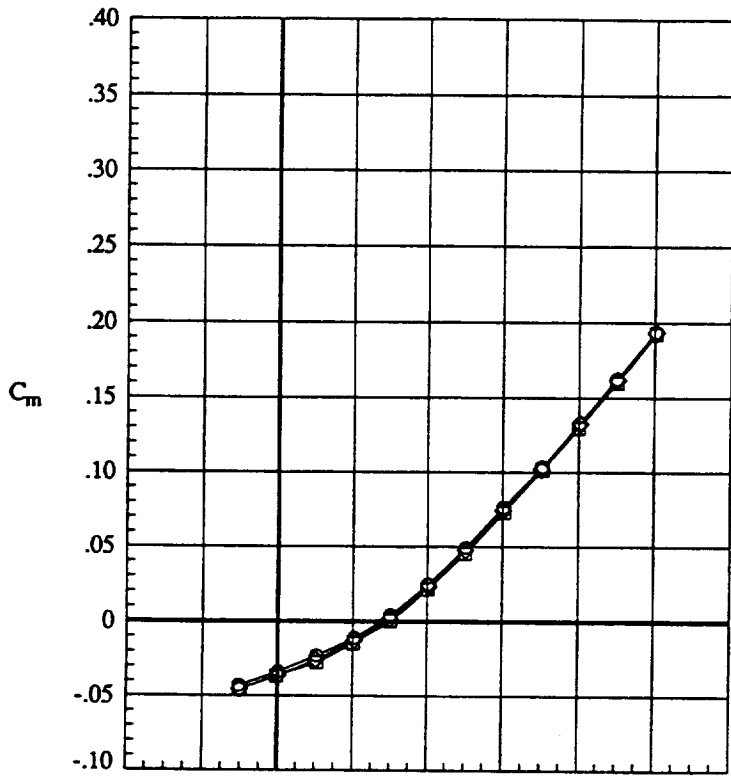


(b) Lateral aerodynamics  
Figure 22. Continued.

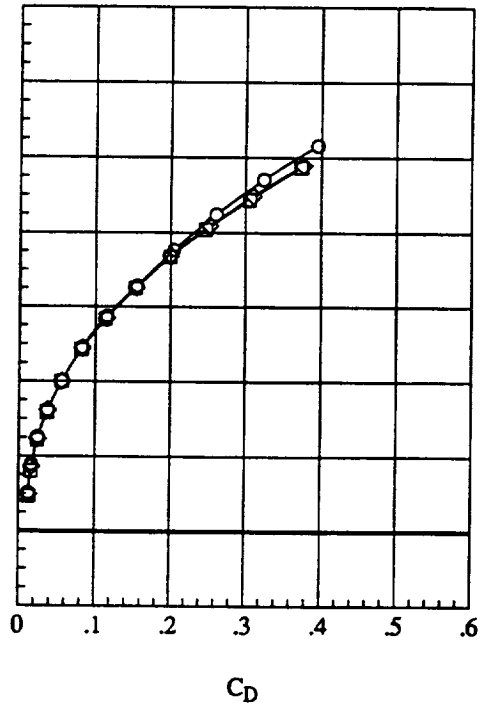
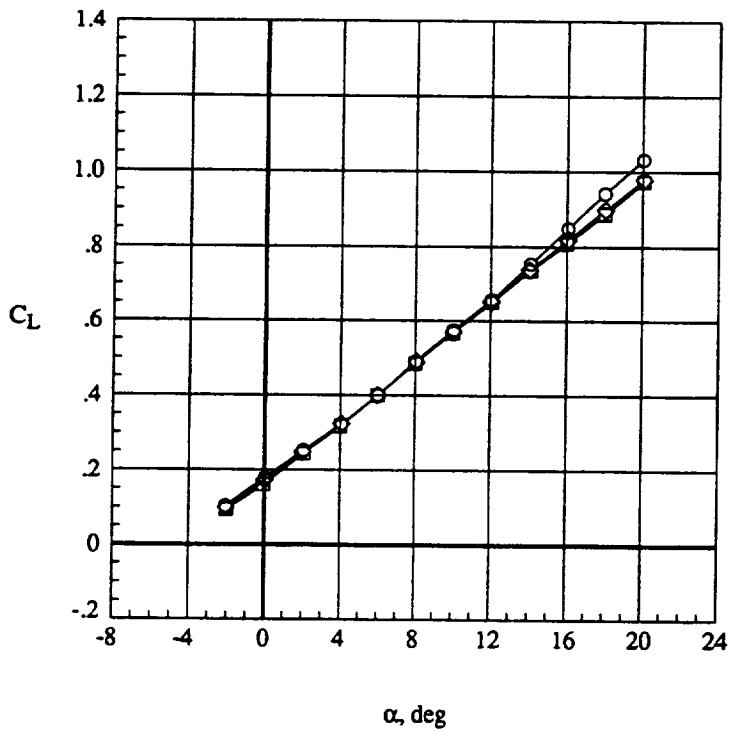
	Run	$\beta$ , deg	Configuration
○	39.	0.	$\delta_L = 0^\circ, \delta_T = 0^\circ$
□	43.	0.	$\delta_L = 0^\circ, \delta_{T_{1/2/3}} = 10^\circ/10^\circ/20^\circ$



(c) Lift / Drag performance  
Figure 22. Concluded.



Run	$\beta$ , deg	Configuration
○	43.	0. $\delta_L = 0^\circ, \delta_{T_{1/2\beta}} = 10^\circ/10^\circ/20^\circ$
□	44.	5. $\delta_L = 0^\circ, \delta_{T_{1/2\beta}} = 10^\circ/10^\circ/20^\circ$
◇	45.	-5. $\delta_L = 0^\circ, \delta_{T_{1/2\beta}} = 10^\circ/10^\circ/20^\circ$

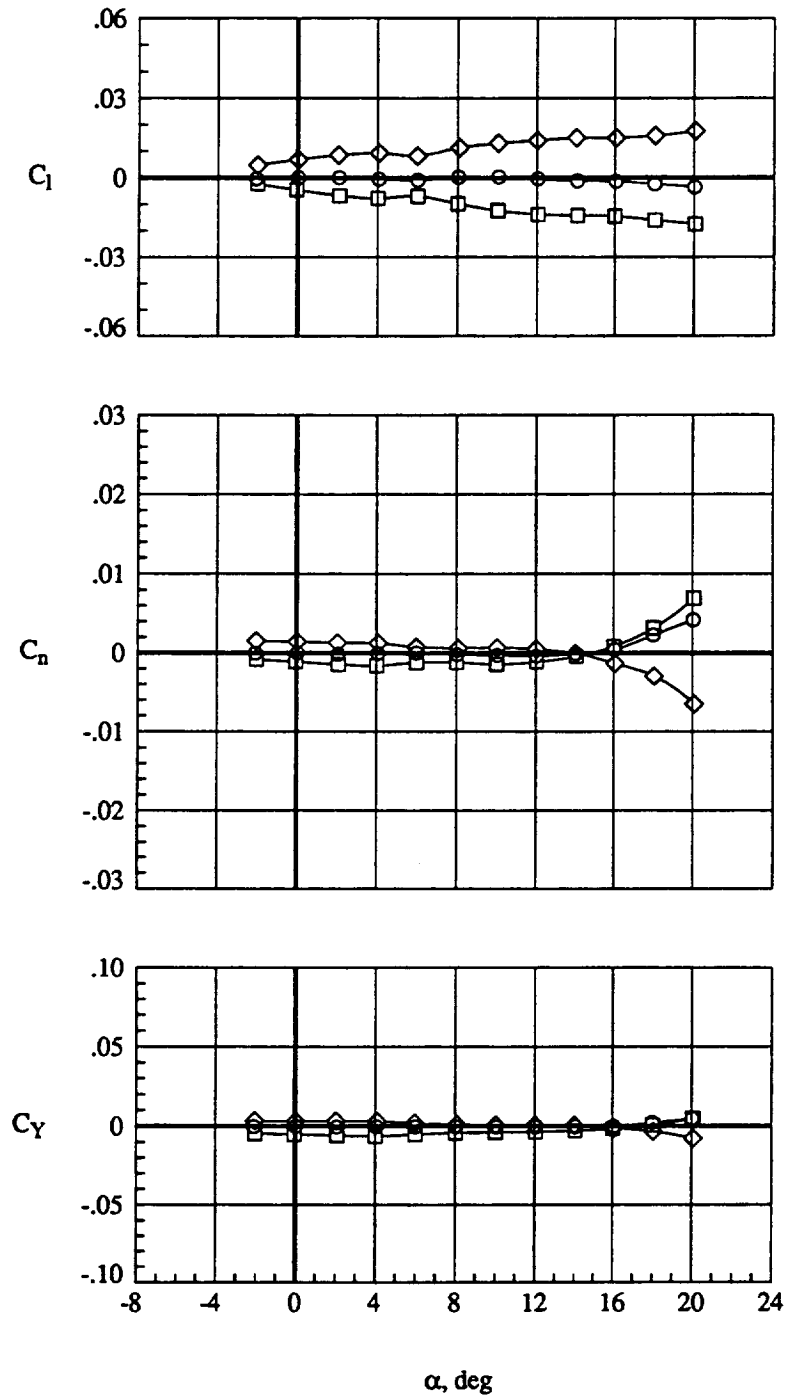


(a) Longitudinal aerodynamics

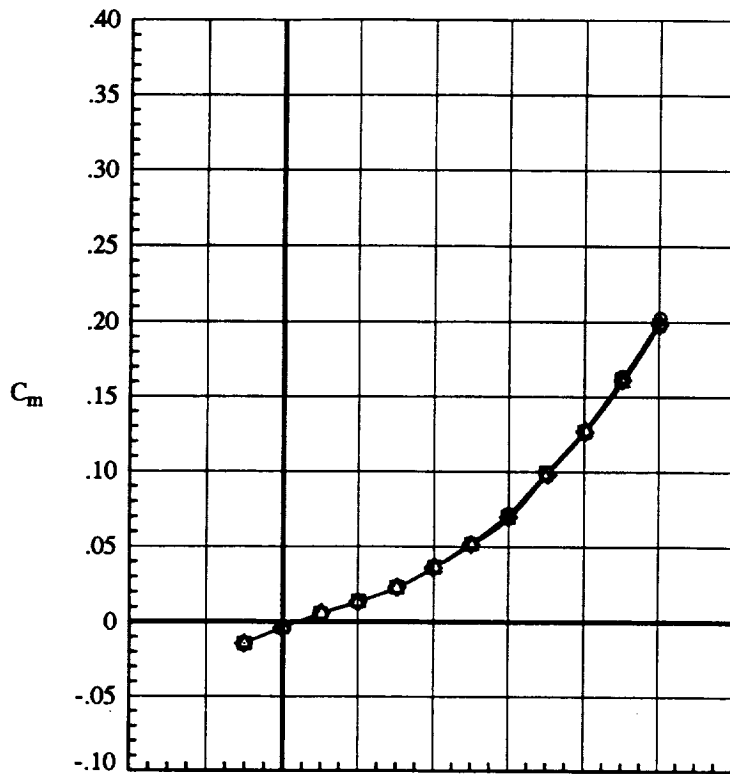
Figure 23. Effect of sideslip on baseline configuration with trailing-edge flaps deflected,  $q=110$  psf.



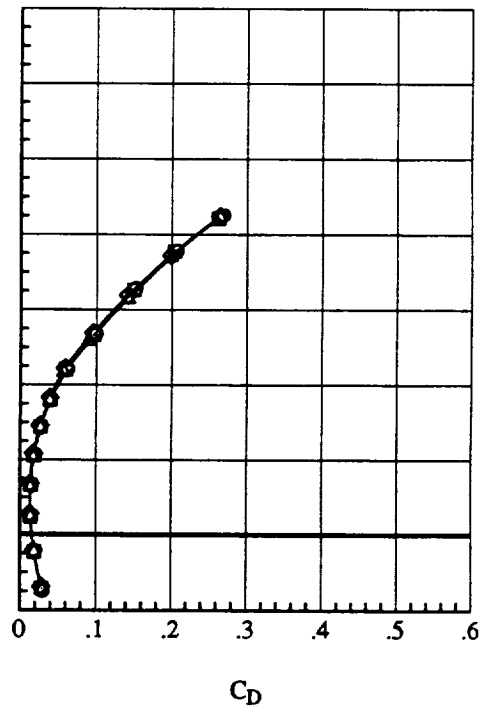
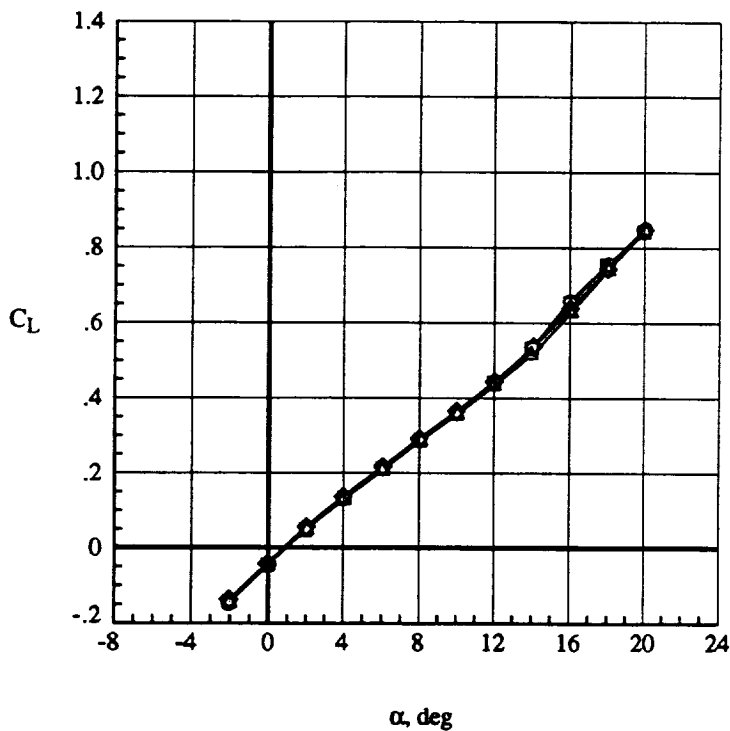
Run	$\beta$ , deg	Configuration
○	43.	$\delta_L = 0^\circ, \delta_{T_{1/2/3}} = 10^\circ/10^\circ/20^\circ$
□	44.	$\delta_L = 0^\circ, \delta_{T_{1/2/3}} = 10^\circ/10^\circ/20^\circ$
◇	45.	$\delta_L = 0^\circ, \delta_{T_{1/2/3}} = 10^\circ/10^\circ/20^\circ$



(b) Lateral aerodynamics  
Figure 23. Concluded.



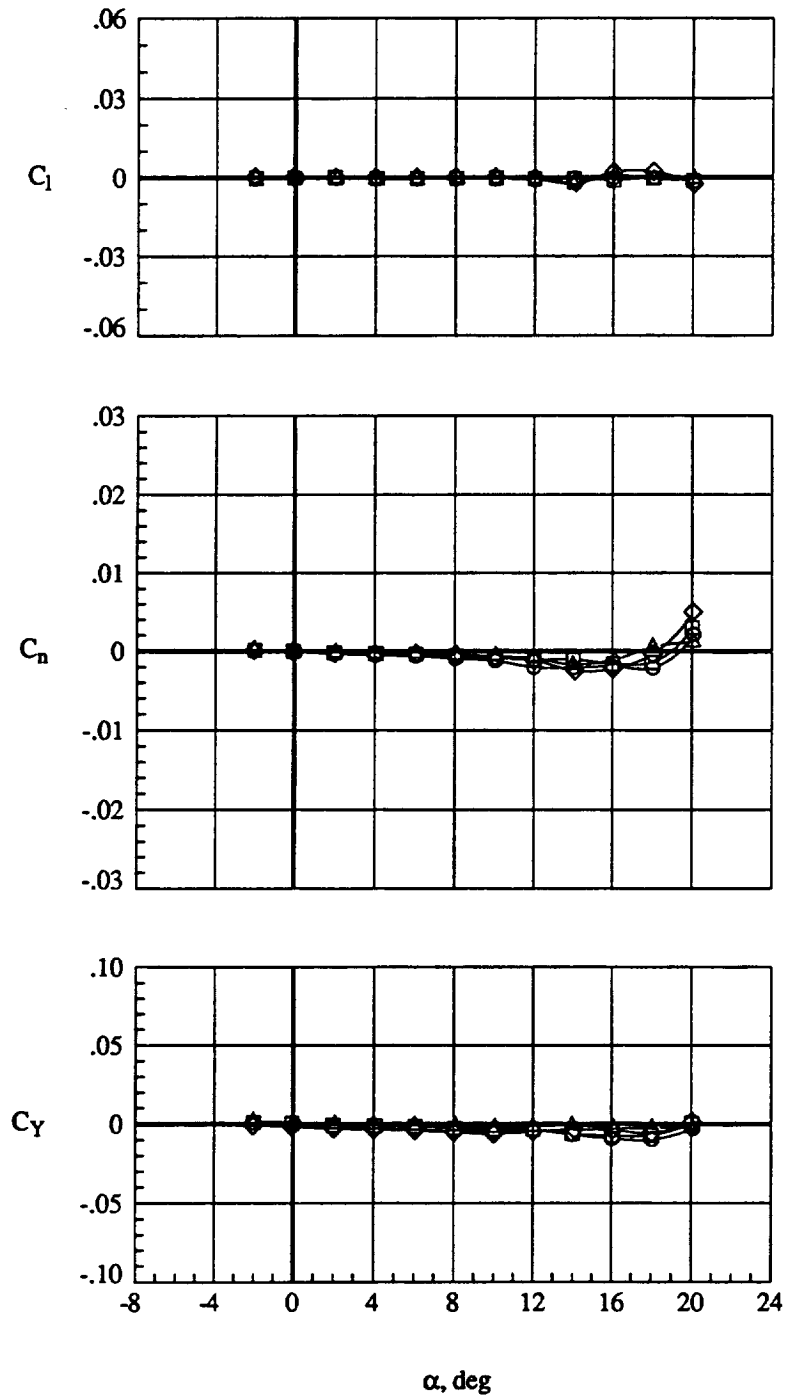
	Run	$\beta$ , deg	q
○	10.	0.	20.
□	11.	0.	50.
◇	14.	0.	70.
△	13.	0.	110.



(a) Longitudinal aerodynamics

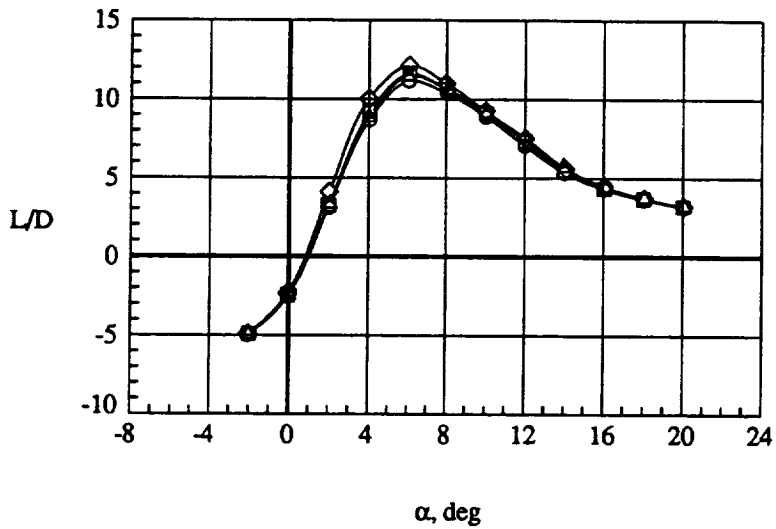
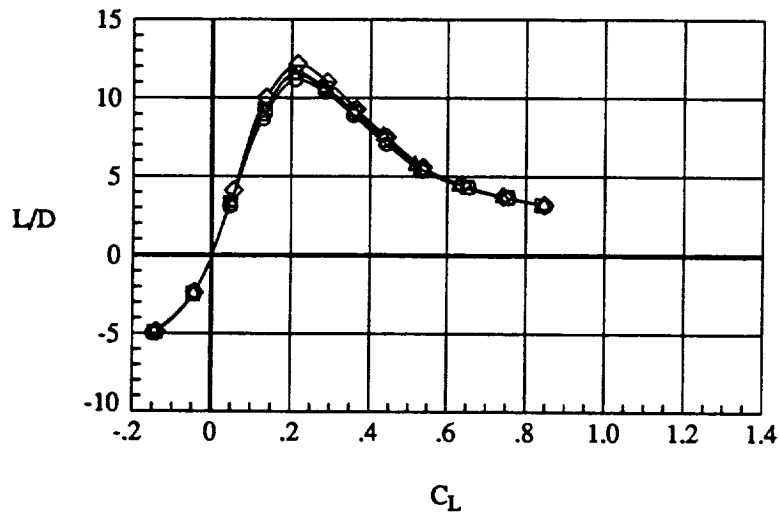
Figure 24. Effect of tunnel dynamic pressure on the mission adaptive flap configuration.

	Run	$\beta$ , deg	q
○	10.	0.	20.
□	11.	0.	50.
◇	14.	0.	70.
△	13.	0.	110.

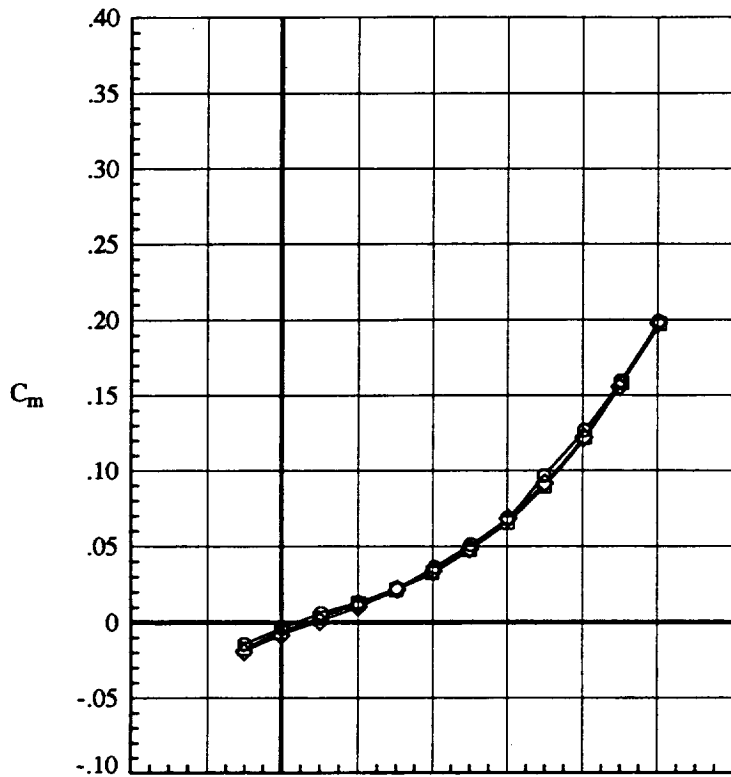


(b) Lateral aerodynamics  
Figure 24. Continued.

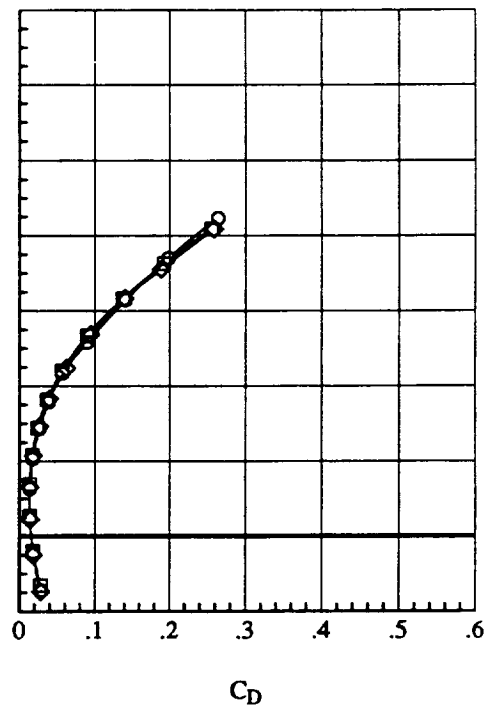
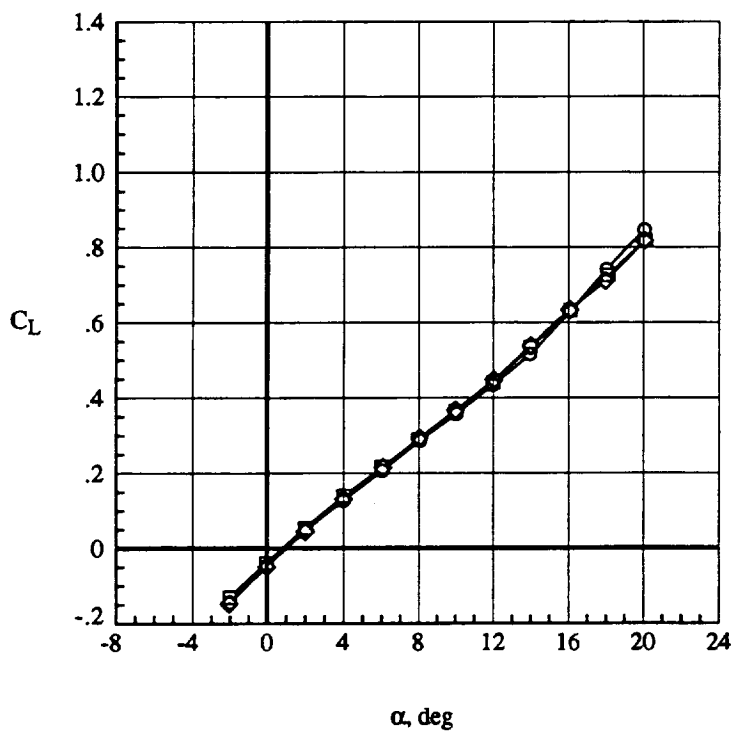
	Run	$\beta$ , deg	q
○	10.	0.	20.
□	11.	0.	50.
◇	14.	0.	70.
△	13.	0.	110.



(c) Lift / Drag performance  
Figure 24. Concluded.



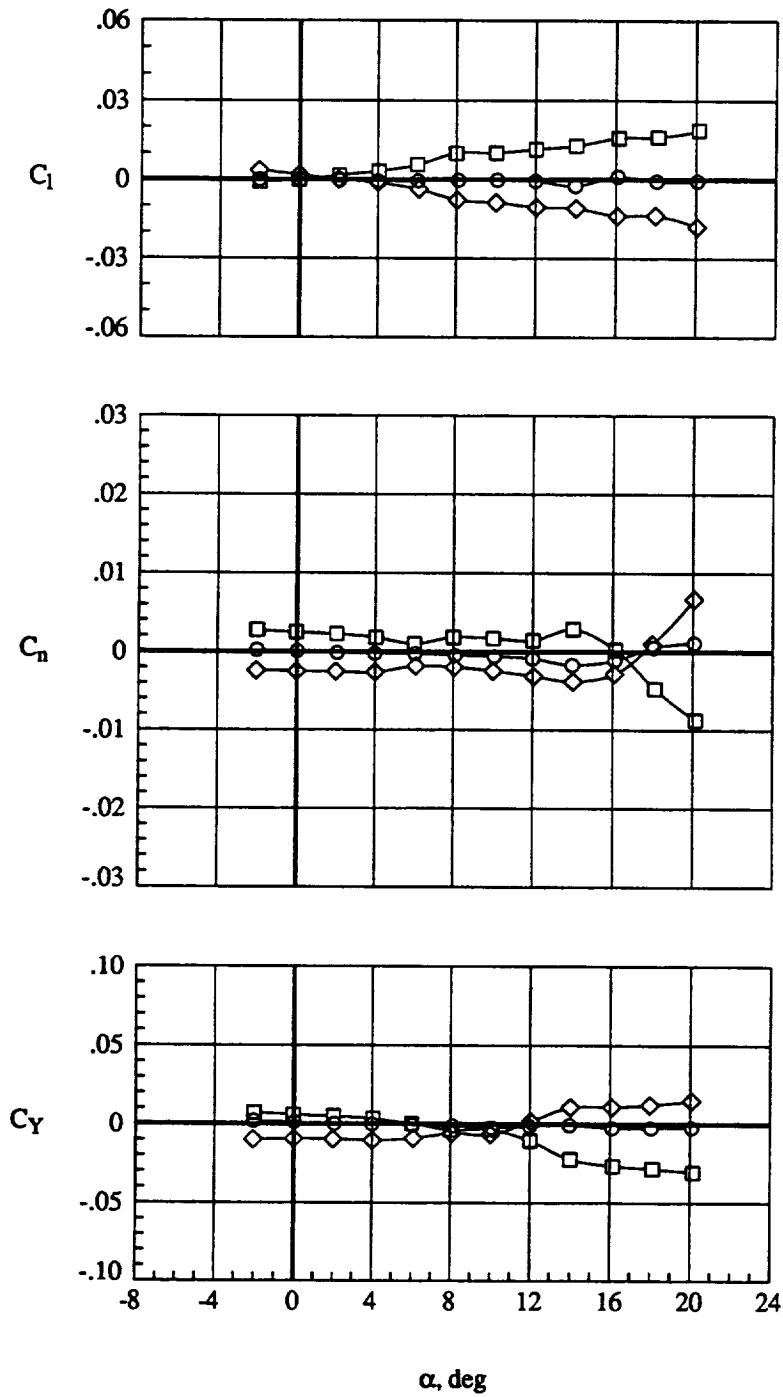
Run	$\beta$ , deg	Configuration
○	13. 0.	$\delta_L = MA, \delta_T = 0^\circ$
□	15. -5.	$\delta_L = MA, \delta_T = 0^\circ$
◇	16. 5.	$\delta_L = MA, \delta_T = 0^\circ$



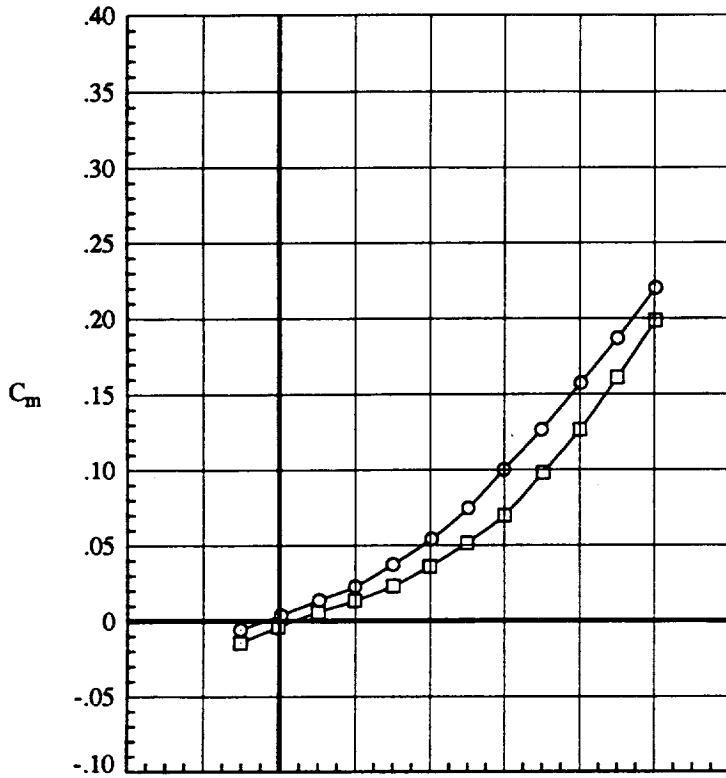
(a) Longitudinal aerodynamics

Figure 25. Effect of sideslip on the mission adaptive flap configuration,  $q=110$  psf.

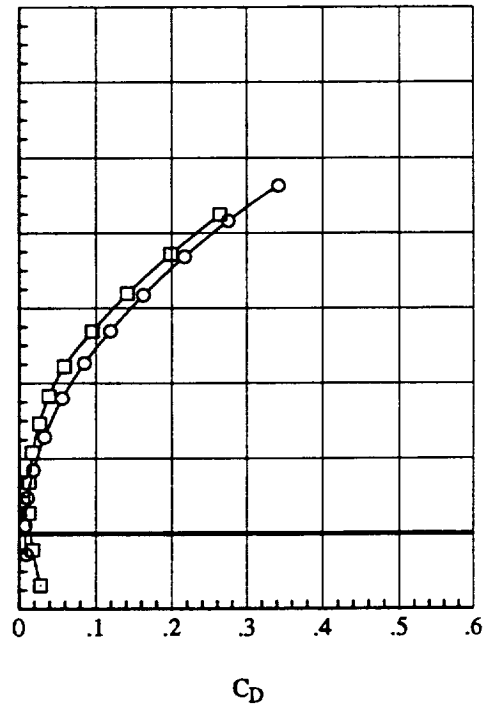
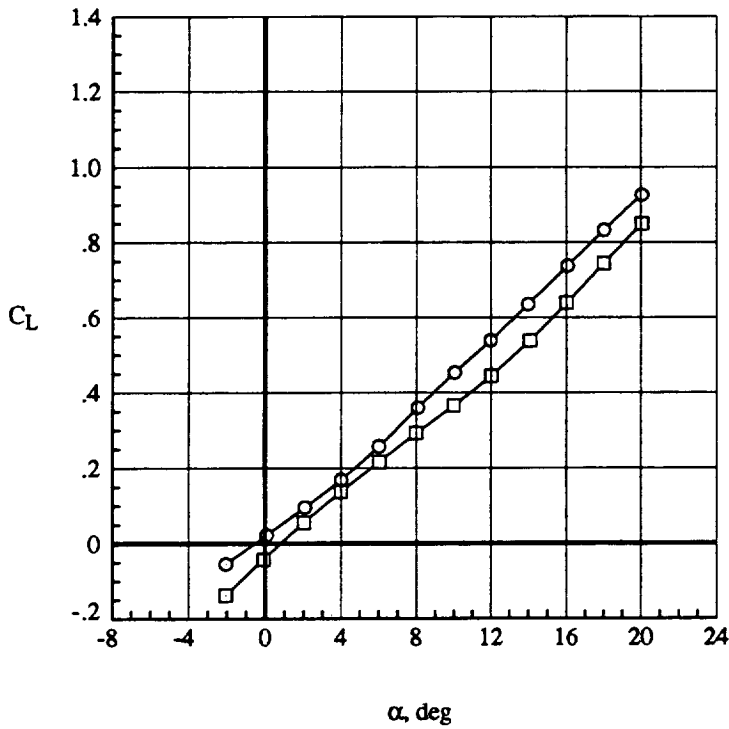
Run	$\beta$ , deg	Configuration
○	13.	0. $\delta_L = MA, \delta_T = 0^\circ$
□	15.	-5. $\delta_L = MA, \delta_T = 0^\circ$
◇	16.	5. $\delta_L = MA, \delta_T = 0^\circ$



(b) Lateral aerodynamics  
Figure 25. Concluded.



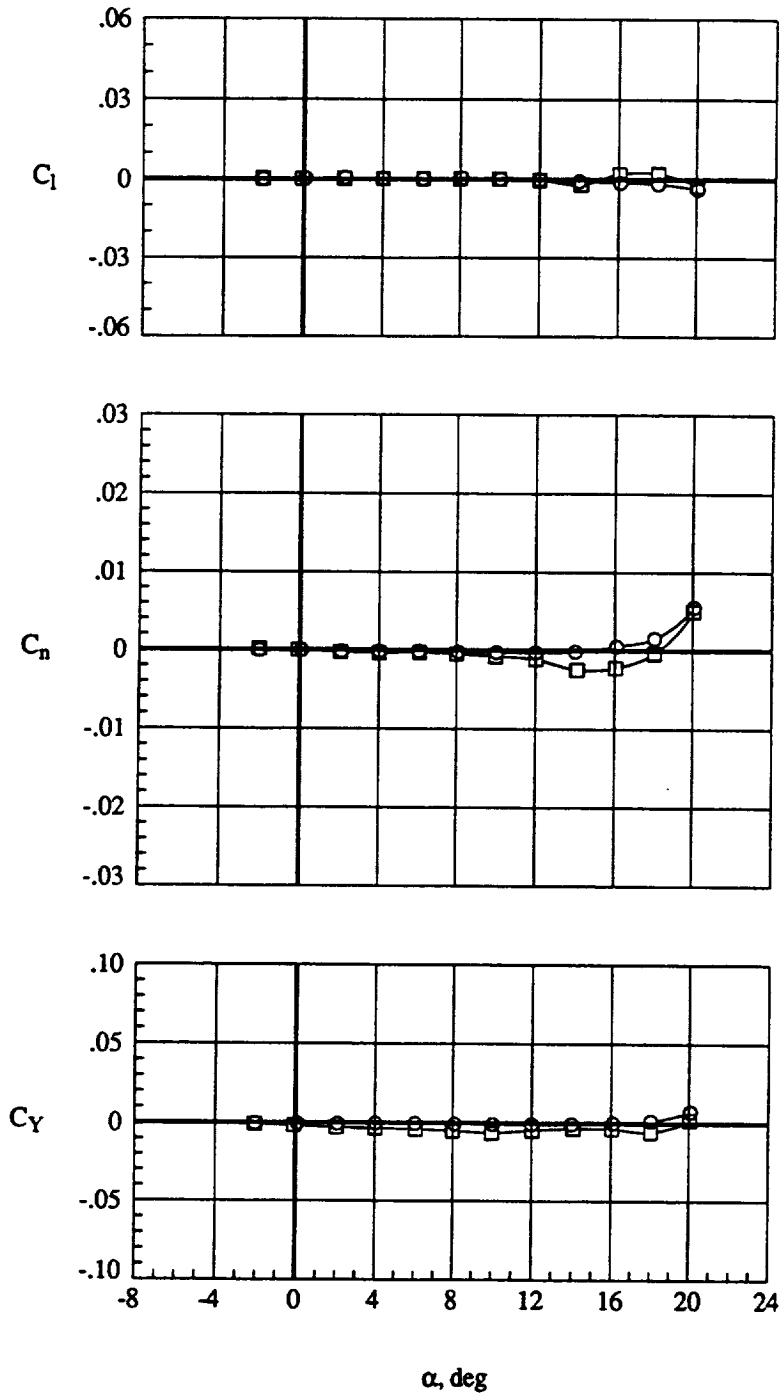
Run	$\beta$ , deg	Configuration
○	38.	$\delta_L = 0^\circ, \delta_T = 0^\circ$
□	14.	$\delta_L = MA, \delta_T = 0^\circ$



(a) Longitudinal aerodynamics

Figure 26. Effect of mission adaptive leading-edge flap with  $\delta_T = 0^\circ, q=70$  psf.

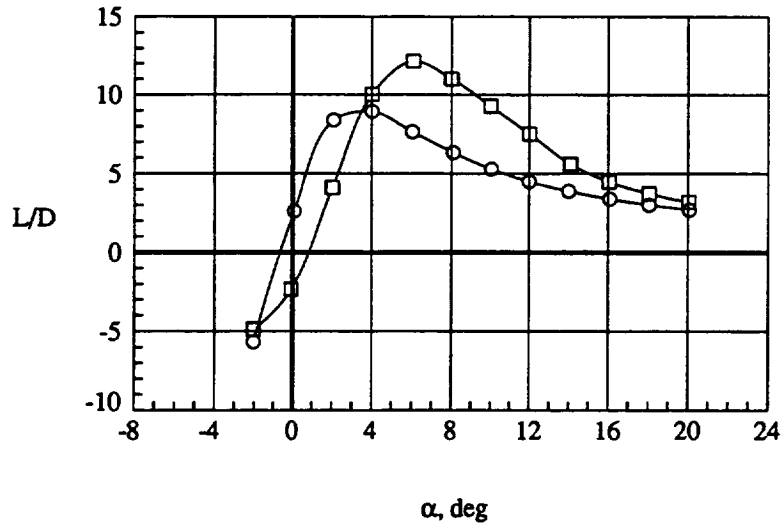
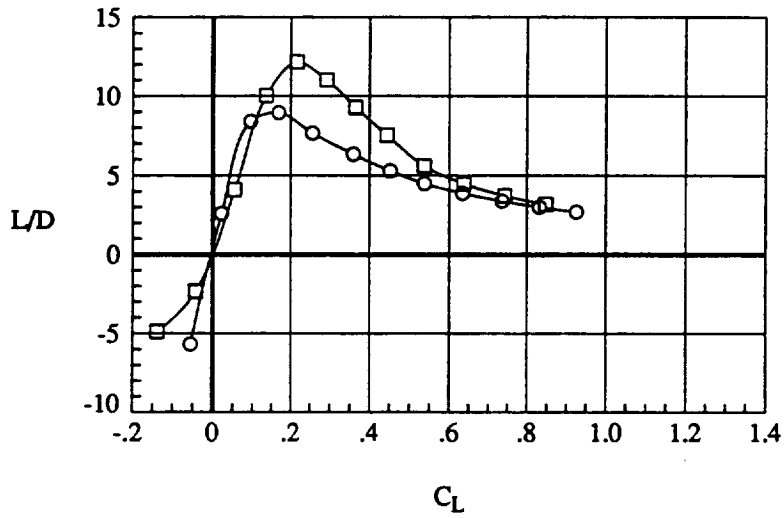
	Run	$\beta$ , deg	Configuration
○	38.	0.	$\delta_L = 0^\circ, \delta_T = 0^\circ$
□	14.	0.	$\delta_L = MA, \delta_T = 0^\circ$



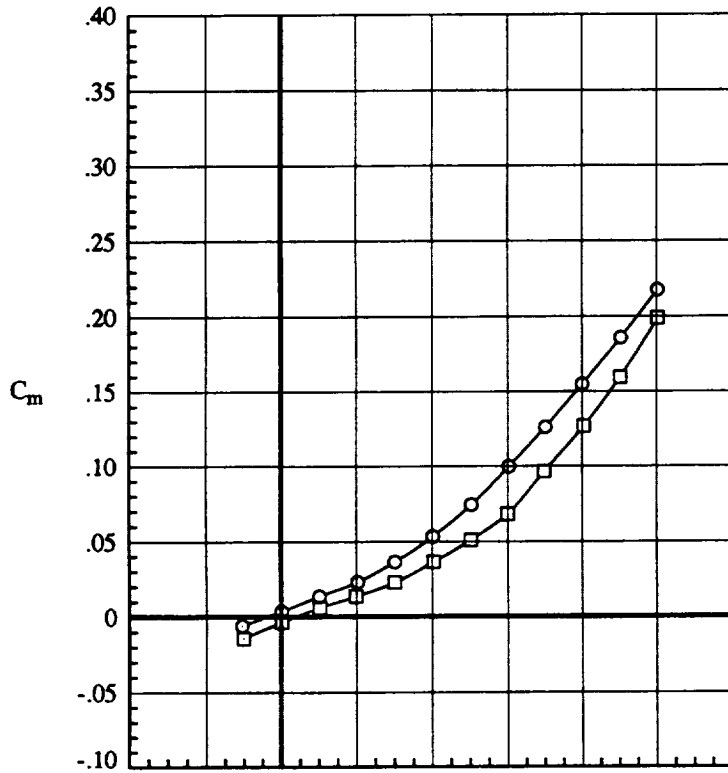
(b) Lateral aerodynamics  
Figure 26. Continued.



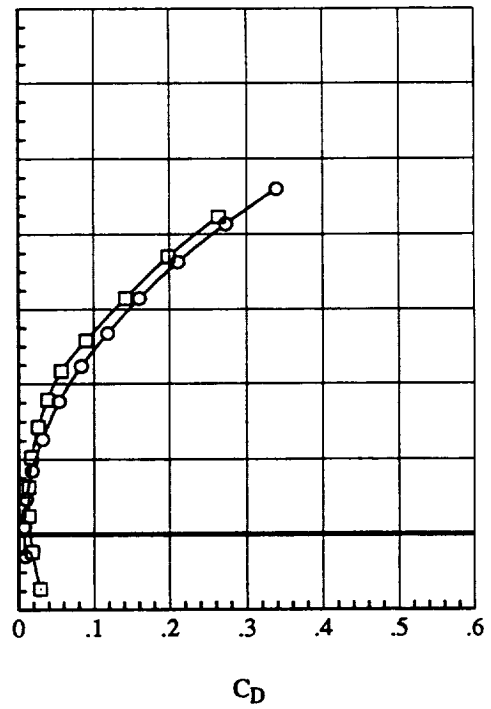
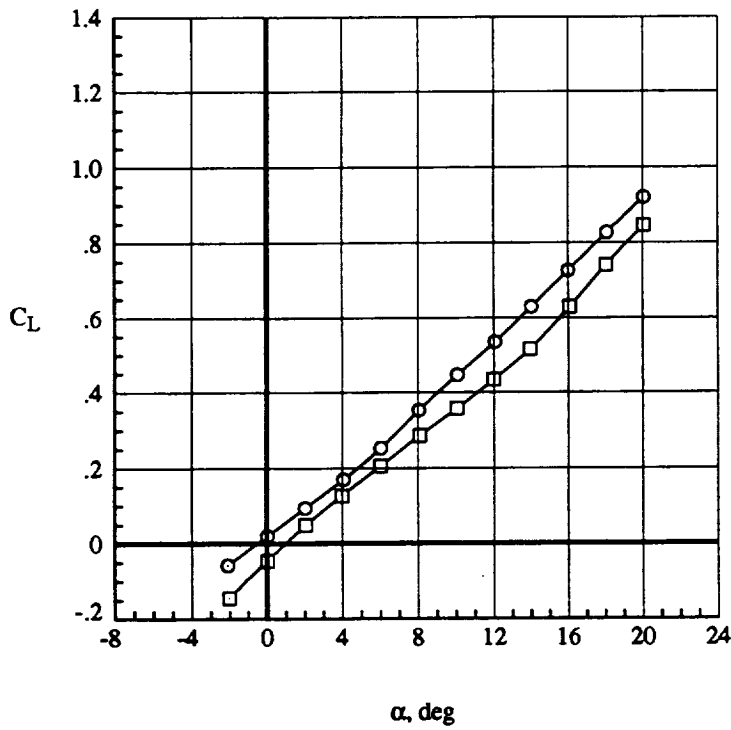
	Run	$\beta$ , deg	Configuration
○	38.	0.	$\delta_L = 0^\circ, \delta_T = 0^\circ$
□	14.	0.	$\delta_L = MA, \delta_T = 0^\circ$



(c) Lift / Drag performance  
Figure 26. Concluded.



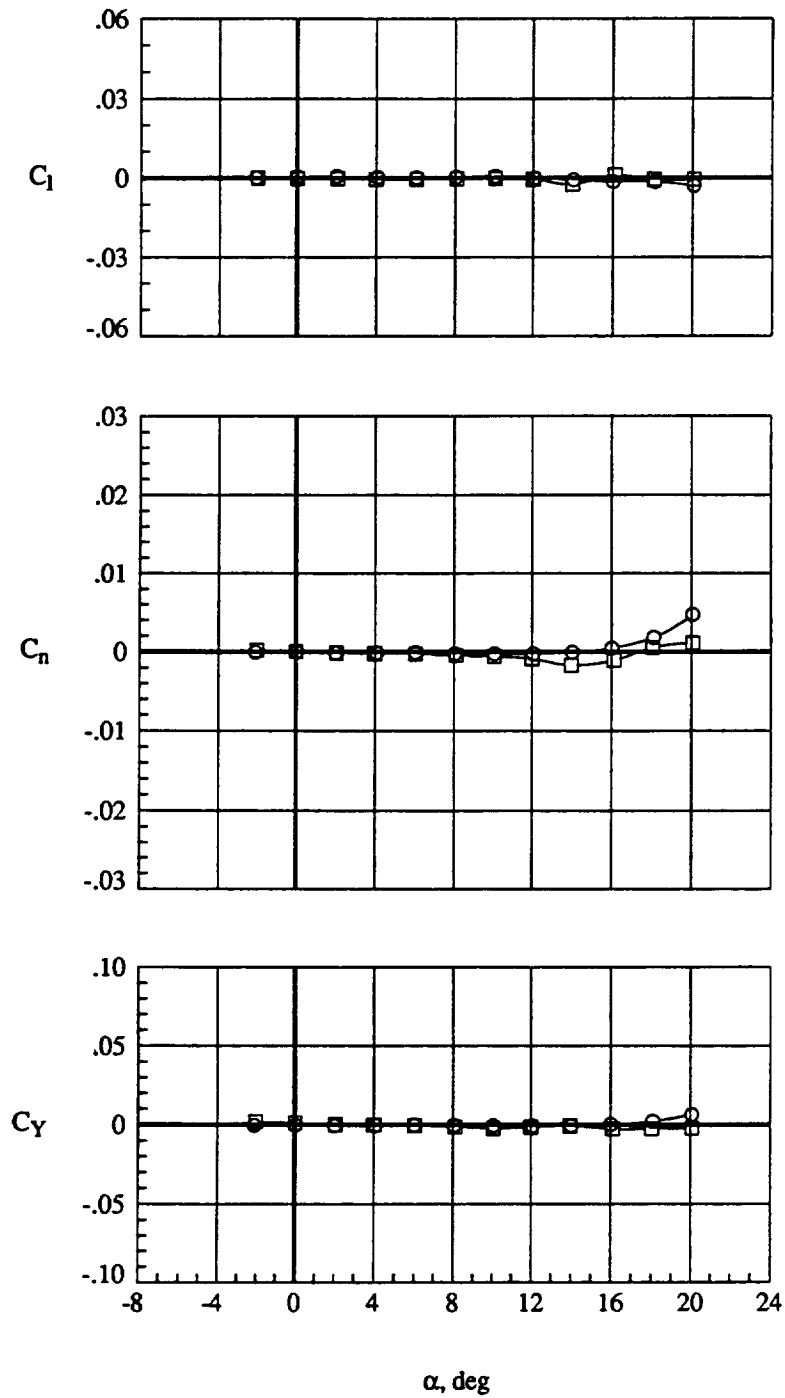
Run	$\beta$ , deg	Configuration
○	39.	$\delta_L = 0^\circ, \delta_T = 0^\circ$
□	13.	$\delta_L = MA, \delta_T = 0^\circ$



(a) Longitudinal aerodynamics

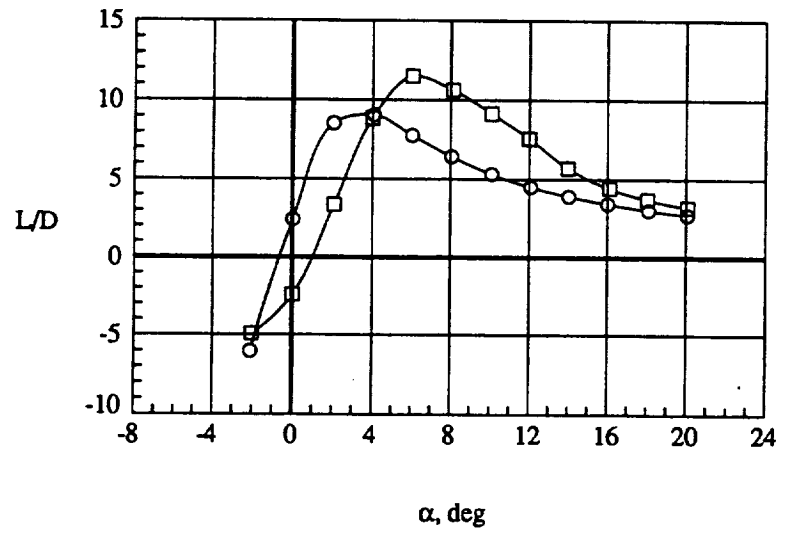
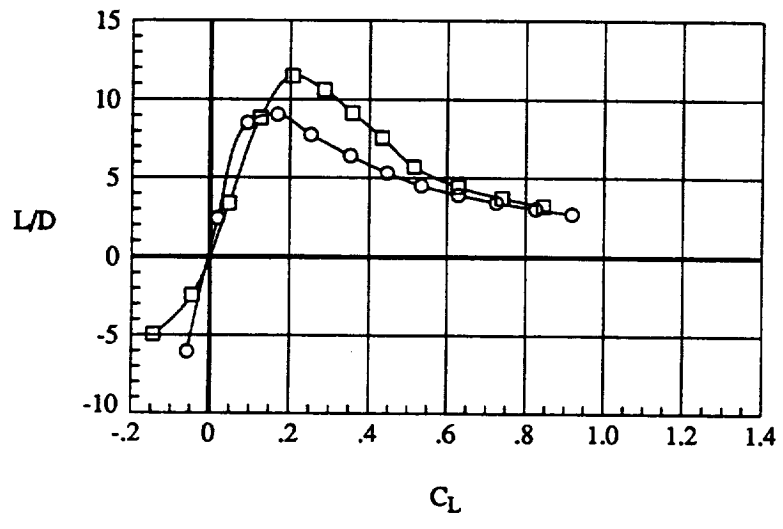
Figure 27. Effect of mission adaptive leading-edge flap with  $\delta_T = 0^\circ, q = 110$  psf.

	Run	$\beta$ , deg	Configuration
○	39.	0.	$\delta_L = 0^\circ, \delta_T = 0^\circ$
□	13.	0.	$\delta_L = MA, \delta_T = 0^\circ$

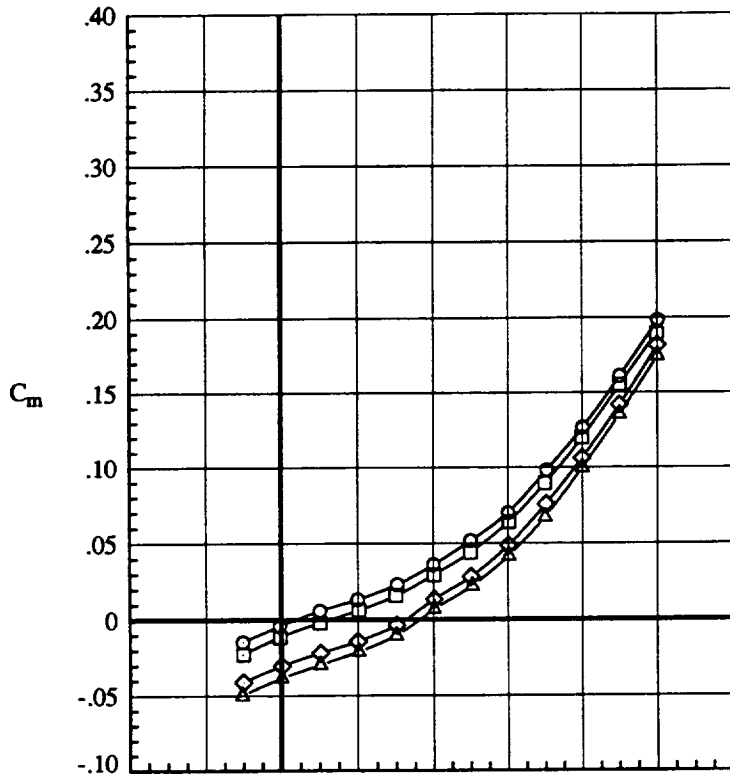


(b) Lateral aerodynamics  
Figure 27. Continued.

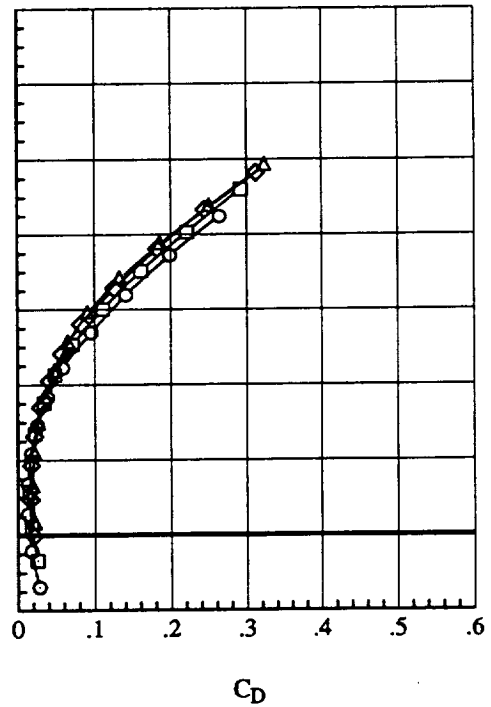
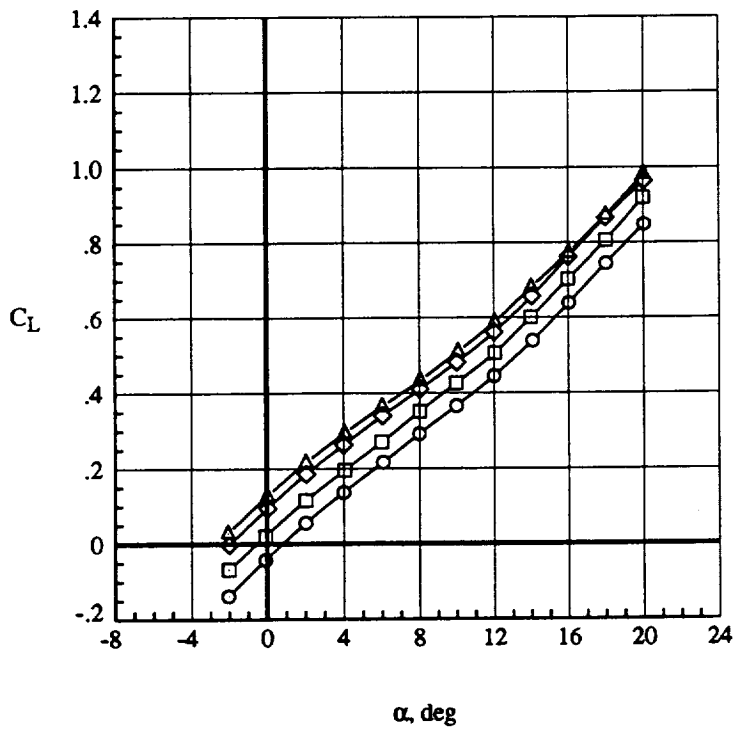
Run	$\beta$ , deg	Configuration
○	39.	$\delta_L = 0^\circ, \delta_T = 0^\circ$
□	13.	$\delta_L = MA, \delta_T = 0^\circ$



(c) Lift / Drag performance  
Figure 27. Concluded.



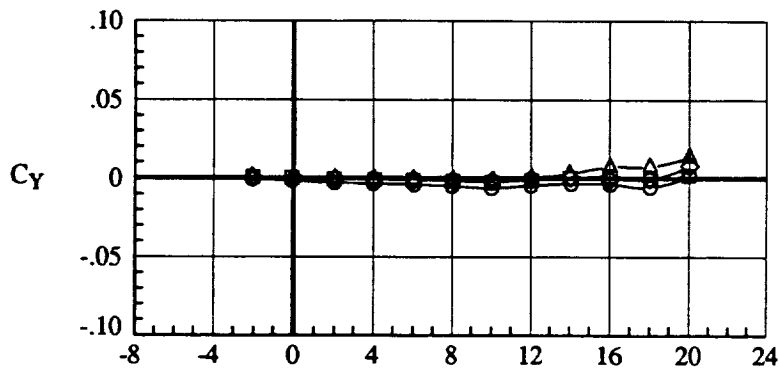
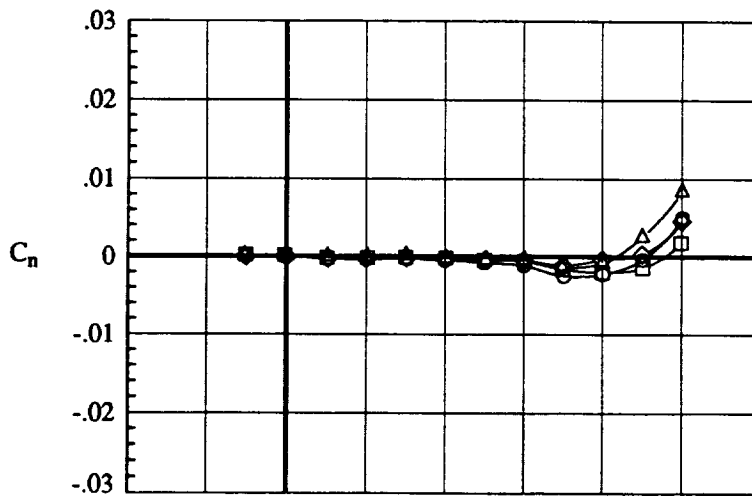
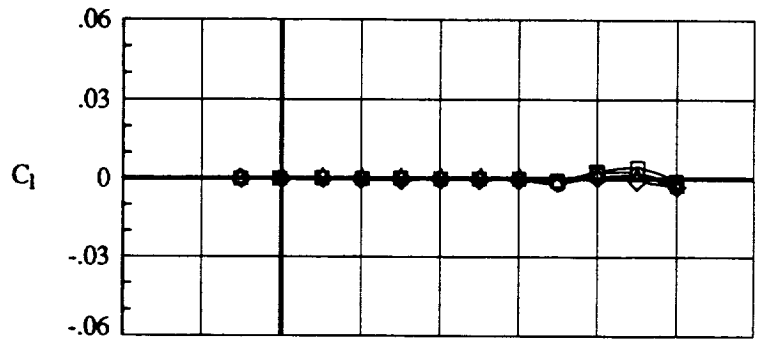
Run	$\beta$ , deg	Configuration
○	14.	0. $\delta_L = MA, \delta_T = 0^\circ$
□	17.	0. $\delta_L = MA, \delta_{T_{1/2/3}} = 10^\circ/10^\circ/0^\circ$
◇	21.	0. $\delta_L = MA, \delta_{T_{1/2/3}} = 10^\circ/10^\circ/12.9^\circ$
△	25.	0. $\delta_L = MA, \delta_{T_{1/2/3}} = 10^\circ/10^\circ/20^\circ$



(a) Longitudinal aerodynamics

Figure 28. Effect of outboard trailing-edge flap with mission adaptive leading-edge flap,  $\delta_{T_{1/2}} = 10^\circ/10^\circ, q=70$  psf.

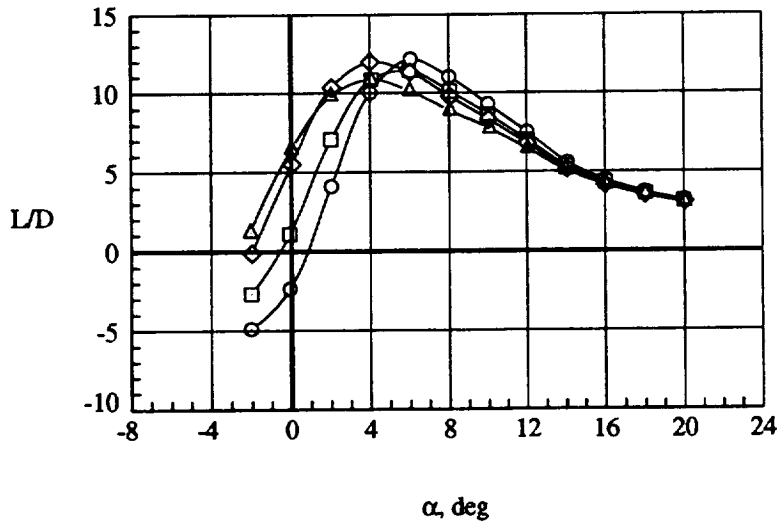
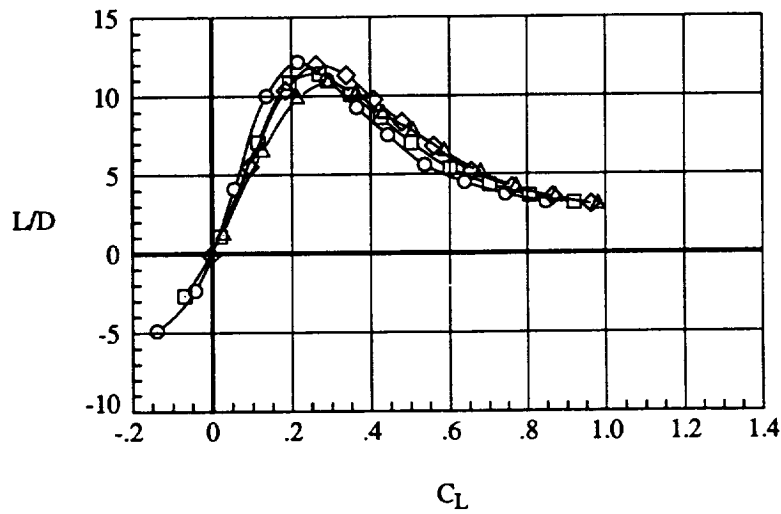
	Run	$\beta$ , deg	Configuration
○	14.	0.	$\delta_L = MA, \delta_T = 0^\circ$
□	17.	0.	$\delta_L = MA, \delta_{T_{1/2/3}} = 10^\circ/10^\circ/0^\circ$
◇	21.	0.	$\delta_L = MA, \delta_{T_{1/2/3}} = 10^\circ/10^\circ/12.9^\circ$
△	25.	0.	$\delta_L = MA, \delta_{T_{1/2/3}} = 10^\circ/10^\circ/20^\circ$



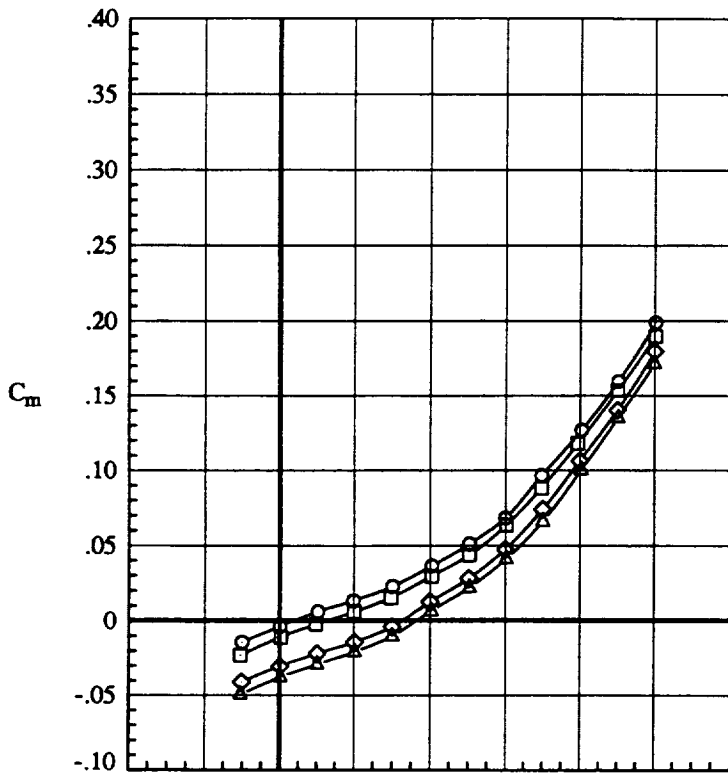
$\alpha$ , deg

(b) Lateral aerodynamics  
Figure 28. Continued.

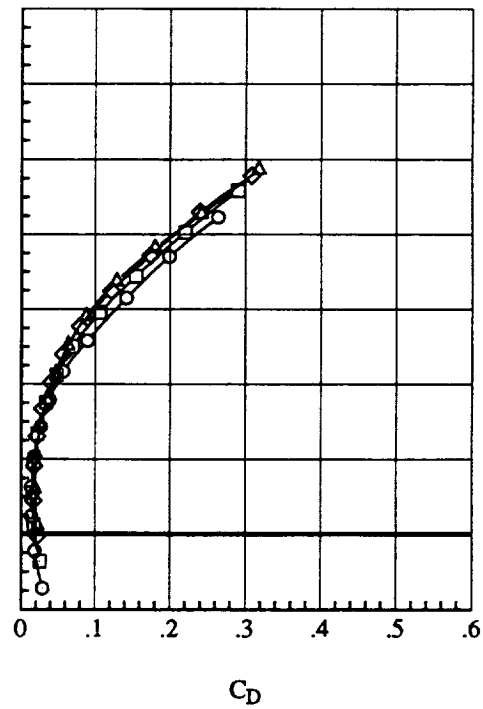
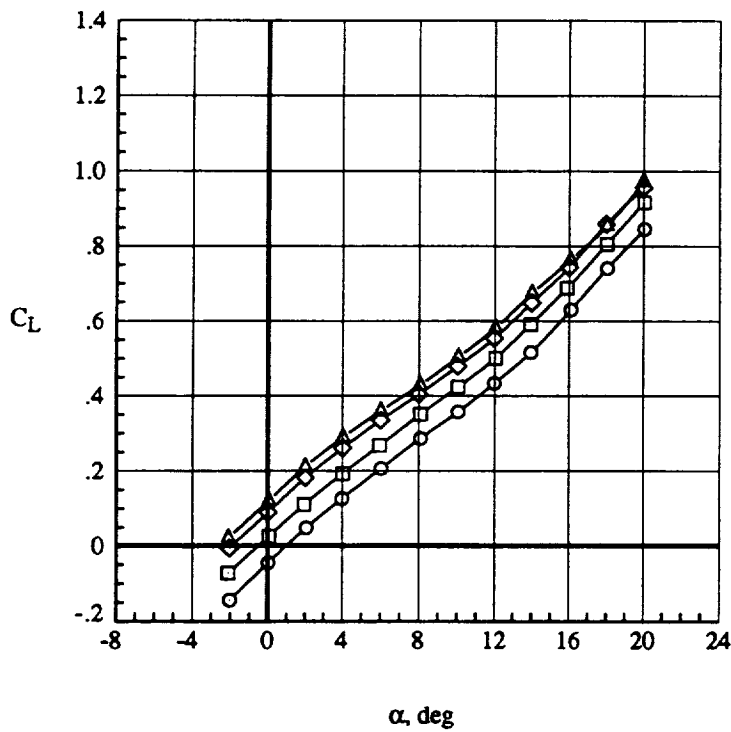
	Run	$\beta$ , deg	Configuration
○	14.	0.	$\delta_L = MA, \delta_T = 0^\circ$
□	17.	0.	$\delta_L = MA, \delta_{T_{1/2/3}} = 10^\circ/10^\circ/0^\circ$
◇	21.	0.	$\delta_L = MA, \delta_{T_{1/2/3}} = 10^\circ/10^\circ/12.9^\circ$
△	25.	0.	$\delta_L = MA, \delta_{T_{1/2/3}} = 10^\circ/10^\circ/20^\circ$



(c) Lift / Drag performance  
Figure 28. Concluded.



Run	$\beta$ , deg	Configuration
○	13.	0. $\delta_L = MA, \delta_T = 0^\circ$
□	18.	0. $\delta_L = MA, \delta_{T_{1/2/3}} = 10^\circ/10^\circ/0^\circ$
◇	22.	0. $\delta_L = MA, \delta_{T_{1/2/3}} = 10^\circ/10^\circ/12.9^\circ$
△	26.	0. $\delta_L = MA, \delta_{T_{1/2/3}} = 10^\circ/10^\circ/20^\circ$

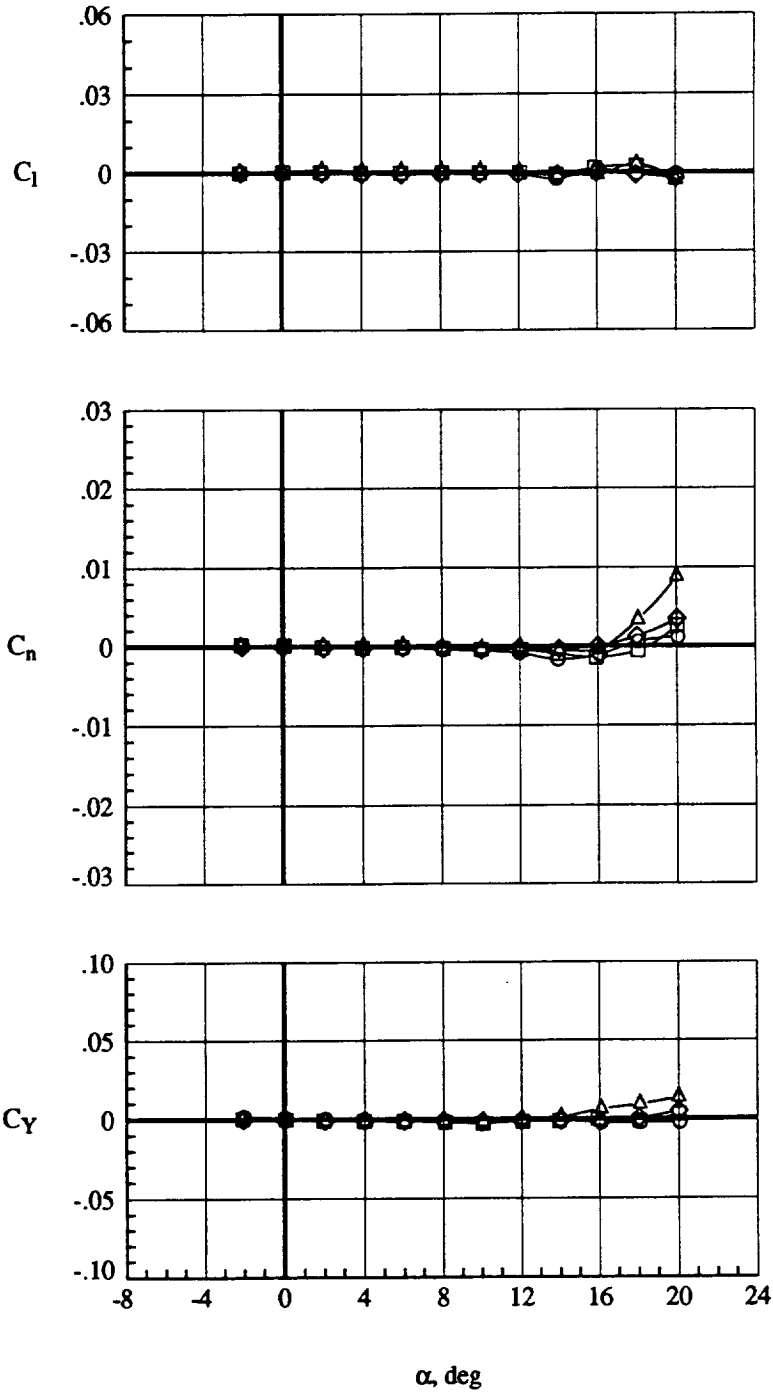


(a) Longitudinal aerodynamics

Figure 29. Effect of outboard trailing-edge flap with mission adaptive leading-edge flap,  $\delta_{T_{1/2}} = 10^\circ/10^\circ, q=110$  psf.

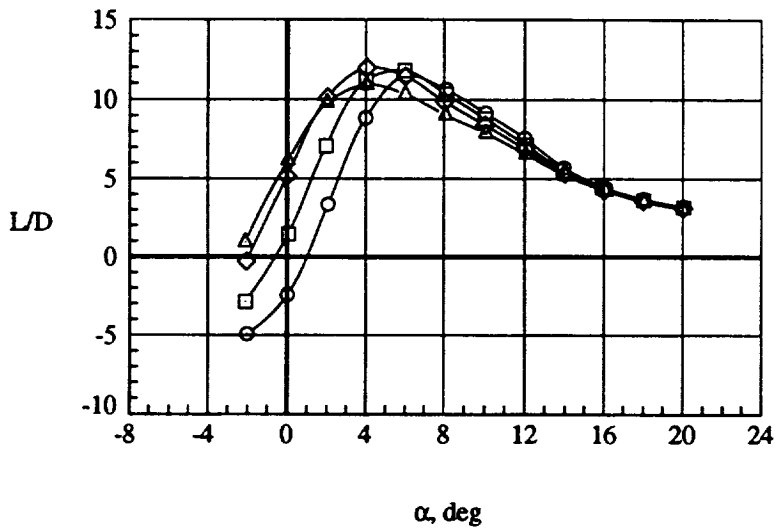
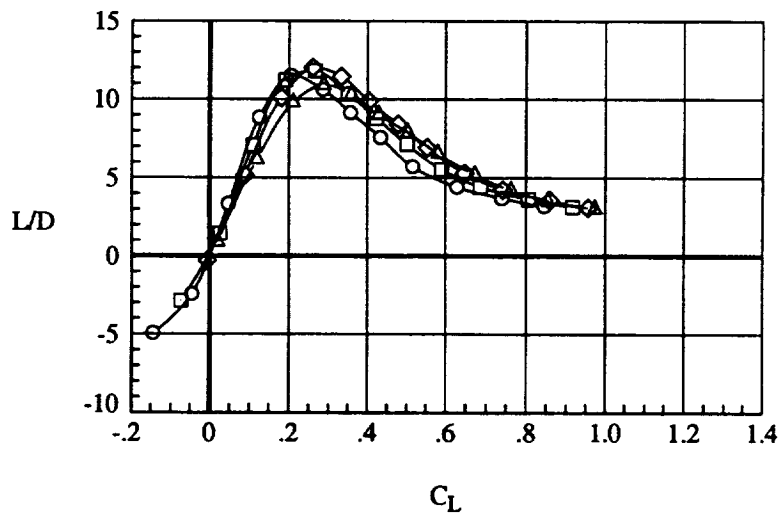


	Run	$\beta$ , deg	Configuration
○	13.	0.	$\delta_L = MA, \delta_T = 0^\circ$
□	18.	0.	$\delta_L = MA, \delta_{T_{1/2/3}} = 10^\circ/10^\circ/0^\circ$
◇	22.	0.	$\delta_L = MA, \delta_{T_{1/2/3}} = 10^\circ/10^\circ/12.9^\circ$
△	26.	0.	$\delta_L = MA, \delta_{T_{1/2/3}} = 10^\circ/10^\circ/20^\circ$

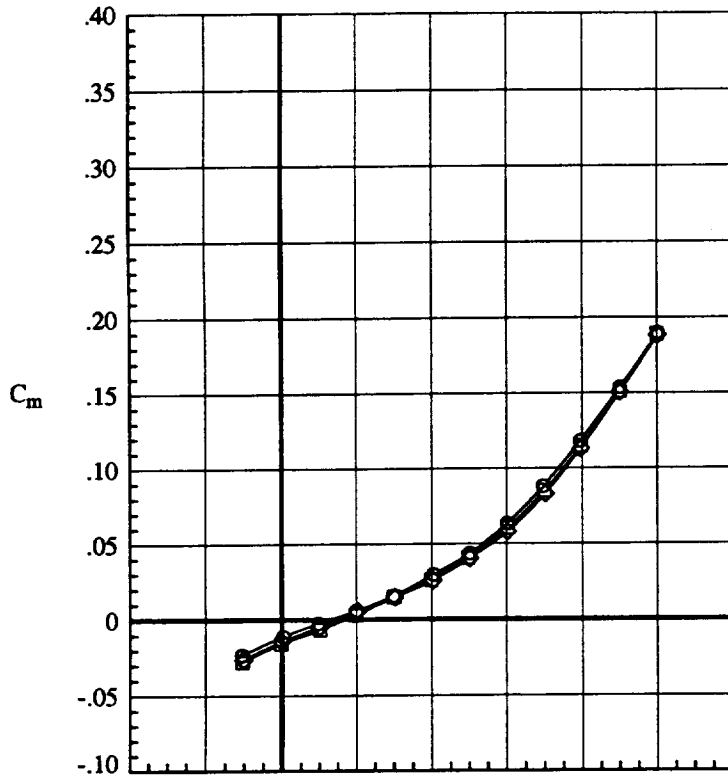


(b) Lateral aerodynamics  
Figure 29. Continued.

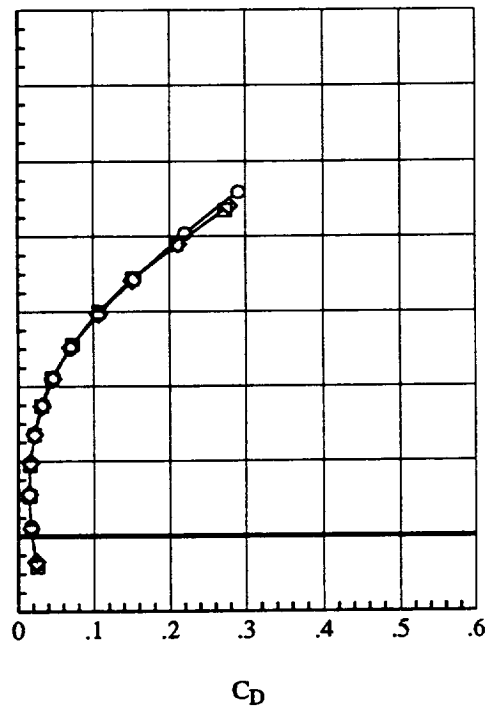
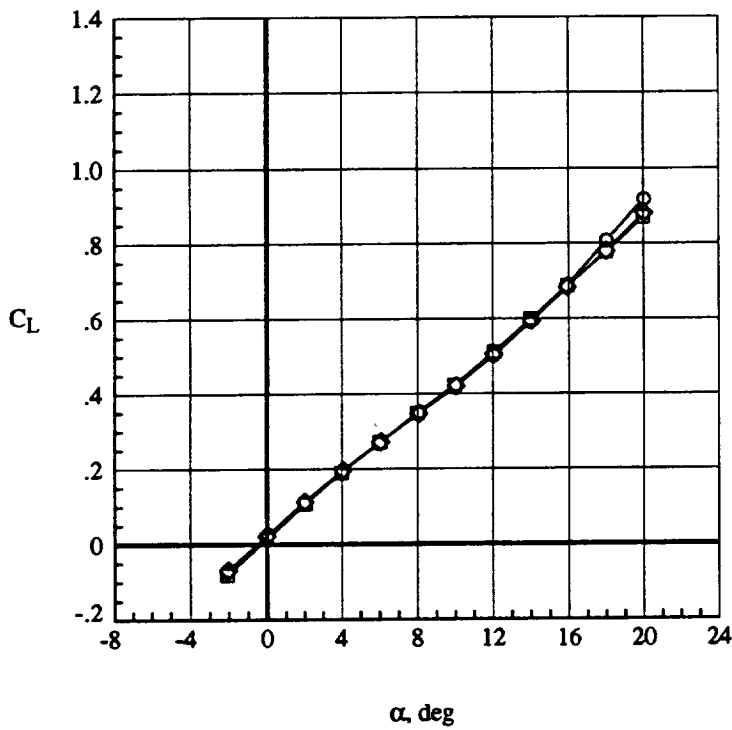
	Run	$\beta$ , deg	Configuration
○	13.	0.	$\delta_L = MA, \delta_T = 0^\circ$
□	18.	0.	$\delta_L = MA, \delta_{T_{1/2/3}} = 10^\circ/10^\circ/0^\circ$
◇	22.	0.	$\delta_L = MA, \delta_{T_{1/2/3}} = 10^\circ/10^\circ/12.9^\circ$
△	26.	0.	$\delta_L = MA, \delta_{T_{1/2/3}} = 10^\circ/10^\circ/20^\circ$



(c) Lift / Drag performance  
Figure 29. Concluded.



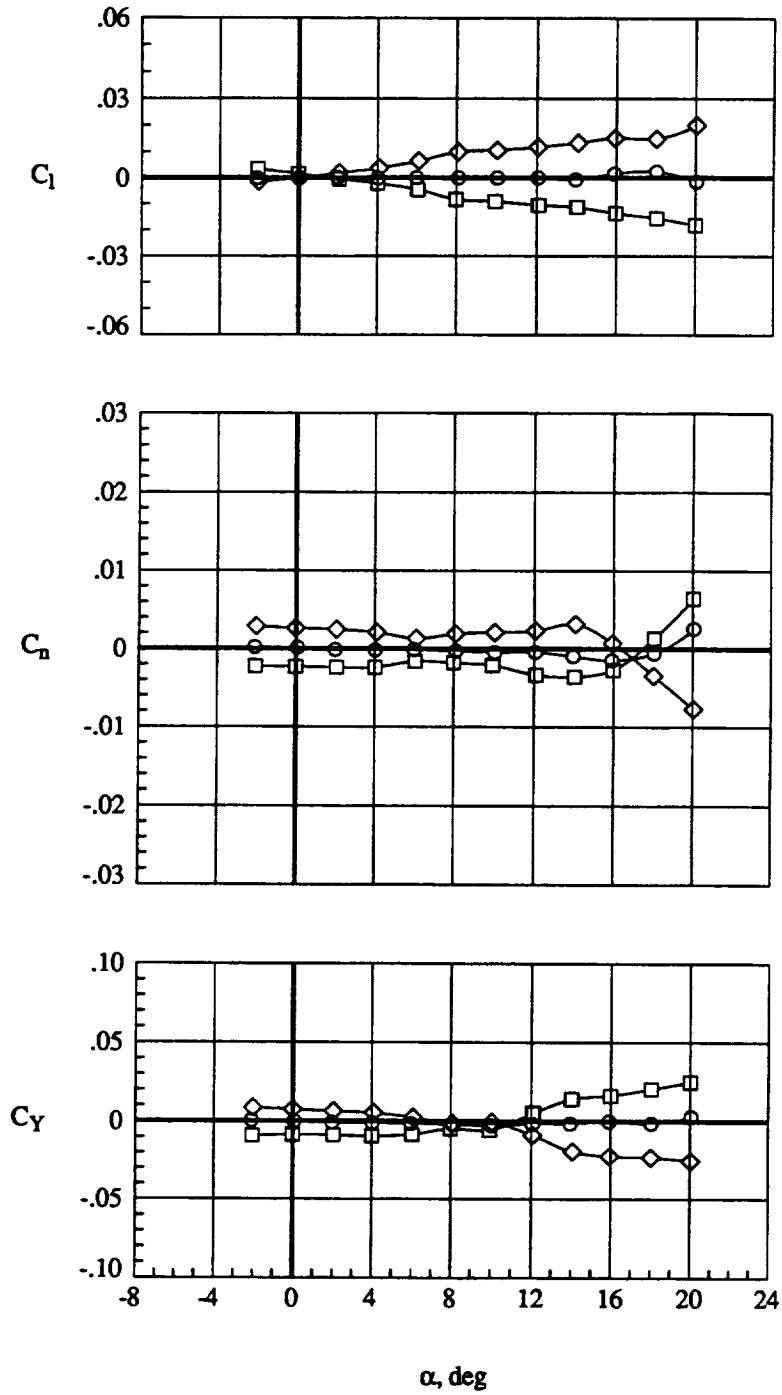
Run	$\beta$ , deg	Configuration
○	18.	0. $\delta_L = MA, \delta_{T_{1/2/3}} = 10^\circ/10^\circ/0^\circ$
□	19.	5. $\delta_L = MA, \delta_{T_{1/2/3}} = 10^\circ/10^\circ/0^\circ$
◇	20.	-5. $\delta_L = MA, \delta_{T_{1/2/3}} = 10^\circ/10^\circ/0^\circ$



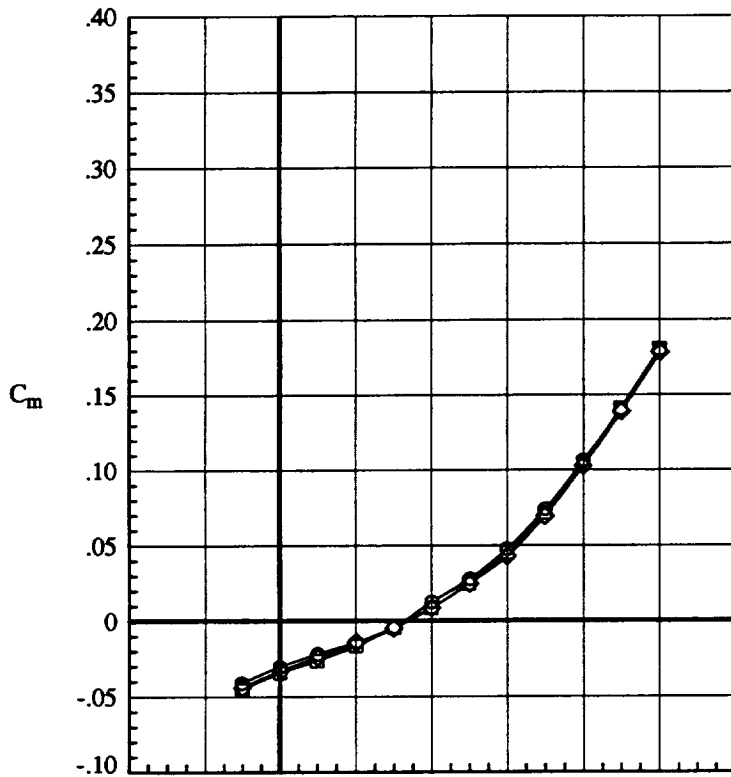
(a) Longitudinal aerodynamics

Figure 30. Effect of sideslip on the mission adaptive leading-edge with  $\delta_{T_{1/2/3}} = 10^\circ/10^\circ/0^\circ$ ,  $q=110$  psf.

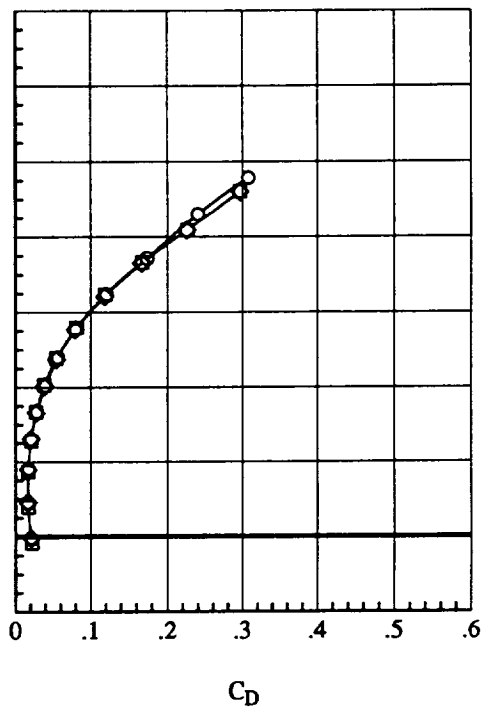
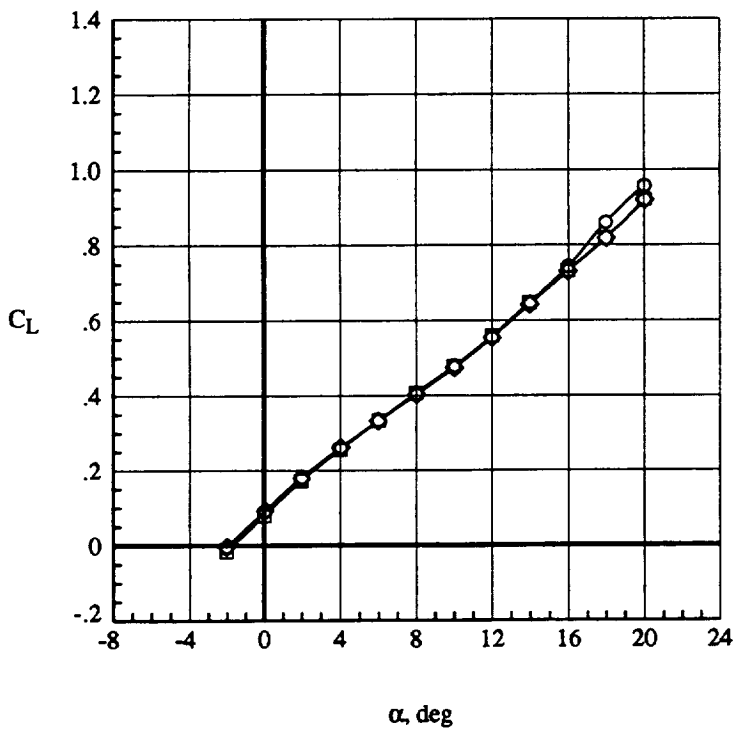
Run	$\beta$ , deg	Configuration
○	18.	0. $\delta_L = MA, \delta_{T_{1/2/3}} = 10^\circ/10^\circ/0^\circ$
□	19.	5. $\delta_L = MA, \delta_{T_{1/2/3}} = 10^\circ/10^\circ/0^\circ$
◇	20.	-5. $\delta_L = MA, \delta_{T_{1/2/3}} = 10^\circ/10^\circ/0^\circ$



(b) Lateral aerodynamics  
Figure 30. Concluded.

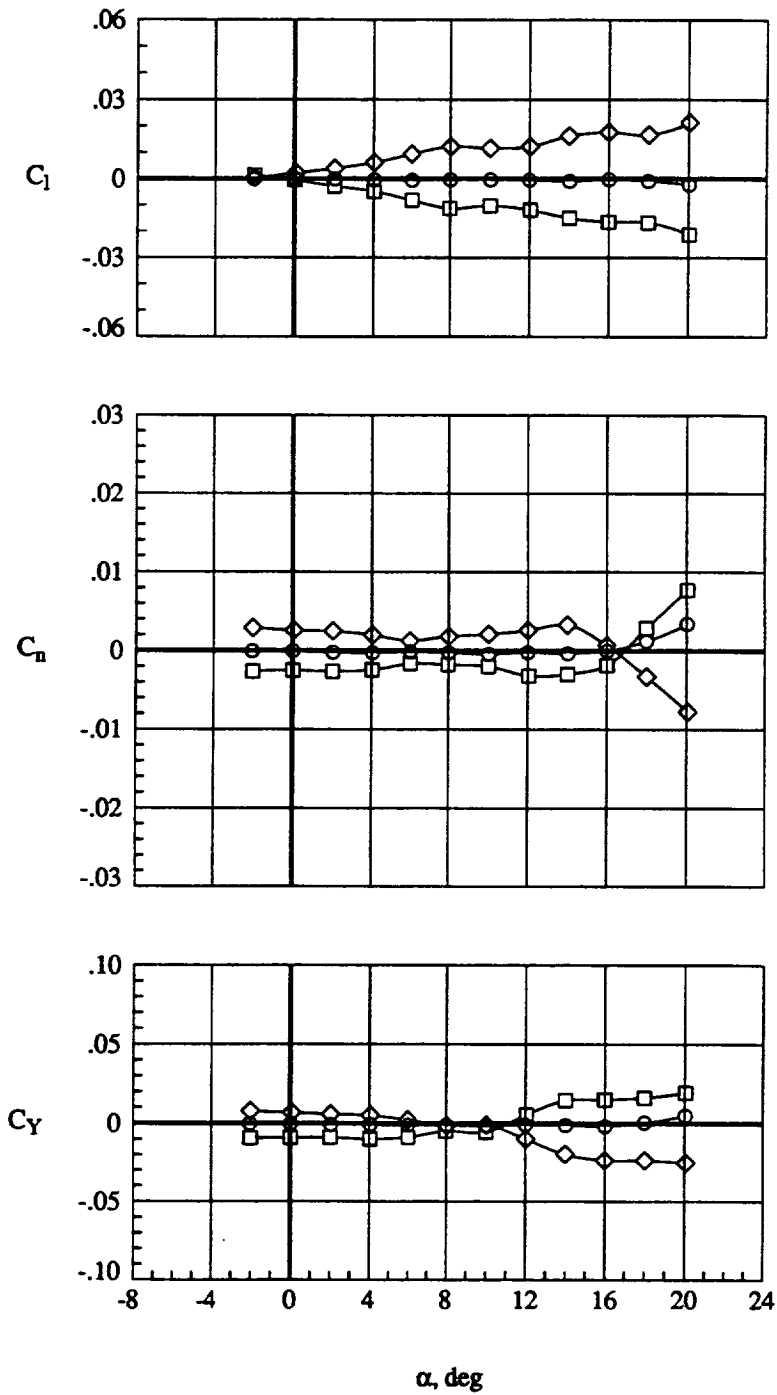


Run	$\beta$ , deg	Configuration
○	22. 0.	$\delta_L = MA, \delta_{T_{1/2/3}} = 10^\circ/10^\circ/12.9$
□	23. 5.	$\delta_L = MA, \delta_{T_{1/2/3}} = 10^\circ/10^\circ/12.9$
◇	24. -5.	$\delta_L = MA, \delta_{T_{1/2/3}} = 10^\circ/10^\circ/12.9$

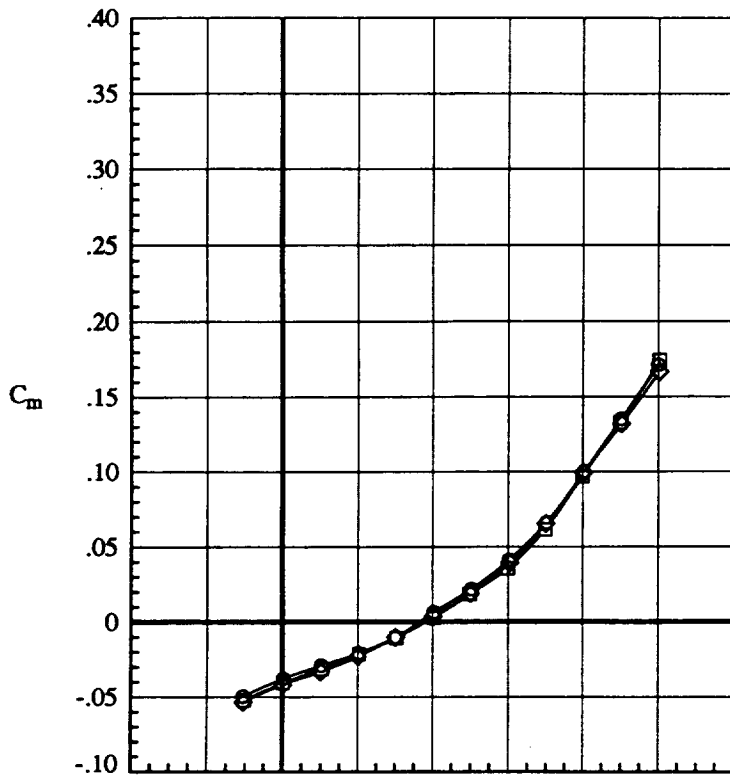


(a) Longitudinal aerodynamics  
 Figure 31. Effect of sideslip on the mission adaptive leading-edge with  $\delta_{T_{1/2/3}} = 10^\circ/10^\circ/12.9^\circ$ ,  $q=110$  psf.

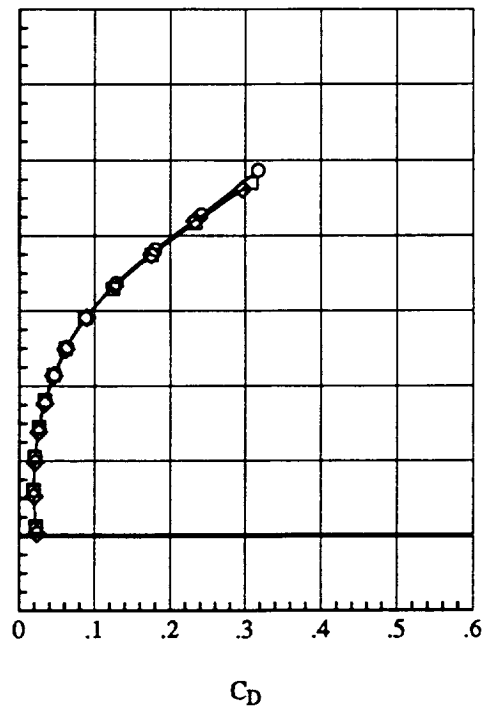
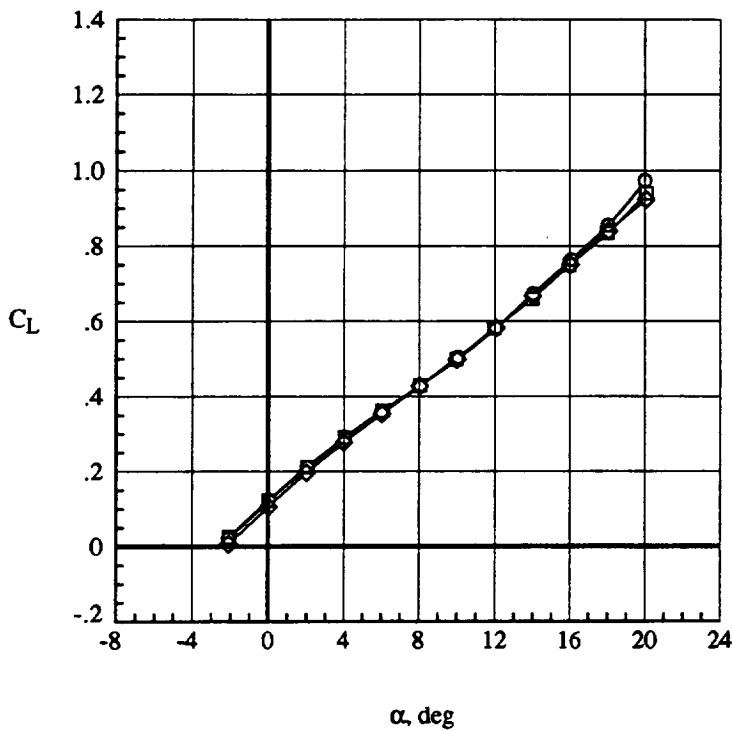
Run	$\beta$ , deg	Configuration
○	22.	0. $\delta_L = MA, \delta_{T_{1/2/3}} = 10^\circ/10^\circ/12.9$
□	23.	5. $\delta_L = MA, \delta_{T_{1/2/3}} = 10^\circ/10^\circ/12.9$
◇	24.	-5. $\delta_L = MA, \delta_{T_{1/2/3}} = 10^\circ/10^\circ/12.9$



(b) Lateral aerodynamics  
Figure 31. Concluded.

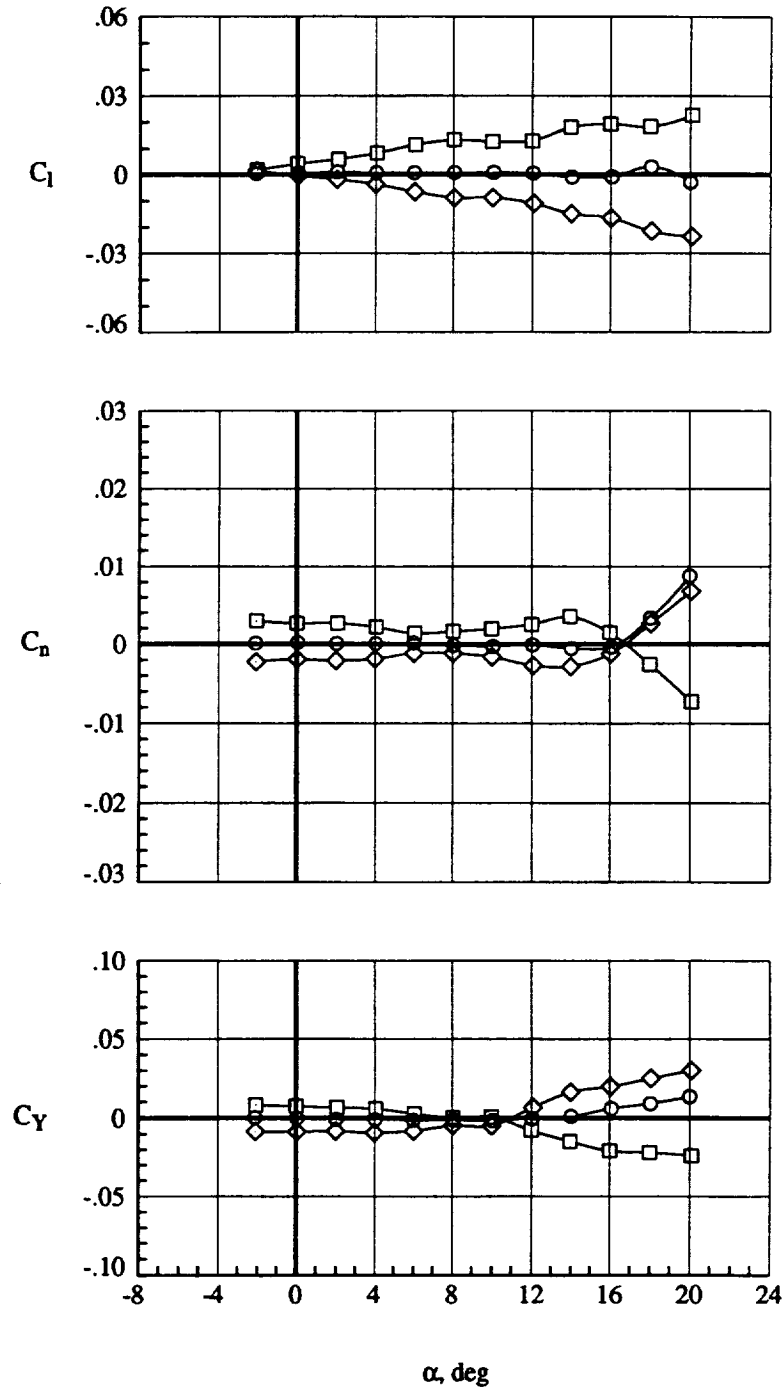


Run	β, deg	Configuration
○	26.	0. δ <sub>L</sub> = MA, δ <sub>T<sub>1/2/3</sub></sub> = 10°/10°/20°
□	27.	-5. δ <sub>L</sub> = MA, δ <sub>T<sub>1/2/3</sub></sub> = 10°/10°/20°
◇	28.	5. δ <sub>L</sub> = MA, δ <sub>T<sub>1/2/3</sub></sub> = 10°/10°/20°



(a) Longitudinal aerodynamics  
 Figure 32. Effect of sideslip on the mission adaptive leading-edge with δ<sub>T<sub>1/2/3</sub></sub> = 10°/10°/20°, q=110 psf.

Run	$\beta$ , deg	Configuration
○	26.	0. $\delta_L = MA, \delta_{T_{1/2/3}} = 10^\circ/10^\circ/20^\circ$
□	27.	-5. $\delta_L = MA, \delta_{T_{1/2/3}} = 10^\circ/10^\circ/20^\circ$
◇	28.	5. $\delta_L = MA, \delta_{T_{1/2/3}} = 10^\circ/10^\circ/20^\circ$



(b) Lateral aerodynamics  
Figure 32. Concluded.



## Appendix A

### Instrumentation Accuracy

Forces and moments were measured with a six-component strain-gauge balance identified as NASA LaRC VST-3. The accuracy and error range for each component is as follows:

Component	Max Load Range (lb or in-lb)	Error Range
Normal Force	±3000	±0.6%
Axial Force	±500	±0.75%
Pitching Moment	±10000	±0.5%
Rolling Moment	±7500	±1.1%
Yawing Moment	±4500	±1.4%
Side Force	±1800	±0.8%

The angle-of-attack sensor had an accuracy of  $\pm 0.01^\circ$ . Tunnel and atmospheric conditions were measured using standard facility instrumentation as described in reference 11.

## References

1. Campbell, Bryan A.; Applin, Zachary T.; Kemmerly, Guy T.: *Subsonic Assessment of Several Vortex Flow Management Devices on a High-Speed Civil Transport Configuration*. NASA/TP-1999-209693, 1999.
2. Campbell, Bryan A.; Applin, Zachary T.; Kemmerly, Guy T.; Coe, Paul L., Jr.; Owens, D. Bruce; Gile, Brenda E.; Parikh, Pradip G.; Smith, Don: *Subsonic Investigation of a Leading-Edge Boundary Layer Control Suction System on a High-Speed Civil Transport Configuration*. NASA/TM-1999-209700, 1999.
3. Campbell, Bryan A., Hom, Kam W., and Huffman, Jarrett K.: *Investigation of Subsonic Maneuver Performance of a Supersonic Fighter Cranked Wing*. NASA TP-2687, 1987.
4. Coe, Paul L., Jr.; Huffman, Jarrett K., Fenbert, James W.: *Leading-Edge Deflection Optimization for a Highly Swept Arrow-Wing Configuration*. NASA TP-1777, 1980
5. Scott, Samuel J.; Nicks, Oran W.; and Imbrie, P.K.: *Effects of Leading-Edge Devices on the Low-Speed Aerodynamic Characteristics of a Highly-Swept Arrow-Wing*. NASA CR-172531, 1985
6. Rao, Dhanvada M.: *Subsonic Flow Investigation on a Cranked Wing Designed For High Maneuverability*. NASA CR-178046, 1986.
7. Rao, Dhanvada M.: *Low-Speed Wind Tunnel Study of Longitudinal Stability and Usable-Lift Improvement of a Cranked Wing*. NASA CR-178204, 1987.
8. Rao, Dhanvada M.; Campbell, James F.: *Vortical Flow Management Techniques*. Prog. Aerospace Sci. Vol. 24, pp173-224, 1987.
9. Frink, Neal T.: *Concepts for Designing Vortex Flap Geometries*. NASA TP-2233, 1983

10. Carlson, Harry W.; Darden, Christine M.: *Validation of a Pair of Computer Codes for Estimation and Optimization of Subsonic Aerodynamic Performance of Simple Hinged-Flap Systems for Thin Swept Wings*. NASA TP-2828, 1988.
11. Gentry, Garl L., Jr.; Quinto, P. Frank; Gatlin, Gregory M.; and Applin, Zachary T.: *The Langley 14- by 22-Foot Subsonic Tunnel: Description, Flow Characteristics, and Guide for Users*. NASA TP-3008, 1990.
12. Rae, William H., Jr.; Pope, Alan: *Low-Speed Wind Tunnel Testing*. John Wiley & Sons, Inc., 1984.
13. Herriot, John G.: *Blockage Corrections for Three-Dimensional-Flow Closed-Throat Wind Tunnels, With Consideration of the Effects of Compressibility*. NACA Rep. 995, 1950.

REPORT DOCUMENTATION PAGE			Form Approved OMB No. 0704-0188	
Public reporting burden for this collection of information is estimated to average 1 hour per response, including the time for reviewing instructions, searching existing data sources, gathering and maintaining the data needed, and completing and reviewing the collection of information. Send comments regarding this burden estimate or any other aspect of this collection of information, including suggestions for reducing this burden, to Washington Headquarters Services, Directorate for Information Operations and Reports, 1215 Jefferson Davis Highway, Suite 1204, Arlington, VA 22202-4302, and to the Office of Management and Budget, Paperwork Reduction Project (0704-0188), Washington, DC 20503				
1. AGENCY USE ONLY (Leave blank)	2. REPORT DATE December 1999	3. REPORT TYPE AND DATES COVERED Technical Memorandum		
4. TITLE AND SUBTITLE Subsonic Investigation of Leading-Edge Flaps Designed for Vortex- and Attached-Flow on a High-Speed Civil Transport Configuration			5. FUNDING NUMBERS WU 537-03-22-02	
6. AUTHOR(S) Bryan A. Campbell, Guy T. Kemmerly, Kevin J. Kjerstad, and Victor R. Lessard				
7. PERFORMING ORGANIZATION NAME(S) AND ADDRESS(ES) NASA Langley Research Center Hampton, VA 23681-2199			8. PERFORMING ORGANIZATION REPORT NUMBER L-17919	
9. SPONSORING/MONITORING AGENCY NAME(S) AND ADDRESS(ES) National Aeronautics and Space Administration Washington, DC 20546-0001			10. SPONSORING/MONITORING AGENCY REPORT NUMBER NASA/TM-1999-209701	
11. SUPPLEMENTARY NOTES Campbell, Kemmerly, and Kjerstad: Langley Research Center, Hampton, VA; Lessard: ViGYAN, Inc., Hampton, VA.				
12a. DISTRIBUTION/AVAILABILITY STATEMENT Unclassified-Unlimited Subject Category 02 Availability: NASA CASI (301) 621-0390			12b. DISTRIBUTION CODE Distribution: Nonstandard	
13. ABSTRACT (Maximum 200 words) A wind tunnel investigation of two separate leading-edge flaps, designed for vortex- and attached-flow, respectively, were conducted on a High Speed Civil Transport (HSCT) configuration in the Langley 14- by 22-Foot Subsonic Tunnel. Data were obtained over a Mach number range of 0.12 to 0.27, with corresponding chord Reynolds numbers of $2.50 \times 10^6$ to $5.50 \times 10^6$ . Variations of the leading-edge flap deflection angle were tested with outboard leading-edge flaps deflected $0^\circ$ and $26.4^\circ$ . Trailing-edge flaps were deflected $0^\circ$ , $10^\circ$ , $12.9^\circ$ and $20^\circ$ . The longitudinal and lateral aerodynamic data are presented without analysis. A complete tabulated data listing is also presented herein. The data associated with each deflected leading-edge flap indicate L/D improvements over the undeflected configuration. These improvements may be instrumental in providing the necessary lift augmentation required by an actual HSCT during the climb-out and landing phases of the flight envelope. However, further tests will have to be done to assess their full potential.				
14. SUBJECT TERMS High-Speed Civil Transport; HSCT; HSR; Vortex flap; Attached-flow flap; Mission adaptive flap			15. NUMBER OF PAGES 108	
			16. PRICE CODE A06	
17. SECURITY CLASSIFICATION OF REPORT Unclassified	18. SECURITY CLASSIFICATION OF THIS PAGE Unclassified	19. SECURITY CLASSIFICATION OF ABSTRACT Unclassified	20. LIMITATION OF ABSTRACT UL	